

Mechanisms of the Removal of Metals from Acid and Neutral Mine Water under varying Redox Systems

A thesis submitted for the Degree of Doctor of Philosophy

by

Kay Florence, MSc

School of Engineering, Cardiff University

September 2014

DECLARATION

This work has not been previously accepted in substance for any degree and is not concurrently submitted in candidature for any degree

Signed Date

STATEMENT 1

This thesis is being submitted in partial fulfilment of the requirements for the degree of PhD

Signed Date

STATEMENT 2

This thesis is the result of my own independent work/investigation, except where otherwise stated. Other sources are acknowledged by explicit references.

Signed Date

STATEMENT 3

I hereby give consent for my thesis, if accepted, to be available for photocopying and for interlibrary loan, and for the title and summary to be made available to outside organisations.

Signed Date

STATEMENT 4: PREVIOUSLY APPROVED BAR ON ACCESS

I hereby give consent for my thesis, if accepted, to be available for photocopying and for interlibrary loans after expiry of a bar on access previously approved by the Graduate Development Committee.

Signed Date

Acknowledgments

Thanks to my Ph.D supervisors Dr Devin Sapsford, Dr Ian Watson and Dr Abby Moorhouse for academic support and guidance throughout the project. Although, particular thanks go to Dr Jennifer Geroni, my Dad Peter Florence and Professor Christian Wolkersdorfer for their help in the field, endless discussions and sheer determination in keeping me focused through to completion of the thesis. I also thank Professor Barrie Johnson and Dr Cath Kay at Bangor University for their collaboration on the microbiological investigations. Phil and Sarah Morgan of Hydro Industries. Ravi Mathers, Jeff Rowland, Kristinna Penmann, Nia Blackwell and Marco Santonastaso for lab assistance and other colleagues at both Cardiff and Aberystwyth University, many of which have become good friends, Gillifer, Tina, Phil, Ruth, Nick, Bill, Brian and John. My family and long term friends who have been so supportive, I have been astonished at the level of encouragement that you have shown throughout this journey, especially Chris, whom I thank dearly for the love and energy that he tirelessly provides – and the nice graphs and images that he helped to design.

Mum, it's not quite the Olympic gold medal I promised you when I was little but none the less, this is for you.

Abstract

This thesis investigates the effectiveness of a passive treatment technology for Fe removal from low pH metal mine water. In addition, the use of electrocoagulation (EC) in removing Zn from circumneutral mine water and acid mine drainage (AMD) was studied. Using an advanced oxidation process (AOP) followed by EC converted Fe(II) from coal mine drainage to a stable magnetic form of Fe. Research also studied the use of Cu electrodes in removing high concentrations of metals and sulphate from AMD.

A 1 m³ field pilot scale vertical flow reactor (VFR) for passively treating an average flow of 0.6 L/min was deployed for 414 days. The system was gravity fed and removed an average of 65% of the Fe from pH 3 AMD. Potential removal mechanisms are a combination of bacterially mediated Fe(II) oxidation by *Ferrovum myxofaciens* and filtration of Fe nanoparticles. The build-up of the ochre bed did not compromise the permeability of the VFR. Mineralogical and microbiological studies combined with PHREEQC modelling show that the main mineral precipitated in the VFR is schwertmannite.

Using EC, it was shown that the addition of Fe from neutral mine water by electrical dissolution of an Fe electrode resulted in Zn to be removed at a near neutral pH through a combination of co-precipitation and adsorption reactions. An inert Pt electrode rapidly removed 70 mg/L of Fe(II) from coal mine water by AOP applying 5 A during 4 min treatment. A second stage treatment adding Fe by electrical dissolution of Fe electrodes generated the required Fe(II):Fe(III) ratio and E_h-pH conditions to form magnetic Fe (magnetite).

Further investigations into EC proved that the removal of sulphate and metals from AMD was highly effective when adding Cu from a copper electrode at 40 min at 5 A with aeration. Sulphate was reduced from 1324 mg/L to 112 mg/L without leaving Cu in solution. ESEM images and mineralogical studies of the precipitates showed that the mineral cuprite is formed. This has future potential implications for metal recycling/recovery from AMD.

Content

Acknowledgments.....	v
Abstract.....	vii
Figures Index.....	xv
Table Index.....	xxi
1 Abbreviations.....	1
2 Introduction.....	2
2.1 Implementation of the EU Water Framework Directive	2
2.2 Mine Drainage in the UK	2
2.3 Metal Mines Strategy for Wales.....	3
2.4 Mine Water Chemistry and Acid Mine Drainage	4
2.5 pH and Redox (E_h)	9
2.6 Considerations for Remediation.....	10
2.7 Motivation	11
2.8 Aims of the Thesis.....	12
3 Literature Review.....	14
3.1 Iron Chemistry	14
3.1.1 Elemental Iron and Iron Speciation	14
3.1.2 Common Iron minerals	15
3.1.3 Fe Oxides and Hydroxides in AMD	18
3.1.4 Iron Solubility	19
3.1.5 Iron Toxicity in the Aqueous Environment.....	20
3.1.6 pH of Hydrolysis	21
3.2 Zinc Chemistry	23
3.2.1 Zinc in the Aqueous Environment	23
3.2.2 Common Zinc Minerals	24
3.3 Metal Removal by Adsorption and Co-precipitation	25
3.3.1 Adsorption	25
3.3.2 Co-precipitation	27
3.4 Source Control	28
3.5 Passive Treatment Options.....	29
3.5.1 Description of Passive Treatment.....	29
3.5.2 Anoxic Limestone Drains (ALD)	30

3.5.3	Oxic Limestone Drains (OLD)	31
3.5.4	Open Limestone Channels (OLC).....	32
3.5.5	Reducing and Alkalinity Producing Systems (RAPS)	32
3.5.6	Constructed Wetlands	33
3.5.7	Aerobic Wetlands	34
3.5.8	Anaerobic Wetlands	35
3.5.9	Sizing Criteria for Wetlands and Settling Lagoons	35
3.5.10	Permeable Reactive Barriers (PRB).....	36
3.5.11	Sand Filters	37
3.5.12	Ochre Accretion and SCOOFI Systems.....	38
3.6	Vertical Flow Reactors.....	39
3.6.1	Introduction.....	39
3.6.2	Development of the Vertical Flow Reactor.....	40
3.7	Active Treatment Options	41
3.7.1	Description of Active Treatment Options	41
3.7.2	Active Abiotic Treatment	42
3.7.3	Bacterial Activity	43
3.7.4	Sulphate Reducing Bacteria.....	44
3.7.5	High Density Sludge Process (HDS)	44
3.7.6	Membrane Filtration.....	45
3.7.7	Ion Exchange	47
3.8	Electrochemistry.....	48
3.8.1	Introduction.....	48
3.8.2	Overview of Reactions Involved	51
3.8.3	Electrode Configuration and Materials.....	53
3.8.4	Advanced Oxidation Process.....	54
3.8.5	Selected Mine Water Applications.....	55
4	Study Areas	57
4.1	Introduction.....	57
4.2	Cwm Rheidol Pb/Zn Mine, Mid-Wales.....	58
4.2.1	Location.....	58
4.2.2	Geology	59
4.2.3	Mining History	60

4.2.4	Mine Water Chemistry	60
4.3	Frongoch Pb/Zn mine, Central-Wales	66
4.3.1	Location.....	66
4.3.2	Mining History.....	67
4.3.3	Geology.....	68
4.3.4	Mine Water Chemistry	68
4.4	Parys Mountain, Anglesey, North-Wales	69
4.4.1	Location.....	69
4.4.2	Mining History.....	70
4.4.3	Geology.....	71
4.4.4	Mine Water Chemistry	71
4.5	Ynysarwed, South-Wales	72
4.5.1	Location.....	72
4.5.2	Mining History.....	72
4.5.3	Geology.....	73
4.5.4	Mine Water Chemistry	73
5	Methods.....	75
5.1	Introduction.....	75
5.2	Laboratory Methods.....	77
5.2.1	Laboratory pH, ORP, Temperature.....	77
5.2.2	Sample Collection, Preservation and Storage.....	77
5.2.3	Laboratory Glassware and Equipment Decontamination	77
5.2.4	Electrical Transformer for Electrocoagulation (EC) Experiments.....	77
5.2.5	Graded Glassware and Laboratory Equipment	78
5.2.6	Sample Acidification.....	78
5.2.7	Sample Storage and Preparation of Synthetic Mine Water.....	78
5.2.8	Buffer Solutions.....	79
5.2.9	Laboratory Grade Chemicals.....	79
5.2.10	Deionised Water	79
5.2.11	Alkalinity.....	79
5.2.12	Cation Analysis: Inductively Coupled Plasma Optical Emission Spectrometry.....	79
5.2.13	Anion Analysis: Ion Chromatography	80

5.3	Spectrophotometry.....	81
5.3.1	Introduction.....	81
5.3.2	Preparation of the Fe(II) Secondary Standard.....	82
5.3.3	Solutions used for Fe(II) Analytical Method.....	83
5.4	Chemical Investigation of Sludges.....	84
5.4.1	Total Digestion.....	84
5.4.2	Sequential Extraction.....	84
5.5	X-Ray Diffraction.....	85
5.5.1	Introduction.....	85
5.5.2	Sample Preparation and Measuring Procedure.....	85
5.6	Environmental Scanning Electron Microscopy.....	85
5.6.1	Introduction.....	85
5.6.2	ESEM Principles.....	86
5.6.3	Analytical Procedure for the ESEM Analysis.....	87
5.7	CS-Analysis.....	87
5.8	Terminology for Filtered/Unfiltered/Total Concentrations.....	87
5.9	Design and Construction of the VFR.....	88
5.9.1	Design Criteria.....	88
5.9.2	Tank Construction.....	89
5.9.3	Connection at the Adit.....	91
5.9.4	Inflow.....	91
5.9.5	Overflow.....	92
5.9.6	Position of the VFR at Cwm Rheidol.....	92
5.9.7	Maintenance of the VFR During Operation.....	94
5.10	VFR Field and Laboratory Methods and Experiments.....	94
5.10.1	Water Sample Collection and Preservation.....	94
5.10.2	Alkalinity Determination.....	95
5.10.3	On-site Parameters.....	95
5.10.4	Sludge Sample Collection.....	96
5.10.5	Fe Oxidation and Adsorption Experiments.....	97
5.10.6	Determination of Volume of Dry Ochre.....	99
5.10.7	Fe Adsorption Experiments at Cwm Rheidol and Parys Mountain.....	99
5.10.8	Limestone Experiments.....	100

5.10.9	Aeration Experiments.....	102
5.10.10	Stirring Experiments.....	103
5.10.11	Centrifugation, Coagulation and Flocculation Experiments.....	104
5.10.12	Ultracentrifugation.....	105
5.10.13	Settling Velocity of Cwm Rheidol Precipitates.....	106
5.10.14	Microbiological Sampling and Analysis.....	107
5.10.15	VFR Decommissioning.....	107
5.11	Electrochemical Methods and Equipment.....	109
5.11.1	Adsorption vs Co-precipitation of Zn (Frongoch).....	109
5.11.2	Advanced Oxidation (Ynysarwed).....	110
5.11.3	Electroprecipitation.....	111
5.11.4	Zinc Titration.....	112
5.12	PHREEQC Modelling.....	112
5.13	Statistical Investigations.....	113
6	Results and Discussion.....	117
6.1	Reasons for the VFR Experiments Conducted in the Project.....	117
6.2	Introduction to the Cwm Rheidol VFR Field Study.....	117
6.3	Hydraulics.....	119
6.3.1	Flow Rate through the VFR.....	119
6.3.2	Hydraulic Conductivity of the VFR.....	121
6.3.3	Upscaling of the VFR.....	121
6.4	Physicochemical Parameters of the Cwm Rheidol Mine Water.....	122
6.4.1	Fe Concentrations in the VFR.....	122
6.4.2	On-site Parameters.....	128
6.4.3	Alkalinity.....	133
6.4.4	Metals and Main Ion Concentrations (field data).....	134
6.5	Fe Removal Investigations.....	138
6.5.1	Introduction.....	138
6.5.2	Cwm Rheidol Aeration and Adsorption Experiments.....	138
6.6	Limestone Experiments.....	150
6.6.1	Cwm Rheidol Open System Limestone Experiment.....	150

6.6.2	Cwm Rheidol Closed System Limestone Experiment to Assess the Potential for a RAPS System as a Second Treatment Stage for Zn Removal Following a VFR.....	152
6.6.3	Parys Mountain Limestone Experiment	153
6.7	Ultracentrifugation of Cwm Rheidol Water.....	155
6.8	VRF Microbiology (by Bangor University).....	158
6.9	VFR Ochre Characterisation	160
6.9.1	Results of Sequential Extractions.....	160
6.9.2	TOC and Sulphur Analysis.....	160
6.9.3	Results of XRD Analysis	161
6.9.4	Results of ESEM Analysis.....	162
6.10	Total Digest of VFR Ochre.....	164
6.11	Settling of VFR Precipitates	165
6.12	Geochemical Modelling.....	169
6.13	Zinc Removal.....	170
6.13.1	Characterization of Mine Water.....	170
6.13.2	Electrocoagulation of Frongoch Mine Water (steel electrodes)	170
6.13.3	Zinc Solubility Titration.....	172
6.13.4	Co-precipitation vs. Adsorption of Zn in Neutral Mine Water.....	172
6.14	Advanced Oxidation of Ynysarwed Coal Mine Drainage	178
6.15	Electrochemical Treatment of Cwm Rheidol Water.....	185
6.16	Vertical Flow Reactor (VFR).....	189
6.17	Electrochemistry for Fe and Zn Removal.....	192
6.17.1	Zn removal Before and After EC Using Iron Electrodes	192
6.17.2	AOP for Fe Removal at Ynysarwed.....	192
6.17.3	Electroprecipitation at Cwm Rheidol Using Cu Electrodes.....	192
6.18	Relevance for Mine Water Treatment and Further Work.....	193
6.18.1	VFR Relevance	193
6.18.2	Zn Removal	194
6.18.3	Advanced Oxidation and Electrocoagulation	195
7	Literature.....	196

Figures Index

Figure 1: Map showing the priority metal mines in Wales (modified after Johnston, 2004); study sites in this thesis indicated.	4
Figure 2: Metal solubility as a function of pH; from Wolkersdorfer (2013), amended and supplemented according to Cravotta (2008); Original data obtained from Charles A. Cravotta III, pers. comm. 2013.	8
Figure 3: Pourbaix diagram for Fe-species with the pH-E _h -ranges in which thiobacteria and iron bacteria are commonly found (modified from and after Baas Becking et al., 1960, Tischendorf and Ungethüm, 1965). Superimposed are the pH- (red) and E _h -conditions (green) for the Cwm Rheidol Lower Number 9 Adit mine water. Means are given as solid horizontal and vertical lines.	15
Figure 4: Discharge of mine water from the abandoned Ynysarwed colliery into the River Neath (courtesy of Ch. Wolkersdorfer).....	21
Figure 5: E _h -pH diagram for the system Zn-O ₂ -CO ₂ -S-H ₂ O; activities: Zn = 10 ⁻⁶ and 10 ⁻⁴ , C = 10 ⁻³ and S = 10 ⁻³ (from Brookins, 1988).	25
Figure 6: Membrane filter sizes and separation types (modified from Wolkersdorfer 2013).	46
Figure 7: Conceptual representation of the electrical double layer (from Vepsäläinen, 2012).	50
Figure 8: Comparison of sludge settling rates from aerated and electrolysed ferrous mine water (from Franco and Balouskus, 1974).	51
Figure 9: Schematic representation of typical reactions during the EC treatment (from Vepsäläinen, 2012).	53
Figure 10: Potential electrode configurations for EC treatment (modified from Comminellis and Chen, 2010).	54
Figure 11: Digital Elevation map showing the four sites, Cwm Rheidol, Parys Mountain, Frongoch and Ynysarwed studied in this thesis (contains Ordnance Survey data © Crown copyright and database right).	57
Figure 12 Map showing the boundary of the Cwm Rheidol abandoned Pb/Zn and its position in relation to the River Rheidol. The small red circle on the western edge of the boundary marks the flows from the adit discharge pipes. © Crown Copyright/database right 2014. An Ordnance Survey/EDINA supplied service.	59
Figure 13: The sparsely vegetated spoil tips at the Cwm Rheidol former Pb/Zn mine.....	61
Figure 14: Old filter beds at Cwm Rheidol that are blocked AMD from the adit discharge pipes flowing into the adjacent River Rheidol.	61

Figure 15: Cwm Rheidol No. 9 adit portal. In the foreground the discharge pipe for the mine water flowing in the middle of the image can be seen. The adit surface and the walls are covered with ochre..... 62

Figure 16: Cwm Rheidol Mine water discharge pipes (left: No. 6 adit, right: No. 9 adit)..... 63

Figure 17: Pilot scale passive system installed by Natural Resources Wales in 2010 for the removal of Zn from the Cwm Rheidol upper adit water. 65

Figure 18: Sludge formation in the 2010 trials..... 66

Figure 19: Boundary of the Frongoch abandoned Pb/Zn mine. Mine water discharges from the adit west of the site. © Crown Copyright/database right 2014. An Ordnance Survey/EDINA supplied service. 67

Figure 20: Adit and manmade channel at the Frongoch mine site. Width of adit approximately 1 m..... 69

Figure 21: Boundary of Parys Mountain copper mine. Red circle indicates the north Dyffryn Adda (north adit) where water from the mine drains into the Afon Goch North. © Crown Copyright/database right 2014. An Ordnance Survey/EDINA supplied service..... 70

Figure 22: Location of the Ynysarwed active and passive treatment plants..... 74

Figure 23: Sludge sample from VFR for sequential extraction (diagonal 7 cm).. 85

Figure 24: Schematic of the VFR pilot plant used in the field trial at Cwm Rheidol. 89

Figure 25: Left is the coiled drainage pipe to the outflow. Right is the gravel layer placed on top of the pipe and the coarse gravel layer..... 90

Figure 26: Cwm Rheidol mine water discharge pipes; Left: Is the set up for piping water from the lower number 9 discharge pipe to the VFR. Right: The discharge point of both upper number 6 and lower number 9 adits.... 91

Figure 27: Initial stages of filling the VFR. Left: Shortly after seeding the VFR; right: First time filled VFR plus inflow pipe..... 92

Figure 28: Schematic cross section of the upper number 6 adit and the lower number 9 adit and the location of the VFR at Cwm Rheidol. masl: meters above sea level..... 93

Figure 29: Map showing the aerial position of the VFR at the old filter bed area at the Cwm Rheidol site. The orange line shows the feed pipe from the number 9 adit into the tank. Digimap ® – © Crown copyright/database right 2014. Ordnance Survey/EDINA supplied service. FOR EDUCATIONAL USE ONLY. 93

Figure 30: Left: partial dewatering of the ochre collected from the VFR at Cwm Rheidol; right: set-up of the laboratory Fe adsorption experiments on Cwm Rheidol VFR sludge..... 98

Figure 31: Ochre from the VFR added to untreated mine water in adsorption experiments..... 100

Figure 32: Cwm Rheidol mine water with limestone added.....101

Figure 33: Left image is the Limestone reactor (closed system) Right image, parameters being measured prior to the stripping phase.102

Figure 34: Experimental set up for stirring experiments.104

Figure 35: Left is the ochre bed of the VFR after having been drained. Right is a section of the ochre bed taken for lab analysis.108

Figure 36: Flow rate in L/min over time; the secondary axis shows the cumulative volume treated throughout the trial period.....120

Figure 37: Filtered and unfiltered VFR Inflow and outflow Fe(total) concentrations over time.124

Figure 38: Nominal retention time in the VFR (median unfiltered Fe: 71.0 %; median filtered Fe: 67.8 %).125

Figure 39: Filtered and unfiltered Fe(total) removal rate and flow rate of the VFR over time.125

Figure 40: Inflow and outflow Fe(II) concentrations for some of the sample points throughout the trial period.127

Figure 41: Fe concentrations and Fe-removal rate vs. flow rate of the VFR. Though there is a trend to lower removal rates at higher flows, the low regression coefficients indicate that there is no correlation between the removal rate and the flow.....128

Figure 42: inflow and outflow temperature for the sample points throughout the trial period.....129

Figure 43: pH of the VFR inflow and outflow water over time.129

Figure 44: EC measurements for the VFR inflow and outflow over time.131

Figure 45: VFR inflow and outflow dissolved oxygen (DO) concentrations over time.....132

Figure 46: ORP corrected values of the VFR inflow and outflow water over time.....133

Figure 47: VFR Zn concentrations of the inflow and outflow water over time. 134

Figure 48: VFR Pb concentrations of the inflow and outflow water over time. 135

Figure 49: VFR Cd concentrations of the inflow and outflow water over time. 136

Figure 50: VFR SO_4^{2-} concentrations of the inflow and outflow water over time.....137

Figure 51: VFR Cl^- concentrations of the inflow and outflow water over time..138

Figure 52: Fe filtered and unfiltered concentration in the raw mine water during aeration over time at Cwm Rheidol (pH 2.3, E_h 772 mV).139

Figure 53: Fe oxidation lab experiment to determine concentration of Fe(III) in raw mine water in contact with VFR ochre over time. Results compare Fe concentrations analysed by the Merck Spectrophotometer and the ICP-OES.....141

Figure 54: Cwm Rheidol field adsorption experiment, Fe(II) and Fe(total) concentration of aerated raw mine water in contact with VFR sludge over time. Note the different scales for Fe total and Fe(II).142

Figure 55: Results of filtered Fe concentrations during the field adsorption experiments at Parys Mountain. Blue arrows indicate the times (0, 150 and 270 min) at which the VFR ochre was added in the following respective quantities: 1 L, 0.5 L, 1 L.143

Figure 56: Filtered Fe total, Fe(II) and Fe(III) concentrations in aerated/agitated and static setup of Cwm Rheidol inflow mine water after 50 h reaction time (compare with the results in Figure 59).....145

Figure 57: Course of the Fe total concentrations in aerated/stirred and static Cwm Rheidol inflow water over time (lab experiment). Fe(II) was measured at 0 mg/L at beginning of experiment.147

Figure 58: Fe total concentrations in aerated/agitated and laboratory static setup of Cwm Rheidol inflow mine water after 48 h reaction time (compare with the results in Figure 56).147

Figure 59: Fe total concentrations in aerated/agitated, stirred and static samples of Cwm Rheidol inflow water over time (lab experiment). 35 min Fe total in fast stirred experiment extrapolated (lighter bar); Fe(II) data for the aerated experiment after 180 min not available due to malfunction of the spectrophotometer.149

Figure 60: Distribution of Fe in the non-turbid and turbid samples used in the Fe removal experiments. 0.05 μm is considered the threshold of the centrifuging experiments, 0.2 μm is the filter size used in the field and lab experiments.....149

Figure 61: Time dependend Fe total concentrations in aerated/stirred sample of Cwm Rheidol outflow water (lab experiment).....150

Figure 62: pH and filtered (semi-)metal concentrations in Cwm Rheidol inflow water in contact with limestone.....151

Figure 63: Cwm Rheidol closed system limestone experiment followed by air stripping.....153

Figure 64: pH and metal concentrations in Parys Mountain water after contact with Cwm Rheidol VFR sludge and then in contact with limestone (closed system followed by air stripping after 54 h 30 min).155

Figure 65: Results of the centrifuge experiment to determine the Fe particle size in the Cwm Rheidol inflow water. Error bars based on duplicate ion determinations.....157

Figure 66: Results of the centrifuging experiment to determine the Zn particle size in the Cwm Rheidol inflow water.....158

Figure 67: XRD analysis of VFR ochre. The peaks at around 15, 35 and 45°2 θ are characteristic for schwertmannite.161

Figure 68: SEM image showing the amorphous structure of the Cwm Rheidol Fe precipitates collected from the VFR when it was in operation162

Figure 69: SEM image of amorphous structure of the Cwm Rheidol Fe precipitates (as solid ochre) collected from the VFR after it had been drained down.....162

Figure 70: SEM image showing the amorphous structure of the ochre collected from the Cwm Rheidol discharge pipe162

Figure 71: Sampling location of the Cwm Rheidol pipe sludge at the end of the No. 9 adit drainage pipe. Width of pipe 300 mm.....164

Figure 72: Height of the Fe precipitates in the VFR during the trial is approximately 40 cm from the top of the gravel. Inflow temporarily turned off.....166

Figure 73: Height of Fe precipitates in the VFR after it had been drained is approximately 6–7 cm from the top of the gravel bed.....167

Figure 74: Fe precipitates immediately after the sample was taken from inside the VFR.....167

Figure 75: Settling properties of the precipitates that formed in the VFR at 15, 60, 120, 194, 240 and 284 s settling time.....167

Figure 76: Settling rates of the VFR sludge. 50% settling after the first 120 s. Between 284 and 600 s, extrapolated data.....168

Figure 77: Settling velocities of the VFR sludge. Settling velocity decreases rapidly after 50% of the sludge has settled.....169

Figure 78: Results for pH, filtered Zn and total Fe removal from Frongoch mine water using steel electrodes at 1.5 A and 30 V.171

Figure 79: Solubility curve for Zn titrated through the pH range 2–12.....172

Figure 80: Results for Zn removal from Frongoch mine water by electro co-precipitation with Fe from a sacrificial electrodes spaced 30 mm apart. 1 A, variable voltage. Compare Table 10 for meaning of abscissa.....174

Figure 81: Results for Zn removal by electro co-precipitation with Fe from sacrificial electrodes spaced 30 mm apart. 1 A, variable voltage. Compare Table 10 for meaning of abscissa.175

Figure 82: Results for Zn removal by adsorption to HFO particles that were added and precipitated electrically using Fe electrodes spaced at 30 mm 1 A, variable voltage. using Zn added at the end of the EC stage, before stirring. Fe unfiltered and filtered concentrations after 15 min stirring were identical, therefore the data plots on the same data point. Compare Table 10 for meaning of abscissa.....176

Figure 83: Results for Zn removal by adsorption to HFO particles that were added and precipitated electrically using Fe electrodes spaced 30 mm apart, 1A, variable voltage. Zn added at the end of the EC stage, before

stirring and the experiment extended to include a 40 min settling time. Compare Table 10 for meaning of abscissa.....176

Figure 84: Results for Zn removal by adsorption to HFO particles that were added and precipitated electrically using Fe electrodes spaced 30 mm apart, 1A, variable voltage. Zn added after the stirring phase and before the settling phase. Compare Table 10 for meaning of abscissa.....177

Figure 85: Fe(II) concentration of Ynysarwed coal mine water at increasing current using Pt electrodes. 4 min reaction time.....178

Figure 86: Filtered Fe(II) concentration of Ynysarwed coal mine water through the temperature range 15–45 °C.....180

Figure 87: Diagram showing the conversion of Fe(II) to Fe(III) in the diffusion layer between the Pt electrode and the sample (modified after Lefrou et al., 2012).....180

Figure 88: left: Magnetic Fe phase in Ynysarwed sample after oxidation followed by addition of Fe using sacrificial electrodes. Middle: Magnetic material adhered to the cathode. Left: Dried magnetic material from Ynysarwed sample.....182

Figure 89: Pourbaix-diagram for Fe-S-O-H and Fe-O-H phases with superimposed E_h -pH-conditions at the end of the experiment. Temp: 40 °C, $p = 1$ bar, $Fe(aq) = 10^{-2.7}$, $H_2O(aq) = 1$, $SO_4^{2-}(aq) = 10^{-2.7}$. Diagrams constructed using Geochemist’s Workbench 9.....184

Figure 90: ESEM images of the electrochemically produced magnetic sludge formed in Ynysarwed water after a two stage process of AOP followed by EC with Fe electrodes.184

Figure 91: Unfiltered Cwm Rheidol sludge and dried sludge produced in the EC reactor after 60 min treatment time with Cu + Al electrodes.187

Figure 92: ESEM images of the sludge from the Cu + Al electrode treated water. The cubic mineral in the centre is probably cuprite (Cu_2O).....188

Figure 93: Stability diagram for Cu phases using the analysis in Table 26 at 40 °C. Diagram constructed using Geochemist’s Workbench 9. Conclusions.....189

Figure 94: Cross section of the Cwm Rheidol mine and the mechanisms leading to the mine water chemistry and the Fe oxidation/precipitation reactions occurring in the VFR. Mine layout based on literature mentioned in the text and dozens of underground images found in the internet.....190

Table Index

Table 1: The Formulae and names of the major Iron Oxides and Oxide Hydroxides (Schwertmann and Cornell, 2000).....	16
Table 2: pH of hydrolysis of ions from dilute solution (from Levinson 1974).....	22
Table 3: Coordinates for each of the sites investigated.....	58
Table 4: Summary of treatment types investigated at each of the sites. A more detailed compilation is provided in Table 6.....	58
Table 5: Pb and Zn concentrations (%) in river sediments and soils affected by mine sites in the Frongoch and Cwm Rheidol area (Griffith, 1919).....	60
Table 6: Experiments and methods conducted during the course of the project. Detailed explanations and reasons for conducting the tests are provided in the relevant chapters.....	76
Table 7: Phases targeted by the sequential extractions performed on the VFR ochre.....	84
Table 8: Description of terminology used within this thesis. All filtered samples filtered through a 0.2 µm filter.....	88
Table 9: Centrifuge parameters and calculated values.....	106
Table 10: Experimental procedure for Zn adsorption vs co-precipitation experiments.....	110
Table 11: Results of the Paired Samples <i>t</i> -Test, 95% confidence Interval to test the treatment efficiency of the VFR.....	115
Table 12: Results of the Pearson Correlation of the physicochemical VFR parameters in Appendix 4. Only the relevant correlations are discussed in the text.....	116
Table 13: Comparison of mean values for inflow and outflow parameters ('pair') and the Fe unfiltered/filtered concentrations (Pair 9). The statistical significance of the differences is presented in Table 11. pH recalculated arithmetic average for [H ⁺] and standard deviations as well as Std, Error Mean from measured pH-values.....	123
Table 14: Average filtered and unfiltered Fe total and Fe(II)-concentrations in the inflow and outflow water of the VFR in mg/L.....	126
Table 15: Fe concentrations in aerated and static bucket experiments after 50 h.....	144
Table 16: Starting Fe total concentrations in fresh and aged Cwm Rheidol mine water samples (see also Appendix 4).....	146
Table 17: Filtered Fe(III) concentrations in inflow and outflow mine waters after selected centrifuge treatments (3000 rpm, 15 min). Only the results for the 60 mg/L AlSO ₄ -solution are shown.....	156

Table 18: Weight% of constituents of the VFR ochre. ^a VFR sludge, ^b Canadian Active Treatment plants, ^c US coal mine sludges, ^d active treatment of fluorspar mine sludge.....	160
Table 19: Sulphur and carbon content by weight % of the Cwm Rheidol VRF ochre.....	161
Table 20: Emission spectrum data from ESEM analysis of ochre samples from Figure 68, Figure 69 and Figure 70.....	163
Table 21: Results of the total digest for the VFR and lower number 9 adit discharge pipe (Figure 71) sludges (%). B, Be, Bi, Co, Mo, Ni, Sb, Se and Tl below the detection limit. 0.0 means that the element was measured above the detection limit, but below 0.05%.	165
Table 22: Settling rates (v, cm/s) of the VFR sludge.....	168
Table 23: Change in parameters at the end of each amperage step (el. cond.: electrical conductivity; ORP uncorrected). Pt electrodes, 4 min reaction time.....	179
Table 24: Parameters for untreated and EC treated Cwm Rheidol water in mg/L; Cu anode with Al, Pt, Cu and Fe cathode materials and a treatment time of 40 min at 5 A. ORP is uncorrected.	186
Table 25: Emission spectrum data from ESEM analysis of the cubic mineral in Figure 92.....	188
Table 26: Results for the total digest of sludges from the EC treatment of Cwm Rheidol and Ynysarwed water (%). 0.0 means that the element was measured above the detection limit, but below 0.05%.	188
Table 27: Fe removal processes occurring in the VFR at Cwm Rheidol.	191

1 **Abbreviations**

AMD	acid mine drainage
AO	advanced oxidation
AOP	advance oxidation process
BART	Bangor Acidophile Research Team
ccp	cubic close packed
DNA	deoxyribonucleic acid
DO	dissolved oxygen
EC	electrocoagulation
EQS	environmental quality standard
hcp	hexagonally close packed
HDS	high density sludge
HFO	hydrous ferric oxide
HRT	hydraulic residence time
IC	ion chromatography
ICP-OES	inductively coupled plasma atomic emission spectroscopy
LDS	low density sludge
masl	meters above sea level
MMO	mixed metal oxide
ORP	oxidation reduction potential
PCR	polymerase chain reaction
RAPS	reducing alkalinity producing systems
rDNA	ribosomal deoxyribonucleic acid
rpm	revolutions per minute
SAPS	successive alkalinity producing systems
SRB	sulphate reducing bacteria
SSSI	Site of Special Scientific Interest
VFR	vertical flow reactor
WFD	water framework directive

2 Introduction

2.1 Implementation of the EU Water Framework Directive

Abandoned mines can contaminate local watercourses and cause substantial damage to the ecosystem (Younger et al., 2002). In addition, a major environmental concern has been highlighted since the introduction of the EU Water Framework Directive (WFD). This important piece of legislation has been transposed into UK law; the directive stipulates that all inland water bodies are to be of 'good ecological status' by 2015 (2006/11/EC) and sets stringent targets for water quality standards that are to be met in order for surface water and groundwater to comply with the directive's terms. Because rivers and streams polluted by historic mining practices often contain levels of contaminants that grossly exceed water quality standards (Mullinger, 2007), it is essential to address those contaminants with practical technology.

2.2 Mine Drainage in the UK

National and EU law now states that remedial work following mining activity are the responsibility of the mine operators ("polluter pays principle"). Prior to this, the mine operators commonly would have walked away from a site once excavations were complete. Consequently, it is estimated that there are hundreds to thousands of 'abandoned' mining facilities, including onshore mining and quarrying sites in England and Wales (Palumbo-Roe and Colman, 2010). Jarvis et al. (2007), based on National Resources Wales data, reports that more than 100 km of Welsh streams are subject to mine water pollution. Since the introduction of the Water Framework Directive, the responsibility for the clean-up of these contaminated waters has often fallen upon local authorities and non-profit making bodies such as Natural Resources Wales. All of them are currently under pressure to ensure water quality on catchment wide scales in order to comply with EU legislation (European Parliament, 2006).

The attention on remediation of Fe-rich waters has generally focused on coal mine drainage which, in part, is due to the government funding the 'Coal Authority' set up in 1994 to take on the responsibility for the management of coal mine discharge following mine closures (Johnston et al., 2007). Yet, numerous

metalliferous mines in the UK need attention and cost effective treatment options have to be developed or already existing ones to be implemented and improved.

2.3 Metal Mines Strategy for Wales

In 1996, Natural Resources Wales, formerly known as the Environment Agency of Wales secured funding from the National Assembly to develop a Metal Mine Strategy for Wales and commenced monitoring of 5042 km of river stretches in Wales. It was found that 506 km failed to comply with the River Ecosystem objectives, with 108 km being directly attributed to mine pollution (Mullinger, 2007). This research deemed the problem as substantial and led to the development of a strategy to seek and identify priority sites for remediation (Johnston, 2004). In July 2002, the Metal Mines Strategy for Wales finally was published (Rees et al., 2004). A list of the top fifty worst polluting abandoned mines that Natural Resources Wales aim to remediate was selected from the National Rivers Authority database of 1337 mines. Thirty eight of these top fifty polluting mines are located in County Ceredigion (Figure 1) and impact the three main rivers: the Rheidol, Ystwyth and Clarach which drain the mid-Wales Orefield (Johnston, 2004). Three of the abandoned mines studied in this thesis are listed in the top 50 polluting sites, two of which are located in the Ceredigion area. The fourth site is, in contrast, an abandoned coal mine and therefore not part of the metal mines strategy for Wales. Yet, the site is however an intermittent contributor of pollution to the River Neath in South Wales.

The scale and persistent nature of the problem of pollution from abandoned metal mines in Ceredigion is evident. There is a clear emphasises on the need for the development of cost effective remediation methods that can be employed to control polluting effluent from metal mines in the area. The Coal Authority is now working in conjunction with Natural Resources Wales to develop and implement cost effective long-term treatment options at priority sites in the UK. The work presented in this research was co-funded by the Coal Authority and Cardiff University to advance knowledge in the field of metal mine water treatment with a focus on Fe removal from acid mine drainage (AMD) and Zn removal from circumneutral mine waters at abandoned mine sites in Wales.

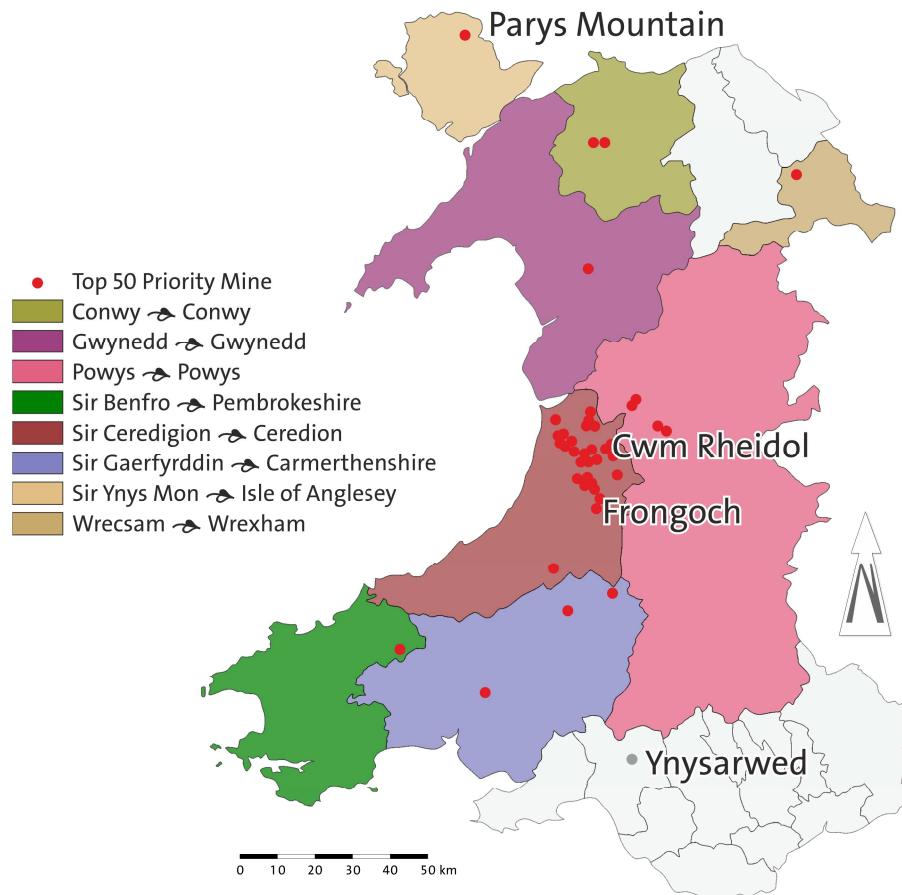


Figure 1: Map showing the priority metal mines in Wales (modified after Johnston, 2004); study sites in this thesis indicated.

2.4 Mine Water Chemistry and Acid Mine Drainage

The two most important reactions that occur in the aqueous environment involve either protons or electrons (Drever, 1997). The transfer of protons affects the pH of a system whereas the transfer of electrons affects the redox potential, signified as the 'E_h' or 'pe'. In summary, protons and electrons in chemical reactions are interdependent of each other and govern the oxidising power and acidity (Stumm and Morgan, 1996).

Metal rich drainage occurs when metal sulphide minerals are exposed to physical and chemical processes. When either surface or groundwater comes into contact with primary and secondary minerals at mine sites under oxic conditions, problematic mine drainage generally develops as dissolution reactions between the water and the ore and rock forming minerals (Wolkersdorfer, 2008). Characteristics of polluting mine waters can vary considerably depending on the geochemical conditions at point source of weathering and the chemistry of the host rocks and gangue minerals. These characteristics determine

whether waters will be acidic and ferruginous, net alkaline and ferruginous, circumneutral or saline (Gandy and Younger, 2002). The mid Wales Orefield, in which the sites of primary focus of this study are located, is generally characterised by circumneutral mine drainage because of the lack of pyrite in the ores. However, pyrite and marcasite are present in a few rare cases such as at the former Cwm Rheidol Pb and Zn mine which is the source of noteworthy water quality failures for potentially harmful elements for up to 16 km downstream of the abandoned mine site (Fuge et al., 1991). In general terms, acidic drainage is generated by the reaction of pyrite or marcasite (FeS_2) with water and an oxidant such as atmospheric as well as dissolved O_2 or Fe(III) . Occasionally, this reaction is supported by a catalyst, for example MnO_2 or microorganisms. Depending on the oxidant present, reactions occur in both oxygenated and anoxic systems. Furthermore, the commonly complex process involves chemical, biological and electrochemical reactions (Blowes et al., 2003, Stumm and Morgan, 1996).

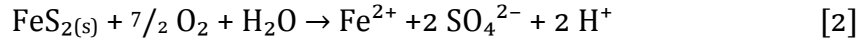
The overall equation for the oxidation of pyrite by atmospheric oxygen is given as:



However, there are a number of sub-reactions that occur which ultimately generate the sulphuric acid as in equation 1. In addition, the precipitation of iron oxides and oxyhydroxides, collectively known as iron ochre, forms the characteristic orange staining that can be seen coating river beds and streams. This staining can be seen in the streambeds for large distances downstream of the outcrops of the pyritiferous host rocks (Fuge et al., 1994).

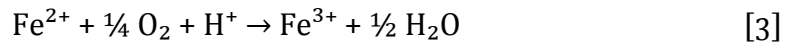
Acid mine drainage (AMD) is found around the world as a result of naturally occurring processes and activities associated with land disturbances such as mining. AMD might cause a number of environmental problems such as ground and surface water pollution by dissolved and particulate metals, in some areas it is also responsible for degrading the quality of soils or aquatic habitats (Adler, 2007). The problem is extensive at abandoned historic mines where, once mining has ceased, the water pumps have simply been turned off or water is allowed to discharge in an uncontrolled manner from the adits; the groundwater

rebound then floods the underground workings (Wolkersdorfer, 2008, Younger et al., 2002) and exposed mineral surfaces then enter into oxidation and hydrolysis reactions. The reaction of pyrite with oxygen and water results in hydrogen ion release, sulphate ions and soluble metal ions (Stumm and Morgan, 1996) as shown in equation 2:

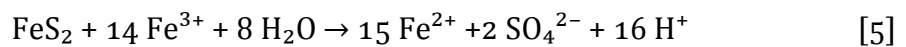
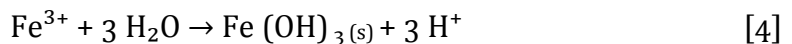


The process of oxidation by atmospheric oxygen is generally slow in undisturbed systems. Yet, the reaction rate is enhanced by a factor of at least 10^5 by iron and sulphate oxidising bacteria at low pH-values (pH <4) such as *Acidithiobacillus thiooxidans* or *Acidithiobacillus ferrooxidans* (Blowes et al., 2003, Kelly and Wood, 2000, Singer and Stumm, 1969, Singer and Stumm, 1970a). More recent studies into biotic oxidation of Fe(II) in low pH mine waters have led to the isolation and characterisation of the Fe oxidising bacteria *Ferrovum myxofaciens* (Rowe and Johnson, 2009). These bacteria are active in pH <2 and were used to oxidise and precipitate Fe in a pilot plant in Nochten, Germany (Hedrich and Johnson, 2012, Johnson, 2014).

Once the water from within the mine reaches the surface and comes into contact with atmospheric oxygen, the amount of dissolved oxygen in the water increases quickly to near saturation. Sufficient oxygen causes the oxidation of ferrous iron Fe(II) to ferric iron Fe(III) as described by equation 3



Ferric iron can either precipitate as the iron oxyhydroxides, e.g. $\text{Fe}(\text{OH})_3$, as in reaction 4 or it can react directly with pyrite to produce more ferrous iron. Oxidation of pyrite by Fe^{3+} generates 16 moles of protons per mole of pyrite as described by equation 5



Consequently, when ferrous iron is produced by equation 5 in the presence of sufficient dissolved oxygen, the cycle of reactions 3 and 4 are perpetuated (Singer and Stumm, 1969, Singer and Stumm, 1970a). Fe(II) is further oxidised

to Fe(III) by oxygen and subsequently, Fe(III) becomes reduced by pyrite to generate more Fe(II) and adds proton acidity to the water (Singer and Stumm, 1970a). In such cases where there are no buffering minerals present, the pH of the water continues to decrease. These reactions describe how the presence of pyrite in the host rock leads to the generation of acid mine water. The proton activity expressed as the pH of mine water can vary quite considerably and is found to be in the range of -3.6 (Richmond Mine at Iron Mountain, California, USA) to 12 (Lake Velenje, Slovenia) in nature (Nordstrom, 2011, Nordstrom et al., 2000, Wolkersdorfer, 2013).

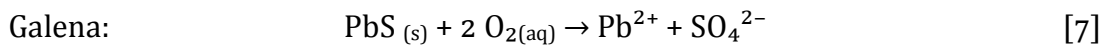
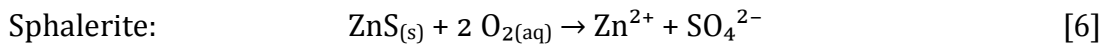
In oxidising conditions, when the pH is raised above the pH at which Fe forms insoluble ferric hydroxides (Stumm and Morgan, 1996), iron is removed from the system. However, where oxygen levels are low, reaction 5 continues to completion and waters will have elevated concentrations of Fe(II) (Jennings et al., 2008).

Metal solubility is controlled by the pH and redox conditions making these factors the principal control on element mobility in the secondary environment. Stumm and Morgan (1996) therefore call the pH the “Master Variable” in aquatic chemistry. As such, the mobility of other potentially harmful elements that may be present in sulphide deposits can be increased upon acid generation from pyrite weathering. The amphoteric nature of metals means that metal cations tend to dissolve at low pH whereas anionic species have a tendency to dissolve at high pH (Cravotta, 2008, Langmuir, 1997). Chemical dissolution of these other elements present in the host rock leads to a metal-laden discharge that may contain high concentrations of potentially contaminating metals such as Fe, Cu, Zn, Pb, Cd, Ni, Cr, Al and metalloid species such as As (Nordstrom, 2011).

Because of the aforementioned characteristics, mine water treatment in terms of removing metals by precipitation is achieved by altering the pH and the redox environment of the water. This limits the solubility of undesirable constituents that compromise water quality. Constituents that might be present, which are potentially toxic to aquatic organisms or humans, include multivalent metals such as Fe(II) and Fe(III), Zn(II), Cd(II), Pb(II), Cu(II), Mn(II), Mn(III), Al(III),

excess hydrogen ions and excess sulphur usually as sulphate (Walton-Day, 2003).

Sulphide minerals are highly reactive and break down easily to release metals and semi-metals into the environment. Waters reacting with sulphide minerals do not necessarily generate acidity. For example, the non-ferrous metal sulphides such as sphalerite and galena break down to release soluble (semi-)metal cations into solution as described by the following equations (Younger et al., 2002):



Absence of pyrite in the ores thus produces metal rich waters without a substantial release of H^+ ions. Circumneutral waters (pH 6–8) are generated where any acidity produced by pyrite or marcasite is neutralized by the dissolution of carbonate and aluminosilicate minerals in the host rocks (Levinson, 1974, Nordstrom, 2011). Circumneutral mine waters therefore contain contaminating metal and metalloid species such as Cd, Zn, As, Se and Pb, which are soluble over a wide range of pH values (Figure 2).

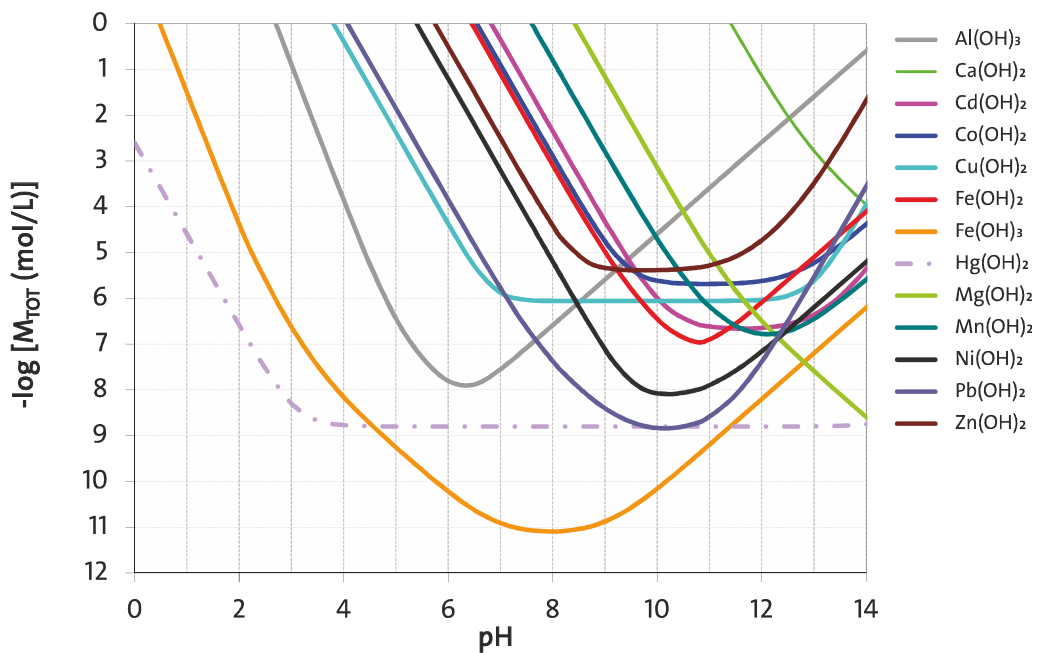


Figure 2: Metal solubility as a function of pH; from Wolkersdorfer (2013), amended and supplemented according to Cravotta (2008); Original data obtained from Charles A. Cravotta III, pers. comm. 2013.

2.5 pH and Redox (E_h)

Metal precipitation occurs when the pH is raised above the metal's pH of hydrolysis as the solubility of the hydrolysed species and the hydrolysis product are correlated with each other (Stumm and Morgan, 1996). There are only a few elements that are not extremely sensitive to pH in aqueous environments and remain soluble over the entire pH range, for example, acid radical forming elements such as nitrogen and chlorine, the alkaline earth metals Ca, Sr, and Mg and alkali earth metals such as Na, K and Rb (Levinson, 1974). These two parameters, pH and E_h , are very important in mine drainage as they determine the stability limits of minerals within an aqueous system (Gill, 1996). pH is a numerical expression for the proton activity (Levinson, 1974, Sørensen, 1909) defined by the expression:

$$\text{pH} = -\log_{10}\{\text{H}^+\} \quad [8]$$

pH is a logarithmic function; consequently, a change of one pH unit represents a tenfold change in proton (hydrogen ion) activity $\{\text{H}^+\}$. In an acidic solution the hydrogen ion activity is greater than 1.0×10^{-7} mol and in a basic solution less than 1.0×10^{-7} mol, placing the neutrality of pure water at 25 °C at pH 7. So far, the lowest pH ever measured was -3.6, in California's Iron Mountain mine (Nordstrom et al., 2000). Since water dissociates into H^+ - and hydroxyl OH^- -ions and the dissociation constant of water is 10^{-14} mol/L, both the hydrogen and hydroxide ion concentration can be given on a pH scale. This means that a pH of 2 corresponds to a hydrogen ion concentration of 1.0×10^{-2} mol/L and a hydroxide ion concentration of 1.0×10^{-12} mol/L (Atkins and Beran, 1992).

pH, considered the "master variable", is a parameter that can be established by electrochemical methods with a pH meter (Stumm and Morgan, 1996) measuring the voltage between a reference electrode and a specially designed glass electrode (Levinson, 1974). Furthermore, the pH value determines the potential reactions in an aqueous system (Faure, 1998). Redox (reduction-oxidation) or oxidation reduction potential (ORP) is defined as the electron activity (Acero et al., 2006) and is a measure of the potential for electrons to be donated to electron accepters within a system. Because oxidation reduction reactions involve the transfer of electrons, it is fundamentally an electrical property that is rec-

orded in either volts or millivolts (Levinson, 1974). This measure can be presented as either pe for the electron activity or as E_h when quoted in volts.

$$pe = -\log_{10}[e^-] \quad [9]$$

Whilst pe and E_h are both used in representing the redox potential, they are not interchangeable parameters. Care should therefore be taken to retain the correct unit of measure for the redox potential. It is possible to convert E_h to pe by the following equation:

$$pe = \frac{F}{2.303RT} E_h \quad [10]$$

Where F is Faraday's constant (96,485.3365 J V⁻¹ g⁻¹ [sA mol⁻¹])

R is the gas constant (8.3144622 J K⁻¹ mol⁻¹)

T is the temperature expressed in K ([K] = [°C] + 273.15)

2.303 is the conversion from natural log to base 10 log.

To measure the E_h within an aqueous system, an inert electrode such as platinum and a secondary reference half-cell electrode are used. The voltage between the two is measured and the value corrected against the reference standard hydrogen electrode to give an E_h value in Volts. Values of E_h and pH can be used to construct E_h /pH diagrams which provide valuable information about the relationship between different metal species under set conditions (Levinson, 1974).

2.6 Considerations for Remediation

Mine water treatment has developed considerably over the past two to three decades. Treatment systems are designed to fit sustainably into the local environment and sometimes to operate in perpetuity with a minimum of maintenance. Systems employed to remediate contaminated waters are passive or active and generally involve the reversing of some of the reactions that cause mine drainage or using other physical/chemical/biological methods to limit the solubility of contaminants (Brown et al., 2002, Walton-Day, 2003, Wolkersdorfer, 2013).

A number of factors need to be considered when designing a system to be employed at a specific site such as: hydrological regime, topography and locality, the longevity of the system, cost and the geochemical nature of the environment (Cravotta, 2007). Also, systems must be designed in compliance with planning criteria, the requirements of which often dictate the type of treatment that can be employed. Efficiency, aesthetics and the provision to enhance the environment are important factors for a lot of passive and semi-passive systems (Brodie, 1991).

2.7 Motivation

Treatment of AMD poses very different challenges to the treatment of low Fe circumneutral waters. This study focuses on iron chemistry and aims to improve understanding of the mechanisms for removing Fe from low pH AMD as well as investigating the effects of adding Fe to circumneutral mine water in order to remove potentially harmful elements such as Zn, Cd and Pb.

The aims of this thesis are to examine different metal mine waters and assess the effectiveness of innovative treatments to remove metals (the main focus on Fe and Zn). The main branch of this thesis follows on from the success of the vertical flow reactor (VFR). This reactor consists of a tank with a gravel bed in its lower part and the mine water follows the hydraulic gradient and flows through the gravel bed. On top of this gravel bed, ochre accretes, building into a layer and the Fe is removed by a combination of heterogeneous catalysis in the ochre bed and oxidation in the water column. Vertical down flow means that the size of the treatment system can be greatly reduced compared to conventional systems. The VFR has been developed at Cardiff University through previous lab studies and field trials. Until this project, the VFR has only been applied at net alkaline and net acidic coal mine sites: Taff Merthyr and Ynysarwed respectively (Barnes, 2008, Geroni, 2011). The VFR was shown to be successful at Taff Merthyr in removing Fe(II) at a substantially higher rate of 16 g/m²/d, compared to wetland and settling lagoons. The Fe removal mechanisms were thought to be a combination of oxidation in the water column and heterogeneous catalysis within the ochre bed.

The question of whether the VFR would be effective at treating very low pH metal mine water coincided with the Coal Authority's taking on the responsibility of the abandoned metal mines. AMD from metal mines sets out different challenges from coal mine water at the sites studied in this thesis, such as the pH, which is much lower at the metal mines and the acidity much higher. In coal mine water treatment, oxidation rates and settling rates are the key parameters. In very low pH metal mine water, pH and redox conditions are much further from the ideal in terms of being in the range for least solubility of metals. Removal of metals by precipitation is usually achieved through the addition of chemicals which raise solution pH and precipitate the contaminant metals. One of the key motivations for this thesis was to investigate alternative chemical free methods to treat low pH, multi element mine water. Three potential treatment methods are examined:

- 1) The Vertical Flow Reactor (VFR)
- 2) Electrocoagulation
- 3) Advanced oxidation

These three treatments form two main branches of this thesis, the VFR and electrochemical treatment. The VFR is an entirely passive system which until this thesis, has been used to remove Fe from coal mine discharges. The novelty of the VFR in this thesis is that for the first time a pilot scale VFR was constructed and installed to remove Fe from a low pH mine water (pH 2.9) metal mine site.

In contrast, electrocoagulation (EC), was investigated as a potential method for the removal of Zn from circumneutral mine water and the application of the advanced oxidation process (AOP) was examined as an electrochemical alternative to chemical dosing for removal of Fe from coal mine drainage.

During the course of this thesis, 2 papers and posters in journals and conferences were produced. They are attached in Appendix 5.

2.8 Aims of the Thesis

The following bullet points describe the aims of the thesis. Four different mine waters were used. Potential treatment options designed to tackle specific contaminants associated with each water 'type' are examined.

- To assess the effectiveness of the Vertical Flow Reactor (VFR) at passively removing problematic iron from low pH mine water.
- To determine the removal mechanisms of iron removal in the VFR
- To investigate how effective electrochemical treatment of mine water is by traditional EC methods using sacrificial electrodes on circumneutral mine water for the removal of Zn.
- To determine whether the advanced oxidation (AO) process will accelerate Fe(II) oxidation in the near neutral pH range and to report any promising findings.
- To determine if Zn can be removed by electrocoagulation with iron electrodes.
- To determine whether more Zn can be removed by co-precipitation with Fe than can be removed by adsorption to Fe using electrochemical methods.
- To determine the effectiveness of different electrode materials such as Al and Cu in removing metals from low pH mine water.

3 Literature Review

3.1 Iron Chemistry

3.1.1 Elemental Iron and Iron Speciation

Iron, though it only constitutes 4.7% of the Earth's crust, makes up 30 % of the Earth's total mass, 80% of which is found in the core. It is the fourth most abundant crustal element. Iron is chemically a very versatile element due to its variable oxidation states. Its chemical character allows it to co-ordinate to sulphur, nitrogen and oxygen atoms. It also has the ability to bind with small molecules (Cox, 1995).

Iron (Fe) with the atomic number 28, is a d block element that resides in group 8 of the periodic table above ruthenium (Ru) and Osmium (Os). Iron has characteristics of a transition element. Although the electron structure for these elements is d^6s^2 , Fe can exist in the 0, II and III oxidation state and has valences forming a number of complexes in both the Fe(II) and Fe(III) states (Faure, 1998).

Ferrous iron exists as dissolved Fe(II), as solid Fe(II) or as haem which is Fe complexed with decomposing vegetation. Fe can also exist as a compound, where Fe(II) is bound in the centre of an organic ring called a porphyrin. Ferric Fe exists as dissolved Fe(III) or solid Fe(III) (Hunt, 2003). The form in which the Fe species exist in the natural environment is controlled by pH and redox conditions (Figure 3). The Fe pair can exist side by side, for example, where stratification of lake and river waters means that both aerobic and anaerobic conditions exist (Baird, 1995). This is particularly evident in the warmer seasons where less dense warm air at the surface is close to saturation with respect to dissolved oxygen, so Fe(III) dominates, whilst at the same time, the reduced anaerobic conditions in the colder, more dense layer means that Fe(II) will dominate (Baird, 1995). Also in minerals, ferric and ferrous iron can coexist, such as in copiapite (Bayless and Olyphant, 1993).

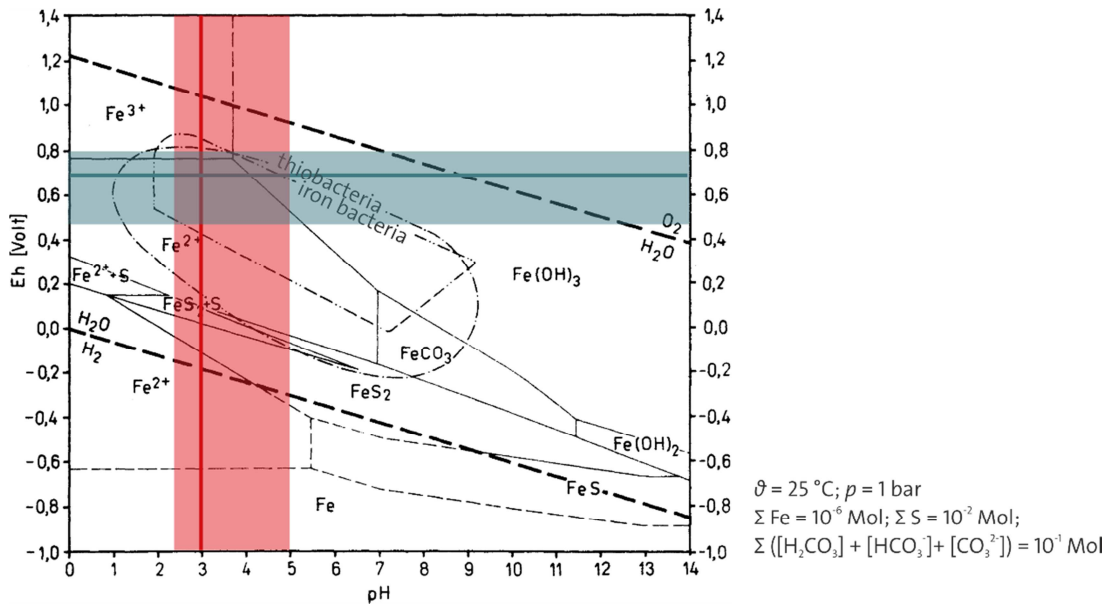


Figure 3: Pourbaix diagram for Fe-species with the pH- E_h -ranges in which thiobacteria and iron bacteria are commonly found (modified from and after Baas Becking et al., 1960, Tischendorf and Ungethüm, 1965). Superimposed are the pH- (red) and E_h -conditions (green) for the Cwm Rheidol Lower Number 9 Adit mine water. Means are given as solid horizontal and vertical lines.

3.1.2 Common Iron minerals

Iron minerals in igneous and metamorphic rocks are the primary source of iron in the aqueous environment. Pyroxenes, amphiboles, biotite and magnetite (silicates and aluminosilicate) have a relatively high iron content (Hem, 1985) which may replace aluminium and magnesium. It is the Fe(III) in the octahedral position which allows for part substitution of other trivalent metals of similar size, which is known as isomorphous substitution. Fe oxides can have other metal cations of similar ionic radii such as Zn(II), Cd(II) or Pb(II) incorporated into their structure (Schwertmann and Cornell, 2000). Iron has borderline lithophilic/chalcophilic properties being common in both sulphide mineral and oxide forms (Cox, 1995). Pyrite (FeS_2) and magnetite (Fe_3O_4) are common minor minerals.

As consequences of the breakdown of these iron bearing rocks by chemical weathering, Fe is mobilized and redistributed. Fe is mainly mobilized as Fe(II) until it reaches oxygenated environments where it exists mainly as Fe(III) oxyhydroxides (Langmuir, 1997). This process has been essential in the chemical evolution of the Earth's surface. The primitive atmosphere had little O_2 and sedimentary rocks containing Fe(II) were formed. As photosynthesis developed, Fe

exposed to the atmosphere was oxidised to Fe(III), thus explaining large deposits of oxide minerals such as haematite (Fe_2O_3) and magnetite (Fe_3O_4) which have been a primary source of Fe since 1200BC (Cox, 1995).

Table 1: The Formulae and names of the major Iron Oxides and Oxide Hydroxides (Schwertmann and Cornell, 2000).

Oxyhydroxides		Oxides	
$\alpha\text{-FeOOH}$	Goethite	$\text{Fe}_5\text{HO}_8 \cdot 4\text{H}_2\text{O}$	Ferrihydrite
$\beta\text{-FeOOH}$	Akaganeite	$\alpha\text{-Fe}_2\text{O}_3$	Hematite
$\gamma\text{-FeOOH}$	Lepidocrocite	$\gamma\text{-Fe}_2\text{O}_3$	Maghemite
$\delta\text{-FeOOH}$	Feroxyhyte	Fe_3O_4	Magnetite

Fe oxides can to some extent be classified by colour, which varies in accordance with structure and Fe concentration and Fe(II) Fe(III) ratio (Cox, 1995) as well as particle size and cation substitution (Schwertmann and Cornell, 2000). Colours of iron minerals include purple, black, red, brown, orange, yellow and green/blue. Hue and chroma can be matched against a colour chart classification system such as the Munsell and CIE-Lab types which have been developed using chroma meter measurements of 265 synthetic samples (Schwertmann and Cornell, 2000).

In addition, Fe is an important source of colour in rocks and soils (Fitzpatrick and Self, 1997). In simple terms, where Fe(III) dominates, the minerals range from yellow to brown but when there are mixtures of Fe(II) and Fe(III) an almost black mineral is produced (Cox, 1995).

The extraction of iron from its oxides is a process that has a high energy demand; for this reason, the iron is a desirable element for recycling (Cox, 1995). All Fe(III) oxides have a an octahedron as their basic structural unit. According to Schwertmann and Cornell (2000), “each Fe atom is surrounded by either combinations of O and OH ions or by six O atoms which form layers, which are either approximately cubic close packed (ccp) as in lepidocrocite and maghemite and are termed α phases or hexagonally close packed (hcp) as in goethite and hematite which termed γ phases. In both ccp and hcp structures, tetrahedral interstices exist between three O and OH in one plane and the anion in the above plane”. Out of the fifteen iron oxides, hydroxides and oxide hydroxides currently known, eight are considered the most important (Table 1). With

the exception of ferrihydrite, and ferrioxalate, these compounds can be well crystallised.

Understanding the crystalline structure of the different mineral phases is important, because it allows us to understand both the impacts that individual precipitates might have on the environment and their properties as a remediation material. For instance, despite the detrimental impact that ochres have on aquatic systems, Fe minerals can be used to remove contaminant anion and cations by a variety of mechanisms: substitution, adsorption, co-precipitation, chelation and complexation reactions (Farley et al., 1985, Stumm and Morgan, 1996). The extent at which removal of contaminants can be achieved is dependent on the mineral phase present which in turn, is dictated by the synergistic environmental conditions.

The term hydrous ferric oxide (HFO) is used to describe the amorphous, ferric or iron oxyhydroxides which are formed upon rapid hydrolysis of ferric iron solutions. They can be produced in the laboratory at temperatures of 20–30 °C. When the resulting precipitate is analysed by XRD, peaks are not always definitive, except on occasions when a few broad reflections indicate that there is some crystalline character, not dissimilar to the naturally formed iron oxide ferrihydrite (Dzombak and Morel, 1990). As precipitated particles coagulate, they form a very porous and therefore hydrated, poorly ordered structured gel-like sludge. Ageing of HFO transforms it to a crystalline iron oxide such as goethite, the rate at which this occurs is dependent on the Fe(III) concentration, pH and temperature. The higher the values, the quicker the crystal forms. As an example, between 2 and 10% of HFO is transformed to goethite after 12–15 days (Crosby et al., 1983).

Usually, the growth rate of the crystallization of HFO can be hours to days in water with several mg/kg of dissolved iron (Langmuir, 1997). Growth rate of a crystalline phase detectable by either x-ray diffraction or SEM increases with increase in temperature. The proportion of Fe(II) relative to temperature is an important parameter for the crystallization, more so than the proportion of Fe(III) present (Langmuir, 1997).

The potential use and metal removal properties of common Fe minerals are well documented in the literature (Dzombak and Morel, 1990, Fernandez-Martinez et al., 2010, Sahoo et al., 2012, Valente et al., 2012). Speciation of iron and sulphate in AMD relates to the crystalline structure and definition of the Fe-SO₄²⁻ minerals, where studies have shown that the more crystalline goethite incorporates higher ratios of sulphate than the poorly formed ferrihydrite and schwertmannite minerals. In addition, age is an important factor that influences the chemical composition and crystal structure of the precipitate (Majzlan and Myneni, 2004, Peretyazhko et al., 2009).

The group of Fe(II, III) hydroxy salts are the green rusts which have an essential structural component, although not oxide/hydroxides in a strict sense (Schwertmann and Cornell, 2000). These oxyhydroxyl salts have been shown to accelerate the removal of inorganic contaminants from mine water by a combination of surface catalysis reactions and alteration of the redox conditions, thus altering the oxidation state and mobility of metal ions. Bearcock et al. (2011) conducted batch experiments adding natural green rusts to mine water with 70, 80 and 8.5 mg/L of Al, Cu, Fe from low pH mine water and found that metals were completely removed within one hour contact time.

3.1.3 Fe Oxides and Hydroxides in AMD

Various authors describe iron precipitates in mine drainage as being a “Variety of poorly ordered oxides and hydroxysulphates which are effective sorbents of trace metals and oxyanions” (Gagliano et al., 2004). Water quality in AMD, such as the amount of acidity developed is determined by the Fe(III) precipitates that form (Acero et al., 2006, Dold and Fontboté, 2001). The main Fe(III) minerals that are usually related to AMD are jarosite [KFe₃(SO₄)₂(OH)₆], which forms in pH <3 with high sulphate concentrations. Goethite (α-FeOOH) and ferrihydrite (Fe₅OH₈·4H₂O) precipitate at circumneutral pH (Schwertmann and Carlson, 2005). The most common Fe mineral that forms by direct precipitation from pH 3–4 water and sulphate concentrations between 1000 and 3000 mg/L is schwertmannite, a ferric oxyhydroxysulphate which is poorly crystalline and therefore difficult to characterise (Bigham et al., 1994). Schwertmannite has the ideal formula [Fe₈O₈(OH)_{4.8}(SO₄)_{1.6}] (Bigham and Nordstrom, 2000, Bigham et al., 1996, Gagliano et al., 2004). In fact, its crystalline structure has not yet been

fully determined. However, Fernandez-Martinez et al. (2010) have proposed a structure similar to that of ankageneite where there is a deformed frame of iron octahedra. Their simulations aim to provide knowledge of the position of the sulphates in the structure which is thought to help in understanding the scavenging properties that schwertmannite has in its ability to harness exchange processes with trace element contaminants and oxyanions. In terms of precipitation from mine water, schwertmannite is formed as large quantities of nanoparticulate Fe(III) when bacterially mediated oxidation of Fe(II) is exposed to the atmosphere.

Schwertmannite is a metastable structure, which means that it transforms to the more crystalline phases such as goethite within weeks to months (Acero et al., 2006, Regenspurg et al., 2004). The geochemical stability of iron precipitates in mine drainage is important, because transformations of poorly formed ferrihydrite and schwertmannite to more stable forms, such as goethite, means changes in the efficiency as contaminant sorbents (Bigham et al., 1996).

3.1.4 Iron Solubility

Oxyhydroxides are amphoteric with the solubility being a function of pH. A decrease in solubility of up to 10^7 times occurs between the amorphous and well crystalline phase such as goethite or hematite. Between pH 5–10, Fe(III) concentrations will be at or below detection limit (Langmuir, 1997). That said, in surface and ground waters, suspended colloidal Fe oxy hydroxides can exist between pH 3–8. Colloidal suspension can be destabilized by the adsorption of specific species in conditions where strong electrolyte concentrations give rise to an increased ionic strength.

Colloids are least stable and therefore likely to agglomerate or flocculate at a pH where the surface charge of the oxy hydroxide is uncharged. This is called the point of zero net proton charge (PZNPC), which is pH 8 (pH of minimum solubility) for ferric hydroxides in pure water. At the point of zero charge, the particles do not repel each other. The charge on the particle surface has a net positive charge below this pH where the surface is OH⁻ deficient above pH 8, surface has an excess of OH⁻ and is therefore negative. The colloids are therefore most sta-

ble in solutions where the charge is furthest from PZNPC and the repulsion forces are mutual (Langmuir, 1997).

The oxidation state of Fe is important in terms of the effects of the solubility. The majority of the iron in the Earth's crust is present as Fe(II) but is rapidly oxidised at the Earth's surface to Fe(III) which is very insoluble in water at neutral conditions. Below pH 3 to 4, dissolved Fe(III) and Fe(III) inorganic complexes are mobile in oxidised surface waters and sediments. Fe(III) ferric organic complexes are also mobile in surface waters and soils between pH 5 and 6. Fe²⁺ as the free ion can occur when conditions are reducing and the pH is below 7–8 (Langmuir, 1997). Iron is much more soluble under reducing conditions where it is mobile, usually as the dissolved uncomplexed Fe²⁺ form at pH 7–8.

3.1.5 Iron Toxicity in the Aqueous Environment

Fe released in natural waters can have a detrimental effect on the ecology, as such, the maximum permitted concentration of the EQS (environmental quality standards) for Fe in surface rivers and streams is 1 mg/L (2006/11/EC). This is a challenging target for ferruginous mine water discharges that can exceed these limits by 10–1000's mg/L. When low pH ferrous rich mine water enters watercourses, the oxygen concentrations in the water are depleted while ferrous Fe(II) progressively oxidises to ferric iron Fe(III). Fe ochrous precipitates slowly settle out and coat the vegetation in stream and river beds. Fine flocs of Fe precipitates remain suspended for long periods of time and reduce light penetration causing interference with photosynthesis. Besides this, Fe precipitates can encrust rocks and stones, covering all benthic biota (Kelly, 1988). Consequently, ochre can have a devastating effect on aquatic ecosystems. Periphyton and benthic invertebrate abundances in rivers are greatly reduced where ochre precipitates are present (McKnight and Feder, 1984). The fine grained silty texture of iron ochres chokes aquatic vegetation which becomes chlorotic, weak and unhealthy. This can be clearly seen along sections of rivers that are impacted by AMD (Figure 4). One of the challenges is the time scales for which the impacts of AMD can persist; mine water can continue to pollute for many decades.

Untreated AMD can cause stream pollution in a number of ways and the acidity is harmful not only to the ecology but accelerates the corrosion process of

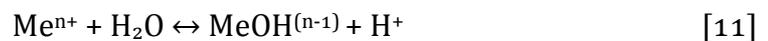
manmade structures, concrete in dams and bridge abutments for example (Franco and Balouskus, 1974).



Figure 4: Discharge of mine water from the abandoned Ynysarwed colliery into the River Neath (courtesy of Ch. Wolkersdorfer).

3.1.6 pH of Hydrolysis

In geochemistry, hydrolysis is a term used to describe reactions in which either (or both) of the O-H bonds in water are broken (Gill, 1996). This happens because metal ions in water behave as Lewis acids and are free to accept electrons whilst water behaves as Lewis base and is willing to share its two unshared oxygen-associated pair of electrons. As such, strong H₂O metal interactions dissociate the H⁺ on the water molecule producing lower pH water (reaction 11)



The degree of dissociation of water with cation (Meⁿ⁺) is determined by the metal hydrolysis constant found in published data (Evangelou, 1998). The larger the hydrolysis constant, the stronger the interaction between H₂O and the metal, thus the lower the solution pH will become. Free metal cations in aqueous environments form aquo complexes and are therefore hydrated. Precipitation of metal cations in aqueous solutions occurs when the coordinated water molecules exchange for preferred ligands of free metal ions. Hydrolysis reactions are important in mine water treatment where elements of intermediate ionic potential such as Fe(III) or Al are soluble in fairly acidic conditions, and mixing

with a less acidic solution (neutralisation) will cause precipitation of metal hydroxides as a result of hydrolysis (Gill, 1996, Langmuir, 1997). Consequently, cations released into solution combine with the OH^- to form a parental base. This removal of OH^- from solution causes the solution to become more acidic and explains, how the hydroxide precipitation is directly related to the hydroxide ion concentration (pH). However, as shown, the pH of hydrolysis of metal hydroxides varies with metal species (Table 2) and the pH required to achieve minimum solubility also changes with ionic strength and the hydrolysed species (Levinson, 1974, Stumm and Morgan, 1996).

Table 2: pH of hydrolysis of ions from dilute solution (from Levinson 1974).

Ion	pH	Ion	pH
Fe^{3+}	2.0	Cd^{2+}	6.7
Zr^{4+}	2.0	Ni^{2+}	6.7
Sn^{2+}	2.0	Co^{2+}	6.8
Ce^{4+}	2.7	Y^{3+}	6.8
Hg^+	3.0	Sm^{3+}	6.8
In^{3+}	3.4	N^{2+}	7.0
Th^{4+}	3.5	Nd^{3+}	7.0
Al^{3+}	4.1	Pr^{3+}	7.1
U^{6+}	4.2	Hg^{2+}	7.3
Cr^{3+}	5.3	Ce^{3+}	7.4
Cu^{2+}	5.3	La^{3+}	8.4
Fe^{2+}	5.5	Ag^+	7.5–8
Be^{2+}	5.7	Mn^{2+}	8.5–8.8
Pb^{2+}	6.0	Mg^{2+}	10.5

These values of pH of hydrolysis as well as the surface charge, specified by the pH of the point of zero charge, also exhibit different solubilities at different pH values. The lowest solubility (as pH) for metals is at the lowest point in the u-shaped curve, which corresponds with the sum of all hydrolysed species of that metal (see Figure 2). The solubility of metal hydroxide as a function of the pH means it can be difficult to precipitate two metals as hydroxides simultaneously (Evangelou, 1998). Minimum solubility of a metal hydroxide can be affected by other constituents in the water (Metcalf & Eddy, 2002). The free hydrogen ion H^+ is considered to be the barest of metal ions (Faure, 1998, Stumm and Morgan, 1996).

3.2 Zinc Chemistry

3.2.1 Zinc in the Aqueous Environment

Zinc (Zn), atomic number 30, is a transition element that resides in group 12 of the periodic table of elements. Elements in this group have the electron configuration $d^{10}s^2$ which form the +2 ions (Faure, 1998).

Solubility curves for metal ions (relevant to this study 'zinc' and 'iron') have been published by several authors (Cravotta, 2008, Langmuir, 1997, Nordstrom and Alpers, 1999, Stumm and Morgan, 1996) and all of them are consistent with each other in representing the relationship between the influence of hydrolysis products on the solubility of metal hydroxides over a broad pH range. Taking one example, Nordstrom and Alpers (1999) clearly showed the amphoteric nature of zinc and iron and their pH dependence of solubility. This is important in understanding the complex behaviour of soluble metal ions and control of contaminant mobility in the natural environment. Published solubility curves often show solubility of various metal hydroxides on the same graph, providing a quick reference to assess the pH at which these metals or metal complexes are most or least soluble. Whilst these theoretical values are a critical step in understanding metal solubility, it is important to understand the other reactions that take place when Fe is introduced or present in the system. Acid and hydroxide titrations to study the solubility of Zn in the presence of iron showed that combining charged species has a substantial effect on concentrations of metals in the system. This behaviour is due to a combination of adsorption and co-precipitation reactions. In the presence of Fe, other charged species are caught up (trapped) in the Fe precipitation phase, as they are adsorbed to the surface of the Fe particle (Noubactep, 2012).

Care needs to be taken with the term co-precipitation in the Zn and Fe system as it does not necessarily mean that the Zn is simultaneously precipitating with the iron. As Dzombak and Morel (1990, p 260 figure 8.8) showed, 100% adsorption of 10^{-7} mol/L Zn is reached at 10^{-3} mol/L of hydrous ferric oxide (HFO) at pH 7.5. The graph also indicates that there is only 30% less adsorption at much higher ion strengths of the solution. From the literature, co-precipitation (by entrapping (semi-)metals during Fe precipitation) and adsorption onto the sur-

face of HFO are one of the key Zn removal mechanisms. Reliable and comprehensive databases of thermodynamic values for metal ion complexes means that reactions can be modelled using geochemical modelling software such as PHREEQC (Cravotta 2008; Parkhurst 2013; Plummer et al. 1979) to predict the concentrations and behaviour of metals in complex multi-metal contaminated waters.

3.2.2 Common Zinc Minerals

Zinc is the 23rd most abundant element within the Earth's crust. According to Hem (1985), Zn can be found in most natural waters at concentrations up to 1 µg L⁻¹. Because Zn is a major constituent of the ore mineral sphalerite (ZnS), Zn concentrations in mine impacted waters can be several orders of magnitude higher. As described, Zn is fairly soluble over a relatively broad pH range (Florence, 1980) with a minimum between pH 9 and 11 (Figure 2). Zn can be present as the free ion Zn²⁺ or combined with sulphide, oxide and carbonate complexes (Kelly, 1988), as can be seen in Figure 5. Elevated concentrations of Zn can therefore be found in both AMD and neutral mine waters. Because Zn²⁺ in aqueous solutions is extremely ecotoxic, it can negatively affect plants and invertebrates as well as vertebrate fish. This ecotoxicological behaviour in even micromolar amounts of Zn²⁺ is described by the Free Ion Activity Model (Smith and Huyck, 1999). An example by Muysen et al. (2006) showed that just 6 µmol killed 93% of all *Daphnia* in water. Studies in the UK have shown that the concentrations of Zn found in aquatic organisms such as the free living *Trichoptera* larvae, followed the concentrations found in mine water impacted rivers (Brown, 1977).

Zn toxicity to some freshwater fish species is considered to be affected by water hardness as well as pH. Therefore, Zn is listed as a priority substance under list II of the EU dangerous substances directive (76/464/EEC) and (2006/11/EC), and has imperative water quality standards that vary with water hardness from between 0.008 –75 mg/L. Yet, Zn in trace quantities is essential for the health of humans and animals (Sanders et al., 1999) and the recommended daily intake for zinc in humans is 15 mg (Fosmire, 1990). Manifestations of toxicity symptoms at high intake (100–300 mg d⁻¹) include nausea, vomiting, epigastric pain, lethargy and fatigue (Bothwell et al., 2003). Even for lower concentrations of

intake, reports of negatively affecting the cholesterol level or interferences with the Cu and Fe metabolism are known. Users of Zn supplements should be aware of this (Fosmire, 1990).

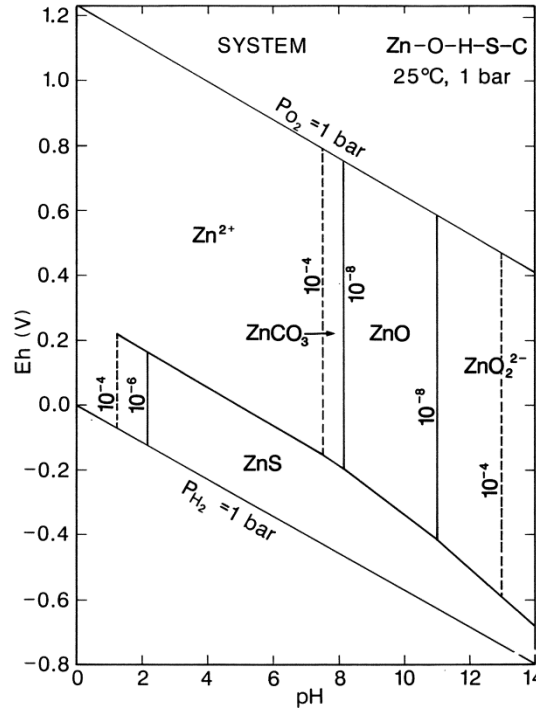


Figure 5: Eh-pH diagram for the system Zn-O₂-CO₂-S-H₂O; activities: Zn = 10⁻⁶ and 10⁻⁴, C = 10⁻³ and S = 10⁻³ (from Brookins, 1988).

3.3 Metal Removal by Adsorption and Co-precipitation

3.3.1 Adsorption

A solid surface of iron oxide exposed to a solution becomes surrounded by a layer of tightly bound water molecules to form a solvation shell (International Union of Pure and Applied Chemistry, 2012). This layer may also incorporate some solute ions and molecules that are being held near or within this shell by electrostatic forces. The charge that develops on the surface of the hydrous oxide, which attracts oppositely charged ions, is the result of equilibrium reactions at the oxide surface and not within the solid (Dzombak and Morel, 1990). The removal or exchange of solute species with one another, which does not substantially affect the solid's surface properties, is known as adsorption and implies that these processes occur at the water-solid interface (Hem, 1985). Consequently, metals such as Zn, Cu, Cd which are usually very mobile in slightly acidic solution can become concentrated in ochre precipitates (Dyck, 1968,

Langmuir, 1997). Because of their characteristics, Schwertmann and Cornell (2000) describe precipitating ochres as having the largest sorption capacity of any material in the environment. Some of those factors determining sorption and desorption reactions are the concentration of the metals in solution, pH and the presence of organic material.

Modelling adsorption capacities of hydrous oxides has developed in more recent years (Acero et al., 2006, Dzombak and Morel, 1987, Dzombak and Morel, 1990, Rhee and Dzombak, 1998, Stumm and Morgan, 1996). During earlier studies, Dyck (1968) found that it was possible to quantitatively represent the adsorption of Ag^+ from very dilute solutions onto freshly precipitated hydrous ferric oxides using the Freundlich adsorption equation (Freundlich Isotherm):

$$\frac{x}{M} = kC^{\frac{1}{n}} \quad [12]$$

x/M is the ratio of the amount of silver and iron in the precipitate at the equilibrium adsorbent concentration C , k the adsorption constant, and n an empirical constant to fit the results to the equation. Dyck (1968) constructed a series of adsorption isotherms which clearly showed the influence of pH on the amount of Ag^+ adsorbed, thus proving the pH dependence of metal ion adsorption concentrations.

Freundlich's adsorption equation was successfully applied and therefore in agreement with the findings because this was a simple system. However, there are a number of parameters that need to be considered in calculating adsorption capacities of solid surfaces and this has led to the development of surface complexation modelling. In order to gain understanding of the sorption mechanisms, a great deal of effort in developing theoretical models of the oxide/water interface resulting in a unified description of surface complexation modelling and provision of a sorption model that is generally applicable (Dzombak and Morel, 1987, Dzombak and Morel, 1990). This generalised two layer model incorporates the diffuse layer model (Stumm et al., 1970), the multistate model (Benjamin and Leckie, 1981) and the surface precipitation model (Farley et al., 1985). It is however important to realise that the two-layer sorption model presented by Dzombak and Morel (1990) is designed to fit certain kinds of experi-

mental data. A thorough understanding of the constraints on data is necessary when considering the validity for use in surface complexation modelling.

3.3.2 Co-precipitation

Reactions involving dissolution or precipitation of a solid ultimately occur at the interface between the solid and solution phases. It is known that as hydrous iron and manganese oxides precipitate in alkali or oxidising conditions and have the ability to incorporate (by co-precipitation) other elements that would normally be unaffected by changes in E_h - and pH-conditions (Levinson, 1974).

The terms adsorption and co-precipitation are closely linked. As described above, adsorption is the process whereby cations and anions are attached to the hydroxyl groups of the hydrated molecules but are not incorporated into the structure as in co-precipitation. Karthikeyan et al. (1997) pointed out that a lot of publications about metal adsorption to HFO exist, while there is a lack of quantitative adsorption vs. co-precipitation comparisons. These authors conducted experiments to study the mechanisms of adsorption and co-precipitation and how they govern Cu solubility at less than ppm level. In their experiments they added Cu before and after the precipitation of HFO and compared the concentrations of dissolved Cu in the final solutions. Adding the Cu after precipitation of HFO resulted in adsorption reactions whereas adding Cu before HFO precipitation caused co-precipitation of Cu with HFO. Consequently, the experiments showed that more Cu was incorporated into the HFO when added before the precipitation phase and they concluded that this was most likely the result of a number of mechanisms. In the context of their work they defined co-precipitation as:

“the simultaneous removal of a foreign ion (e.g., Cu^{2+}) during the formation of a primary metal precipitate such as HFO or HAO (hydrous aluminium oxide) Co-precipitation can entail (a) Cu adsorption onto freshly formed hydrous oxide colloids, (b) solid solution formation by Cu incorporation into the hydrous oxide lattice, (c) mechanical enclosure of Cu-containing solution by the precipitate, or (d) a combination of these processes” (Karthikeyan et al., 1997).

However, the earlier works by Dyck (1967) looked at the adsorption and co-precipitation of silver with HFO and found that under equilibrium conditions, the amounts adsorbed/co-precipitated were identical.

3.4 Source Control

Contaminated mine water discharges occur when ore minerals are exposed to oxygen and water. Therefore flooding and sealing the mine could be considered a source control option (Fernández-Rubio et al., 1987). Dissolved oxygen concentration would be rapidly depleted by microbial activity and oxidising reactions and the system stabilised. The challenge is the common scarcity of knowledge of the underground working at historic mine sites. Since the main period of mining in the UK was between 1840 and 1920, many thousands of sites are unmapped. Voluntary registration of abandoned mine plans was not encouraged until 1840 when the first Government Mining Records office was established in London. Plans following closure of mines were not officially required to be deposited by the secretary of state until 1872 and even then, only the boundaries had to be documented. Yet this requirement applied only if the mine had more than twelve people working below ground (British Geological Survey, 2014). The British Geological Survey (BGS) have been working to identify previously unmapped mine sites across the UK and at the time of writing this thesis, 3000 historic sites had been found. Therefore, source control under these circumstances would be rather difficult, as the extent of the mining below ground or the locality of the shafts is largely unknown, implying that there can be no guarantee that the mine is completely sealed.

Source control is not limited to the underground workings and discharges from the mine adits. Surface waters can be diverted in order to help reduce the amount of water entering the mine (Skousen et al., 2000). Tailings are usually kept below water to prevent contact with oxygen. Waste rock piles are also a major source of diffuse pollution. Exposure to the atmosphere and weathering causes the metals in the waste tips to leach into nearby water courses and percolate down through the sediments below and is therefore a potential risk for contaminating ground water. Capping of such areas with soil or organic layer helps to reduce this risk by limiting the diffusion of oxygen (Johnson and Hallberg, 2005). In addition, capping of the waste tips can also help prevent the

spread of the contaminated fines material that is easily transported by wind to the surrounding areas (Herbert Jr, 1999). To prevent AMD from forming at source is very difficult; consequently, the only way to control pollution coming from abandoned mines is often to use treatment technologies that clean the water prior to discharge to water courses. The type of treatment option used depends on many factors. Besides the site specific criteria such as inflow water chemistry, flow rate, discharge consent, topography and land availability, the cost, operations management, waste disposal, access and security are but a few of the critical measures that contribute to the overall success of a mine water treatment system (Coulton et al., 2003).

3.5 Passive Treatment Options

3.5.1 Description of Passive Treatment

Passive mine water treatment technology was first published in Hedin et al. (1994) and has been improved since then. Yet, the first work relating to passive water treatment was conducted by Kickuth (1977) and Seidel (1996) using wetlands to treat municipal water from Othfresen/Germany. By chance this system also treated mine water from the Ida-Bismarck mine (Wolkersdorfer, 2008, Wolkersdorfer, 2013) and might therefore be considered the first artificial passive mine water treatment system.

Passive treatment can broadly be described as being a natural self-purification-system (Younger et al., 2002). Passive treatment got its name because it uses only naturally available energy sources (gravity, microbial metabolic energy and photosynthesis) as methods for the deliberate improvement of water quality (PIRAMID Consortium, 2003, Younger et al., 2002) without the need for constant human intervention (Nkwonta and Ochieng, 2009). This makes passive treatment a favourable option due to low initial set up cost, use of non-hazardous materials and low maintenance requirements (Walton-Day, 2003); an important consideration given that abandoned mines can continue to pollute for tens to hundreds of years (Benner et al., 1999, Leblanc et al., 2000, Razowska-Jaworek et al., 2008)

A passive system may consist of a number of stages or cells through which metal rich or acidic waters are passed. These cells, which may be linked to operate

in series, parallel or both are each designed to treat a different aspect of the water chemistry (Walton-Day, 2003). In artificial wetlands for example, the combined effect of organic matter, bacteria and algae removes metals by filtration, adsorbance and precipitation reactions. Those combined effects also reduce the water's acidity. In addition, Reducing-and-Alkalinity Producing Systems (RAPS) and limestone filter beds can be used to alter the redox condition thus increasing solution pH to reduce contaminant mobility. This process encourages precipitation of Fe (oxy) hydroxides which in turn causes the co-precipitation or sorption of other contaminant metal ions (Blowes et al., 2003). Alternatively, cells can also be designed as closed systems to create anoxic conditions under which bacterial sulphate reduction promotes the precipitation of insoluble metal sulphides effectively removing them from solution. Yet, there are limitations concerning the quantity of water or metal loading that the system can effectively cope with. Such systems are commonly designed for the treatment of Fe rich waters and are ineffective in removing Pb, Cd and Zn from circumneutral waters. Without the use of active chemical dosing, alkaline channels or drains, the pH cannot be raised sufficiently enough to cause precipitation of these contaminants.

3.5.2 Anoxic Limestone Drains (ALD)

Anoxic limestone drains consist of trenched beds filled with crushed limestone aggregate through which AMD is channelled. Limestone (CaCO_3) is usually a cheap material that dissolves when in contact with AMD. Dissolution of limestone into AMD works two fold in that it neutralises proton acidity and adds bicarbonate alkalinity to the system. In turn, this raises the pH of the water and precipitates out metals that would otherwise remain in solution at the pre-treated 'lower' pH (Brodie et al., 1991, Hedin et al., 1991, Skousen, 1991a). The problem with limestone dissolution is that precipitation of Fe and Mn rapidly armours the limestone, passivating the system if not kept in anoxic conditions. To prevent armouring from Fe and Mn hydroxides, the limestone channels are buried below ground thus keeping the system anoxic; Fe and Mn are consequently retained in their reduced state (Skousen, 1991a). Maintaining a closed system also prevents degassing of CO_2 to the atmosphere which helps in the process, because dissolved CO_2 adds more bicarbonate alkalinity and causes a

higher pH in the water than if it is allowed to equilibrate with the atmosphere (Cravotta and Trahan, 1999, Kirby et al., 2009, Younger et al., 2002).

If the mine water contains dissolved Fe(III) or is already oxidised, the pores of limestone aggregates will eventually clog with Fe(OH)₃ or MnO because oxidation and hydrolysis of Fe will be likely to occur in water with dissolved O₂ (DO) concentrations over 1 mg/L. ALDs are not considered appropriate unless the inflow water is reduced, which means having less than 1 mg/L DO concentration (Brodie et al., 1991). In addition, for maximum alkalinity generation, a minimum retention time of 14 h is required (Younger et al., 2002).

Care needs to be taken when discussing failure of ALDs due to clogging. Younger et al. (2002) describes cases in which ALDs failed to treat water after just 6 months because the first 10–15 % of the ALD had armoured. If this portion were to be replaced and maintained regularly the system would continue to work. The point being made is that the system might not necessarily be considered passive if frequent maintenance is required.

3.5.3 Oxidic Limestone Drains (OLD)

Oxidic limestone drains are also known as open channel limestone reactors (OCLRs), as an alternative to ALD and RAPS where water contains moderate concentrations of O₂, Fe³⁺ or Al³⁺ (Cravotta, 1998). The OLD is an open channel alternative to the ALD for treating water with higher DO concentrations. This system also harnesses the higher alkalinity produced by closed system CaCO₃ kinetics (Cravotta, 2007). The theory behind OLDs is that metal hydroxide precipitation is encouraged prior to the contact period with the limestone in the open channel (Cravotta, 2010). This can be accepted as long as the precipitated particles are kept in suspension by controlling the flow velocity (> 0.1 m/min), which prevents staining from ochre precipitates. Yet the residence time must be below 3 h (Cravotta, 2007, Cravotta and Trahan, 1999). The metal hydroxides are carried through to either settling ponds or aerobic wetlands where they are allowed to settle or are filtered respectively. Although it was found that armouring does still occur, acid neutralizing capacity is merely hindered rather than compromised altogether (Ziemkiewicz et al., 1997) because the initial rate of calcite dissolution is much higher than in ALDs (Cravotta and Trahan, 1999).

This system might have applications in some situations; Cwm Rheidol for example where the AMD is already oxidised and the topography lends itself to higher flow velocities being achieved. Besides retention time differences between OLDs and ALDs, which result in the minimum flow velocities required for OLD systems, the only other difference in design criteria is the water quality. OLD's are suited to water types that are saturated with respect of DO and with moderate concentrations of Fe(III) (10–20 mg/L) and Al(III) and a total acidity of <90 mg/L as CaCO₃ (Younger et al., 2002).

3.5.4 Open Limestone Channels (OLC)

Whilst passive treatment by ALDs and constructed wetlands have been successful in treating AMD, both these methods require large areas of land to fulfil the required residence times, in addition, wetlands are only applicable to mildly acidic water with relatively low flow rates and there are of course situations where suitable land areas are restricted. As described above, ALDs operate in such a way that the precipitation of ferric hydroxide is suppressed until after the acidity is neutralised under anoxic conditions to prevent armouring of the neutralising material (limestone). However, extensive studies by Pearson and McDonnell (1974) showed that dissolution rates of limestone diminish to 1/5th of unarmoured limestone. The rate of limestone dissolution under AMD loading can be quantified and so open limestone channels are channels filled with limestone that are open to the atmosphere and can be applied to treat AMD under certain conditions. Open limestone channels must be long enough and the amount of limestone required can be estimated based on the work of Ziemkiewicz et al. (1994).

3.5.5 Reducing and Alkalinity Producing Systems (RAPS)

Originally termed “Successive and Alkalinity Producing Systems” (Kepler and McCleary, 1994), abbreviated to SAPS, “Reducing and Alkalinity Producing Systems” (RAPS) are constructed to remediate acidic mine drainage by means of a limestone bed beneath an organic substrate that is covered by a layer of water (Younger, 2000). The water layer is required to be of a specific depth in order to maintain a constant driving head for gravity fed down flow through the treatment bed (Younger et al., 2002). However, the RAPS systems require less land

than traditional wetlands. The compost layer provides an energy source for microbes that consume the dissolved oxygen to maintain a reducing environment for bacterial sulphate reduction (BSR) to occur. The principal of BSR aids in a number of ways: by keeping the system anoxic, precipitation of sulphide and also an increase in alkalinity by dissolution due to the increased pressure of CO₂ released by the bacteria (Johnson and Hallberg, 2005, Matthies et al., 2012). Long term performance of RAPS systems has been reported by Demchak et al. (2001) for a number of sites in Pennsylvania. At the Howe Bridge site no decrease in treatment performance over a six year period was observed and the authors state that construction cost the RAPS was the equivalent to seven years worth of dosing with NaOH. Based on their observations the authors prompted certain construction recommendations such as the need to refresh or replace the compost occasionally. They also stated that the compost layer should have a minimum depth of 50 cm to prevent the formation of deeply oxidised zones within the compost resulting from preferential flow paths in a compost layer which is too thin. Other studies around this time (early 2000) have reported performance inconsistencies from the influence of variation in system design and influent chemistry (Rose and Dietz, 2002).

More recent studies by Matthies et al. (2012) suggest that BSR does not contribute as much as previously thought. Her work concludes that the Fe oxidation and hydrolysis reactions are responsible for the generation of acidity, and the overall reduction of metals concentrations occurs by precipitation of metal hydroxides deeper in the sediments by means of proton neutralisation from the dissolution of calcite.

3.5.6 Constructed Wetlands

Currently, the most common passive treatment systems are constructed wetlands having achieved 'proven technology' recognition in most areas of the world due to their widespread success in treating net alkaline mine water where the main contaminant of concern is Fe (PIRAMID Consortium, 2003, Younger et al., 2002). This success of wetland systems is in part a result of the specific design criteria that can be referenced in order to minimise the risk of failure. If the guidelines are followed then the system will usually work. These systems are also favoured to active treatment where applicable as they provide

an effective treatment for the removal of metals for comparably low initial capital cost and with low long term operating costs as well as low energy demand compared to that of conventional methods such as chemical dosing (Sheoran and Sheoran, 2006). But life cycle cost is not fully appreciated yet.

3.5.7 Aerobic Wetlands

Aerobic wetlands are surface flow wetlands that are relatively shallow and work by providing an oxidising environment in which the oxidation of Fe(II) and the subsequent hydrolysis of Fe(III) produces acidity. This release of protons that follows hydrolysis precipitation reactions deems aerobic wetlands only suitable for net-alkaline drainage. If used for the purpose to treat net-acidic mine water, these reactions would cause a drop in pH to a value usually <5 in which metals will dissolve and therefore be re-mobilised (Younger et al., 2002). In addition to Fe, Mn has also been reported as being effectively removed from aerobic wetlands. The presence of MnO_2 and FeOOH in aerobic wetlands acts as a catalyst for the oxidation and precipitation of Mn(II) from solution by providing adsorption surfaces for the catalysis of the Mn(II) oxidation. This reaction is considered to be the main removal mechanism over co-precipitation reactions occurring during oxidation of Fe(II) to solid FeOOH particulates for removal of Mn (Hedin et al., 1994).

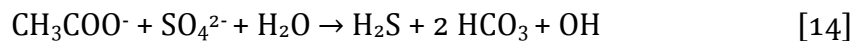
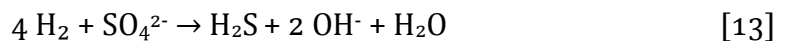
The main function of the reeds is to regulate the flow of water through the system, prevent channelling and support the filtering of ochre particles to aid in the sedimentation of precipitated metals. Where the wetland is treating a flow with Fe concentrations around 1 mg/L, the uptake of metal by the reeds themselves can be a contributing factor to the remediation process (Younger et al., 2002), yet the process is usually not of significance in the system. Those aforementioned behaviours have led to wetlands also being constructed as final polishing steps for low metal concentrations such is the case at the Ynysarwed coal mine water treatment system, where the bulk of the Fe is removed by aeration, chemical dosing and clarification. In the final step, the discharge is then sent through a wetland to filter fine particles (Brown et al., 2002).

Wetlands often require a large land-take but reed beds can provide an aesthetically pleasing image of a mine water treatment system whilst providing good

wildlife habitats (Younger et al., 2002). Yet, wetlands are not considered suitable treatment for discharges where more potentially toxic elements such as As and Cd might be present. Other metals such as Zn and Cu usually show poor removal rates in aerobic wetlands (PIRAMID Consortium, 2003).

3.5.8 Anaerobic Wetlands

Anaerobic wetlands can be used to treat net acidic mine water. They are constructed so that the contaminated water flows about 1 m deep through a thick organic anoxic substrate. This substrate, which can be formed from organic waste such as manure, sawdust or mushroom compost, provides a reducing environment in which bacterial sulphate reduction can occur. Proton acidity, which results from the hydrolysis of metals such as Al(III) and Fe(III) can then be consumed whilst at the same time, bicarbonate alkalinity is added to the system. Bacterial sulphate reduction produces either H₂S which sometimes degasses to the atmosphere or usually reduces metals to form metal sulphides, both processes consuming protons (Lottermoser, 2007, Wildeman et al., 1993). The complete reduction of sulphate to hydrogen sulphide is an 8 e⁻ reduction process which requires several 2e⁻ reductions at a time by reactions 13 and 14 (Konhauser, 2006):



Protuberances in the upper layer of the substrate have also been studied and show that there are a number of complex interactions contributing to reducing the acidity and remove mixed metal contaminants (Younger et al., 2002). Compost wetlands can therefore be used to treat AMD from metal mines.

3.5.9 Sizing Criteria for Wetlands and Settling Lagoons

There is no one size fits all treatment option for mine water treatment. The mechanisms for Fe removal from coal mine water discharges are considered to be 'well understood' and the principles of aqueous Fe chemistry are being applied to a number of UK ferruginous coal mine water discharges. Those are being successfully treated with the installation of settlement lagoons and aerobic

reed bed wetlands and Fe is typically removed as Fe(III) hydroxyl oxides (Barnes, 2008).

These systems can be applied to net-alkaline mine waters or net-acidic (Hedin et al., 1994) waters that have been previously passed through a RAPS, ALD or OLD system (Barnes, 2008). However, according to PIRAMID Consortium (2003) wetland design guidelines state that wetlands are only considered appropriate as a final polishing stage for discharges less than 5 mg/L Fe. Concentrations higher than this will require up front Fe removal in the form of settlement lagoons. The sizing of settlement lagoons for these systems is based on three rule of thumb guidelines:

- i. Using a nominal hydraulic residence time (HRT) of 48 h.
- ii. Sizing based on 100 m² of lagoon per L/s of mine water flow, and
- iii. Assuming an iron removal rate of 10 g/m²/d

These guidelines indicate that substantial land take is required (Barnes, 2008) and therefore restrict the application in a topographic sense. In the context of ferruginous metal mine water discharges, where iron concentrations can reach several 100's of mg/L, the low pH is an additional problem and these sizing criteria, and thus the treatment option itself, are commonly considered unrealistic.

3.5.10 Permeable Reactive Barriers (PRB)

Mining activity can affect groundwater both chemically and hydrodynamically. Treating aquifers that have been polluted with high metal concentrations and associated acidity or alkalinity is more difficult than treating point source discharges (Wolkersdorfer, 2008). In 1995, permeable reactive barriers (PRBs) were reported as an emerging alternative to pump and treat systems to treat hazardous subsurface contaminant plumes (Blowes et al., 1995, Waybrant et al., 1998). The way in which PRBs work is relatively simple: a reactive, permeable medium is placed in the flow path of the contaminated plume. PRBs are designed to allow the flow to pass through the reactive media. Geochemical reactions that reduce toxic species to their less harmful form or simply immobilize them by entrapment of precipitated phases occur as the contaminants contact the media. This improves the overall water quality of the water that has passed

through the barrier. PRBs are passive systems, as the flow of water through the barrier moves under a natural hydraulic gradient (Blowes et al., 1995).

PRBs have been used worldwide for a number of applications and proved effective at removing organic and other contaminants such as uranium and chromium. In these instances, zero valent iron (ZVI) is used to reduce contaminant concentrations by precipitation of metals and the breakdown of organics (PIRAMID Consortium, 2003). Yet, ZVI can worsen the situation in some acid mine waters by adding Fe to the surrounding water. Other materials have been successfully investigated for subsurface AMD treatment. These generally include combinations of a material such as sand and pea gravel with calcite chips and an organic waste material (Amos and Younger, 2003). In these cases, the reactions that occur are similar to RAPS. Sulphate reduction generates alkalinity which increases pH to precipitate the metals as metal sulphides (Benner et al., 1999, Blowes et al., 2000). PRBs also have the potential to treat contaminated circumneutral mine water with elevated concentrations of Zn, Pb, and Cd by using other essentially waste materials to increase solution pH enough to precipitate these metals as their hydroxides. For example, fly ash and basic oxygen furnace slag (BOS), which have a high CaO content, were used in field trials with promising results (Warrender et al., 2011). A build-up of precipitates will undoubtedly reduce the permeability and reactivity of the media over time. These systems need to work for up to decades in order to be cost effective. Design is therefore critical in the long term success of such systems (Blowes et al., 2000).

3.5.11 Sand Filters

Sand filtration has been used for the purification of drinking water since the early 1800's (Huisman and Wood, 1974) and has proved to effectively remove a number of different contaminants, including parasitic microbes (WHO, 2004) for a variety of situations. There are two types of sand filtration: slow sand filtration and rapid sand filtration. In slow sand filtration systems, water is filtered down through a bed of fine sand particles supported by a graded coarse gravel layer. Water is fed by gravity at a very slow flow rate. During its course through the sand, a combination of biological, physical and chemical processes, occurring predominantly on top of the gravel bed layer, removes the microbes and particulates from the water. This is where a biologically active layer forms

from dead and alive microorganisms called a *schmutzdecke*. This *schmutzdecke* plays an important part of the removal of contaminants and acts as a natural coagulant reducing chemical dosing costs (WHO, 2004). Rapid gravity filters, also known as roughing filters, use a coarser grain size for faster flow velocities. This reduced contact time means that coarse filters are usually employed as a pre filter to remove bigger particles up front of a fine filter. Fe and Mn removal can be achieved in rapid sand filters by autocatalysis within the filter bed and the metals therein are deposited as oxides. Microbial oxidation by *Gallionella ferruginea* rapidly increases the rate of Fe removal in these systems. Consequently, sand filters can be used as low flow mine water treatment systems where residual metal concentrations do not cause the rapid clogging through build-up of precipitates. However, sand filters can be regularly backwashed and the backwash water recycled for treatment in the clarification stage for higher water recovery (Schoeman and Steyn, 2001).

3.5.12 Ochre Accretion and SCOOFI Systems

SCOOFI (Surface Catalysed Oxidation of Ferrous Iron) reactors are trickling filters in which water trickles down over a supported large surface area. Water comes in contact with the air as it passes over this surface and Fe^{3+} precipitates. Ferric solids adhere to this surface to form an accreted layer which provides an adsorption surface onto which dissolved Fe and Mn species adsorb. These are then oxidised by surface catalytic oxidation which leads to rapid precipitation of more Fe(III) (Jarvis and Younger, 2001, Younger, 2000). This system has potential to reduce the footprint of treatment systems because surface catalysed oxidation is more rapid than the oxidation of Fe(II) by dissolved oxygen and therefore requires less residence time compared to wetlands and settling ponds (Sapsford et al., 2007). SCOOFI reactors are considered to be best suited to net-alkaline mine water where the main contaminant for removal is Fe (Dey et al., 2003, Sapsford et al., 2006). An early example of the SCOOFI reactor used a tank packed with brushwood to aid in aeration and provides a high surface area for accretion of ochre (Best and Aikman, 1983). Because the build-up of ochre is rapid on the media surface, consideration needs to be given to replacement or maintenance of the system during the design phase (Younger et al., 2002).

SCOOFI reactors can be divided into two categories: saturated and unsaturated flow reactors. The PIRAMID guidelines state that saturated systems, which can be orientated either vertically or horizontally are only suited to mine water that is already well oxygenated which ensures that all of the dissolved Fe(II) is oxidised with the given reaction time, and are therefore only considered appropriate when the Fe concentration is <50 mg/L. Saturated systems provide more intimate contact between the media and the water than unsaturated systems and are therefore more efficient at reducing Fe concentrations. Unsaturated reactors do not require pre aeration steps as the nature of the flow makes them less efficient than saturated systems, yet substantial reductions in Fe and Mn can be achieved. Because unsaturated systems have a gravity fed vertical flow path, sizing is often restricted by the available driving head (PIRAMID Consortium, 2003).

3.6 Vertical Flow Reactors

3.6.1 Introduction

The VFR was originally trialled following observations at a UK RAPS site that a substantial proportion of the Fe was being removed above the compost layer (Barnes, 2008). A VFR operates similar to the SCOOFI process except that there is no need to add a high surface area medium, because ochre accretes to itself from a reactive bed much like the *schmutzdecke*. On its course through the system, minewater passes down through a gravel supported accreting bed, eliminating the need for additional support media to aid in the accretion of ochre solids.

A first installation of this novel 'low footprint' system for mine water treatment was constructed at the Taff Merthyr colliery, which has a net-alkaline mine water with 9 mg/L Fe. The pH of the mine water at Taff Merthyr is 6.9 (Sapsford et al., 2007). The results showed that the vertical flow reactor typically achieves higher removal rates between 10 and 20 g/m²/d) compared to on site settling lagoons (typically < 5 g/m²/d). These rates are achieved with smaller residence time, often half that of the settling lagoon. Mn was also removed at a rate of 50% in 24 h compared to 5% in 24 h (Barnes, 2008, Sapsford et al., 2007, Sapsford et al., 2006). The Taff Merthyr VFR was shown to substantially increase Fe(II) re-

removal properties compared to settling lagoons and wetlands with an average removal rate of $16 \text{ g/m}^2/\text{d}$. The mechanism for iron removal in this trial was thought likely to be a combination of oxidation in the water column of the VFR tank and heterogeneous catalysis in the ochre bed (Barnes, 2008, Sapsford et al., 2006).

3.6.2 Development of the Vertical Flow Reactor

On recognising the difficulty with land take requirement for passive treatment of Fe rich discharges based on the PIRAMID guideline sizing criteria for settling lagoons and wetlands, it became necessary to consider alternative treatment options.

Cardiff University has driven research into the applicability of VFRs to remove Fe at different pH coal mine water discharges. Field trials were conducted at Taff Merthyr, a net alkaline discharge (Barnes, 2008). Preliminary trials were also conducted at Ynysarwed which discharges net acid coal mine drainage (Geroni, 2011). In conjunction with the field trials, extensive work had been done by both Barnes (2008) and Geroni (2011) to develop an understanding of the Fe removal mechanisms within the VFR, particularly at Taff Merthyr, as well as Fe oxidation rates in both field and laboratory settings and the settling rates of Fe precipitates. Combined, this work has advanced knowledge into sizing of mine water treatment systems. Barnes (2008) found that the major mechanism for removal in the VFR at Taff Merthyr was almost certainly filtration of HFO particles and not heterogeneous catalysis of Fe(II) oxidation in the ochre bed. Geroni (2011) concludes that the low dissolved Fe(II) concentrations ($< 1 \text{ mg/L}$) at the Ynysarwed VFR at pH 4.6 were a result of the high Fe(II) oxidation rates and residence times. She observed that oxidation and the decrease of Fe(II) occurred already within the water column, prior to passing through the ochre bed. As has been shown by Barnes (2008) and Geroni (2011), a VFR is an effective Fe removal system for both net-acidic and net-alkaline coal mine drainage. Consequently, the VFR has a potential as a passive Fe removal option for acidic, low pH mine waters.

A number of authors are recognising the limitations of common practice passive treatment systems for the treatment of multi contaminant AMD (Macías et al.,

2012) which suffer from passivation of Fe precipitates. AMD treatment is also progressing towards the idea of Fe removal as an initial treatment stage to extend the system operating time and avoid multi element contaminated sludge, which would have a substantial higher disposal cost. The benefit of a clean HFO sludge is its reuse as an adsorbent or pigment (Hedin, 2003, Zinck, 2005, Zinck, 2006).

3.7 Active Treatment Options

3.7.1 Description of Active Treatment Options

Active mine water treatment is the usual way of treating mine water in operating mines and in those cases where the environment might be adversely polluted. At abandoned mines, “active treatment is generally only adopted” when it is difficult to “treat passively or where other considerations such as land availability prevent the use of passive treatment” (Coulton et al., 2003).

Active treatment can be classified into a number of technologies:

Active treatment uses conventional mine water treatment unit processes that requires a number of steps: first, addition of lime to precipitate metals then chemical coagulation through the addition of chemical reagents, rapid mixing and flocculation, followed by floc removal via sedimentation and flotation. Active systems are therefore quite demanding in chemical use, energy input and mechanical parts as well as skilled manpower (Nkwonta and Ochieng, 2009). Yet, these systems have the advantage of being able to accurately control treatment in response to fluctuation in influent water chemistry and consume less land because treatment plants can be located directly at the mine site (Walton-Day, 2003). The disadvantages include high perpetual operation and maintenance costs and the production of substantial quantities of contaminated sludge (as in passive treatment) which can be problematic to handle, requiring additional disposal and transportation costs (Coulton et al., 2003). In relation to abandoned mine sites, active treatment plants require connections to basic infrastructure for transportation, access and power source. Active treatment is therefore not considered appropriate for the long term treatment of mine waters discharging from abandoned mines except where environmental reasons require this method.

The acronym ODAS is a commonly used term that encompasses the stages of the process that are required when adding chemicals to treat mine water. These stages are **o**xidation, **d**osing with **a**lkali and **s**edimentation. Used together, they complete the active process but the order in which they are implemented changes depending on the geochemical characteristics of the water. For instance, very acidic water would require the addition of alkali chemicals as the first step to raise solution pH in order to improve the oxidation kinetics whereas a carbonated water that is high in CO₂ would be first aerated to degas the CO₂ to raise the pH, which in turn increases the rate of oxidation (Younger et al., 2002). Separation or sedimentation of the precipitates from the water is carried out in the clarification phase.

3.7.2 Active Abiotic Treatment

Addition of chemicals is the most common way to treat AMD. This raises the pH in order to precipitate metal and metalloid contaminants. Alkali reagents used for the neutralisation process include NaOH, NaCO₃, CaO, Ca(OH)₂, MgO, Mg(OH)₂, limestone, soda ash briquettes are used (Maree et al., 2013, Skousen, 1991b). Most of these chemicals are added either as liquids, powdered or in a slurry form. Besides limestone, CaO, known as lime or burnt lime is the cheapest and most readily available chemical; it comes in powdered form or slaked as a bulky substance having the disadvantage of producing a high volume of sludge. In contrast, NaOH usually is the most expensive chemical but with a fast reaction time and comes in liquid form allowing it to be added using a dosing pump. Treatment can be achieved in a relatively small vessel which is useful when treating multi contaminant AMD. In such a case it might be necessary to have a multi stage treatment where each stage targets the specific pH for the minimum solubility of that particular element. Where Fe is present, oxidation of the Fe(II) and precipitation at pH 8–9 will remove many of the metals by co-precipitation (Dzombak and Morel, 1990). In principle, rapid reaction times cause smaller floc sizes and longer settling times and consequently, the addition of coagulants might be necessary to speed this stage up. Because there are several advantages/disadvantages against each chemical, an appropriate selection needs to consider all the ODAS stages in terms of cost of operating, land availability, treatment time, transportation and disposal. Aside from the metals,

chemical addition can be used to reduce sulphate concentrations, as in the barium chloride process that is sometimes used to remove radium and sulphate (Maree et al., 2004).

Limestone can also be added to neutralise the acids or an integration of both limestone (CaCO_3) and lime (Ca(OH)_2) can be employed (Deul and Mihok, 1967). This is a multi-staged process for the treatment of AMD where metals and sulphate concentrations need to be reduced. In this process, water is neutralised by the addition of limestone which raises the pH close to 7. Further addition of lime raises the pH to 12 leading to the precipitation of gypsum for partial removal of sulphate and other metals of concern which have a higher pH of hydrolysis. With a final stage of pH correction being required to lower the pH, it is possible to precipitate the CaCO_3 and recover the CO_2 produced in the first stage (Geldenhuis et al., 2003).

3.7.3 Bacterial Activity

The presence of bacteria is commonly seen in the form of biofilms, where they have deposited ferric iron as a gelatinous slime which surrounds them. Fe oxidising bacteria use Fe as an energy source through conversion of Fe(II) to Fe(III) and are found in most iron bearing waters in the natural environment (Figure 3). The solubility of Fe(II) and Fe(III) is dependent on the pH and redox conditions and the bacteria are not able to modify the chemical thermodynamic behaviour of the reactions, but catalyse them. Consequently, they live in the pH- E_h -conditions favourable for Fe-Oxidation. Abiotic oxidation of Fe at pH <3.5 is very slow regardless of the oxygen saturation and, consequently, Fe(II) oxidising bacteria are important players in speeding up the oxidising process in these environments (Stumm and Morgan, 1996). To understand biotic oxidation rates at low pH, laboratory investigations with only one species of acidophilic iron-oxidizers (*Acidithiobacillus (At.) ferrooxidans*) have been carried out. However, the kinetics varies between species and more recently, *Ferrovum (Fv.) myxofaciens*, a novel autotrophic iron-oxidiser, were investigated (Hedrich and Johnson, 2012). These bacteria have been found to be the most efficient iron oxidisers in this environment and produce extracellular polymeric substances, which creates acid-streamers in moving mine water. *Fv. myxofaciens* also precipitates the mineral Schwertmannite and experiments using synthetic pH 2.1

mine water have shown promising results for the bacteria to act as polishing treatment by lowering soluble Fe concentrations from about 280 mg/L to <1 mg/L (Hedrich and Johnson, 2012).

3.7.4 Sulphate Reducing Bacteria

Active biological treatment plants use specific bacteria to selectively precipitate metals thereby recovering and recycling metals from the waste stream. Sulphidogenic bioreactors are used in systems to control the biogenic production of H₂S. This process works by generating alkalinity to precipitate metals as insoluble sulphides. Sulphate reducing bacteria (SRBs) are sensitive to acidity and need to be protected from this in order for bioreactors to be a stable form of remediation (Johnson and Hallberg, 2005). Yet the performance of active biological treatment plants is more controllable than for passive biological treatment. However, the added benefit of the reduction in sulphate as a proven technology (PIRAMID Consortium, 2003) as well as the ability to selectively remove metals such as Zn and Cu, means that some of the high capital and operating cost could partly be offset by metal recovery in the future (Smith et al., 2013).

3.7.5 High Density Sludge Process (HDS)

One of the biggest cost factors in active treatment is the disposal of the sludge from metal precipitation and the added alkali (Morin and Hutt, 2006, Zinck, 2006). Sludge handling includes the collection, transportation and disposal, usually into designated landfill or underground, which makes the sludge volume a key consideration. The development of the HDS system by Kostenbader and Haines (1970) has benefits in active mine water treatment and works to improve overall treatment efficiency in several ways. Part of the sludge produced at a plant is recycled back into the system as seeds for the iron-oxyhydroxide-formation and causes metals to precipitate on the surface, this produces a higher density sludge which not only improves the settling rates and dewaterability of the ochre, it also improves the efficiency of the chemicals used. Early trials gave promising results with sludge containing 15–40% solids equating to 15–40% less sludge volume and thus dramatically reduced storage, disposal and chemical costs. The HDS process is therefore well suited to the treatment of AMD with high ferrous to ferric ratios which are notoriously difficult to treat (Kostenbader and Haines, 1970). Recirculation of precipitates back

into the feed solution also enhances the dewatering and settling rates of sludges due to higher sludge densities (Suvio et al., 2010). Due to these advantages, the HDS-process since then, became the most prominent water treatment process in the mining industry with a trend towards installing those systems (Senes Consultants Limited, 1994).

3.7.6 Membrane Filtration

Microfiltration (MF), ultrafiltration (UF), Nanofiltration (NF) and reverse osmosis (RO) are pressure driven membrane technologies that are being favoured for used in removal particulates and microorganisms from water sources (Abdulgader et al., 2013). Until the 1970's the main use of membrane technology was to purify salt water for drinking water purposes and in the 1990's substantial technological changes occurred, making membrane technologies a feasible option for mine water treatment. Since the attention on trace metal contamination has increased over the past couple of decades, in line with tightening legislation on water quality standards, the interest in developing these technologies for removal of problematic cations and anions from AMD has also increased.

Membrane technologies work by removing both dissolved and particulate contaminants from water by passing the feed water at high pressure over and parallel to a membrane consisting of very small pore sizes (Strathmann, 2012). This pressure-driven crossflow allows for continuous treatment. Particles greater than the membrane pore size are separated from the water which passes through to the membrane's other side (Figure 6). The contaminants become concentrated into liquor on the other side of the membrane. This concentrate then has to be removed and disposed of appropriately (Cartwright, 2012, Younger et al., 2002). Membranes are categorised by pore size and therefore selected for specific treatment purposes in accordance with the contaminant(s) of concern.

RO is a commonly used treatment for the desalination to drinking water. Whilst it has the potential to treat mine water, maintenance (membrane replacement) and the high energy demand of the operating pressures restrict the application of RO to certain economic conditions where there are no alternative. In terms of membrane technology, nanofiltration is reported as being appropriate for mine

water treatment. However, the commercially available membranes must be selected with set criteria in mind, for example, in nonferrous mine water, the main considerations reported are (Andrews et al., 2009): first, to adequately reduce metal concentrations, separating them from the sulphate and secondly, ensure that the sulphate can be concentrated sufficiently for removal by chemical precipitation. However, the authors also reported that although there are benefits in using NF in that a lower osmotic pressure is required than with RO systems, in order for maximum performance to be achieved in both stages of treatment, antiscalants need to be used to prevent fouling.

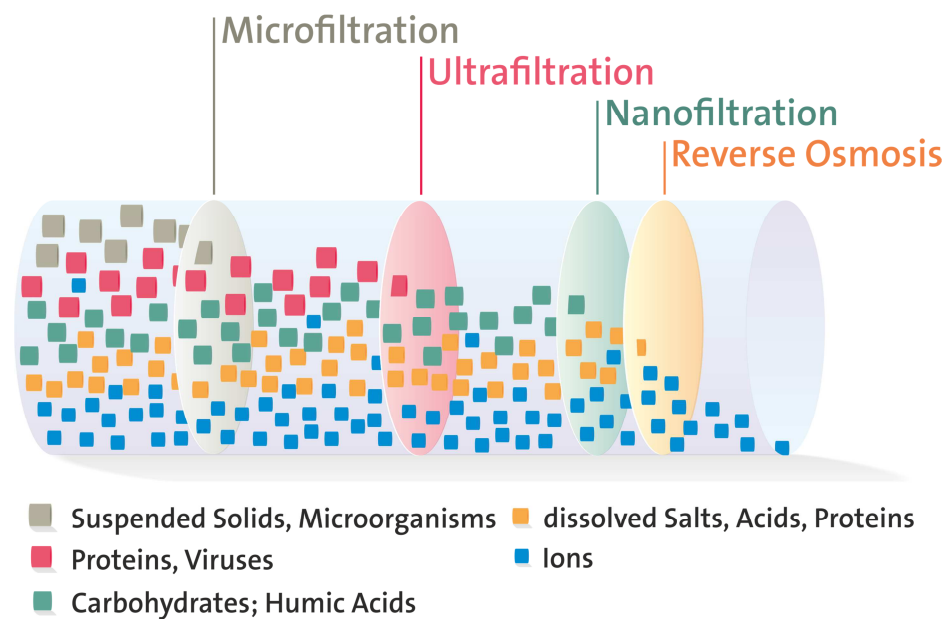


Figure 6: Membrane filter sizes and separation types (modified from Wolkersdorfer 2013).

More recently, nanofiltration has been reported as being highly effective in removing the metals Pb and Hg and the semi metals Sb and As from low pH mine water at the Los Rueldos mine in Northern Spain with only moderate pressure required (Sierra et al., 2013). Here again, the nature of the treatment dictates that fouling will continue to be the problem when using membranes for mine water treatment. As has been shown, the success of membrane technology is highly dependent on the operation pressure, feed temperature and pH as well as the concentration of metals to be removed. An increase in feed pressure causes an increase in rejection but decreases with an increase in feed temperature. The chemistry of the water and engineering are the two dominant fields

that need to be understood for success of the technology in mine water treatment.

3.7.7 Ion Exchange

Natural and synthetic zeolites and other mineral mixture products were being used for ion exchange before 1930 when the first plastic 'resins' were developed for cation exchange. It wasn't until 1949 that anion resins were developed, this enables the process of demineralisation of water to become available (Skelly and Loy, 1974). Since then, the application of the ion exchange principle has been widely applied to water treatment. Ion exchange treats water hardness, inorganic chemicals and radionuclides.

Ion exchange in water treatment refers to a reversible process where selected function groups that are pre-treated with mono valent ions on the surface of a solid medium are used as 'ion exchangers'. The medium is porous, allowing mine water to pass through so that these ionic 'exchanges' can take place. Background of the method is that cation exchanges (using cationic resins) and anion exchanges (using anionic resins) occur as the contaminated water passes and therefore, the toxic elements in the water are replaced/exchanged for nontoxic contaminants. For example, in mine water, common multi valent contaminants such as Cu(II), Fe(II), Fe(III), Cd(II), SO_4^{2-} are easily exchanged with less harmful mono valent ions such as Na^+ , H^+ , K^+ , OH^- , Cl^- (Skelly and Loy, 1974). An Ion exchange medium can be a resin that is often made of a complex crosslinked polymer matrix (Abdulgader et al., 2013). Resins are preferred to natural materials such as zeolites, which are a class of aluminosilicate mineral (PIRAMID Consortium, 2003), as the resins can be backwashed using acid or alkalis to remove the contaminants and thus allowing the material to be regenerated for further use. Zeolites however, need to be disposed of which adds to the overall operating cost (Wolkersdorfer, 2013). The use of resins also has the advantage over chemical dosing because it produces relatively low volume sludge with substantially better dewatering properties (Pollio and Kunin, 1967). Ion exchange resins are also simple to use with no energy requirement for the exchange phenomenon to occur (Abdulgader et al., 2013). However, the correct resin type must be selected for the contaminant concentration, and the operating parameters such as pH in order for the ion exchange process to be efficient,

mineralisation and the metal toxicity can limit the performance of field ion exchangers (Gaikwad, 2010).

3.8 Electrochemistry

3.8.1 Introduction

In this part of the chapter, a short introduction to electrochemistry will be given. It is mainly based on the books published by Comninellis and Chen (2010), Lefrou et al. (2012), Rajeshwar and Ibanez (1997) and Wendt et al. (2012) without referring to them in all detail throughout this introduction.

Electrocoagulation for treating waste water was initially proposed in the UK as far back as 1889 when the first EC plant was constructed in London for treating sewage by mixing it with sea water and subsequent electrolysis. Various electrochemical methods were being patented in the early 1900's. Electrocoagulation (EC) with aluminium and iron electrodes, for example, was patented in the US in 1909, but only in 1946 the first large scale EC plant for the treatment of drinking water was applied in the US (Holt et al., 2002). Relatively large capital investment and high energy demand made this 'new' technology expensive for the time. Research into the EC process was mostly driven by the US and the former USSR and has progressed over the past sixty years in line with increasing pressures to comply with strict environmental regulations on drinking water quality and wastewater discharge (Chen, 2004).

The earliest report about electro oxidation (electrolytic oxidation) of mine water provides details of bench and field trials aimed at determining the economics of using electro oxidation for the treatment for AMD from coal mines (Jasinski and Gaines, 1972). This report describes the method of direct oxidation using a packed bed reactor where a packed bed of semi-conductive carbon particles are placed between a cathode and an anode. Trials demonstrated that operating costs at this time were too high compared to conventional aeration. In a subsequent investigation by Franco and Balouskus (1974), performance at low pH was reported to have been affected by a number of side reactions: 1) the back reduction of Fe(III) at the cathode, 2) the chemical reaction with H generated in highly acidic water and 3) electrode fouling. Nonetheless, this substantial work examined the effects of numerous operating parameters, materials as

well as design and optimisation strategies for the application of EC as a treatment technology of AMD. In addition to information contained within those publications, new knowledge is applied in this thesis, since power electronics have developed such that EC is regaining interest from the mining sector as a potential mine water treatment technology.

Electrochemistry differs from classical chemistry in that it provides an additional, adjustable degree of freedom. Oxidation-reduction shifts can therefore be controlled by an electric current or with a voltage. In the context of mine water, this forced manipulation of redox conditions is a beneficial 'additional' parameter for treatment operations.

Modern electrochemical processes are taking advantage of the presently known physical and chemical reactions that occur within the electrochemical cell. Those processes encompass electrocoagulation, electroflotation, electroflocculation, electroprecipitation, electroforming and the advanced oxidation process (AOP). All of these terms are often imprecisely referred to as 'electrocoagulation' without immediately specifying which process might have been meant by the author.

Conventionally, the term electrocoagulation is used in water treatment to describe the process in which metal ions are added to contaminated water by electrical dissolution of a sacrificial anode, usually made of Fe or Al (Sasson et al., 2009). Once these charged ions are released from the sacrificial electrode into the electrolyte, they destabilise suspended, emulsified or dissolved contaminants by reducing the repulsive energy barrier between the particles and cause the aggregation of metal ions in the same way as in conventional treatment (Barkley et al., 1993). Colloidal stability and instability is governed by the balance between London forces or van de Waal's forces of attraction and repulsive electrostatic forces (Weiner, 2010). When adding aqueous metal ions to water, the positively charged Fe(III) or Al(III) ions are sorbed to the surface of the negatively charged colloids, neutralising their charge and a double layer forms around the colloid (Figure 7). Subsequently, these otherwise suspended particles are able to coagulate and flocculate, which increases their size and density and causes their sedimentation. Sometimes, especially in electrocoagulation,

gases are attached to the flocs and results in floating of the coagulates. In any case, they can be more easily separated and removed from the water by filtration or sedimentation (Barrera-Díaz et al., 2011).

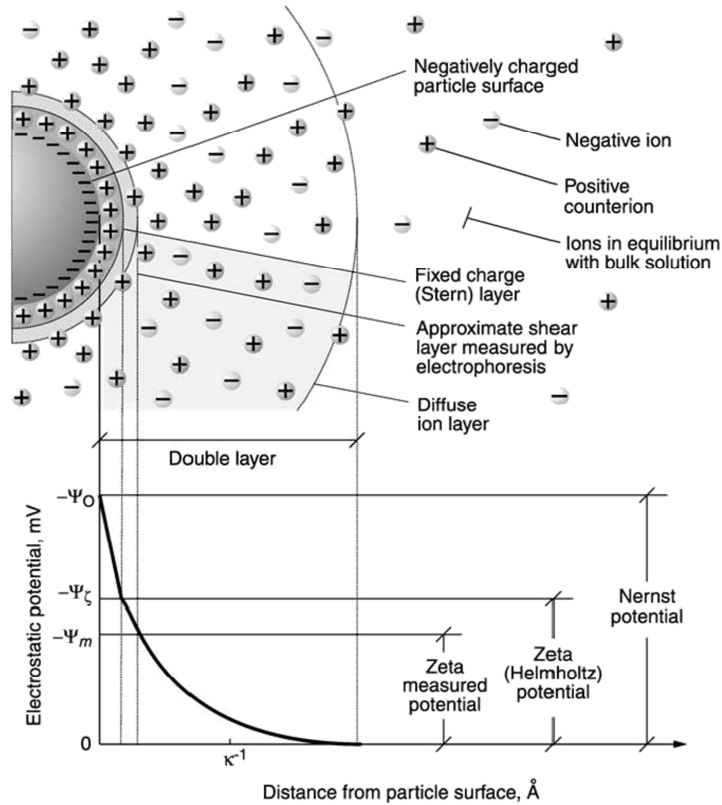


Figure 7: Conceptual representation of the electrical double layer (from Vepsäläinen, 2012).

EC has many advantages over conventional waste water treatment methods besides ease of operation: The main advantage is that it usually does not require the addition of chemicals (Sasson et al., 2009). Furthermore, flocs from electrocoagulation have a thinner solvation sphere, show a higher shear resistance, can be filtered more easily (Barkley et al., 1993) and, as can be seen in Figure 8, show higher sludge settling rates (Franco and Balouskus, 1974). Despite the potential for EC to extensively eliminate the disadvantages of classical treatment methods, it has received little scientific attention in the mine water community (Figuroa and Wolkersdorfer, 2014) and the mechanisms are not understood in detail, particularly the factors that influence the effective removal of metallic ionic species. The focus has been mostly been to optimise for minimal electrical consumption and maximise effluent throughput rates (engineering) and less on the physicochemical parameters (Mollah et al., 2001).

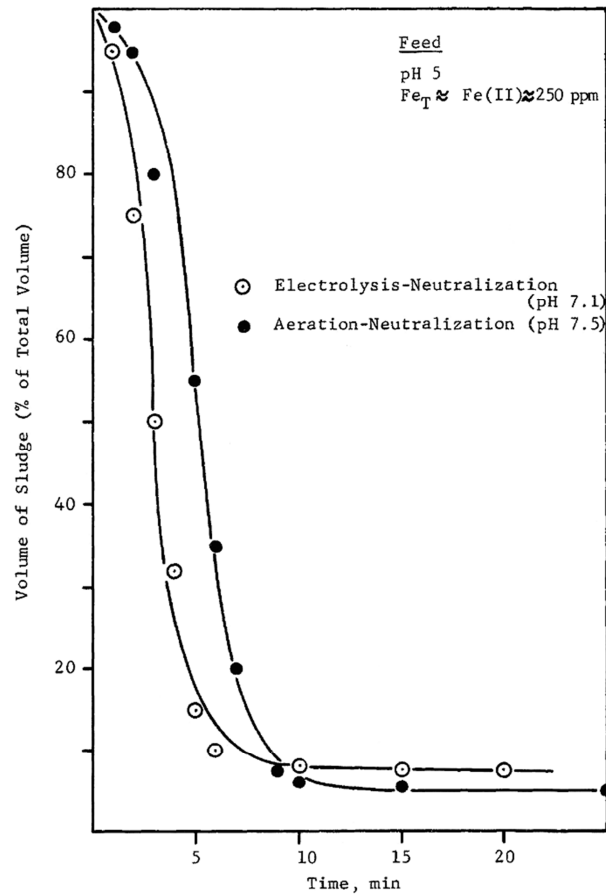
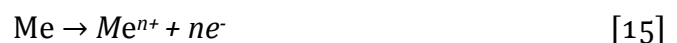


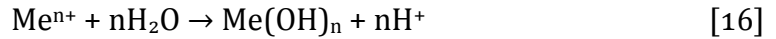
Figure 8: Comparison of sludge settling rates from aerated and electrolysed ferrous mine water (from Franco and Balouskus, 1974).

3.8.2 Overview of Reactions Involved

A very simplified version of an electrochemical reactor would consist of two electrodes, usually made of Al or Fe immersed in an aqueous solution. An electric current is applied so that the electrodes act as a positive anode and a negative cathode. In electrochemical reactions it is important to quantify the electricity usage, which is calculated by measuring the current density. The electric current was first defined by Ampère in 1820 as “the overall movement of charges in a conductor” (after Lefrou et al., 2012). This electric current oxidises the metal at the anode, causing it to corrode and releasing metal ions into solution by the following reaction:

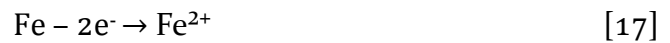


Metal ions are able to enter into further reactions, for example, if the E_h -pH conditions are suitable for hydrolysis of metal ions. In those cases, precipitation can occur by the following equation:



A variety of electrode materials are used in electrochemical water treatment, whereas the choice of materials directly relates to the treatment required. For instance, sacrificial electrodes are conventionally used when the treatment requires coagulant dosing in the form of metal ions. According to Chen (2004), metal ion generation takes place at the anode by the following reactions:

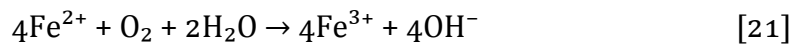
For an iron or aluminium anode:



In alkaline conditions:



In acidic conditions:



In addition to the dissolution of metal ions from the anode, the following reactions take place within the EC system (Figure 9):

- Hydronium ion or proton ion consumption and hydroxyl production causes an increase in pH
- Reduction of metal ions at the cathode
- Electrochemical decomposition of water molecules results in the production of hydrogen gas at the cathode and oxygen at the anode by reactions:



The operation of the coagulation unit and its cell configuration influences many parameters including pH, floc stability, agglomeration size and bubble size. In

addition, the dominant removal mechanisms (*e.g.* settling or flotation) might change, as the reaction progress will most certainly alter when the operating parameters and pollutant types are modified (Holt et al., 2005).

The relative mass m of metal [g cm⁻²] that is added to the water by EC can be calculated using Faraday's law (modified from Comninellis and Chen, 2010):

$$m = \frac{ItM}{nF} \quad [25]$$

Where:

I : Current density, A m⁻²

t : Time of electrolysis, s

M : relative molar mass of metal used, mol g⁻¹

n : number of electrons in the red-ox reaction, –

F : Faraday constant, 96,485.3365 J V⁻¹ g⁻¹ [sA mol⁻¹]

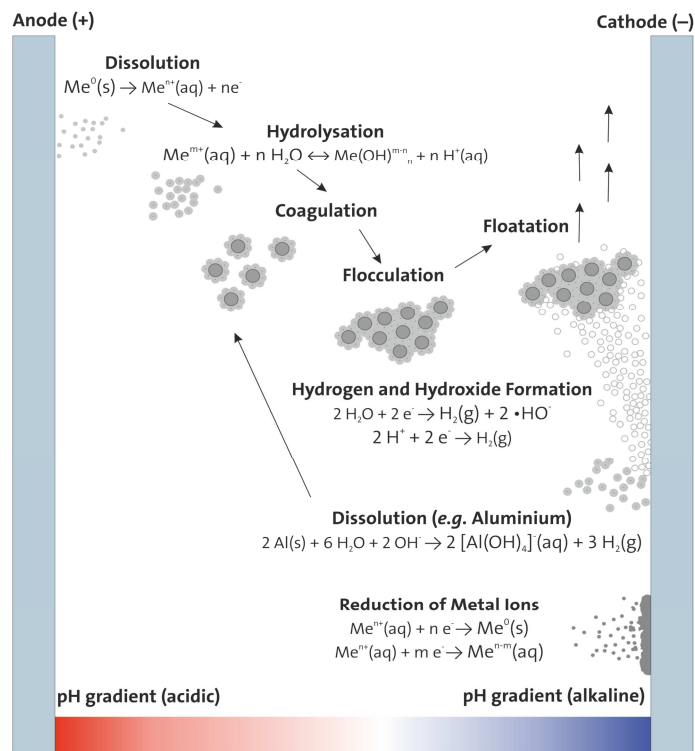


Figure 9: Schematic representation of typical reactions during the EC treatment (from Vepsäläinen, 2012).

3.8.3 Electrode Configuration and Materials

The choice of electrode configuration largely depends on the treatment requirements. Usually, electrodes are monopolar or bipolar (Figure 10) and the

flow through the cells can be in series or parallel (Mollah et al., 2001, Pretorius et al., 1991, Vepsäläinen, 2012).

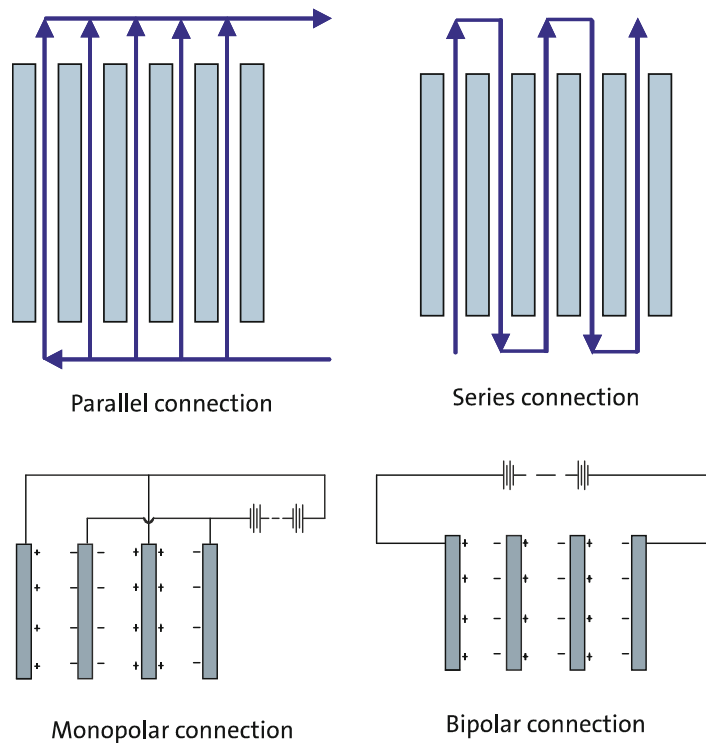


Figure 10: Potential electrode configurations for EC treatment (modified from Comninellis and Chen, 2010).

A simple monopolar electrode arrangement means that each anode and each cathode is connected with each other through the power supply. Bipolar configurations differ in that sacrificial anodes, which are not connected to the power supply, are placed between a monopolar cathode and anode which are connected to the power supply. The electric current passes through the two electrodes thus charging the neutral sides of each of the sacrificial anodes. They then become oppositely charged on both sides and during electrolysis, cathodic reduction and anodic oxidation reactions occur on opposite sides of the same electrode, thus redeeming them bipolar (Comninellis and Chen, 2010).

3.8.4 Advanced Oxidation Process

As described earlier, electrochemical treatment is a collective term which includes a variety of electrochemical processes and techniques such as the advanced oxidation process (AOP), a term originally defined by Glaze et al. (1987) as “*The oxidation processes that generates hydroxyl radicals in sufficient quantity to affect water treatment*”.

The advanced oxidation process (AOP) is different from electrocoagulation in that 'inert' or 'non-sacrificial' electrodes, which are commonly made of carbon, Pt coated Ti or other mixed metal oxides (MMO) such as PbO_2 , IrO_2 , $\text{Ti/SnO}_2\text{-Sb}_2\text{O}_5$ are used. These types of electrodes are able to generate highly oxidative species, thus providing an effective and efficient process for oxidation. The hydroxyl radical ($\cdot\text{OH}$) that is produced on the surface of the electrode is a powerful, non-selective chemical oxidant that acts rapidly with most organic compounds (Trapido, 2008). This is also known as anodic oxidation or direct oxidation (Chen, 2004, Rajeshwar and Ibanez, 1997).

3.8.5 Selected Mine Water Applications

Various electrode materials have been investigated in experiments to assess electroprecipitation as a treatment for acid mine waters. Jenke and Diebold (1984) studied the electroprecipitation of metals from synthetic non-ferrous mine water. In their experiments, polished steel rods were used as the cathode and various anode materials including steel, zinc and lead were trialled. By using a stainless steel rod anode, they observed in 30 min treatment time an increase in pH from 2.8 to 4.7, a 100% reduction in Cu concentrations, and 90% Zn reduction from the original concentrations of 300 mg/L and 1000 mg/L respectively. They concluded that Fe from the steel was responsible for the coprecipitation of the dissolved metals. Similarly, when using a Zn anode, almost 100% of the Cu was removed in the 30 min treatment time. Furthermore, they reported that the Pb anode being the most effective for the removal of sulphate due to the low solubility of lead sulphate. High pH, up to pH 12, within 6 min using the Pb anode, was explained by the decomposition of Pb(II) which does not actively compete for hydroxide being generated at the cathode. Yet, the electrode is quickly poisoned with PbSO_4 which, at this stage, makes the method unsuitable for sulphidic mine waters.

Casqueira et al. (2006) studied Zn-removal from synthetic, Zn-rich water (20 mg/L) at an initial pH of 7 and various electrical set-ups. They noticed that the optimum electrical configuration is 15 V and 400 mA and that the stoichiometric metal:collector ratio plays an important role in forming floating flocculants. Using their optimal configuration, they gained a current density of 8 mA/cm² and removed 96 % Zn by electroflocculation.

Whilst there is potential for high rates of metal removal as described earlier, there can be adverse reactions in the EC process, such as fouling of electrodes due to the formation of a hydroxide or sulphate layer on the surface of the electrode. This inhibits metal ion production causing detriment to the operating efficiency over time (Mollah et al., 2001). Workers have found that simply cleaning the electrode before each experiment and switching direction of current every 10–30 min was sufficient to limit the formation of a passivation layer (Heidmann and Calmano, 2008). Yet, this would not be practical in a pilot or full scale operation. Another disadvantage is that the process of oxidation of the sacrificial electrodes in order to dissolve metal into the waste water stream, means that the electrodes have to be regularly replaced (Matteson et al., 1995). Some of these issues can be avoided by combining the basic EC system with other technology such as ultrafiltration or carbon adsorption. Yet, large scale applications for mine water treatment do not exist at present due to feasibility considerations (Figuerola and Wolkersdorfer, 2014).

In this thesis, the applicability of EC to a variety of mine waters is considered. EC is an active process. It is examined in this thesis as a potential alternative to treat water types that require chemical dosing. A particular interest exists in the removal of Zn from low Fe waters by adding Fe, from a sacrificial electrode to encourage co-precipitation of Zn with Fe precipitates. EC was also investigated for its applicability to treat multi-metal contaminated, low pH AMD and scoping studies were also performed to investigate AOP as a practical method for the oxidation of Fe(II) in coal mine drainage. In addition, potential differences in the mineralogical structure of electro generated Fe precipitates and naturally aged ochres are considered.

4 Study Areas

4.1 Introduction

In this thesis, mine water from four sites, Cwm Rheidol, Parys Mountain, Frongoch and Ynysarwed was used. With the exception of Ynysarwed, which is a former coal mine, the sites are all abandoned metal mines located in Wales. Figure 11 shows the locations of the four sites used and the co-ordinates for each of the sites are given in (Table 3).

Cwm Rheidol was chosen as an appropriate AMD site to trial the VFR because the topography is such that a system can be gravity fed and therefore passive. Also, the site has good access and security which are important considerations for running a field trial. Mine water from Parys Mountain, another well-known AMD producing site was also investigated during the VFR trial to identify if there could be an application for the VFR in the future.



Figure 11: Digital Elevation map showing the four sites, Cwm Rheidol, Parys Mountain, Frongoch and Ynysarwed studied in this thesis (contains Ordnance Survey data © Crown copyright and database right).

Table 3: Coordinates for each of the sites investigated.

Location	UTM ETRS89 coordinates
Cwm Rheidol	E 30440902 N 5804479
Parys Mountain	E 30410200 N 5917015
Frongoch	E 30439283 N 5800449
Ynysarwed	E 30449297 N 5727570

In contrast, mine water from Frongoch, which has high Zn concentrations but low Fe circumneutral pH water, was chosen for the electrochemical experiments for Zn removal. Ynysarwed was investigated because its water chemistry showed potential for electrochemical treatment using AOP. Table 4 gives the treatment type applied to each of the waters used in this thesis.

Table 4: Summary of treatment types investigated at each of the sites. A more detailed compilation is provided in Table 6.

Treatment type investigated	Cwm Rheidol	Parys Mountain	Frongoch	Ynysarwed
VFR ☉	✓			
AOP ☼			✓	✓
EC ☼	✓		✓	✓
AOP + EC ☼				✓
Co-precipitation ☼			✓	

VFR: Vertical Flow Reactor; AOP: Advanced Oxidation Process; EC: Electrocoagulation;

☉: field experiment; ☼: lab experiment

4.2 Cwm Rheidol Pb/Zn Mine, Mid-Wales

4.2.1 Location

The Cwm Rheidol or Ystumtuen mine is located within the mid-Wales Orefield approximately 12 km east of Aberystwyth north of the river Rheidol (Figure 12) and 190 km NNW from Cardiff University. The mine is part of a big mine complex situated just below the village of Ystumteum, on the steep southerly face of the Rheidol Valley which runs ESE to WNW. The drainage is issued from two adits that intercept the steeply dipping Castell Lode (Jones and Pugh, 1935). The lower number 9 adit, the number referring to the former working level, is approximately 100 m above sea level. Directly above, at approximately 175 m above sea level is the number 6 adit. These adits were originally mined more than 400 m into the hillside and join with a number of other mines underground

to form a main drainage point. According to Jones (1922), the upper adit crosses the Castell lode at a distance of 428 m and the lower adit at 494 m.

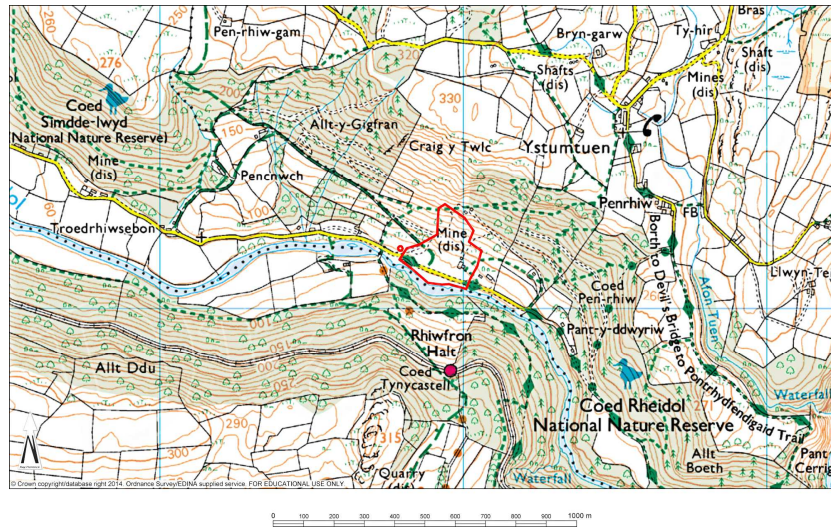


Figure 12 Map showing the boundary of the Cwm Rheidol abandoned Pb/Zn and its position in relation to the River Rheidol. The small red circle on the western edge of the boundary marks the flows from the adit discharge pipes. © Crown Copyright/database right 2014. An Ordnance Survey/EDINA supplied service.

4.2.2 Geology

Many mines in the mid-Wales Orefield are located along the Castell Lode. The primary ores are sphalerite, galena, chalcopyrite, arsenopyrite, some pyrite and marcasite, which is present within quartz, barite and a carbonate gangue. Cwm Rheidol is on the down throw side of the E–W trending Ystwyth fault on the steep southerly face of the Rheidol Valley (Jones, 1922). The ores are hosted as veins in Lower Silurian siliceous sediments which were originally deposited in a deep marine basin by turbidity currents (Cherns et al., 2006). Sediments were later folded into an ENE trending sequence of structures (Raybould, 1973) and the extensive faulting and fracturing that accompanied this episode, opened up pathways for mineralizing fluids. Late stage hydrothermal mineralisation of the Caledonian Orogeny then characterised the region by the presence of many non-ferrous metalliferous ores which are concentrated along a 10 km stretch of the ENE trending Camdwr fault (Johnston, 2004). The mines at Cwm Rheidol exploited the part of Castell Lode, hosted in the Devil’s Bridge Formation. Although the Castell Lode was worked for lead zinc and copper, sphalerite was the main ore mined there. The high pyrite and marcasite content at the Cwm

Rheidol mine is unusual for the Castell Lode (Jones, 1922), a region where mines are generally characterised by a low Fe circumneutral discharge (Jones and Howells, 1975).

4.2.3 Mining History

Past records for mining at Cwm Rheidol exist from 1848, and records state that the mine produced 119.4 kg of silver, 5158 t of galena, 111,113 t of sphalerite and 3926 t of pyrite utilised for the production of sulphuric acid (Jones, 1922). Production peaked in 1905 and the mine finally closed in 1917. Since then, no responsibility for the pollution from the site was taken from and consequently, the mine still discharges substantial loads of metals, including zinc into the River Rheidol which flows into the Celtic Sea near Aberystwyth, 15 km to the west. Griffith (1919) described the influences of the Cwm Rheidol mine on the Rheidol river sediments and soils downstream of the mine site and reported that Pb and Zn negatively influenced those compartments (Table 5). The legacy of past mining is still clearly evident from the 60,000 m² of sparsely vegetated spoil tips that can be seen in Figure 13 (Fuge et al., 1991) as well as the ochreous drainage overflows into the River Rheidol (Figure 14).

Table 5: Pb and Zn concentrations (%) in river sediments and soils affected by mine sites in the Frongoch and Cwm Rheidol area (Griffith, 1919).

Compartment	Element	Frongoch	Cwm Rheidol
river sediments	Pb	0.92	0.35
	Zn	1.2	Traces
soil	Pb	1.56	0.1
	Zn	1.97	0.12

4.2.4 Mine Water Chemistry

Despite this mine complex having been abandoned for almost a century, Edwards and Potter (2007) report that AMD from this site alone contributes almost half the Zn and Pb loading found along the 15 km stretch from the mine to the sea. Concentrations exceed the EU Water Framework Directive's Water Quality Standard for good ecological status by several orders of magnitude (European Parliament, 2006). Remediation attempts were made in the early 1960's following the construction of the Cwm Rheidol Hydroelectric Power Sta-

tion. This reduced the volume of flow that passed the mine, thus increasing the metal loading by loss of dilution.



Figure 13: The sparsely vegetated spoil tips at the Cwm Rheidol former Pb/Zn mine.



Figure 14: Old filter beds at Cwm Rheidol that are blocked AMD from the adit discharge pipes flowing into the adjacent River Rheidol.

The siliceous nature of the host rock means there is little buffering of AMD from carbonates. To counteract this, a limestone filter bed was constructed for the purpose of neutralising the AMD prior to discharge into the Rheidol River. Initially, this was successful in reducing Zn and Pb, until the Lower Adit blew out in 1969, causing the filter bed to block with ochre. The filter bed has been left

unmaintained since an overhaul in 1976 and has therefore been deemed ‘ineffective’ (Edwards and Potter, 2007). It is worth noting that the water chemistry at Cwm Rheidol is probably not best suited to ALD treatment given the high Fe concentrations and that there is filterable Al in the drainage. Younger et al. (2002) explain that Al can be problematic for ALD’s if dissolved concentrations of more than 2 mg/L Al exist. This is because it prevails in the Al(III) state and hydrolyses by the following reaction (equation 26)



in anoxic conditions and will subsequently precipitate at the higher pH conditions that are created at the surface of the limestone aggregates, thus clogging the pores over time.

The drainage chemistry of the two adits differs, which is attributed partly to the increase in pyrite and marcasite with depth in the Castell Lode. This gives rise to the Lower number 9 Adit (Figure 15) issuing drainage with high Fe thus low pH and higher sulphate than the Upper Adit (Raybould, 1973) and partly because the Upper number 6 Adit water is a mixture of mine water and surface water giving rise to dilution. Adit number 6 has an average flow of 11 L/s and adit number 9 a flow of 3 L/s (Edwards and Potter, 2007).

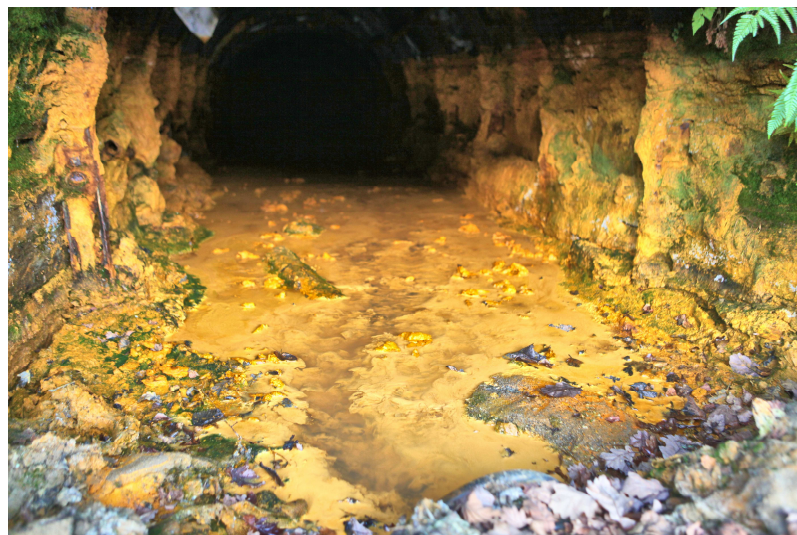


Figure 15: Cwm Rheidol No. 9 adit portal. In the foreground the discharge pipe for the mine water flowing in the middle of the image can be seen. The adit surface and the walls are covered with ochre.

National Resources Wales (formerly Environment Agency Wales) managed a project in partnership with Welsh Assembly Government and The Coal Authority with further financial support from the European Union to undertake works to reduce the impact of mine water on the Afon Rheidol (Edwards and Potter, 2007). This began with piping water from both the Upper Adit and the Lower Adit to the base of the spoil tips on the opposite side of the road from the river (Figure 16). Prior to this, mine water discharging from both adits flowed uncontrolled and overland down the steep sided banks and directly into the river. The steep slopes are made up of poorly vegetated spoil and fines from former mining. Mine water was therefore percolating through the spoil and the discharge into the river was a mixture of both point source and diffuse pollution. In Johnston (2004), the Cwm Rheidol complex is stated as contributing at least 40% of the metal load of the Afon Rheidol.



Figure 16: Cwm Rheidol Mine water discharge pipes (left: No. 6 adit, right: No. 9 adit).

Cwm Rheidol is classified as one of the top 50 polluting metal mines in Wales and put forward as a priority site for remediation in the Metal Mines Strategy for Wales report by Johnston (2004). Works were carried out to improve the land quality by the measures described above. The author of this thesis measured the AMD from the lower number 9 adit as typically being of low pH averaging pH 2.9 in the Fe-buffer range, with concentrations of Fe < 90 mg/L, Zn up to 125 mg/L, Al 25 mg/L, Pb and Cd 0.1 mg/L as well as SO_4^{2-} concentrations being typically in the range of 1500–2000 mg/L. Water from the Upper Adit is a mix-

ture of mine water and surface water, the pH is typically 3.7–4.1 in the Fe-buffer range with Fe concentrations of 2.5–25 mg/L. Zn from the Upper Adit ranges between 10 and 30 mg/L and is therefore in breach water quality standards. Whilst works were successful in diverting the mine water from each of the adits to the base of the mine, which has improved the land quality at the opening of the lower number 9 adit, the water quality did not improve by this measure. Before that modification, AMD spilled out to form a highly metal contaminated pond in the plateaux adjacent to the No 9 adit. This water now discharges at the base of the slope alongside the piped upper number 6 Adit discharge. The two flows are mixing the drainage channel which flows beneath the road into the area of the former limestone filter beds. Currently, this area is flooded and the mine water flows directly over the wall into the River Rheidol. Zn is the main element of concern there, as the River Rheidol is failing water quality standards for Zn for 15 km downstream of the mine where it flows into the Atlantic Ocean (Edwards and Potter, 2007).

In 2007, the HERO group at Newcastle University had carried out laboratory trials to test materials for use in a pilot scale passive treatment system to treat the Zn from the less Fe containing Upper Adit water. A number of materials were tested as suitable substrates to increase alkalinity, encourage adsorption, promote microbial sulphate reduction and precipitate metals as sulphides, carbonates or oxides. The pilot plant for treating the water from the upper number 6 adit (Figure 17) consists of a tank initially filled with wood chippings, compost, digested sludge (which provide an energy source for SRBs) and whelk shells (to produce alkalinity). The system essentially acts as a RAPS, utilising sulphate in the system to treat the Zn by bacterial reduction of Zn to ZnS (Edwards and Potter, 2007). This has been implemented as per the recommendation put forward in 2004 following a scoping study that identified and suggested possible active and passive treatment systems for the site (Rees et al., 2004). The field pilot scale mine water treatment system began operation in 2010 and is still ongoing. In October 2011, a progress report by the Environment Agency wales provided a brief summary of interim results associated with the scheme. Initial results were promising with 97% Zn being removed in the first sample period during September, which declined to less than 50% in the

December samples, with an increase again from December to February when 80% removal was achieved. However, the report does not provide actual concentrations and there is reference to higher removal possibly being attributed to lower Zn concentrations at the inflow.

Cwm Rheidol is a site that is representative of AMD in terms of acidity and high dissolved metal concentrations. As such, it is a popular site for pilot studies used by researchers and government agencies such as National Resources Wales (Edwards and Potter, 2007). It should be noted that the Newcastle trial is treating Upper Adit water, contrary to this thesis which aims to improve the lower adit water.

In 2010, the author engaged in an MSc dissertation project at Aberystwyth University to trial the effectiveness of reactive waste materials for removing Zn from the Lower Adit AMD. Trials were terminated prior to breakthrough after just eight days because of the rapid decrease in flow rates due to the precipitation of Fe-(oxy) hydroxides (Figure 18).



Figure 17: Pilot scale passive system installed by Natural Resources Wales in 2010 for the removal of Zn from the Cwm Rheidol upper adit water.

Based on those previous results, some form of two stage treatment with an up-front Fe removal system would be required to enable testing the material's longevity in terms of saturation from Zn precipitation or adsorption. For this reason the Cwm Rheidol mine was chosen as the study site for the VFR previously trialled by Cardiff University at net alkaline coal mine drainage (Barnes, 2008,

Sapsford et al., 2007, Sapsford et al., 2005) and net acidic coal mine drainage (Geroni, 2011). The intention was to test the VFR on the Lower Adit water of the abandoned Cwm Rheidol mine.



Figure 18: Sludge formation in the 2010 trials.

4.3 Frongoch Pb/Zn mine, Central-Wales

4.3.1 Location

Frongoch abandoned Pb Zn mine is at grid reference SW 72427 73587. It is one of the largest mines in North Ceredigion. The mine is listed in the Metal Mines Strategy for Wales as one of the priority sites for remediation (Environment Agency, 2002). The mine is located in a remote, isolated upland area (Figure 19) 15 km ESE of Aberystwyth near Pontrhydygroes in central Wales (Bick, 1996). It is situated in the Nant Cwmnewydion catchment, a tributary of the River Yswyth and is upstream of the River Ystwyth which flow west in the direction of the Irish Sea (Bearcock et al., 2010). The site is covered with old derelict mine workings and the spoil tips have been designated as a SSSI because they contain rare secondary minerals. For this reason, the tips were moved to the opposite side of the road to protect them from damage caused by the wood mill that is currently in operation at the site (Hartley, 2009).

4.3.2 Mining History

Frongoch was one of the most successful Zn mines located within the mid-Wales Orefield due to the abundance of sphalerite, particularly south of the Rheidol (Lewis, 1967; Foster-Smith, 1979). Frongoch was mined between 1795 and 1903 and produced more than 60,000 t of Pb ore and 51,000 t of Zn ore (Bick, 1996). Mining was not continuous at the site due to fluctuating Pb prices, which caused a series of closures and lease transfers. In 1834, the mine closed until 1875. By this time, Pb prices improved substantially and the mine was then taken over by John Taylor & Sons who worked as the Lisburne Mine Co. They operated the mine successfully for the next 44 years until making their first loss. The mine was then let to John Kitto who worked the sphalerite as well as the Pb ore and used the waste rock to backfill some of the large stopes. In 1897, Kitto retired from the mine, which was passed to the Society Anonyme Des Mines De Frongoch. A dressing plant for processing the Zn ore was constructed at the site and the lower part of the mine flooded from 154 fathoms, the mine shaft down to 90 fathoms repaired. Mining techniques were primitive and therefore slow and costly. Mining finally ceased in 1903. However, sphalerite on the waste rock dumps was worked between 1920 and 1930 (Bick, 1996).

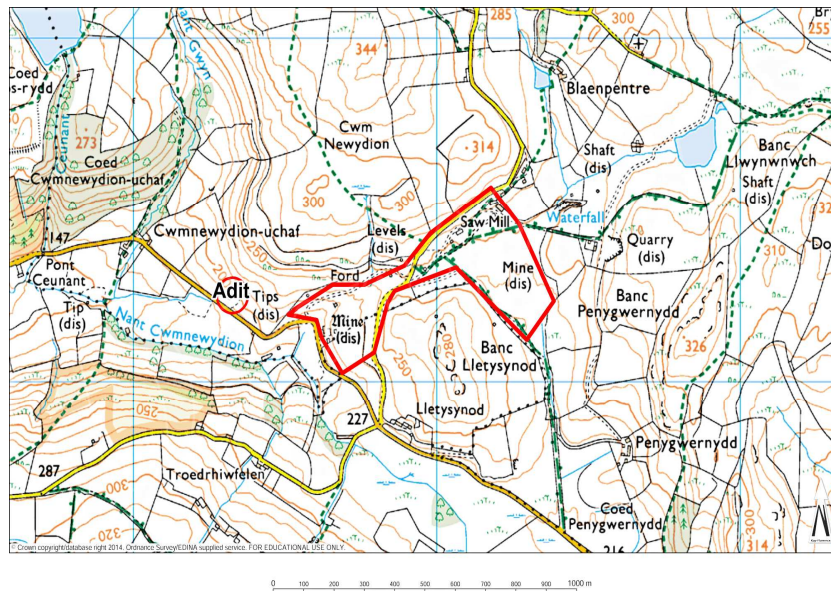


Figure 19: Boundary of the Frongoch abandoned Pb/Zn mine. Mine water discharges from the adit west of the site. © Crown Copyright/database right 2014. An Ordnance Survey/EDINA supplied service.

Frongoch is located on a steep upland slope. The hydraulic gradient made it possible to process the ore by gravity fed water wheels which were replaced with an electrically driven ore processing plant in 1899 (Bick, 1978, Bick, 1996, Jones, 1922, Richardson, 1974). Large volumes of water were used in the ore processing. Fines and contaminated water were discharged directly into the Ystwyth. Griffith (1919) analysed sediments and soils affected by the Frongoch mine site and found considerable amounts of Pb and Zn in the samples (Table 5). He concluded that the negative effects observed on crops and cattle are a result of contamination from the mine spoil heaps.

4.3.3 Geology

Frongoch mineralisation is hosted in Silurian deposits of the Llandovery series. This falls under the Devil's Bridge Formation, which consists of interbedded turbidites of layered sandstone and mudstones. These turbidites are reported to a depth of approximately 470 m at the Frongoch site. According to Davies et al. (1994) the Frongoch site is at the centre of the Teifi Anticline that formed after the turbidites during the early to mid Devonian orogeny. The mid-Wales ore field consists of mineralised veins set within characteristic steeply dipping loads described by Jones (1922) as wall-like ore bodies, adjacent to which shafts were sunk in order to work the ore-bodies. The mineralization was the result of periods of tectonic activity that caused the migration of hydrothermal fluids which were responsible for episodes of fracturing and brecciation.

The Yswyth Fault is an ENE trending fault that cross cuts the anticline and thus through the Frongoch site. The fault is mineralized with two galena rich lodes that are separated by barren rock consisting of an intrusive breccia and the formation also contains phosphatic pockets. Those two branches, namely the north and south loads, extend the length of the mine (Bick, 1996) and later stage mineralization contains assemblages of widely spaced fragments of quartz. This late stage deposit occurs at both Frongoch and Ystumteun (Mason, 1997).

4.3.4 Mine Water Chemistry

During the course of this project the author measured the adit discharges mine water to the south of the site as having an average flow rate of about 200 L/min (Figure 20) and a circumneutral pH with very low Fe concentrations

<0.01 mg/L. The main element causing environmental quality standards failure is Zn. Figure 2 shows that Zn remains soluble in the pH for Frongoch water and Zn is predominantly present in the dissolved Zn(II) state. The average concentration of Zn in the mine water is 12–15 mg/L. Fe concentrations are very low at Frongoch, which eliminates co-precipitation reactions that might otherwise aid in the removal of Zn.

4.4 Parys Mountain, Anglesey, North-Wales

4.4.1 Location

Parys Mountain, grid reference SH 443 903, former copper mine, is situated 2.5 km south of the coastal town of Almwch, Anglesey, Wales. The mine covers an area of approximately 2.5 km² and lays at 147 m above sea level at the highest point on the Isle of Anglesey, North West Wales (Figure 21).

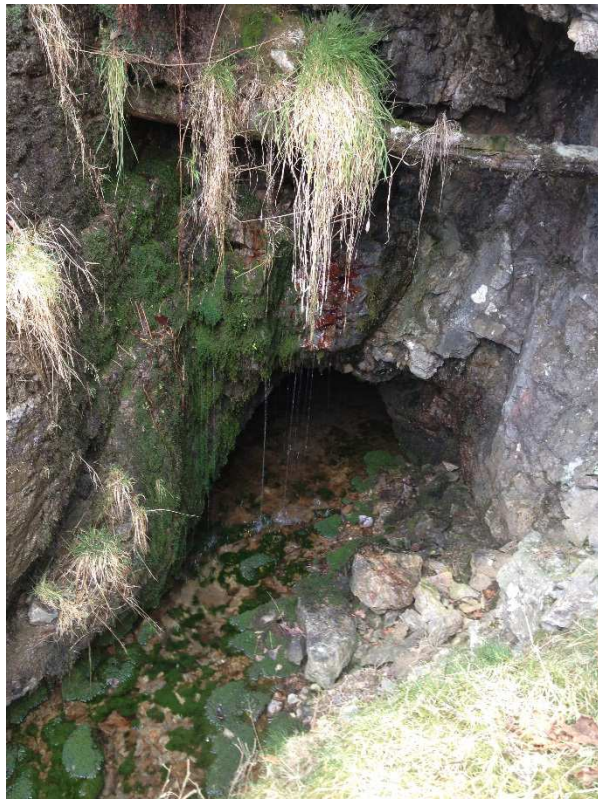


Figure 20: Adit and manmade channel at the Frongoch mine site. Width of adit approximately 1 m.

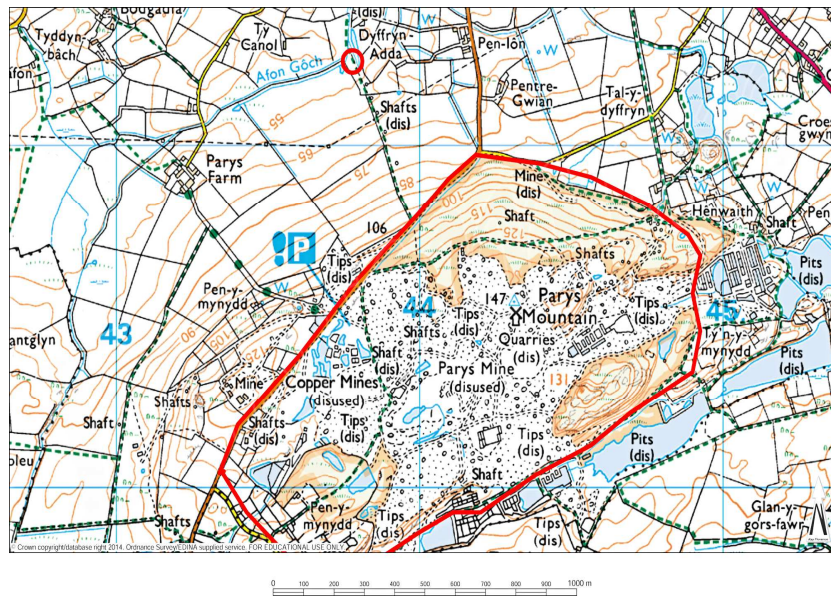


Figure 21: Boundary of Parys Mountain copper mine. Red circle indicates the north Dyffryn Adda (north adit) where water from the mine drains into the Afon Goch North. © Crown Copyright/database right 2014. An Ordnance Survey/EDINA supplied service.

4.4.2 Mining History

Parys Mountain constitutes an industrial archaeological monument of international importance (Countryside Council for Wales website). There is evidence to suggest that the mine has been worked for copper since the Bronze Age and it is widely thought that the site was also mined by the Romans (Ixer and Budd, 1998). In historical times, the site has mainly been exploited for copper ores but zinc and lead were also mined (Bearcock, 2007). The main period of extraction did not commence until 1760. Peak production was reached in the late 18th and early 19th Century at which time Parys Mountain dominated the global copper market as the biggest copper producer in the world, extracting approximately 3000 tonnes annually (Pearce, 1994).

Underground production ceased in the 1880's and by 1920 mining had stopped completely (Fuge et al., 1994). Cu was still being extracted as a precipitate from mine waters that were passed through brick lined tanks containing Fe metal. This method recovered 50% of the Cu after smelting, but it was however considered very labour intensive and the process did not continue past the 1950's (Ríos et al., 2008).

In 1995, 5.5 million tonnes of Zn, Cu and Pb reserves were discovered after the site had been acquired by Anglesey Mining Exploration Limited. Since then, the site has changed hands a number of times. More recently (1985), it was owned by Anglesey Mining plc who were responsible for sinking a deep exploratory shaft with a view to future production should economic conditions permit (Pers comm., Pearce, Perkins, 2009). There has been little activity over the past twenty years but intensive exploration is still ongoing by Anglesey Mining Exploration Limited since 2012 (Wales Online, Aug 02 2013 17:35). Recently, it was announced through the London Stock Exchange (2 July 2014 LSE:AYM) that Micon International Limited, who is reviewing the deposit's economic value, will finish the report about Parys mountain's mineral potential shortly and that this will enable better future planning for Zinc mining there.

4.4.3 Geology

Parys Mountain is the most famous mineral deposit in Wales, where volcanogenic ores have been described as Kuroko-type deposits due to their similarity to the exhalative deposits found in Kuroko in Japan (Swallow 1990 in Bearcock 2007). The main sulphide minerals present are pyrite, chalcopyrite, arsenopyrite, galena and lead. The Zn-Pb-Cu sulphides are characterized by the occurrence of concordant massive to banded sulphide lenses formed during the late Ordovician (Barrett et al., 2001) by the circulation of hot (170–300°C) mineralizing fluids on the sea floor (Pearce, 1993). These lenses occur at and near the contact between Ordovician shales and overlying rhyolites. Parys Mountain is the only example of a volcanic associated massive sulphide type deposit (VMS) in Britain and therefore attracts many visitors.

4.4.4 Mine Water Chemistry

Parys Mountain is a very sparse, poorly vegetated site, where evidence of past mining can be clearly seen. The mine is littered with spoil heaps and the country rock is exposed to weathering. Minerals within the spoil heaps are easily oxidised, and the oxidation of pyrite and other sulphidic minerals are catalysed by the presence of acidophilic bacteria found at the site. Walton and Johnson (1992) found various species of iron and sulphate oxidising bacteria contributing to the formation of AMD: *Acidithiobacillus thiooxidans* (sulphur oxidisers), *Acidithiobacillus ferrooxidans* (sulphur and ferrous iron oxidisers) and *Leptospira*

rillum ferrooxidans (ferrous iron oxidisers). Combined with the low neutralising capacity of the host rocks, these spoil heaps leach a characteristic low pH 2.5, ferruginous, metal and sulphate rich mine water. Initially, there were lakes in the bottom of the Great Opencast and water from the mine drained into both the Afon Goch North and from the south-east into the Avon Goch South both of which were heavily impacted by the mine drainage, hence the translation from the Welsh 'Avon Goch' being 'red river' (Fuge et al., 1994, Pointon and Ixer, 1980, Walton and Johnson, 1992).

In summer 2003, a dewatering project was implemented by the Environment Agency; this included the dewatering of the lakes in the Great Open Cast. Drainage was then directed towards the Dyffryn Adda adit draining the mine from the North section of the site to the sea at Amlwch.

Rees (2005) reported that the water discharging from the Dyffryn Adda Adit contained SO_4^{2-} as high as 3020 mg/L, Fe often <500 mg/L and concentrations of up to 58.5 mg/L, 0.2 mg/L, 0.4 mg/L and 44.4 mg/L for Zn, Cd, Pb and Cu respectively, with a pH typically between 2.67–3.08. As such, Parys Mountain is considered a notorious producer of what might be considered typical 'AMD'. Traditionally, the treatment of such waters is conducted by adding substances (such as lime) to increase the pH and encourage the co-precipitation of metals with Fe oxyhydroxides. Parys Mountain was chosen as a site to investigate the use of HFO as a remediation material and study the metal removal mechanisms which might indicate the practicalities of using a VFR at a low pH site other than Cwm Rheidol.

4.5 Ynysarwed, South-Wales

4.5.1 Location

The Ynysarwed mine is in the South Wales Coalfield located along the lower Neath Valley (SS 806 015) near Neath (Figure 22).

4.5.2 Mining History

Mining ceased at Ynysarwed in 1938. According to Evans et al. (2006), initially only minor ferruginous flow was discharged and the mine adit was maintained as a safety escape route for the nearby Blaenant mine which continued to oper-

ate until 1993. At this time, the pumps were switched off and the mines flooded, Ynysarwed being the main drainage point. The flow increased substantially thereafter and the water quality worsened (Ranson, 1999 in Bearcock, 2007).

4.5.3 Geology

The Rhondda Number Two seam was the principal coal seam that was exploited at this mine and was overlain by the Upper Coal Measures, which were mainly fluvial Pennant Sandstones with only a few unworked coal seams. The coal in this area contains 2–4% pyrite and thus has a high S content (Evans et al., 2006).

4.5.4 Mine Water Chemistry

Ynysarwed mine water is net acidic. During the initial stages of flooding, the mine released pH 3.5 water with peak flows of 36 L/s and the discharge was reducing with ferrous Fe concentrations > 400 mg/L recorded in 1994. This flowed directly into the Neath canal and required urgent remediation (Figure 4).

A hybrid/combined active and passive system was installed (Figure 22). Mine water flows from the adit to a well on the opposite side of the road, then pumped to a tank and aerated. Active lime and flocculent dosing was the next stage of treatment, was then passed through a lamellar plate clarifier and the cake sent to landfill. Thereafter, the water was directed approximately 0.5 km south west of the active plant through parallel settling lagoons as a final polishing stage before discharging to the River Neath. The long term decline in Fe concentration in the mine water was predicted and accounted for in the treatment scheme.

As the Fe concentration has diminished over time, so too has the acidity. In early 2000, Fe concentrations have reduced to 150 mg/L and at the time of writing this thesis, Fe concentrations are around 80 mg/L and the lime dosing plant is no longer in operation as it is thought that the wetlands are removing all the Fe. However, the wetlands have recently been reported as being saturated and blocked and therefore not functioning correctly, which is a characteristic maintenance issue. The active part of the treatment system is still in operation at the time of writing this thesis, although there are plans to discontinue use at some time in the future (Authority, 2009).

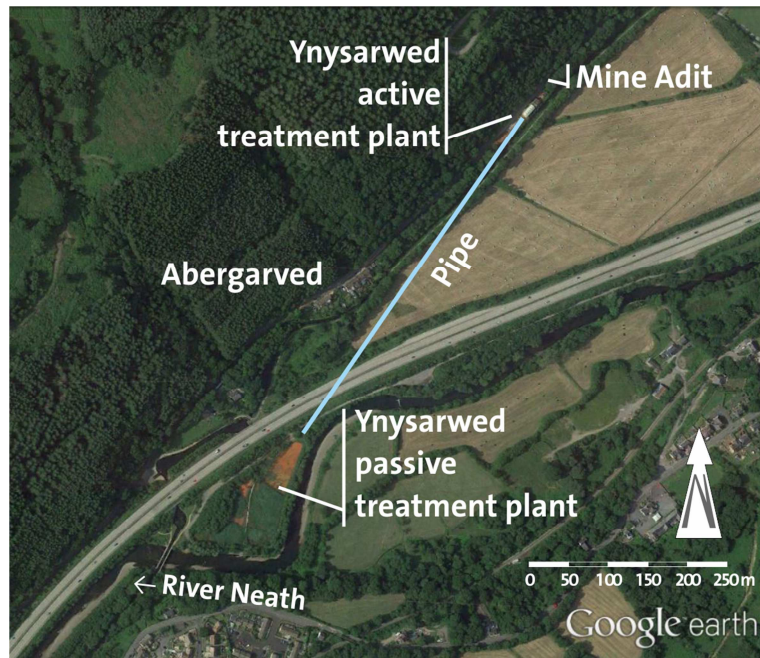


Figure 22: Location of the Ynysarwed active and passive treatment plants.

The mine water chemistry at this site was chosen for experiments using the advanced oxidation process (AOP) to remove ferrous Fe by rapid oxidation. Interesting in this regard are the other possible advantages of using electrochemistry for treating mine water such as improved settling times, less sludge volume and possible native Fe recovery from the treatment process.

5 Methods

5.1 Introduction

Until now, there has been no straightforward way to choose an appropriate treatment method for mine water. In most cases it is necessary to conduct field or laboratory experiments to identify a treatment option for a given mine water. In order to characterize the mine water chemistry at the sites in this study, and identify potential treatment options, numerous field and laboratory experiments were conducted (Table 6). They are described at the beginning of this chapter, in sections 5.2 to 5.8. Descriptions of those experiments are given in sections 5.10.5 to 5.10.10.

Focus of this thesis is the installation, operation, characterization and decommissioning of the VFR passive treatment system. All the field experiments conducted to reach this goal are described in sections 5.9 to 5.10.6.

Because the removal of Zn from the mine waters did not reach the expected removal rate, alternative methods for Zn and Fe removal were examined. This examination identified electrochemical methods (e.g. electrocoagulation) and advanced oxidation as potential treatment options for the investigated mine waters. Therefore, in addition to the passive VFR treatment method, electrochemical experiments were conducted and are described in section 5.11.

At the end of this chapter, the statistical methods used and the procedure for the chemical-thermodynamic modelling are explained (5.13 and 5.12).

.

Table 6: Experiments and methods conducted during the course of the project. Detailed explanations and reasons for conducting the tests are provided in the relevant chapters.

Experiment/Method	Cwm Rheidol	Parys Mountain	Ynysarwed	Frongoch	Laboratory	Field	Chapter
Oxidation	✓				✓	✓	5.10.5, 5.10.5.1, 5.10.5.2
Adsorption	✓	✓			✓	✓	5.10.7
Limestone	✓	✓			✓	✓	5.10.8, 5.10.8.1, 5.10.8.2
Agitation/Stirring	✓				✓	✓	5.10.9, 5.10.10
Centrifuging	✓				✓		5.10.11, 5.10.12
Microbiology	✓				✓		5.10.14
VFR hydraulics	✓					✓	5.10.15.2
Zinc titration					✓		5.11.4
Electrochemistry	✓			✓	✓		5.11, 5.11.1, 5.11.3
Advanced oxidation			✓		✓		5.11.2
Analytical methods							
ICP-OES	✓	✓	✓	✓	✓		5.2.12
IC	✓	✓	✓	✓	✓		5.2.13
Spectrophotometry	✓	✓	✓		✓	✓	5.3
Total digestion	✓		✓		✓		5.4
Sequential extraction	✓				✓		5.4.2
XRD	✓				✓		5.5
ESEM	✓		✓		✓		5.6.2, 5.6.3
CS analysis	✓				✓		5.7
On-site parameters	✓	✓	✓	✓	✓	✓	5.10, 5.10.1

5.2 Laboratory Methods

5.2.1 Laboratory pH, ORP, Temperature

Hanna combination meters HI-9828 were used in bucket experiments that were conducted in the laboratory and were calibrated prior to use as per the method described. For Bench scale experiments, pH was measured using a Metler Toledo InLab Pro pH-probe with integrated temperature compensation. This instrument was calibrated using a two point calibration (pH 4, 7) using manufacturers recommended calibration solutions before each set of experiments. The ORP probe on the Metler Toledo instrument was an LE510 redox probe with a platinum pin. The electrode was standardised using a reference solution and the offset value of the probe measured as the relative reduction potential (Rel, mV). An adjustment based on equation 33 was added to the Rel. mV reading to give the true ORP measurement.

5.2.2 Sample Collection, Preservation and Storage

Samples collected during experiments in the lab were handled in precisely the same way as for field samples (section 5.10.1).

5.2.3 Laboratory Glassware and Equipment Decontamination

Glassware and reusable laboratory equipment such as pipette tips, watch glasses and crucibles used in all laboratory experiments, was washed with laboratory grade detergent prior to soaking in an acid bath of 10% (v/v) HNO₃ solution for 24 h. After this treatment, they were rinsed three times with tap water and subsequently three times using deionised water and left to air dry on clean paper towels before use.

5.2.4 Electrical Transformer for Electrocoagulation (EC) Experiments

To conduct electrocoagulation (EC) experiments, a Consort® D.C. EV261 Transformer was used. The transformer uses a floating voltage whereby the conductivity of the sample dictates the voltage which is drawn to maintain a fixed current set on the instrument. The current can be used at 1–8 A. The amperage required was set depending on the type of experiment Anode and Cathode Materials

In the electrochemical experiments, general purpose iron and steel metal strips supplied by Fisher Scientific were used. The dimensions of these electrodes was $20 \times 1.5 \times 0.1$ cm. Fe electrodes supplied by Hydro Industries are of a standardized size $20.6 \times 3 \times 1$ cm whereas the Al, Cu, Pt coated Ti electrodes, also supplied by Hydro Industries, were $20.6 \times 3 \times 0.3$ cm. Electrodes were cleaned with 30% (v/v) HCl, then rinsed under tap water, followed by deionised water between each experiment to ensure no cross contamination occurred and to remove any scale or build-up on the electrode surface.

5.2.5 Graded Glassware and Laboratory Equipment

Grade A glassware was used in the preparation of chemicals where the volume was critical to the accuracy of the procedure. Grade B glassware was used in bench scale experiments. Consistency was kept throughout, for example, if three beakers were used in stirring experiments, the same grade of glassware would be used for each beaker.

5.2.6 Sample Acidification

To make up the 20 (v/v) % HNO_3 acid for acidifying samples, 20 mL of concentrated nitric acid was added to 80 mL of deionised water in a volumetric measuring cylinder; the cylinder was inverted ten times to ensure sufficient mixing and labelled as a stock solution of 20% (v/v) HNO_3 . This was used for acidifying field and laboratory samples for the ICP-OES as described in section 5.10.1.

5.2.7 Sample Storage and Preparation of Synthetic Mine Water

Cwm Rheidol and Ynysarwed waters are high in Fe which precipitated rapidly after collection. Therefore, when possible, experiments were carried out in the field or on the same day as the mine water was collected in order to keep conditions as close to the natural environment as possible. On occasions when mine water had to be stored, it was kept in the dark at 4°C until required, at which time it was left to reach ambient temperature before starting test work. Fe concentrations at Frongoch are <1 mg/L and the pH is circumneutral. For this reason, the water chemistry did not change noticeably and it was considered acceptable to store it until needed for experiments. For the early electrochemical experiments, synthetic mine water was used to represent the discharge at Frongoch. A 1000 mg/L stock solution was prepared by accurately weighing

4.398 g of $\text{ZnSO}_4 \cdot 7\text{H}_2\text{O}$, adding to 1 L of deionised water in a volumetric measuring cylinder and inverting to mix. The stock solution was kept in a sealed round bottom flask. From this, the dilutions were made to the desired concentration of 12 mg/L to represent the total Zn concentration found in the Frongoch mine water samples

5.2.8 Buffer Solutions

pH buffer solutions were purchased from the manufacturer 'Hanna' in compliance with the operating instructions for the Hanna combination meters HI-9828 and the laboratory instruments. Fresh buffer solution was used each time instruments were calibrated. Remaining solution was stored in the cool and dark. Only solutions that were within the expiry date were used.

5.2.9 Laboratory Grade Chemicals

All chemicals used in this thesis were laboratory grade from either Fisher Scientific or Sigma Aldrich. Chemicals were stored and used as per the issued MSDS sheets. For the Fe(II) analysis, 2,2 Bipyridyl, acetic acid, potassium chromate were used.

5.2.10 Deionised Water

High purity 18 M Ω deionised water was collected from dispenser in the laboratory directly into decontaminated containers for use in both the laboratory and the field work, as required.

5.2.11 Alkalinity

Alkalinity was measured with a Hach Digital Titrator as described in section 5.10.1.

5.2.12 Cation Analysis: Inductively Coupled Plasma Optical Emission Spectrometry

Inductively Coupled Plasma-Optical Emission Spectrometry (ICP-OES) is a method used for the detection of trace metals. The solution is aspirated into very high temperature plasma. It uses inductively coupled plasma to excite the atoms which produce a signature wavelength of light. This emission is then detected by the spectrometer which can determine the intensity and therefore the concentration of the elements (Mermet et al., 2004).

The instrument is useful in that it is able to analyse multiple elements at the same time. Throughout this thesis, ICP-OES was used to determine the concentrations of metals and semi-metals and the instrument used was a Perkin Elmer Optima 2100DV ICP-OES with AS90 plus auto-sampler using WinLab 32 software. Analysis was conducted by trained staff in the CLEER laboratories at Cardiff University. For the VFR work, analysis was for Fe, Zn, Cd and Pb. An initial full suite of metals/semi metals (As) were analysed on each of the mine waters to determine the background chemistry for use with chemical-thermodynamic software for geochemical modelling purposes. The instrument was calibrated using three calibration standards to construct a calibration curve used to cover the detection range required for expected concentrations in samples. Standards are made up from certified analytical standards quoted by the manufacturer as being within $\pm 0.2\%$ of the stated concentration. The standards and an analytical blank of 2% (v/v) HNO₃ in deionised water were analysed after every ten samples to check for drift in analysis.

5.2.13 Anion Analysis: Ion Chromatography

Unacidified water samples were analysed for nitrate (NO₃⁻), chloride (Cl⁻) and sulphate (SO₄²⁻) using ion chromatography. The instrument used was a Dionex[®] ICS-2000 Ion Chromatography System with a Dionex ionpac[®] AS11-HC column and samples were loaded into a Dionex[®] AS40 auto sampler. Analysis of samples was against a set of synthetic standards used to determine peak area values from which to construct a calibration curve. The curve gives a straight line equation; re-arranged appropriately, this was used to work out the concentration from the peak area value quoted by the instrument. The equation is used as follows, where Peak area = slope × concentration + intercept. Therefore, (volume - intercept) / slope = concentration in $\mu\text{g mL}^{-1}$. Any dilution factor was multiplied up at the end of the calculation.

Analysis was carried out by technicians at the CLEER laboratories. Analytical blanks of deionised water were regularly analysed. Samples that were out of range of the instrument were diluted where necessary using deionised water and re-analysed. It was possible in some instances, to re-integrate results that gave unusual peaks using the instrument's software.

5.3 Spectrophotometry

5.3.1 Introduction

Spectrophotometry is an analytic method that measures the intensity of light of a specific wavelength passing through the sample. A colour complex is used and when photons of light encounter the analyte molecules, they are absorbed, thus reducing the intensity of the beam through the sample. Absorbance (the measure of light intensity) is related to concentration in the sample as expressed by the Beer-Lambert Law in equation 27:

$$I_t = I_o \times e^{-kct} \quad [27]$$

I_t = Intensity of light – intensity of transmitted beam

I_o = Intensity of incident beam (intensity of radiation of particular wavelength)

k = Constant

c = Concentration/ colour intensity of the solution

t = Thickness of the vessel the light passes through

For this study, spectrophotometry was chosen to determine concentrations of Fe(II) in samples. Two instruments were used by the author: when available, a portable Merck SQ NOVA60 spectrophotometer with appropriate Spectroquant® Fe test kits for filtered Fe(II) concentrations. This instrument has the advantage in that it is small, convenient to use on site and gives an instant reading for concentrations of Fe(II), Fe total and Fe(III) by applying equation 28:

$$[\text{Fe}_{\text{total}}] - [\text{Fe(II)}] = [\text{Fe(III)}] \quad [28]$$

The test cells use 2,2' bipyridyl as the complexing agent, which is the common method used to distinguish between Fe(II) and Fe(III) species in natural waters (Heaney and Davison, 1977). Test kits are supplied with a blank to calibrate the instrument prior to analysis for Fe.

1 mL of filtered sample was added to the Spectroquant® Fe test cells which have a working range of 0–50 mg/L. From one sample. Where samples exceeded this concentration, a 1:9 dilution was made using deionised water. Results of filtered

Fe total measured by this method were compared with ICP-OES measurements for filtered Fe total to assess the accuracy of the instrument.

When the portable instrument was not available, samples were acidified with HCl and analysed in the laboratory using a Hitachi U1900 spectrophotometer. Samples not analysed on the same day as collection were stored at 4°C and analysed the following day, or frozen for analysis as soon as possible if longer than one day.

To calibrate the instrument, a series of Fe(II) standards 2, 5, 10, 20, 30, 40, 50 mg/L were prepared (as described in section 5.3.2), the instrument reading was first set to zero using a zero standard solution, the standards were then measured and plotted to construct a calibration curve used to calculate the concentrations in the samples. The wavelength was set at 520 nm.

2 mL of sample for Fe(II) analysis that were pre acidified with HCl were added to 5 mL of an ammonium acetate buffer (AWWA, 1998) which contained two drops of 2'2-bipyridyl solution and thoroughly mixed. 2 mL of the mixed sample in the buffer was then added to a 1.5 mL semi-micro cuvette, the absorbance was measured at 520 nm and the reading calculated as concentration of Fe(II) in that sample using the equation from the calibration curve.

5.3.2 Preparation of the Fe(II) Secondary Standard

All glassware was decontaminated as per the method described in section 5.2.3. 10 g/L Fe(II) stock solution was made up by dissolving 49.752 g of Fe(II)SO₄.7H₂O in 1 L of 1.3 molar H₂SO₄, then transferred to a dark coloured glass bottle and stored in the fridge at 4 °C. An acid solution is necessary to maintain the pH below 2 to slow down oxidation and the dark cool conditions prevent photo redox effects.

The Fe(II) secondary standard was made by diluting the stock solution by 50% with 1.3 Molar H₂SO₄ by pipetting 50 mL of the secondary standard into 100 mL grade A volumetric flask and making up to 100 mL with the 1.3 Molar H₂SO₄. This was calibrated using K₂Cr₂O₇, which was prepared by adding 12.285 g of the solid (which had been oven dried at 60 °C until the mass was constant) to

100 mg of deionised water. This was stirred at 100 rpm for 24 h. The calibration of the secondary standard was as per the method described (AWWA, 1998):

- 1) 3×25 mL of the 41.69 nM $K_2Cr_2O_7$ standard was added to a conical flask using a class B volumetric pipette and stood in the fume cupboard.
- 2) 75 mL of deionised water followed by 30 mL of concentrated H_2SO_4 was added to each flask in 10 mL aliquots, swirled and left to cool to room temperature.
- 3) 3 drops of 1:10 dilution ferroin redox indicator 1:10 were prepared (AWWA, 1998) by adding 1.485 g 1.10-phenanthroline monohydrate and 0.695 g of $Fe(II)SO_4 \cdot 7H_2O$ to 100 mL of deionised water and added to the cooled $K_2Cr_2O_7$ solutions.
- 4) The $K_2Cr_2O_7$ solution was used to standardise the 50% secondary standard by titrating each of the three flasks through the orange/green transition ($Cr_2O_7^{2-}$ to Cr^{3+}) to a dark colour, marked as the ferroin end point, using a 50 mL burette.
- 5) A set of 100 mL calibration standards were made up in class A volumetric flasks by diluting the initial 1 in 200 $Fe(II)$ secondary with 1.3 molar H_2SO_4 . 2, 5, 10, 20, 30, 40 and 50 mg/L standards were made.

Each of the standards were analysed as described in section 5.3. A calibration curve was constructed, using a linear correlation to determine the concentration of Fe^{2+} in samples.

5.3.3 Solutions used for $Fe(II)$ Analytical Method

The following chemicals were used in the preparation of the $Fe(II)$ standards for analysis of Fe^{2+} using the Hitachi U1900 spectrophotometer:

- 1.3 molar solution of HNO_3
- 0.2 molar solution of HCl
- Ferroin indicator
- Ammonium acetate buffer solution
- Potassium dichromate $K_2Cr_2O_7$ standard solution
- 2,2' bipyridyl: 1 g of 2,2' bipyridyl
- $Fe(II)SO_4$ (used for the secondary standard)

5.4 Chemical Investigation of Sludges

5.4.1 Total Digestion

To determine the chemical composition of the sludges, a portion of them was oven dried on a watch glass at 105 °C until there was no further reduction in mass (after approximately 48 h). 0.2 g of the dried ochre was ground and technicians at the CLEER laboratories digested the sample by adding 4 mL of 30 % HCl and 4 mL of 70 % HNO₃ (Aqua Regia) to the sample in a HR 100 pressure vessel. The sample was then heated in an Anton Paar Multiwave® 3000 microwave for 1 hour at 200 °C. An analysis of the sample was conducted by ICP-OES for Fe, Zn, Pb, and Cd.

5.4.2 Sequential Extraction

Sequential extractions were carried out by Marco Santonastaso at the CLEER laboratories, results of which are in Appendix 1. Their procedure was followed in order to determine the composition of the VFR sludge and the specific phases to which the constituents are bound (Table 7). Ochre used for the sequential extractions was collected 48 weeks after the system had been drained down to allow the bed to compact and naturally dewater. A section of the ochre was cut from the bed and taken such as to preserve any stratification (Figure 23). The sample was stored in a sealed plastic container and returned to the lab. A 6 cm vertical section was taken from the sample and divided into the top 2 cm, 2–4 cm and 4–6 cm.

Table 7: Phases targeted by the sequential extractions performed on the VFR ochre.

Terminology	Target Phases
Fe _{carb}	Carbonate Fe, including siderite and ankerite
Fe _{ox1}	Ferrihydrite, lepidocrocite
Fe _{ox2}	Goethite, akaganéite, hematite
Fe _{mag}	Magnetite
Fe _{PRS}	Poorly reactive sheet silicates Fe



Figure 23: Sludge sample from VFR for sequential extraction (diagonal 7 cm).

5.5 X-Ray Diffraction

5.5.1 Introduction

X-Ray Diffraction (XRD) was the method used for mineral characterisation of ochres from the VFR trial and the sludge generated during the EC experiments. A Philips PW3830 X-Ray generator, Philips PW1710 diffractometer controller and X Pert High Score plus software were used to obtain the diffractograms from the dried disaggregated samples. Diffractograms are the powder XRD pattern images of the sample which were compared to the software database for matches that can aid in mineral classification.

5.5.2 Sample Preparation and Measuring Procedure

Samples prepared for XRD were first dried overnight in the oven at 60 °C. Enough sample to cover a glass slide was required, approximately 2 g. Dried samples were finely ground using an agate pestle and mortar, sprinkled into the window area of the slide and covered with a glass plate.

Most samples were analysed with a 6 h scan time. However, some particularly amorphous samples were rescanned applying an additional 12 h scan.

5.6 Environmental Scanning Electron Microscopy

5.6.1 Introduction

The Environmental Scanning Electron Microscopy (ESEM) is commonly used to obtain images of a range of materials such as plants, microfossils, bacteria and minerals. The instrument is capable of producing images of magnification that greatly exceeds that of conventional optical microscopes. Recent advances in detector technology and vacuum control allow the ESEM to operate under low

vacuum conditions. The advantage of this is that it negates the need for samples to be dried and coated with gold. The use of a Peltier stage to cool samples makes it possible to image wet and possibly live samples. X-rays that are generated when the electron beam hits a specimen can be collected for element analysis (Philips Electron Optics and Johnson, 1996).

5.6.2 ESEM Principles

A stable beam of electrons are extracted from a field emission gun (FEG) which is composed of a very fine single crystal tungsten tip at high temperature electric field between the tip and the first anode. An additional anode then accelerates the electrons to the required accelerating voltage. The electron beam focuses to a fine point series of electromagnetic lenses and fine apertures down the column and then directed by a set of scanning coils which move the electron beam over the specimen as in conventional SEM.

The low vacuum system attributed to the ESEM means that the instrument can work in conventional 'high vacuum' as well as low vacuum and environmental 'wet' mode. The ESEM instrument uses a vacuum pumping system to alter pressure gradients between the electron gun column and the sample chamber. In the sample chamber, high pressure conditions are achieved using an imaging gas such as water vapour or nitrogen. Pressure in the chamber when in ESEM 'wet' mode varies between 133 and 2666 Pa and water vapour is the auxiliary gas releasing further secondary electrons.

The signal is detected using a gaseous secondary electron detector (GSED) which used gas ionisation to detect and amplify the signal to produce information about the sample. The different radiation signals are processed such that the secondary electron signal is amplified to determine the image topography. Amplification of this signal produces a picture of the sample surface that can be displayed on a monitor.

In conventional SEM, the sample is irradiated with electrons. To produce a complex signal consisting of secondary electrons, X-Rays (characteristic of the sample materials, thus used for chemical characterisation) and electrons of low energy are accelerated from the sample towards the detector.

5.6.3 Analytical Procedure for the ESEM Analysis

ESEM was used in this research to examine the mineralogical structure of the precipitates from both the VFR and the precipitates formed by electrochemical techniques. Samples were analysed by the author at Cardiff University School of Earth Ocean and Planetary Sciences. The instrument used was a FEI XL 30 FG Environmental Scanning Electron Microscope (ESEM) with a Peltier cooled specimen stage using Oxford Instruments INCA ENERGY x-ray analyser.

Samples were dried at 60 °C until no further loss in mass was observed prior to analysis, the samples were then mounted on self-adhesive 12.5 mm pin stubs and coated with a layer of carbon and analysed.

5.7 CS-Analysis

A LECO furnace model SC-144 DR was used to determine the Carbon and sulphur content of ochre samples (CS-analysis). This is important because it partly characterises the composition which was used in conjunction with ESEM images and data and the XRD data to help classify the mineralogy of the ochre. The LECO furnace instrument is accurate to within $\pm 10\%$.

Fresh ochre from the VFR was dewatered and dried overnight at 60 °C. The ochre was ground to a fine powder using an agate pestle and mortar. 0.350 g of sample was accurately weighed and the weight recorded to 3 decimal places. The sample was added to a foil boat and placed into an open ceramic crucible. The instrument was set to operate at 1300 °C and a baseline reading established. The crucible containing the sample was manually loaded into the furnace and the instrument set to determine the sulphur and carbon content using compatible Laboratory Information Management System (LIMS) software. The results are displayed as the % total sulphur and carbon found in the 0.350 g of sample.

5.8 Terminology for Filtered/Unfiltered/Total Concentrations

Throughout this thesis, Fe and Zn measurements are made in a number of ways. Each method is relevant to determining the concentration of Fe(II), Fe(III) and/or Fe(total) or Zn. Table 8 gives the definitions for those measurements in terms of Fe species and what specifically is meant by filtered, unfiltered or total.

To prevent confusion, the term ‘dissolved’ as commonly used for filtered samples is not used in the thesis.

Table 8: Description of terminology used within this thesis. All filtered samples filtered through a 0.2 µm filter.

Terminology	Merck NOVA60 spectro- photome- ter	Hitachi U1900 spectro- photome- ter	Perkin Elmer Optima 2100DV ICP-OES	Dionex® ICS-2000 Ion Chroma- tography
Fe(II) filtered	✓	✓		
Fe(II) unfiltered		✓		
Fe total filtered ¹	✓		✓	
Fe total unfiltered			✓	
Fe(III) filtered ²	✓			
Cations Zn, Pb, Cd, Mn, Al, Cu, Ca, Mg not speciated, therefore quoted as total (of any species of particular element) in both filtered and unfiltered samples			✓	
All anions SO ₄ ²⁻ , Cl ⁻ are filtered				✓

¹Fe total = Fe(II) + Fe(III); can be either filtered or unfiltered

²Fe(III) = Fe total – Fe(II); see equation 28

³the same terminology as described for Fe is used for Zn

5.9 Design and Construction of the VFR

5.9.1 Design Criteria

Various criteria were necessary in the design and placement of the Cwm Rheidol VFR. Most importantly, the system needed to be entirely passive as the site has no basic infrastructure, such as power. Consequently, the VFR needed to be a gravity fed system. It was also important to ensure that no reactive materials were used in its construction to exclude potential interference with the anticipated removal mechanisms. To exclude interference with the ochre bed by turbulent flow of the feed water, and to ensure a continuous build up of ochre, the inflow pipe needed to be fitted with a valve in order to control the flow.

Fe oxidation rates were unknown at Cwm Rheidol and it was therefore unknown what residence time might be required. Inflow, outflow and driving head height needed to be adjustable so that the system could be brought into steady state after the initial filling phase. It was important that all parts and connections within and to the VFR were easily accessible so that regular maintenance,

potential alteration and necessary repairs could be carried out. Security and accessibility to the VFR as well as the discharge point were also necessary for regular sampling and overall long term running of the system to continue without interference or vandalism.

5.9.2 Tank Construction

The system was adapted by the author and Peter Florence from the original design used in initial field trial at the Taff Merthyr site in South Wales (Sapsford et al., 2006), using a 1 m³ intermediate bulk container (IBC) adapted to become a VFR treatment tank. The principle of the design was also used by Geroni (2011) at Ynysarwed although on a smaller scale. A gravel bed layer is in the base of the tank upon which ochre is allowed to build up from the flow through of mine water. As this layer builds up and the permeability of the bed decreases, the inflow needs to be adjusted in order to prevent the system from overflowing. A down flow of mine water is then maintained through the water column and through the ochre bed (Figure 24).

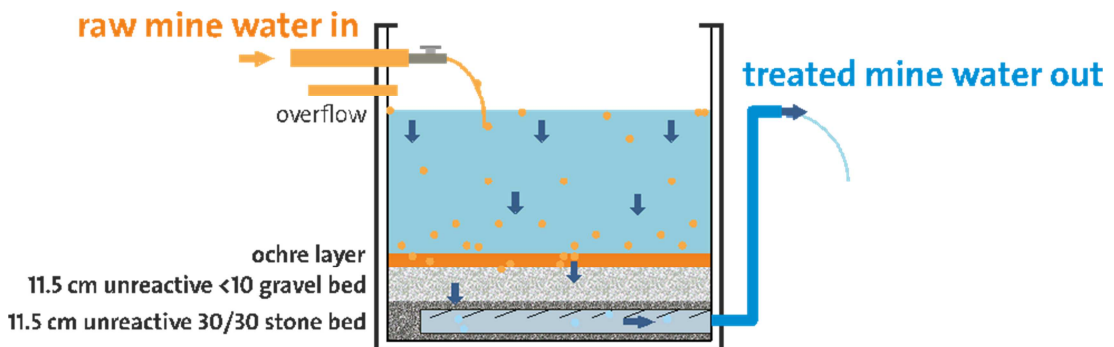


Figure 24: Schematic of the VFR pilot plant used in the field trial at Cwm Rheidol.

For the Cwm Rheidol VFR, the top section of a 1 m³ ICB was completely removed and the inside of the container cleaned using laboratory grade phosphate free surface active cleaning agent (Decon 90) and thoroughly rinsed with water. The procedure was repeated twice to ensure the inside was appropriately decontaminated.

IBC's have an outlet at the bottom of the tank which has a standard fitting which can be opened and closed manually. A length of hose was fitted to that outlet valve to act as a swan neck mechanism so that the head height of the water

within the container could be adjusted; the height was set to 755 mm from the bottom of the container as shown in Figure 24. Towards the end of the trial, the swan neck height was halved in order to reduce the retention time. Inside the tank, a length of coiled drainage pipe attached to the outlet valve was installed. The drainage pipe used was typical farming drainage pipe, which has narrow diagonal slots cut into it; these slots would allow the treated water to be collected and directed up through the swan neck outlet.

30 mm angular coarse grained siliceous chips were added to the container to secure the pipe and provide a stable base on top of which a 200 mm depth layer of 5–10 mm grain size siliceous gravel was added (Figure 25). The slots in the coiled drain pipe were too narrow to allow the chips or gravel to fall through. This formed the filter medium base for the VFR. Gravel and stone chips were sourced from B&Q DIY store in Cardiff and tested prior to use to ensure that they were nonreactive. If limestone chips/gravel were used, then the potential metal removal might have been due to the neutralisation of the AMD by CaCO_3 .

Initially, the inflow was directed through a perforated container in order to distribute the flow energy more evenly over the bed. This was to ensure the least amount of disturbance of any build-up of ochre precipitates in the early stages as it would start to accumulate in the base of the tank. It would also aid in that layer being more evenly distributed once full.



Figure 25: Left is the coiled drainage pipe to the outflow. Right is the gravel layer placed on top of the pipe and the coarse gravel layer.

5.9.3 Connection at the Adit

To direct the mine water from the lower number 9 adit to the tank, a funnel was constructed from a 5 L plastic container. This was fixed to the discharge pipe using plastic cable ties (Figure 26).



Figure 26: Cwm Rheidol mine water discharge pipes; Left: Is the set up for piping water from the lower number 9 discharge pipe to the VFR. Right: The discharge point of both upper number 6 and lower number 9 adits.

20 m of 20 mm Alcatene pipe connected to the bottom of the funnel was trailed down from the adit, under the road and along the purpose built channel where a mixture of both the upper and lower adit mine waters flow. The pipe was fitted with screw lock connectors every 5 m so that it could be deconstructed in sections for cleaning should it become blocked with sediment, fallen leaves, organic debris, detritus from the surrounding environment or directly from the adit. A header tank was placed half way between the adit discharge point and the VFR pilot plant. This was to maintain a driving head above the height of the VFR so that the system could remain gravity fed and therefore entirely passive. The header tank was constructed from a compost barrel with an inflow pipe for raw mine water and an outflow and overflow to maintain the head height in the tank. An outflow pipe was connected from the header tank to the VFR tank by drilling a hole in the side of the tank as close to the top as possible.

5.9.4 Inflow

Initially, a perforated container (Figure 27 left) was used to distribute the inflow water evenly over the bed. After two weeks a layer was beginning to form. However, the decision to fill the tank was made as a 'look see' experiment, to see any Fe oxidation/precipitation would occur within the water column leading to accretion on the gravel bed. For this, a ball and 30 mm valve tap was fitted

so that the inflow water could be controlled. Provisions were made for the tap to be easily removed for cleaning (Figure 27 right) once the tank was filled, the flow rate into the tank was regulated using the tap.



Figure 27: Initial stages of filling the VFR. Left: Shortly after seeding the VFR; right: First time filled VFR plus inflow pipe.

5.9.5 Overflow

An overflow was drilled approximately 6 cm below the inflow connection. This was to ensure that the tank would not overflow should there be any sudden increase in flow due to either high rainfall events or restriction on the outflow rate due to blockage or decreased permeability.

5.9.6 Position of the VFR at Cwm Rheidol

Cwm Rheidol has the advantage of having a secure enclosure parallel to the river. This is the location of the former, now abandoned limestone beds. The VFR was ideally placed within this enclosure which sits topographically well below the mine adit, thus providing a natural downward flow of mine water from the discharge pipe into the VFR (Figure 28). The area has a purpose built hard standing level platform where the VFR was placed. Untreated mine water discharging from the adit flows along the open channel to this point where the VFR was located and is left to overflow the side wall into the River Rheidol (Figure 29). There would be no additional pollution to the Rheidol if the VFR were to fail to treat the raw water passing through it.

The area is fenced off with locking gates and the surrounding landscape is well used by the public for recreational purposes. Security is important to prevent access to this potentially dangerous area. With permission from land owner and site managers, there is access for the vehicles to the site making the set up and

decommissioning of the VFR relatively straight forward. This was also useful when performing field experiments and for access when collecting regular samples and the collection of field testing data.

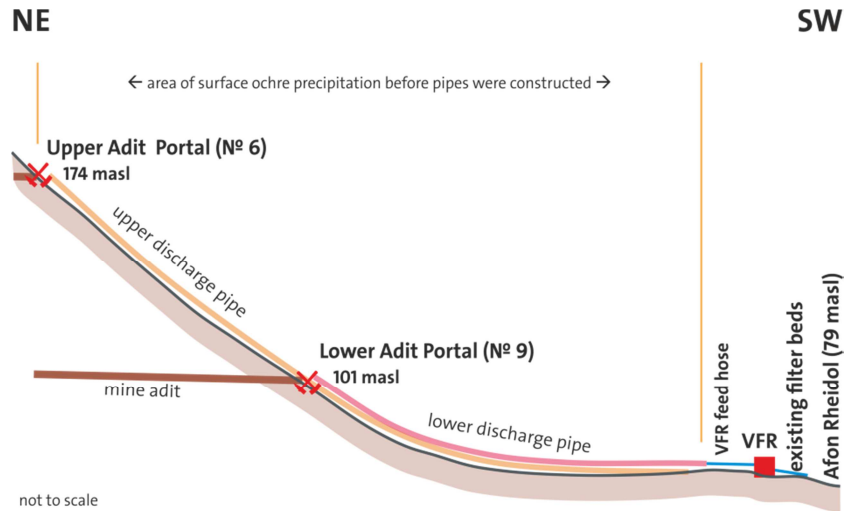


Figure 28: Schematic cross section of the upper number 6 adit and the lower number 9 adit and the location of the VFR at Cwm Rheidol. masl: meters above sea level.



Figure 29: Map showing the aerial position of the VFR at the old filter bed area at the Cwm Rheidol site. The orange line shows the feed pipe from the number 9 adit into the tank. Digimap ® – © Crown copyright/database right 2014. Ordnance Survey/EDINA supplied service. FOR EDUCATIONAL USE ONLY.

The VFR was placed alongside the pilot scale bioreactor that was installed by Newcastle University, as a step towards managing Zn pollution to the river Rheidol from the Cwm Rheidol mine. This project, managed by Natural Re-

sources Wales in partnership with the UK Coal Authority gained additional funding from Welsh Assembly Government and The European Union (Edwards and Potter, 2007). It was started in 2006 by form of diversion of the mine water from the adits, away from the spoil heaps to prevent leaching into the River.

5.9.7 Maintenance of the VFR During Operation

Maintenance of the VFR, particularly the unblocking of pipes that blocked with ochre precipitates, was carried out approximately every four weeks. This was done by backwashing each of the pipe sections using a generator and pump to transport water from the number 6 adit discharge pipe, which has a much higher flow rate and lower Fe concentrations, through the system. The ochre in each section was first loosened by rodding with a strong cable. Each section was then connected to the pump and flushed through until the pipe was clear. The system had to be temporarily stopped on these occasions. Once the pipes were cleared, the head height was re-instated and the flow regulated once more.

5.10 VFR Field and Laboratory Methods and Experiments

5.10.1 Water Sample Collection and Preservation

The same procedure for water sample collection in the field is used throughout this study. Where filtered samples are required, samples were filtered using disposable 0.2 μm Acrodisc PF syringe filters fitted to disposable Plastipak syringes. 0.2 μm filters are considered suitable for removing particles and bacteria from water samples. However, there is some discrepancy in the literature on what particle size is considered to be dissolved/colloidal (Ranville and Schmiermund, 1999, Shiller, 2003). New 30 mL sample containers were used each time and pre-contaminated three times by rinsing with the sample to be collected. Samples that contained Fe were filled to the very top to eliminate exposure to oxygen in the air and the lids replaced. Samples collected for ICP-OES analysis were acidified at the time of collection by adding four drops of 20% (v/v) HNO_3 with a plastic pipette. This was to stabilise the water chemistry by maintaining a pH below 2, at which all the metals analysed for this thesis are in solution, therefore preventing any metal precipitation and minimise sorption. ICP-OES analyses the total concentration in aqueous samples, not the speciation. It is therefore essential to ensure that there are no solids in the samples as

this will interfere with the operation of the instrument. Samples collected on site were placed immediately into a dark cool box and stored at 4° C until analysis was possible. Samples collected for Fe²⁺ analysis in the laboratory using a Hitachi U1900 spectrophotometer, were filtered and acidified with 20% (v/v) HCl as this is a non-oxidising acid. If samples for Fe(II) could not be analysed on the same day, they were frozen as soon as possible to avoid problems losing sample due to freeze expansion of the water only 15 mL of sample would be collected. Samples for ion chromatography analysis were filtered to remove any particulates but not acidified as the solubility of sulphate, chloride and nitrate is much higher than for the metals throughout the pH range of the samples collected in this thesis. This procedure also avoids spikes in the IC analysis.

5.10.2 Alkalinity Determination

Alkalinity was measured using a Hach digital titrator with a 1.6N H₂SO₄ cartridge as per manufacturer's instructions. 100 mL of sample would be collected in a vessel that was rinsed three times with the sample and the titrator controlled with one hand to add the alkalinity consuming acid whilst the other hand swirled the vessel. Alkalinity titrations were performed using bromocresol green-red indicator and the end point was determined by the colour change from green to pink. The units on the titrator are converted to concentration of mg/L CaCO₃ equivalents.

5.10.3 On-site Parameters

All field measurements were taken using Hanna combination meters HI-9828. The dissolved oxygen (DO), electrical conductivity and pH probes were calibrated at each site visit using the manufacturers calibration procedure set out in the operators manual. The meters were kept stored in their original cases, care was taken to ensure the pH/ORP probes were kept in wet in manufacturer's storage solution when not in use. For inflow and outflow measurements (spot measurements) a sample of the water would be collected in a beaker and the meter probe submersed in the sample. The DO Clarke sensor has a built in thermistor to allow for a stable temperature compensated reading within a few seconds. Measurements were recorded as soon as a reading was available as this parameter changes rapidly when the sample is isolated and exposed to the atmosphere. pH, ORP, temperature and electrical conductivity were recorded

once the reading had settled. When used in continuous logging mode, meters were set to log every ten seconds. The data was downloaded from the meters into the manufacturer's software from where it was exported into Excel spreadsheets. After each use, the probes were rinsed thoroughly in DI water. The accuracy of the pH probe is quoted by the manufacturer as ± 0.02 pH units. pH probes were calibrated against pH 4.01 and 7.01 manufacturer's buffer solutions. Accuracy of the ORP probe is quoted as ± 1 mV. The pH and ORP probe use Pt/PtO electrodes combined in a single gel reference electrode. To convert ORP into a true E_h value, a correction temperature and E_h correction using the equation in Wolkersdorfer (2008) was used.

The temperature probe is factory calibrated and quoted as being accurate to ± 0.5 °C. Electrical conductivity has a working range up to 400 mS/cm and quoted with an accuracy of $\pm 1\%$ of reading or 1 μ S/cm, whichever is greater.

The meters were regularly conditioned in the CLEER laboratories by standing the probes in a solution of oxalic acid and ammonium acetate used to complex and dissolve problematic build-up of Fe precipitates.

5.10.4 Sludge Sample Collection

Ochre (hydrous ferric oxide, HFO) collected from within the VFR, was scooped out using a bucket. Care was taken to ensure the least amount of disturbance of the ochre bed as possible. From the bucket, the ochre was partially dewatered by squeezing it through a muslin cloth and then transferred to opaque, Fisher-brand containers with a screw top lid. Samples were then stored in the dark in a cool box until returned to the laboratory where they would be stored in the fridge at 4 °C until ready to use. Once settled, the supernatant was poured off the top so the HFO was retained.

A separate sub sample of the sludge was returned to the lab to work out the ochre concentration in terms of weight per unit volume. A 5 mL sub sample of the dewatered ochre was dried until no further loss of mass was observed and weighed using an analytical balance. The mass in g was then used to work out how much ochre the sludge contained.

Sludge collected for solids analysis for the VFR at the end of the trial was carefully cut from the bed in sections to retain any possible banding or layering that might be present and transferred to a plastic Tupperware box with a lid. Samples were kept refrigerated as described for all other samples until required for further analysis.

5.10.5 Fe Oxidation and Adsorption Experiments

5.10.5.1 Field Experiments at Cwm Rheidol

The purpose of the Fe oxidation experiments carried out at the Cwm Rheidol mine was to determine if the Fe removal rate increased if the water was aerated with a submersible Whale® Water systems self-venting pump. The water was mixed vigorously in an open bucket for 2 h. Alkalinity titration performed at regular intervals throughout the experiment by collecting 100 mL samples of the mine water and titrating using a Hach digital titrator with 1.6N H₂SO₄ and bromocresol green-red methyl indicator used to determine the titration endpoint.

On site, a 10 L bucket was half filled with mine water from the lower number 9 adit discharge pipe. Sample containers were labelled in preparation for filtered and unfiltered samples that were collected every 10 min, acidified with four drops of 20% (v/v) HNO₃ and stored in a portable cold box for transportation back to the CLEER labs where they were analysed by ICP-OES for Fe total and dissolved concentrations. Two Hanna combination meters HI-9828 were calibrated on site and used to continuously log parameters: pH, ORP, electrical conductivity, DO and temperature.

5.10.5.2 Lab Experiments

To investigate the Fe removal mechanism when the iron rich mine water gets into contact with the VFR sludge, batch-wise rate experiments were carried out in the CLEER laboratory by the author with assistance from Dr Jennifer Geroni. These experiments were originally designed to study the oxidation rate of Fe(II) to Fe(III) but were amended once it became clear the Fe in the Cwm Rheidol mine water is already in the ferric state.

Mine water was collected as described above from the inflow pipe of the VFR and several litres of iron precipitates (ochre) from the sludge within the VFR. All other samples were stored at 4 °C in a temperature controlled secure facility in the CLEER Laboratory.

At the start of the experiment, the pH of the ochre containing water and the raw mine water was measured using Hanna combination meters HI-9828. An aliquot of partially dewatered ochre, large enough to produce a 500 mL beaker, was squeezed through a linen sack to remove excess water (Figure 30) and homogenised by stirring. Initial Fe(II) concentrations in the raw mine water were measured using a Merck NOVA60 Spectrophotometer.

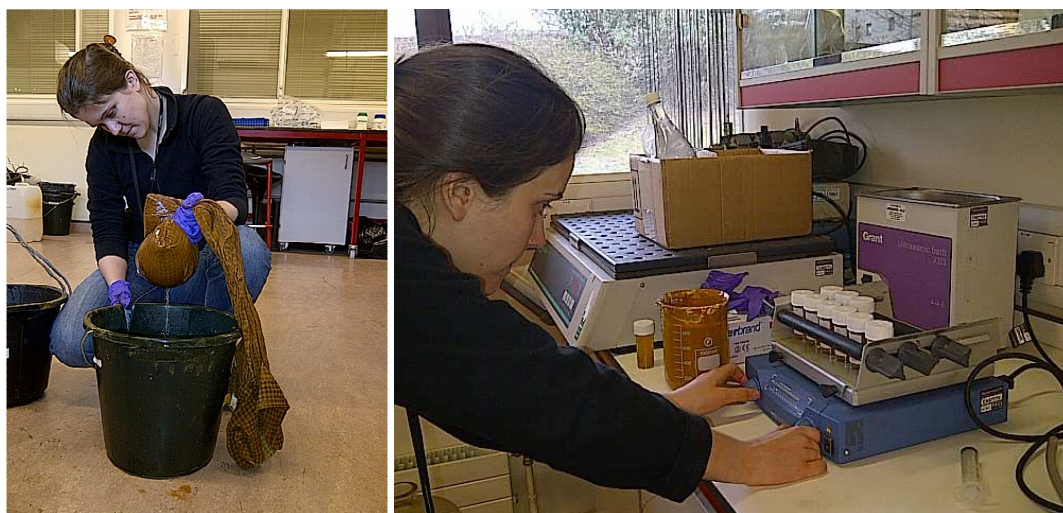


Figure 30: Left: partial dewatering of the ochre collected from the VFR at Cwm Rheidol; right: set-up of the laboratory Fe adsorption experiments on Cwm Rheidol VFR sludge.

New, unused sample containers were labelled and 20 mL of the raw water added to each sample container. 5 mL of the homogenised ochre was carefully measured using a syringe and added to each 20 mL of raw water. A horizontal shaker was set to 400 rpm and a timer started. Each sample was removed from the horizontal shaker at pre-determined time intervals for a 48 h period. Filtered samples were taken for spectrophotometric dissolved Fe(II) and Fe total analysis. Additional 0.2 μm filtered samples were collected and acidified for ICP-OES analysis in order to compare the results of the spectrophotometric analysis with ICP-OES analysis.

5.10.6 Determination of Volume of Dry Ochre

To determine the mass of the ochre in 5 mL of the homogenised decanted sludge used in the Fe oxidation experiments a 5 mL porcelain crucible was acid washed, dried and weighed using a laboratory balance. The mass was recorded to four decimal places. 5 mL of the homogenised, hydrated ochre was syringed into the crucible and the mass of the crucible with the hydrated ochre recorded. The mass of a 125 mm Fisherbrand® filter paper to be used to empty the dry contents onto was also recorded. The crucible with the wet ochre and the filter paper were dried in the oven at 60 °C until a constant mass was measured., this took approximately 60 h. Mass of the dry sludge was then calculated using recorded weights.

5.10.7 Fe Adsorption Experiments at Cwm Rheidol and Parys Mountain

These experiments were conducted in the field in order to determine if Fe would adsorb to solid ochre from the VFR. Cwm Rheidol was the first site. 8 L of raw mine water was collected in a plastic bucket from the lower number 9 adit discharge pipe. Several litres of the hydrated ochre were collected from inside the VFR tank.

The ochre was homogenised by stirring and stored in sealed plastic containers. 1 L of the ochre sludge was added to the bucket of raw mine water and stirred continuously using a submersible Whale® pump. Two Hanna combination meters HI-9828 were calibrated and left in the bucket to monitor pH throughout the experiment as shown in Figure 31. Filtered Fe(II) was measured in the field using a portable Merck NOVA60 instrument. Sample was appropriately diluted for use with 0–50 mg/L Fe test cells. Samples for Fe total Filtered and unfiltered were collected every 5 min for the first 15 min of the experiment then at 10, 15, 20, 30, 50 min with the final sample collected at 24 h. Samples were acidified and stored in a cold box for return to CLEER laboratories for ICP-OES analysis.

This experimental procedure was repeated at Parys Mountain. Ochre collected at Cwm Rheidol was taken to Parys Mountain. There, 8 L of untreated mine water were collected in a plastic bucket. Partially dewatered ochre from Cwm Rheidol was added at specific intervals. The filtered Fe²⁺ concentration were measured in the field using the Merck NOVA60 instrument, samples appropri-

ately diluted to keep within the range of the spectrophotometer. Filtered and unfiltered water samples were collected, acidified and stored cold as for ICP-OES analysis. Hanna combination meters HI-9828 were calibrated and used to log the parameters pH, ORP, electrical conductivity, DO and temperature throughout the 5 h duration of the experiment: Ochre sludge was added at three separate stages during the experiment, at the start, after 2 ½ h, and at 4 ½ h to evaluate the hypothesis that Fe is being removed either by adsorption to the HFO particles at low pH and/or by oxidation through aeration. The final sample was collected after 5 h.



Figure 31: Ochre from the VFR added to untreated mine water in adsorption experiments.

5.10.8 Limestone Experiments

5.10.8.1 *Open System Experiments at Cwm Rheidol*

To assess the effectiveness of the VFR at removing Fe upfront of a limestone bed, an onsite experiment was conducted using 8 L of treated mine water collected from the outflow of the VFR and contacting it with commercially available limestone chips. The principal was to evaluate if it would be possible to precipitate Zn and other metals by increasing the pH of the mine water through limestone dissolution followed by CO₂ degassing. The limestone chips were coarse grained (approximately 20 mm) and angular. Approximately 1 kg of the limestone chips were added to the bucket containing the treated mine water and continuous logging of the pH was started thereafter using the Hanna combination meters HI-9828 (Figure 32). After 30 min, 1 kg of limestone was added and the experiment continued for 5 h 55 min. Filtered samples were collected

every 15 min and acidified for ICP-OES analysis. An initial period of dissolution (gentle stirring) lasted for one hour followed by rapid aeration to strip any CO₂ using a plastic kitchen whisk. Alkalinity titrations were performed using a Hach digital titrator with 1.6N H₂SO₄ cartridge every hour using 100 mL of sample and titrating against red-green bromocresol indicator using the colour change to green as the end point.



Figure 32: Cwm Rheidol mine water with limestone added.

5.10.8.2 *Closed System Experiments at Cwm Rheidol and Parys Mountain*

The left image in Figure 33 show the 10 L plastic container with a screw top lid was used as a closed system reactor for mine waters from both Cwm Rheidol and Parys Mountain. The experiments were repeated for both waters. The reactor was 1/3 filled with limestone chips and filled with raw, untreated mine water. The reactor was sealed and shaken manually at hourly intervals for the first five hours of the first day and periodically thereafter. The system was kept closed for 45 h, for the limestone to react with the low pH mine water except when parameters were measured as shown in the right hand image of Figure 33. Filtered and unfiltered samples of the initial background chemistry was determined by ICP-OES, samples were collected after 2, 4, 10, 25 and 45 h Mg, Fe, Zn, Cu, Pb, Cd, Ni, Mn, As. pH- was measured at the same time the samples were taken. After 45 h, the lid of the container was removed, the contents were tipped into an open plastic bucket to simulate an open system and the pump started to strip any CO₂. pH was logged continuously using two calibrated Hanna combination meters HI-9828 throughout the stripping phase which continued until the pH stabilized at 7.1. There were breaks in the experiment when either the Han-

na probes or the pump required recharging. Samples were collected at hourly intervals when all was running correctly throughout the day but not at night. For both waters the stripping phase lasted for 48 h.



Figure 33: Left image is the Limestone reactor (closed system) Right image, parameters being measured prior to the stripping phase.

5.10.9 Aeration Experiments

5.10.9.1 *Cwm Rheidol Inflow Water Field Experiments*

This experiment was designed as a control against the adsorption experiment (section 5.10.7)

No ochre was added during the course of these experiments to verify if there was a difference in filtered Fe total concentrations between the sample with ochre added. The experiment was run for 50 h in order to replicate the residence time of water in the VFR. A bucket was filled with 8 L of untreated Cwm Rheidol mine water and aerated using the submersible Whale® pump connected to a 12 V car battery. Fe total filtered and unfiltered samples were analysed by ICP-OES and Fe(II) was measured on site using the Merck spectrophotometer. Samples were collected at the start and the end of the experiment.

5.10.9.2 *Cwm Rheidol Inflow Water Laboratory Experiments*

An aeration experiment as in section 5.10.9 was carried out to evaluate if aerating the raw mine water would reduce the Fe concentration compared to a static sample. The term aeration in this context is defined as a method to keep the sample in constant motion introducing oxygen is being introduced at the sample/atmosphere interface. Inflow mine water was collected at Cwm Rheidol from the lower number 9 adit discharge pipe and stored in the dark at 4 °C

overnight. The next day, two identical buckets were filled and one aerated using the submersible Whale® pump while the other one was kept under static conditions. Filtered and unfiltered samples for ICP-OES which were collected and Fe(II) concentrations were measured using the Merck spectrophotometer samples were taken at the start, every 10 min for the first 90min and then after 24 and 48 h. pH, ORP and EC were measured at the start and end of the experiment.

5.10.9.3 *Cwm Rheidol VFR Outflow Laboratory Experiments*

The aeration experiment was repeated in the CLEER laboratories using the outflow (treated) water to determine whether aeration of the treated mine water reduced the Fe concentration. During field sampling it became obvious that the treated outflow from the VFR had a consistent filtered as well as unfiltered Fe concentration of approximately 30 mg/L. This gave rise to the hypothesis that the Fe remaining in the outflow was the dissolved Fe fraction. Therefore, the aeration experiment was repeated as described in section 5.10.9.2 with the treated water to evaluate its effect on the Fe concentration. The experiment was conducted over 24 h with samples collected at 10, 20, 30, 60, 90 and 1440 min.

5.10.10 **Stirring Experiments**

Stirring experiments were conducted to determine if the Fe removal mechanism from the raw Cwm Rheidol mine water is affected by the rate of stirring of the water and view the rate of Fe²⁺ oxidation (where Fe(II) was present) equal volumes of untreated mine water was transferred to four separated 800 mL glass beakers. Three of the four beakers were placed on a Stuart SB 162-3 stirrer as shown in Figure 34. The beakers were set as follows:

- I) No stirring
- II) Stirring speed set to 1.3 at the stirring speed controller
- III) Stirring speed set to 3 at the stirring speed controller
- IV) Aerated (no stirring) using a Dymex2 pump with a perforated tube attached which was submerged into the mine water sample, providing a steady stream of fine air bubbles

Stirred beakers were mixed using a magnetic flea. Filtered and unfiltered samples were collected for analysis of Fe and filtered samples were diluted with deionised water at 1:2 dilution and analysed for Fe(II) using the Merck spectro-

photometer. Fe total was also measured following the addition to the Merck reagent. Samples were collected at the start, after 20, 35, 60, 180 min and 21, 25 and 50 h. pH was measured at the start and end of the experiment using a calibrated Metler Toledo pH probe.



Figure 34: Experimental set up for stirring experiments.

5.10.11 Centrifugation, Coagulation and Flocculation Experiments

A set of experiments were carried out to evaluate if the addition of chemical coagulants would reduce the Fe concentration in the treated Cwm Rheidol outflow water. This was to further investigate if there is a colloidal fraction in the outflow water that would floc, or whether the remaining Fe concentration was all dissolved. Filtered and unfiltered raw mine water samples were collected on site, acidified and taken back to the CLEER labs for metals analysis by ICP-OES. $AlSO_4$ was used as a chemical coagulant and concentrations of 0, 40, 60 and 80 mg/L of $AlSO_4$ were made up from a 1000 mg/L stock solution by diluting with deionised water. To identify, at which $AlSO_4$ concentration the Fe coagulation is at its optimum, the mine water was added to a beaker and made up to 1 L with the correct amount of appropriately diluted $AlSO_4$. Each beaker was placed on a mechanical stirrer at 80 rpm for 1 minute and a further 30 min at a speed of 20 rpm. After stopping the stirrer, the flocculation behaviour of the samples was observed for a further 30 min, and the time of any floc formation recorded. Filtered and unfiltered samples were collected before and after the stirring and acidified for ICP-OES analysis. After the 30 min, 50 mL of sample were transferred to 50 mL centrifuging tubes and centrifuged for 15 min at 3000 rpm. The supernatant was sampled and analysed for Fe total and Fe(II) concentrations.

The same procedure was followed using the untreated inflow and treated outflow water and. The results were compared against each other to determine whether there are colloidal particles in the treated water.

5.10.12 Ultracentrifugation

Centrifuging is a method used to separate particles of different specific density and particle sizes. A centrifuging experiment adapted from Hüttig and Zänker (2004) was used to determine which fraction of the mine water is truly dissolved. In this context, truly dissolved is the fraction that relates to a particle size of less than 50 nm, which is close to the 20 nm cut off between “truly dissolved” and colloids suggested by Shiller (2003).

20 tubes of fresh mine water were collected in the field (10 × 2 to duplicate the experiment). Parallel centrifugation using a SIGMA® 6K15 centrifuge of each 2 × 50 mL of raw water was carried out at rotor speeds calculated as per Table 9 of 300 rpm, 500 rpm, 700 rpm, 1000 rpm, 3000 rpm, 5000 rpm and 3500 rpm in each case over a period of 1 hour (except for the final 3500 rpm which required 2 h due to the limitation of the centrifuge instrument speed). Equivalent RCF values (relative centrifugal force = g-force) at a given point in the centrifuge tube were calculated according to the equation 29:

$$RCF = 11.18 \times r \times \left(\frac{U}{1000}\right) \quad [29]$$

With r : distance between the rotation axis and the particle in the centrifuge tube cm, U : rpm rounds per minute. After centrifuging the supernatant was syringed from the centrifuge tube using a mL pipette. The sample was transferred to a new sample container, acidified with 20% nitric acid and the total unfiltered Fe concentration analysed by ICP-OES.

The maximum size of the particles still present in the supernatant was then calculated with a given density of the colloids and under the assumption of a spherical form of the particles in accordance with equation 30:

$$d = \sqrt{\frac{18\eta \ln \frac{r_1}{r_0}}{(\rho_2 - \rho_1)\omega^2 t}} \quad [30]$$

d : diameter of particle, cm

ρ_2 : density, g cm⁻³; ρ_2 : 3.96 g cm⁻³ for ferrihydrite

r_0 : distance of water level in vial to rotation axis before taking sample, cm

r_1 : distance of water level in vial to rotation axis after taking sample, cm

t : duration of centrifuging, s

η : viscosity of water at 25 °C, 0.008941 g cm⁻¹ s

ρ_1 : density of water at 25 °C, 0.997 g cm⁻³

ω : angular velocity, s⁻¹ = $U \times \frac{2\pi}{60}$

Table 9: Centrifuge parameters and calculated values.

RPM	t , h	g' , -	d , nm
raw	-		
0	1		
300	1	283	683
500	1	474	417
700	1	659	293
1000	1	945	207
2000	1	1889	101
4000	1	4181	50
5000	1	5254	39
3500	2	3913	35

Fraction of Fe relative to particle size in the supernatant were plotted to determine which fraction of the mine water is truly dissolved.

5.10.13 Settling Velocity of Cwm Rheidol Precipitates

Settling velocities (v) of the Cwm Rheidol sludge from within the VFR were calculated by measuring the distance (d) at which the particles settled over time (t) using equation 31

$$v = \frac{d}{t} \quad [31]$$

A 20 L container of water with the precipitates was collected from within the VRF on site and taken back to a laboratory. The experiment was set up so that it could be carried out immediately on arrival in order to minimise any potential change that an artificial environment might have on the structure of the flocs. The sample was shaken and added to a clear 250 mL measuring cylinder to the

250 mL mark and the time for the particles to settle measured and recorded. This method is not as accurate as measuring settling rates with Imhof cones, but was considered sufficient for the purpose of this thesis as a first approximation for the VFR sludge settling rates.

5.10.14 Microbiological Sampling and Analysis

The Cwm Rheidol microbial ecology investigation was carried out at Bangor University Acidophile Research Team (BART). Their methods and materials used for the DNA extraction, 16S rRNA gene PCR and T-RFLP analysis are described in Appendix 2. The sampling procedure described below was carried out by the author as per the instructions given by Professor Barrie Johnson.

Raw water and water from in the VFR tank were collected using pre-sterilised hand pumped filter units from the Cwm Rheidol adit in the VFR tank. The filtration units were sterilised by heating overnight in an oven at 140 °C. Once the filtration units were filled, they were wrapped in foil to eliminate daylight, stored in a cold box and transported immediately to Bangor University where amplification of bacteria DNA from sludge and water samples was carried out in order to determine the dominant microbial community (classification) and the relative abundance of the species in the samples.

5.10.15 VFR Decommissioning

5.10.15.1 Final Measurements in VFR

At the end of the VFR trial, the inflow tap was closed off, final inflow and outflow samples were collected and field parameters measured along with the head height in the tank. Once the final samples and measurements were made, the swan neck was lowered to ground level so that the system could drain down naturally under gravity. A wooden metre measuring stick was held upright in the tank to enable the hydraulic conductivity measurements to be recorded as described in section 5.10.1. Once the VRF was completely emptied of water, the depth of the ochre bed could be estimated. Samples of the ochre bed were collected using a knife to cut through the layer taking care to minimise disturbance of any stratification that might have occurred (Figure 35).

5.10.15.2 Hydraulic Measurements

Flow rate was measured using a 500 mL plastic measuring cylinder and stop watch. The volume in the cylinder was measured after 60 seconds and recorded. This was repeated three times and an average of the three measurements calculated. In addition, the hydraulic head was measured at each visit by measuring the difference between the water surface and the top of the tank and subtracting that from the height of the tank.



Figure 35: Left is the ochre bed of the VFR after having been drained. Right is a section of the ochre bed taken for lab analysis.

To evaluate the VFR's hydraulic conductivity, a permeability test with falling head was conducted. Those tests are generally conducted for measuring the hydraulic conductivity of soils. This method can be used for small scale samples in the lab or for larger scale experiments in the field (*e.g.* with a Guelph permeameter or infiltrometer). The advantage of the method is that tests can be conducted in undisturbed soil or test material conditions and it provides an average of the hydraulic conductivity of the measuring area. Consequently, this method was chosen to measure the hydraulic conductivity of the VFR in undisturbed conditions. Water level measurements are taken at suitable time intervals until the water level returns to equilibrium (Clayton et al., 1995). On the basis of the results sample permeabilities k_f can be calculated using equation 32:

$$k_f = \frac{\alpha \cdot L}{A \cdot \Delta t} \log \frac{h_U}{h_L} \quad [32]$$

L : height of soil in the column (in this case height of gravel bed plus ochre), m

A : the cross section of the sample (in this case the area of the VFR), m²

a : the cross section of the standpipe (in this case the area of the VFR), m^2

Δt : time for the water to flow through the sample in the standpipe, s

h_U : and h_L : upper and lower water levels measured using the same water head reference in the standpipe, m

The measurements were recorded on site at the end of the VFR field trial during the final drain down of the system. The data was used to determine the hydraulic conductivity of the ochre bed.

5.11 Electrochemical Methods and Equipment

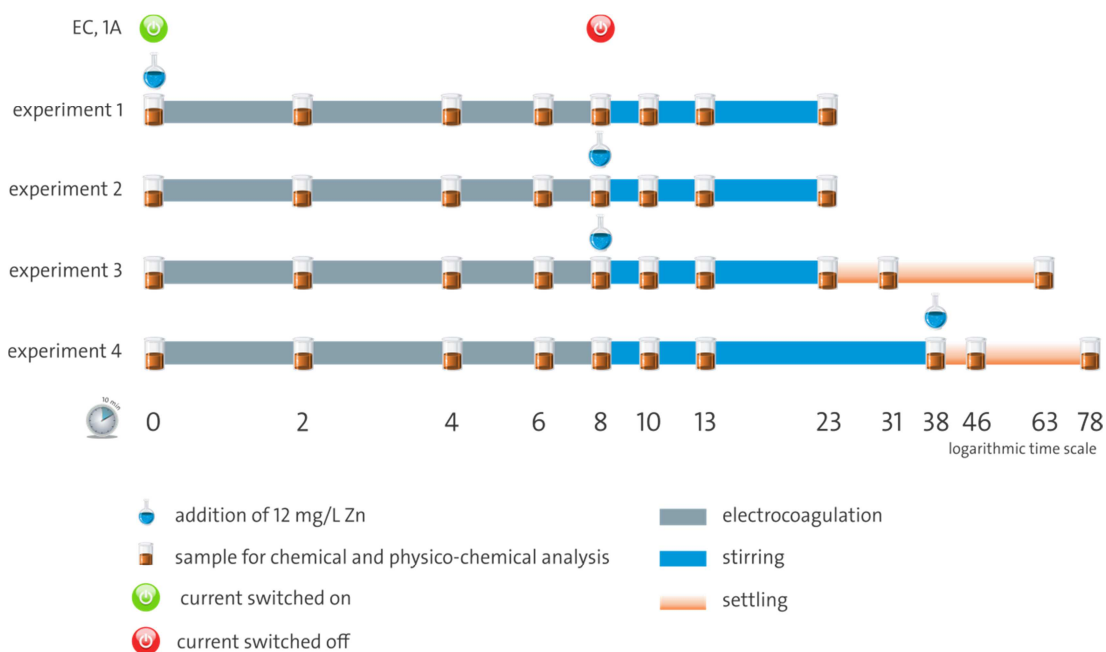
Electrochemical experiments were conducted batch wise. All experiments were performed using 800 mL of sample volume on a magnetic stirrer. Stirring speeds were set and the sample mixed using a magnetic flea. Fresh mine water collected on the same day as the experiment was used each time. Filtered and unfiltered samples were taken according to the standard method described in section 5.10.1 for ICP-OES metal analysis and for IC for anions. In all instances, parameters were measured using calibrated Hanna combination meters HI-9828 with the power supply of the transformer switched off. The area of the electrodes in the sample was recorded to determine the current density for each of the experiments using Faraday's law as described in section 3.8. The distance between the electrodes was always set at 10 mm.

5.11.1 Adsorption vs Co-precipitation of Zn (Frongoch)

An adsorption vs co-precipitation experiment for Zn was conducted with Frongoch mine water. This experiment was performed in triplicate and a blind duplicates and blank samples were analysed to eliminate potential human bias in the analytical results. The experiment was used to determine if more Zn is removed by co-precipitation with Fe added electrically (using two Fe sacrificial electrodes) than by adsorption to HFO particles. As it was unknown if the application of an electric current would affect the Zn removal rate, the same procedure was repeated with the only variable being the time at which the Zn was added to the sample. For the co-precipitation experiment, a 12 mg/L solution of Zn made up from a stock solution of 1000 mg/L Zn from $ZnSO_4 \cdot 7H_2O$ dissolved in tap water. The 12 mg/L Zn solution was representative of the Frongoch mine

water. Two Fe electrodes in monopolar configuration were connected to the power supply which was set at 1 A and a reaction time 8 min was used followed by 15 min stirring. pH, EC, ORP, ORP, voltage, volume and temp were recorded for each sample. Samples were collected at the start, after 2, 4, 6 and 8 min treatment time and after 2, 5 and 15 min of stirring. For the adsorption experiments, exactly the same procedure was followed except the Zn was added after the 8 min treatment time (Table 10) provides a schematic overview of how each of the co-precipitation/adsorption experiments was set out.

Table 10: Experimental procedure for Zn adsorption vs co-precipitation experiments.



5.11.2 Advanced Oxidation (Ynysarwed)

Advanced oxidation (section 3) experiments investigated the effects of using oxygen over potential inert (MMO) electrodes for the oxidation and subsequent precipitation of Fe from coal mine drainage. Advanced oxidation (AO) requires a higher current density than conventional EC methods where the current produces electron holes on the surface of the electrode which provides oxygen potential, rapidly oxidising the sample. The purpose was to compare the method in terms of treatment cost to conventional active treatment methods. The method also examines the characteristics of the settling properties and the sludge

observed in the electro-oxidation process applied to mine water. The relationship between current density and Fe removal was examined. In addition, temperature variation and chemical pH variation tests were carried out to investigate if the reaction was pH dependent. 10 % (v/v) NaOH was added to an untreated sample that was stirred for 2 min and the Fe concentration measured through the pH range 4–7 at 0.25 pH intervals. Similarly, samples were placed on the hotplate, stirred as per the standard procedure and the Fe concentration analysed through the temperature range 15, 21, 22, 26, 37, 39, 41, 45 °C.

Two inert Pt coated Ti electrodes were connected to the power supply in monopolar configuration. Mine water was collected from the adit in plastic containers and filled right to the top to eliminate exposure to the air and taken immediately to the laboratory at Hydro Industries for bench scale batch tests. Hydro Industries is an electrochemical water treatment company based in Llanennech, Wales. This company offered support for the electrochemical studies in the electrochemical section of this research by supplying laboratory time and equipment. Since the conversion of Fe(II) to Fe(III) are the important features in this water, the portable Merck spectrophotometer with appropriate iron test cells (0–50 mg/L) was used so that analysis for Fe(II) and Fe total could be carried out immediately. pH, temp, DO and ORP were measured using the Hanna combination meters HI-9828. A new fresh sample was used for each test. Flash mixing for 2 min after the reaction time helped to floc the precipitates and encourage faster settling. At the end of the experimental procedure, the sample remaining in the beaker was filtered, the sludge retained and dried in the ovens at 60 °C until no further loss of mass was observed, this took approximately 48 h and prepared for further examination by ESEM and XRD to determine its mineralogy.

The AO method was repeated at 1, 2, 3, 4, 5, 6, 7 and 8 A for a treatment time of 4 min.

5.11.3 Electroprecipitation

Experiments using Cwm Rheidol water were to determine if pH correction could be achieved electrochemically in AMD and what precipitates would form under test conditions. Cwm Rheidol water was used because it is a low pH, high

Fe, high sulphate water and therefore possess common AMD characteristics. The stability of these precipitates was considered and sludge formed in experiments was filtered and retained for further analysis by other methods. Pt, Fe, Al, Cu, ceramic and carbon electrodes were tested. Since pH is considered to be the master variable in metal solubility in AMD, the experimental set up was always the same: monopolar electrode configuration, 5 A operating current. The only variables were the time and with or without aeration using a bench top pump with a finely perforated rubber tube attached that was submerged in the sample being treated. Electrode materials that did not show a substantial contribution to the pH increase within 60 min were eliminated from further studies.

Raw, untreated mine water was collected on the day of the experiment. As the Cwm Rheidol mine water is a multi-metal laden discharge, filtered and unfiltered were taken before, at 10 minute intervals and at the end of the experiment and acidified for ICP-OES analysis for Mg, Ca, Zn, Pb, Cd, Fe, Cu, Ni, Al and Mn. Filtered samples were also collected for IC analysis for sulphate and chloride concentrations. At the intervals when samples were taken, the standard parameters temp, ORP, EC and pH were measured using Hanna stick probes and a portable Hanna probes were calibrated using manufactures recommended solutions before each set of experiments.

5.11.4 Zinc Titration

To determine Zn solubility relative to pH under laboratory conditions, a Zn solution of known concentration was prepared and acidified to pH 2. The acidified Zn solution was placed on a stirring plate and the pH monitored continuously. 0.1 M NaOH was then added drop wise from a burette into the Zn solution until the pH settled at an additional pH unit. Samples were collected at each pH unit through the range of pH 2–12. All samples were filtered and analysed by ICP-OES for Zn total filtered concentration.

5.12 PHREEQC Modelling

PHREEQC (Parkhurst and Appelo, 2013) is a numerical computer code that calculates the chemical thermodynamic reactions occurring in aqueous systems. In standard mode, no kinetics or even microbial interactions are considered. The code uses one of various chemical thermodynamic databases such as the

WATEQ4F or the PHREEQC databases, which contains the relevant chemical reactions that potentially can occur in the modelled system and the corresponding stability constants. Based on the input data and the potential reactions contained in the database the code then calculates the species distribution in the sample and the phases as well as their saturation indices that contributed to the water chemistry. Those calculations are based on a set of algebraic equations that describe the chemical reactions occurring. In an iterative process the model solves those equations until the numerical simulation of the chemical system converges. Besides those basic calculations, PHREEQC is capable of performing more sophisticated geochemical calculations such as transport, inverse modelling, mixing processes, advection, kinetics or evaporation (Merkel et al., 2005, Parkhurst and Appelo, 2013). In order to model the behaviour of schwertmannite in the water samples, the original WATEQ4F database was extended with thermodynamic data for schwertmannite.

Only two full water analyses from early 2012 were available for chemical thermodynamic modelling with PHREEQC. One was from Cwm Rheidol (cr25 2012-01-02; Appendix 4) and the other one from Frongoch (kf 1.2 U 2012). For the simulation, PHREEQC interactive Version 3.1.1.8288 (2013-12-05) and the WATEQ4F database (6895 2012-08-21 18:10:05Z) extended with kinetic data of schwertmannite was employed. To calculate the electrical conductivities of the samples and compare them with measured electrical conductivities for analyses adaption, the PHREEQC database was applied instead. The WATEQ4F database was chosen as it contains more species and phases and of the calculated results the species distribution was used to recognize the main species contributing to the water's chemistry. Moreover, the results were used to identify the controlling phases which were in equilibrium with the water and are predominantly responsible for the water's chemical composition. As PHREEQC can't consider microbial activity, the effects of microorganisms are not mirrored by the modelled results.

5.13 Statistical Investigations

Basic statistical analysis of data was done with the statistical package SPSS (Versions 20 – 23). Comparison of inflow and outflow data was done using Paired Samples *t*-tests (Table 11, Table 13). Correlation analysis was done using

the Pearson (2-tailed) correlation test (Table 12). Only the relevant data of these statistical investigations are discussed and presented in the text.

Throughout the thesis, reference to the statistical investigations is given at various sections. To make it easier for the reader, the results of the statistical analysis are already listed here and not – as academic rules usually require – in the results section.

Kay Florence | Removal Mechanisms of Metals from Mine Water

Table 11: Results of the Paired Samples *t*-Test, 95% confidence Interval to test the treatment efficiency of the VFR.

	Paired Differences						t	df	Sig. (2-tailed)
	Mean	Std. Deviation	Std. Error Mean	95% Confidence Interval of the Difference					
				Lower	Upper				
Statistically significant difference									
D.O (ppm) in – out	1.581	1.499	0.289	0.988	2.174	5.480	26	0.000	
D.O (%) in – out	17.561	13.947	2.908	11.530	23.592	6.038	22	0.000	
ORP (mV) in – out	-30.017	48.547	10.123	-51.011	-9.024	-2.965	22	0.007	
Fe Not filtered (mg/L) in – out	64.463	23.256	5.075	53.877	75.049	12.702	20	0.000	
Fe Filtered (mg/L) in – out	52.861	23.370	4.498	43.616	62.106	11.753	26	0.000	
Zn in (mg/L) – out	1.730	2.523	0.495	0.711	2.749	3.496	25	0.002	
Difference statistically not significant									
pH in – out	-0.005	0.187	0.035	-0.078	0.067	-0.151	27	0.881	
Temp (°C) in – out	-0.297	1.476	0.308	-0.936	0.341	-0.966	22	0.344	
<i>Fe % removed unfiltered – filtered</i>	3.326	11.949	2.608	-2.113	8.766	1.276	20	0.217	
Pb filtered in (mg/L) – out	0.002	0.009	0.001	-0.002	0.005	0.842	24	0.408	
Cd filtered in (mg/L) – out	-0.004	0.013	0.002	-0.010	0.002	-1.440	21	0.165	
Sulphate filtered (mg/L) – out	7.383	148.508	31.662	-58.462	73.227	0.233	21	0.818	
Chloride (mg/L) in – out	3.238	19.367	4.330	-5.826	12.302	0.748	19	0.464	
No statistically significant difference									
EC (µS/cm) in – out	44.714	123.518	23.343	-3.181	92.610	1.916	27	0.066	
Mn filtered in(mg/L) – out	-0.261	0.611	0.133	-0.539	0.017	-1.957	20	0.064	

Kay Florence | Removal Mechanisms of Metals from Mine Water

Table 12: Results of the Pearson Correlation of the physicochemical VFR parameters in Appendix 4. Only the relevant correlations are discussed in the text.

	pH in	pH out	EC in	EC out	D.O (ppm) in	D.O (ppm) out	D.O (%) in	D.O (%) out	ORP in	ORP out	Temp in	Temp out	Fe unfiltered in	Fe unfiltered out	SO ₄ filtered in	SO ₄ filtered out	Chlo-ride in	Chlo-ride out	Fe filtered in	Fe filtered out
pH in	-	0.923	0.224	0.176	-0.048	-0.095	-0.076	-0.123	-0.098	<i>-0.456</i>	0.260	0.161	-0.034	0.058	-0.018	0.06	-0.094	-0.043	0.010	-0.012
pH out	0.923	-	0.138	0.050	-0.226	-0.188	-0.136	-0.042	-0.145	-0.279	0.403	0.287	-0.08	0.121	0.029	0.052	-0.030	0.08	0.087	0.076
EC in	0.224	0.138	-	0.933	<i>0.401</i>	0.104	-0.056	-0.394	<i>0.445</i>	0.132	0.372	0.527	0.330	0.403	0.394	<i>0.461</i>	-0.421	0.119	-0.078	-0.162
EC out	0.176	0.050	0.933	-	0.541	0.337	0.112	-0.186	<i>0.431</i>	-0.06	0.167	0.212	0.424	0.570	0.316	0.370	<i>-0.462</i>	-0.021	-0.044	-0.112
D.O (ppm) in	-0.048	-0.226	<i>0.401</i>	0.541	-	0.723	0.928	0.332	0.054	-0.043	-0.382	-0.383	0.103	0.282	0.099	0.178	<i>-0.621</i>	-0.079	-0.071	0.184
D.O (ppm) out	-0.095	-0.188	0.104	0.337	0.723	-	<i>0.497</i>	0.912	-0.109	-0.229	-0.054	-0.243	-0.151	0.142	-0.069	-0.051	<i>-0.489</i>	-0.289	-0.078	0.362
D.O (%) in	-0.076	-0.136	-0.056	0.112	0.928	<i>0.497</i>	-	<i>0.487</i>	-0.562	0.090	-0.031	-0.111	0.137	0.433	-0.322	-0.245	-0.449	0.121	0.259	<i>0.433</i>
D.O (%) out	-0.123	-0.042	-0.394	-0.186	0.332	0.912	<i>0.487</i>	-	<i>-0.509</i>	0.032	0.181	0.02	-0.238	0.188	-0.455	<i>-0.474</i>	-0.079	-0.234	0.034	<i>0.487</i>
ORP in	-0.098	-0.145	<i>0.445</i>	<i>0.431</i>	0.054	-0.109	-0.562	<i>-0.509</i>	-	0.844	-0.334	-0.074	-0.041	-0.372	0.084	0.061	-0.433	-0.028	-0.248	-0.372
ORP out	<i>-0.456</i>	-0.279	0.132	-0.06	-0.043	-0.229	0.090	0.032	0.844	-	0.058	0.182	0.134	0.30	0.04	0.036	0.039	0.241	0.088	0.223
Temp in	0.260	0.403	0.372	0.167	-0.382	-0.054	-0.031	0.181	-0.334	0.058	-	0.880	0.045	0.227	0.080	0.036	-0.103	0.151	0.229	<i>0.458</i>
Temp out	0.161	0.287	0.527	0.212	-0.383	-0.243	-0.111	0.02	-0.074	0.182	0.880	-	-0.023	0.116	0.025	0.015	-0.09	0.249	0.126	0.239
Fe unfiltered in	-0.034	-0.08	0.330	0.424	0.103	-0.151	0.137	-0.238	-0.041	0.134	0.045	-0.023	-	0.660	0.423	<i>0.524</i>	-0.312	0.088	0.908	0.725
Fe unfiltered out	0.058	0.121	0.403	0.570	0.282	0.142	0.433	0.188	-0.372	0.30	0.227	0.116	0.660	-	0.261	0.288	-0.283	0.043	0.755	0.962
SO₄ filtered in	-0.018	0.029	0.394	0.316	0.099	-0.069	-0.322	-0.455	0.084	0.04	0.080	0.025	0.423	0.261	-	0.944	-0.270	0.274	0.064	0.058
SO₄ filtered out	0.06	0.052	<i>0.461</i>	0.370	0.178	-0.051	-0.245	<i>-0.474</i>	0.061	0.036	0.036	0.015	<i>0.524</i>	0.288	0.944	-	-0.285	0.287	0.131	0.075
Chloride in	-0.094	-0.030	-0.421	<i>-0.462</i>	-0.621	<i>-0.489</i>	-0.449	-0.079	-0.433	0.039	-0.103	-0.09	-0.312	-0.283	-0.270	-0.285	-	0.335	-0.059	-0.20
Chloride out	-0.043	0.08	0.119	-0.021	-0.079	-0.289	0.121	-0.234	-0.028	0.241	0.151	0.249	0.088	0.043	0.274	0.287	0.335	-	0.047	-0.083
Fe filtered in	0.010	0.087	-0.078	-0.044	-0.071	-0.078	0.259	0.034	-0.248	0.088	0.229	0.126	0.908	0.755	0.064	0.131	-0.059	0.047	-	0.706
Fe filtered out	-0.012	0.076	-0.162	-0.112	0.184	0.362	<i>0.433</i>	<i>0.487</i>	-0.372	0.223	<i>0.458</i>	0.239	0.725	0.962	0.058	0.075	-0.20	-0.083	0.706	-

Red shaded bold numbers Correlation is significant at the 0.01 level (2-tailed).

Blue shaded italic numbers Correlation is significant at the 0.05 level (2-tailed).

6 Results and Discussion

6.1 Reasons for the VFR Experiments Conducted in the Project

As described in section 2.8, one of the aims of this thesis was to assess the effectiveness of the VFR at removing problematic Fe concentrations from low pH mine water. To achieve this, the experiments described in Table 6 were carried out as follows: **Oxidation**, the aim of these experiments to find out if the VFR ochre oxidised the mine water, converting Fe(II) to solid Fe(III) (heterogeneous oxidation) and subsequent precipitation. It was initially thought that from this, a rate constant for the oxidation of Fe(II) from the lower number 9 adit discharge pipe at Cwm Rheidol could be determined. Based on the results of these experiments, the **adsorption experiments** were done to determine if dissolved Fe(III) adsorbs to the solid ochre in the VFR. As an aside, the **limestone experiments** were designed to assess the potential use of limestone drains following Fe removal from a VFR at both Cwm Rheidol and Parys Mountain. **Agitation/stirring experiments** were used to determine if motion of the water would encourage the coagulation of colloidal Fe(III) particles. **Microbiological analysis** of the VFR ochre and Cwm Rheidol mine water was necessary to determine if bacteria were present in the Cwm Rheidol mine water and therefore likely to be influencing system behaviour. **Centrifugation experiments** were used to determine the particle size distribution in the Cwm Rheidol water so that an explanation could be given for the Fe removal mechanisms in the VFR and to explain quantitatively the performance of the VFR at Cwm Rheidol. Finally, estimations on the **long term performance** and summary of the efficiency of the VFR at low pH could be determined using results of the VFR **hydraulic measurements**.

It should be noted that lines used in the following graphs have been added for making the presented data clearer to the reader and are not necessarily meant to be interpolations between the data points.

6.2 Introduction to the Cwm Rheidol VFR Field Study

The VFR set up at Cwm Rheidol commenced during January 2011. There were a few modifications that had to be made before the VFR was operating correctly;

however, it was possible to achieve flow purely under gravity from the number 9 Adit discharge point into the VFR. Sampling, flow rate and geochemical parameter measurements began on 2011-05-17 and sampling continued until 2012-07-04. There were reasonably regular periods where the flow had to be stopped because of the build-up of ochre in the pipes. This required the system to be shut down whilst the pipes were cleared by back flushing them with a water pump to remove the ochre. On average, this was carried out every four weeks. Sampling frequency was much greater during the initial stages of the trial when the observations were more focused on understanding the water chemistry but were less frequent in later stages as the research shifted towards the microbiology, hydraulic permeability and structure/density of the precipitates. There were also stages during the winter period when the VFR was frozen and also occasions when on arrival, the outflow and overflow were blocked and the system was overflowing. These instances were recorded.

Initially, the plan to set up and run the VFR at Cwm Rheidol followed on from the work of Barnes (2008). In his PhD, the VFR was set up as a passive treatment for Fe removal from net alkaline (pH 6.9) coal mine drainage and the principal design was to achieve Fe removal by surface catalysed oxidation of Fe(II) on the ochre surface and self-filtration of an ochre bed. Cwm Rheidol, on the contrary, is a very low pH multi metal contaminated mine water and the idea was to determine if a VFR can also operate under those conditions employing the same design principle as Geroni (2011) used at the Ynysarwed VFR, a net acidic coal mine drainage (pH 6.1). In both instances, the ochre bed was allowed to form naturally by accretion in the bottom of the treatment tank. In the Ynysarwed VFR case, the inflow rate into the VFR was set to maximum to encourage the seeding of the bed to happen quickly so that the mechanism for Fe(II) oxidation would be by heterogeneous catalysis through adsorption and oxidation on the HFO solids. It was also considered that the precipitates that form in this way rather than by oxidation of precipitates in the water column might form an ochre layer that is more granular with better dewatering properties (Geroni, 2011).

At this stage, it was unknown if a VFR might remove Fe or metal in waters with pH values below 3. Yet, the Cwm Rheidol site is very ochreous, implying that Fe oxidation occurs somewhere between the mine adit in the hills and the filter bed area in the valley (Figure 28, page 93). Consequently, the decision was made to follow the same VFR setup as described in Geroni (2011). The inflow and outflow were left uncontrolled in the initial phase to observe if ochre accretion occurred on the base of the VFR. To avoid scouring of the gravel, the flow was dissipated by being passed through a container with holes drilled in the bottom (page 90, Figure 25). Within the first week, a layer was building up in the bottom of the VFR (page 92, Figure 27, left), and after two weeks the tank was filled with water and the flow rate in and out of the tank controlled by setting the head height to 200 mm. As can be seen from page 92, Figure 27 (left) there was clearly Fe precipitates coating the gravel bed of the VFR already at this initial phase of the experiment.

This section presents the results of the scoping studies that were conducted in relation to the Cwm Rheidol VFR. In addition, the – at first sight – unusual properties of the Fe that enables this system to continuously and passively treat the mine water will be explained.

6.3 Hydraulics

6.3.1 Flow Rate through the VFR

Figure 36 presents all of the 34 outflow measurements that were collected throughout the field trial period. The secondary axis presents the cumulative ‘volume treated’, where the volume between each sampling point was calculated from the inflow rate and added to the previous sample cumulative volume. Using this method, the total volume treated accounts for 274 m³, or approximately 1370 bed volumes of the unreactive gravel bed.

This figure also shows the initial ochre accretion ‘filling’ phase of the tank during the first months after installation when the inflow rate was left uncontrolled, the system was overflowing at this stage, the flow rate reached approximately 4 L/min until day 33. At this time, the flow rate dropped to 0.7 L/min indicating the time at which the head across the tank was fixed using the ad-

justable swan neck and all the flow was through the tank from that time on. However, flow rate data shows that there was a drop in the flow rate as the ochre bed built up between days 33 and 72, at which point the inflow pipes became blocked by precipitates and needed to be backwashed. After the seeding period and initial unblocking of the inflow pipes, the flow rate stabilises between days 33 and 387 (0.1 and 0.4 L/min) with an average flow rate of 0.39 L/min. Several backwashing procedures were needed to clear the pipes of precipitates. These were carried out on days 23, 55, 91, 131, 171 and finally on day 387.

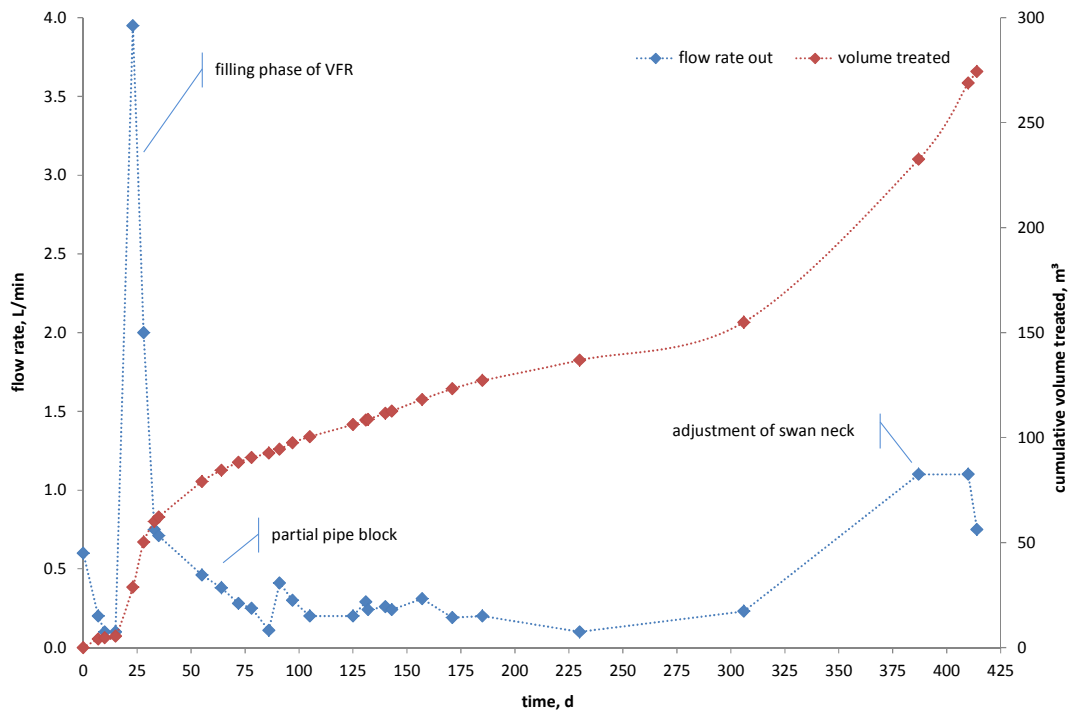


Figure 36: Flow rate in L/min over time; the secondary axis shows the cumulative volume treated throughout the trial period.

No further adjustment to the driving head via the swan neck occurred until day 387 when the swan neck was adjusted to half its previous height giving a greater driving head. This allowed determination of Fe removal efficiency at higher flow rates.

After the swan neck adjustment on day 387, the flow rate increased to 1.1 L/min dropping to 0.75 L/min for the final measurement which was taken on day 414. As the final measurements were recorded almost a month after the swan neck

was adjusted; this decrease in flow rate may be attributed to the pipes starting to block again and not necessarily the hydraulic permeability of the bed.

As can be seen from this data, the flow rate did not substantially change during the build-up of 6–7 cm of Fe precipitates (ochre) in the VFR. This can be considered an indication that the hydraulic conductivity of the ochre and gravel bed did not decrease throughout the trial period.

6.3.2 Hydraulic Conductivity of the VFR

Hydraulic conductivity was measured in the field using a hydraulic conductivity test with falling head, as described in section 5.10.15.2. The falling head was measured every 1–9 min for a duration of 1:19 h. The water temperature in the field was 13 °C and therefore a temperature correction to the standard hydraulic conductivity (k_f) at 20 °C according to Whitlow (2000) was applied. Based on the measurements, the mean effective hydraulic conductivity of the bed is $2.08 \cdot 10^{-5}$ m/s. This, based on DIN ISO/TS 17892-9, can be classified as pervious.

Compared to Barnes (2008), who determined an average hydraulic conductivity of $3.1 \cdot 10^{-5}$ m/s for his 20 mm VFR at Taff Merthyr, the result for the Cwm Rheidol VFR is in exactly the same range. Both VFRs operated for a similar period of time of 287 to 414 days. Consequently, this implies that the hydraulic performance of those systems seems to be very similar. The reason for this behaviour is that the mechanisms that build up the sludge in both VFRs seem to be identical and the sludge therefore appears to have a similar composition which results in similar hydraulic conductivities.

6.3.3 Upscaling of the VFR

When it comes to hydraulic systems, upscaling bench tests or pilot studies is not a simple task as the hydraulic scaling parameters are based on the characteristics of the flow. To calculate the size of a VFR to treat the full flow of the number 9 adit therefore uses a conservative approach with a linear upscaling of the VFR discussed in this thesis.

During the VFR field trial in this thesis, a mean flow of 0.39 L/min was treated in the VFR using an area of 1 m². The mean flow from the number 9 adit is around

3 L/sec; using these values, it can be calculated that a 461 m² VFR would be sufficient to remove an average of 65% of the Fe in the total flow from the number 9 adit for a minimum of one year without maintenance. A VFR of this size would cover an area of approximately 18 m x 25 m. Long term behaviour of a VFR would need to be verified in order to determine how often it would need to be cleaned or at what depth of the VFR sludge the system's hydraulic conductivity would become too low for proper operation.

To establish reliable up-scaling parameters, a full scale VFR would need to be trialled for at least 1 or 2 hydrological years (a hydrological year runs from November to October the following year). This is done because a hydrological year includes a complete rainfall period and consequently flow cycle with the lowest river and spring discharge (base flow) generally occurring in fall. Consequently, a hydrological year is commonly considered to mirror the flow and the removal rates in a representative way (Doležal et al., 2007, Wolkersdorfer, 2008) This measurement was done in 2003/2004 by Natural Resources Wales and showed a flow of 4–24 L/min with an average of 10 L/min. Consequently, 14 L/min would be necessary to treat 90 % of the flow. This would require a 36 m² VFR.

6.4 Physicochemical Parameters of the Cwm Rheidol Mine Water

6.4.1 Fe Concentrations in the VFR

6.4.1.1 Fe(total) Field Data

The VFR's unfiltered inflow Fe(total) concentrations ranged between 23.3 mg/L and 155.1 mg/L with an average inflow concentration of $95.9 \pm \sigma 29.7$ mg/L (Table 13, Figure 37, Appendix 4). Fe(total) unfiltered concentrations in the outflow of the VFR ranged between 14.6 mg/L and 73.3 mg/L and the average concentration was $31.4 \pm \sigma 15.6$ mg/L (Table 13). Data has not been corrected for outliers; therefore the mean 'Fe filtered out', which has a standard deviation of 23.34 mg/L, is higher than 'Fe unfiltered out', which has a standard deviation of 15.97 mg/L.

Table 13: Comparison of mean values for inflow and outflow parameters ('pair') and the Fe unfiltered/filtered concentrations (Pair 9). The statistical significance of the differences is presented in Table 11. pH re-calculated arithmetic average for [H⁺] and standard deviations as well as Std, Error Mean from measured pH-values.

		Mean	n	Std. Deviation	Std. Error Mean
Pair 1	pH in	2.9	28	0.45	0.1
	pH out	2.8		0.49	0.09
Pair 2	EC (µS/cm) in	1544	28	314	59.46
	EC (µS/cm) out	1499		344	64.95
Pair 3	D.O (ppm) in	7.53	27	2.12	0.41
	D.O (ppm) out	5.95		1.85	0.36
Pair 4	D.O (%) in	78.36	23	12.21	2.55
	D.O (%) out	60.80		14.93	3.11
Pair 5	ORP (mV) in	469	23	80.3	16.73
	ORP (mV) out	499		90.3	18.83
Pair 6	Temp (°C) in	13.54	23	2.75	0.57
	Temp (°C) out	13.84		3.10	0.65
Pair 7	Fe unfiltered (mg/L) in	95.89	21	30.47	6.65
	Fe unfiltered (mg/L) out	31.43		15.97	3.48
Pair 8	Fe Filtered (mg/L) in	89.20	27	32.99	6.35
	Fe Filtered (mg/L) out	36.34		23.34	4.49
Pair 9	Fe % unfiltered removed	65.58	21	15.72	3.43
	Fe % filtered removed	62.26		16.61	3.62
Pair 10	Zn in (mg/L)	100.70	26	22.61	4.44
	Zn out	98.97		22.74	4.46
Pair 11	Pb filtered in (mg/L)	0.06	25	0.02	0.00
	Pb filtered out	0.05		0.02	0.00
Pair 12	Mn filtered in (mg/L)	4.79	21	1.53	0.33
	Mn filtered out	5.05		1.24	0.27
Pair 13	Cd filtered in (mg/L)	0.12	22	0.03	0.01
	Cd filtered out	0.13		0.03	0.01
Pair 14	Sulphate filtered (mg/L)	1485.28	22	448.48	95.62
	Sulphate filtered out	1477.90		424.90	90.59
Pair 15	Chloride (mg/L) in	17.08	20	20.56	4.60
	Chloride (mg/L) out	13.84		6.68	1.49

Filtered inflow Fe(total) concentrations, on the other hand, ranged between 16.5 mg/L and 138.7 mg/L with an average inflow concentration of 89.2±σ32.4 mg/L (Table 13, Figure 37). Fe(total) filtered concentrations in the outflow of the VFR ranged between 4.0 mg/L and 86.0 mg/L and the average concentration was 36.3±σ22.9 mg/L (Table 13).

On days 55 and 171, the inflow and outflow Fe concentrations were lower than usual. These sample days coincide with back washing of the pipes which is like-

ly to have caused interference in the system. The flow of clean water through the inflow pipes into the VFR means that the system may not have had sufficient time to adjust to steady state conditions before the samples were collected.

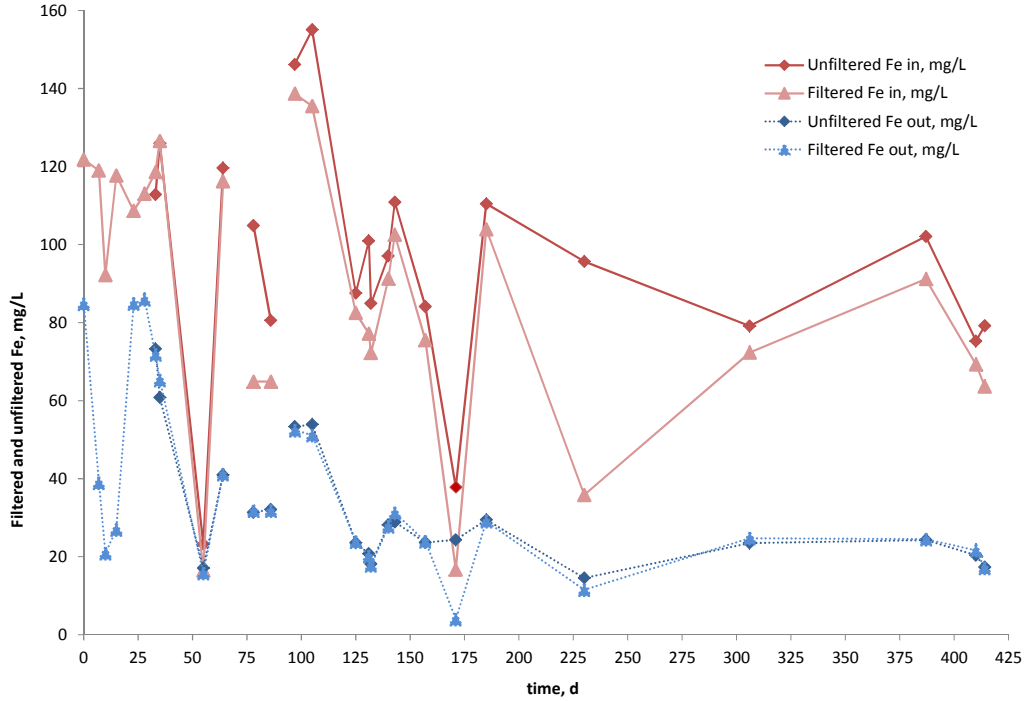


Figure 37: Filtered and unfiltered VFR Inflow and outflow Fe(total) concentrations over time.

Except on days 55 and 171, the VFR was consistent in removing a proportion of the Fe from the inflow, which was observed right from the start of the trial when only filtered samples were collected. Starting on day 33, filtered in addition to unfiltered samples were collected using 0.2 µm filters. As can be seen, a small difference between the Fe(total) filtered and the Fe(total) unfiltered concentrations was observed throughout the trial period for both inflow and outflow (Figure 39).

A paired samples *t*-test with SPSS showed that there is a statistically significant difference in the filtered and unfiltered Fe inflow concentrations (95% confidence interval, Table 11), whilst no statistically significant difference exists for the filtered and unfiltered outflow concentrations.

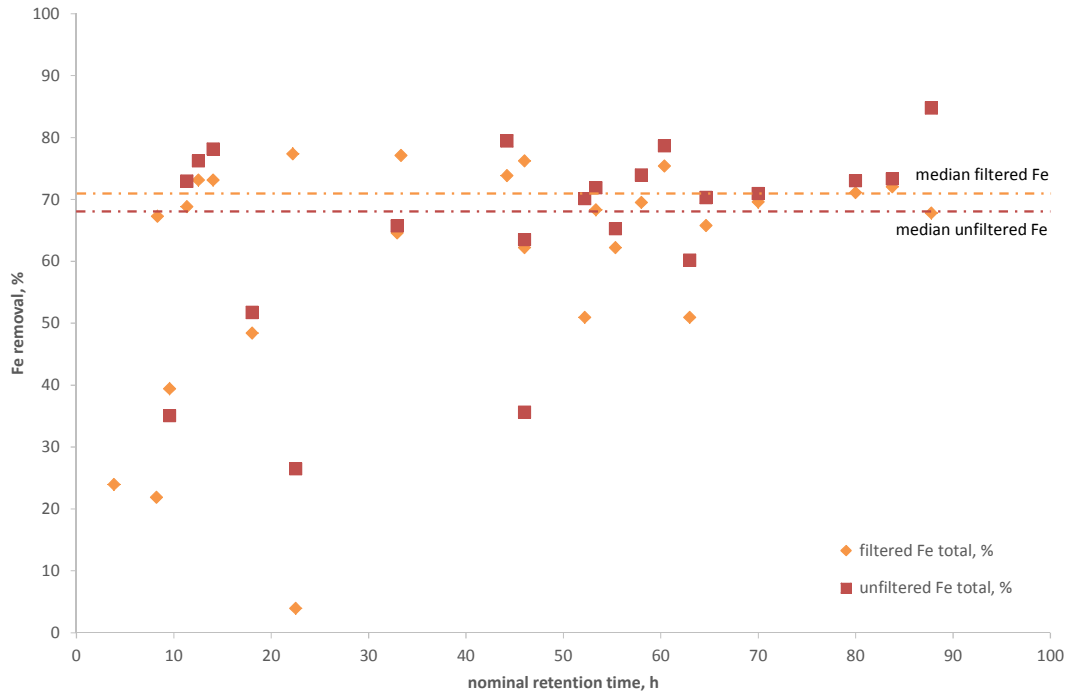


Figure 38: Nominal retention time in the VFR (median unfiltered Fe: 71.0 %; median filtered Fe: 67.8 %).

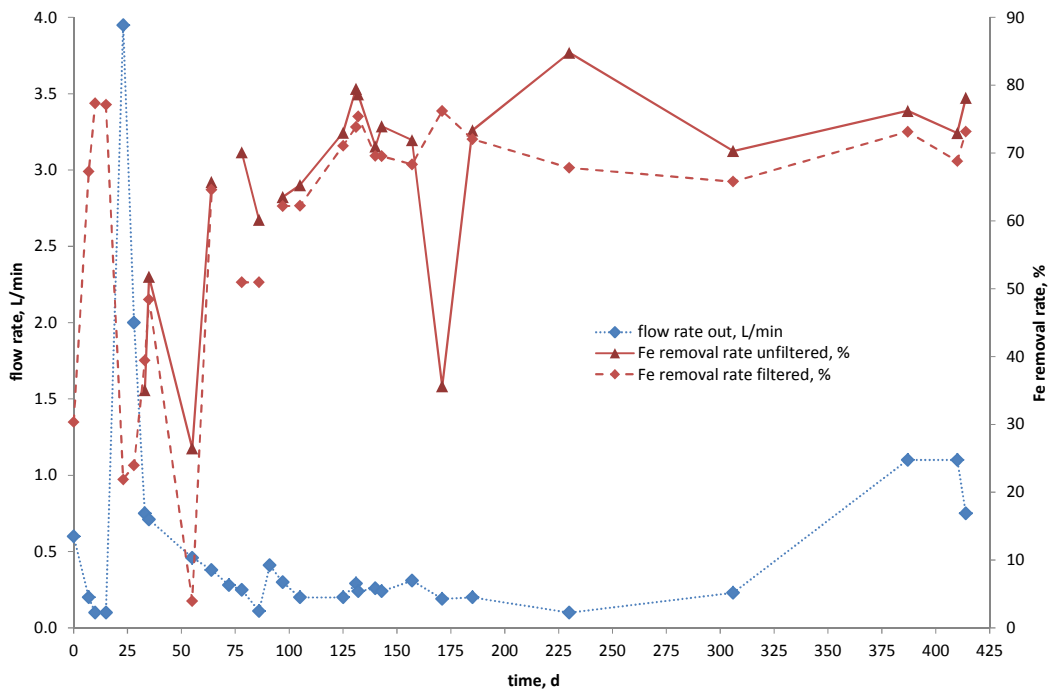


Figure 39: Filtered and unfiltered Fe(total) removal rate and flow rate of the VFR over time.

On average, the removal rate was 65.6% unfiltered Fe(total) and 59.5% filtered Fe(total). Figure 38 shows that this average removal rate does not change sub-

stantially relative to the time that the water is in the VFR. Average Fe removal remains the same whether the treatment time is 5 h or 70 h.

Table 14: Average filtered and unfiltered Fe total and Fe(II)-concentrations in the inflow and outflow water of the VFR in mg/L.

	VFR in		VFR out	
	unfiltered	filtered	unfiltered	filtered
Fe total	95.9	89.2	31.4	36.3
Fe(II)	32.1	20.8	1.0	0.6

6.4.1.2 *Fe Filtered*

In Figure 37, the similarity in the Fe concentrations between filtered and unfiltered Fe can be clearly seen. This is also shown in Table 14, where averages of the filtered and unfiltered Fe total and Fe(II) concentrations are shown. The proportion of Fe that is being retained in the tank is therefore initially passing a 0.2 µm filter. This suggests that the VFR is either

- 1) removing < 0.2 µm colloidal Fe particles, or
- 2) removing dissolved Fe.

The removal rate was consistent throughout the trial, with an approximate 70% of the total Fe concentration of the inflow being removed; consequently, 30% of the total Fe remained in the outflow and was not being removed.

6.4.1.3 *Ferrous Iron – Fe(II)*

Fe(II) was not measured as frequently as Fe(total) and therefore, there are gaps in the Fe(II) data relative to Fe (total) filtered and unfiltered data. A total of 13 samples were analysed for Fe(II). Inflow concentrations varied from 0.58 mg/L to 43.50 mg/L with an average concentration of 20.82 mg/L. The maximum outflow concentration was 4.64 mg/L, but on average, Fe(II) was practically completely removed from the inflow (Figure 40). The Fe(II) concentrations in the inflow were lower than initially expected from the Pourbaix diagram (Figure 3, page 15). This demonstrates that a proportion Fe(II) is already oxidised before reaching the VFR. The difference in Fe(II) in and Fe(II) out concentrations also indicate that there was also some Fe(II) oxidation occurring in the VFR but this cannot be the only Fe removal mechanism in the system because Fe (II) is not

always shown to be in the inflow water and the removal of Fe(II) as a precipitate is unlikely at this pH. The VFR is therefore not exactly acting in the same way as seen in the VFR trial at Taff Merthyr described elsewhere where the pH is more than 3 units higher compared to Cwm Rheidol (Sapsford, 2013).

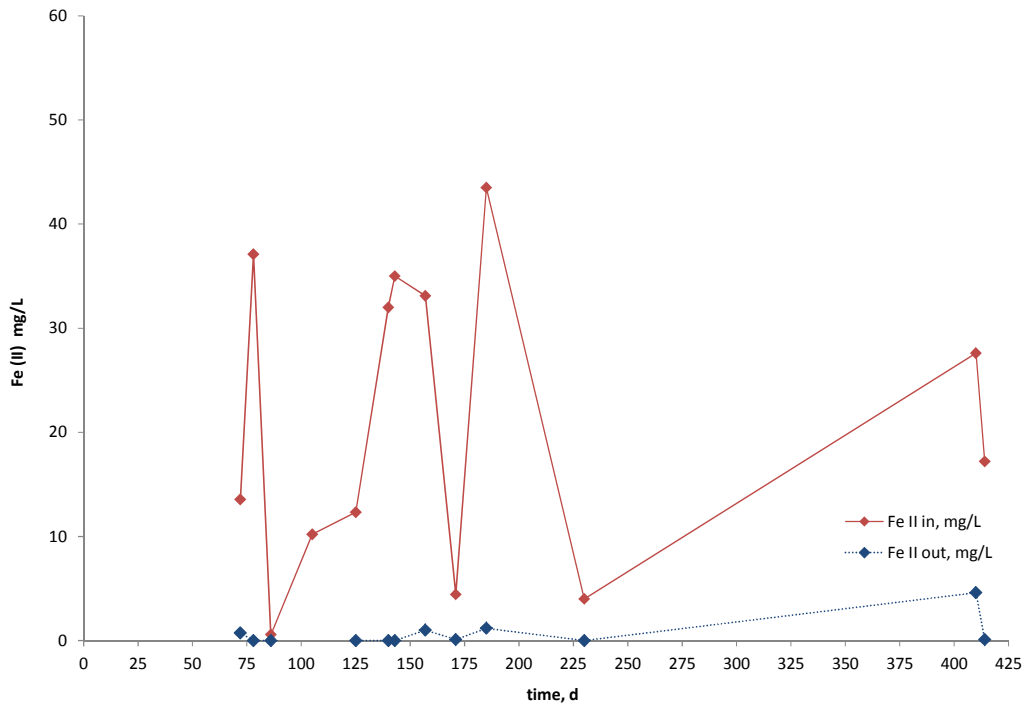


Figure 40: Inflow and outflow Fe(II) concentrations for some of the sample points throughout the trial period.

6.4.1.4 Summary of Iron Removal Performance (field data)

On average of 59–66% of the Fe from the inflow into the VFR is consistently being retained in the VFR. This is independent of the retention time in the VFR (Figure 38) or the flow through the system (Figure 41). To explain this behaviour, several possible hypotheses for the Fe removal mechanisms are considered:

- Filtering of colloidal Fe(III) particles initially in the inflow (< 0.2 μm)
- Microbial oxidation of Fe(II) plus precipitation of resultant Fe(III)
- Sorption of dissolved Fe(II) and Fe(III)

The Experiments used to determine the characteristics of Cwm Rheidol mine water and the mechanisms that are removing Fe from the VFR are summarized in Table 6 and the results presented in sections 6.6, 6.7, 6.9, 6.10, 6.11, and 6.12.

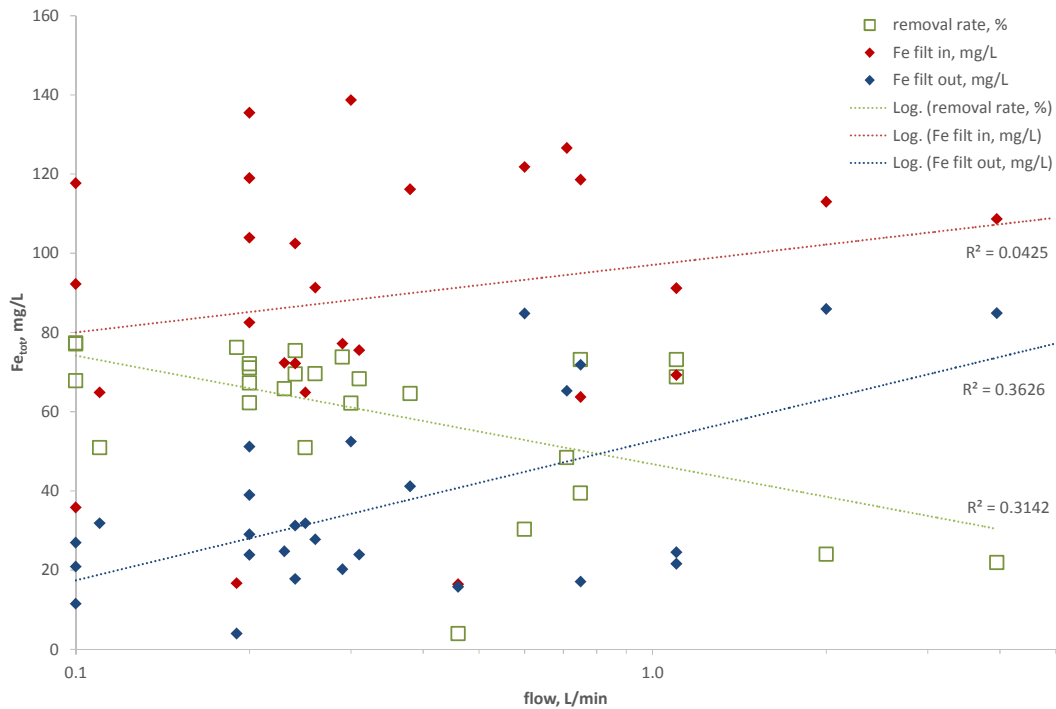


Figure 41: Fe concentrations and Fe-removal rate vs. flow rate of the VFR. Though there is a trend to lower removal rates at higher flows, the low regression coefficients indicate that there is no correlation between the removal rate and the flow.

6.4.2 On-site Parameters

6.4.2.1 Temperature

Figure 42 shows that the inflow temperatures range between 6.8 °C and 18.8 °C with an average of 13.5 ± 2.7 °C and the outflow temperatures between 6.7 °C and 19.7 °C with an average of 13.8 ± 3.0 °C (Table 13). It should be noted that the trial lasted for over a year and that there are obvious seasonal variations. The lowest temperature of 6.7 °C was recorded in January on day 230 and reflects UK winter air temperature. On the next sampling date, the VFR was frozen and the system not operating at all and no data was collected. Though the inflow has a slightly lower temperature than the outflow, a paired samples *t*-test with SPSS showed that there is no statistically significant difference between the inflow and outflow water temperatures (95% confidence interval, Table 11).

Kay Florence | Removal Mechanisms of Metals from Mine Water

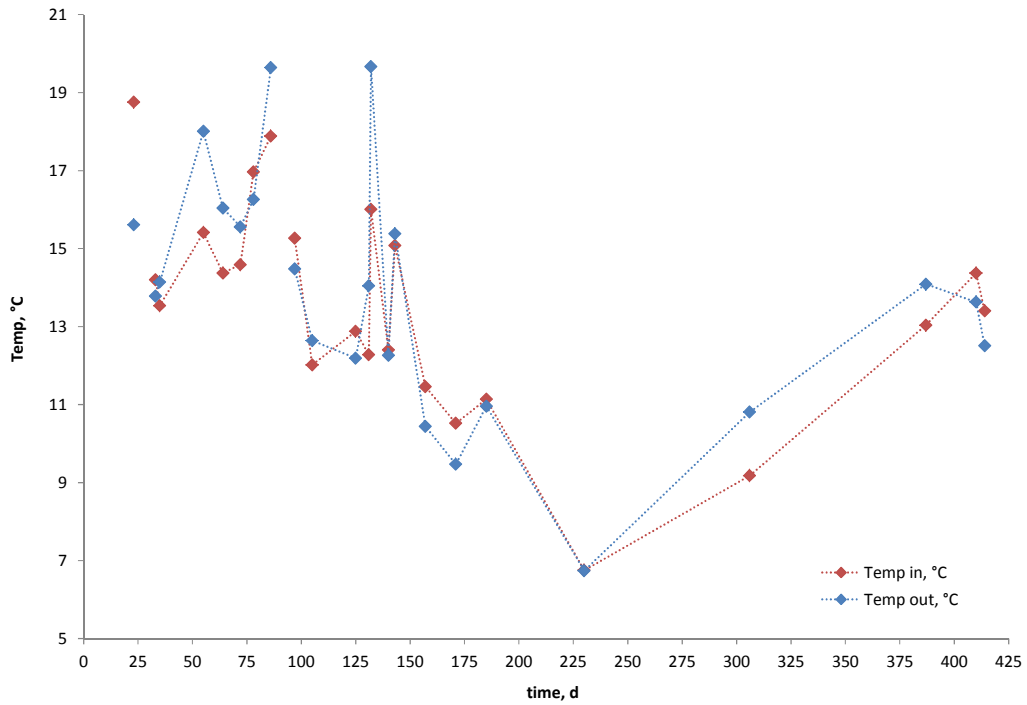


Figure 42: inflow and outflow temperature for the sample points throughout the trial period.

6.4.2.2 *pH (field data)*

The pH of the VFR inflow and outflow was measured every time samples were collected. Figure 43 shows the plot of pH values against the day of the field trial.

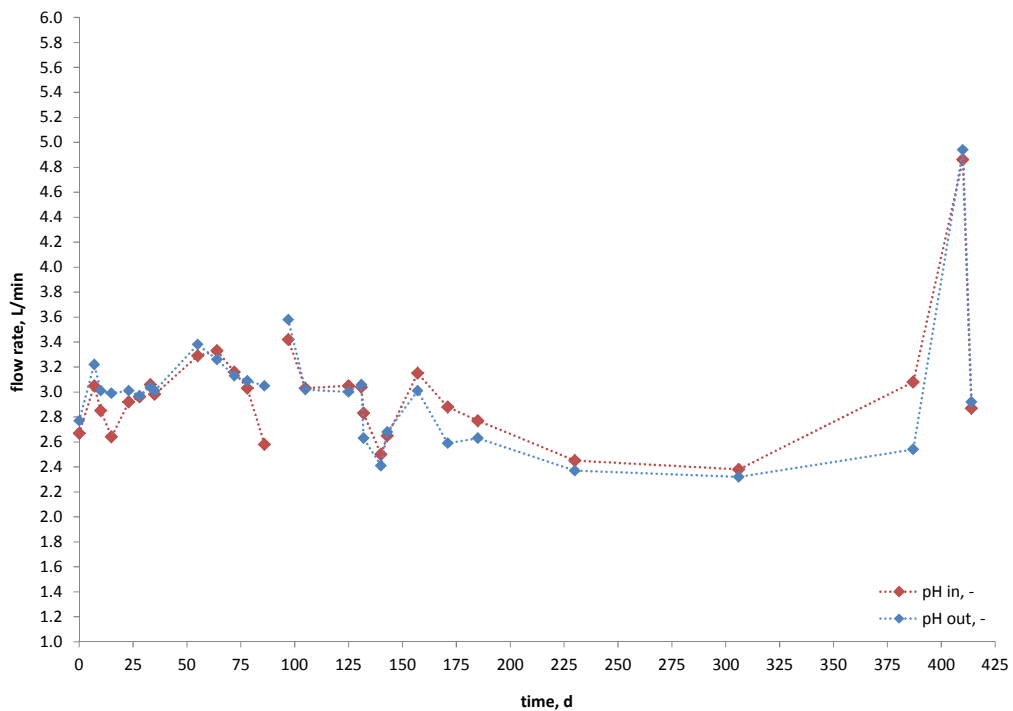


Figure 43: pH of the VFR inflow and outflow water over time.

The pH of both inflow and outflow water ranges from a minimum of 2.3 to a maximum of 4.9, showing only a slight variation over time. The average pH value for both inflow and outflow is $\text{pH } 2.8 \pm 0.5$ (Table 13; average: re-calculated arithmetic average for $[\text{H}^+]$, standard deviation from measured pH-values). There is no statistically significant difference between the pH in and the pH out values (Table 11).

The high pH-value, which seems to be an outlier, was recorded on day 410 and it should be noted that this was just after an intense rainfall event, which caused flooding along the River Rheidol. It could therefore be attributed to dilution by rain water.

As no statistically significant difference in the pH in and out can be seen, hydrolysis of Fe does not seem to be the main Fe removal mechanism in the VFR, even if a small portion of the protons will be buffered by SO_4^{2-} to form HSO_4^- . This observation complies with the E_h -pH-conditions and the thermodynamic properties of the Fe speciation, as can be seen in the Pourbaix-diagram (Figure 3). The hydrolysis and subsequent precipitation of 53 mg/L Fe (0.95 mol) according to equation 4, (page 6) would release 2.9 mol of protons. As there is no significant drop in pH in the tank, it can be suggested that the Fe is not precipitating there.

6.4.2.3 *Electrical Conductivity (EC)*

Both, the electrical conductivity (EC) of the inflow and outflow at the VFR varies over the trial period. The EC of the inflow water has a range of 1010–1982 $\mu\text{S}/\text{cm}$ with an average for the inflow water of 1544 ± 309 $\mu\text{S}/\text{cm}$ (Table 13), which is higher than the average EC of the outflow water which has a range of 843–1972 $\mu\text{S}/\text{cm}$ and an average of 1499 ± 338 $\mu\text{S}/\text{cm}$ (Table 13). Although the average of the inflow is higher than the outflow, individual sampling days might have a higher EC at the outflow than the inflow (Figure 44). The difference between the inflow and outflow is statistically not significant (Table 11). A correlation analysis showed that the EC inflow has a good correlation with the temperature (Table 12).

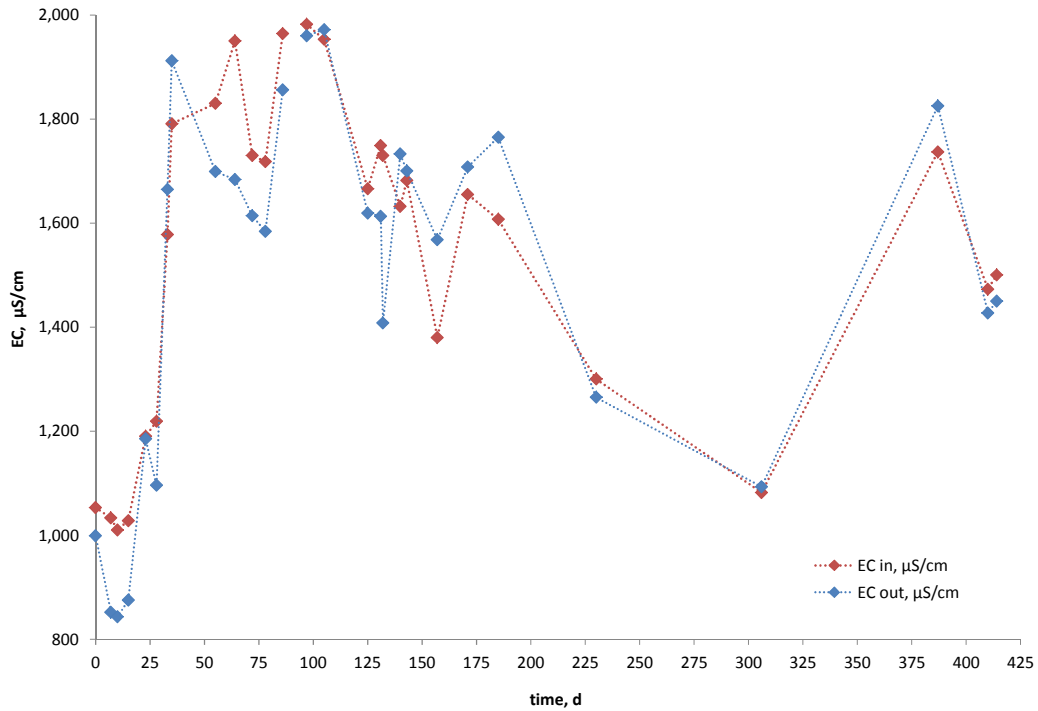


Figure 44: EC measurements for the VFR inflow and outflow over time.

6.4.2.4 Dissolved Oxygen (field data)

Figure 45 shows that the inflow water dissolved oxygen concentrations range between 1.3 mg/L and 10.7 mg/L and 1.4 mg/L to 10.4 mg/L in the outflow. These values are normal for oxidised surface waters. The average is 7.5 ± 2.1 mg/L and 5.6 ± 1.8 mg/L, respectively (Table 13). In regards to the oxygen saturation, the corresponding numbers are 54.5–107.6% in the inflow and 42.3–103.3% in the outflow, with average values of $78.4 \pm 11.9\%$ and $60.8 \pm 14.6\%$, respectively (Table 13). Whilst there is some variation between samples points, DO is less in the outflow than in the inflow. There are three instances when the DO concentration of the outflow is higher than the inflow, which is on days 7, 23 and 55, when the blocked pipes were cleared. The difference between the inflow and outflow DO concentrations are statistically significant (Table 11), indicating that oxygen in the VFR is consumed by oxidising reactions. One of these reactions is the oxidising of Fe(II) when present in the water and the other oxygen consuming process is most likely biological activity in the VFR.

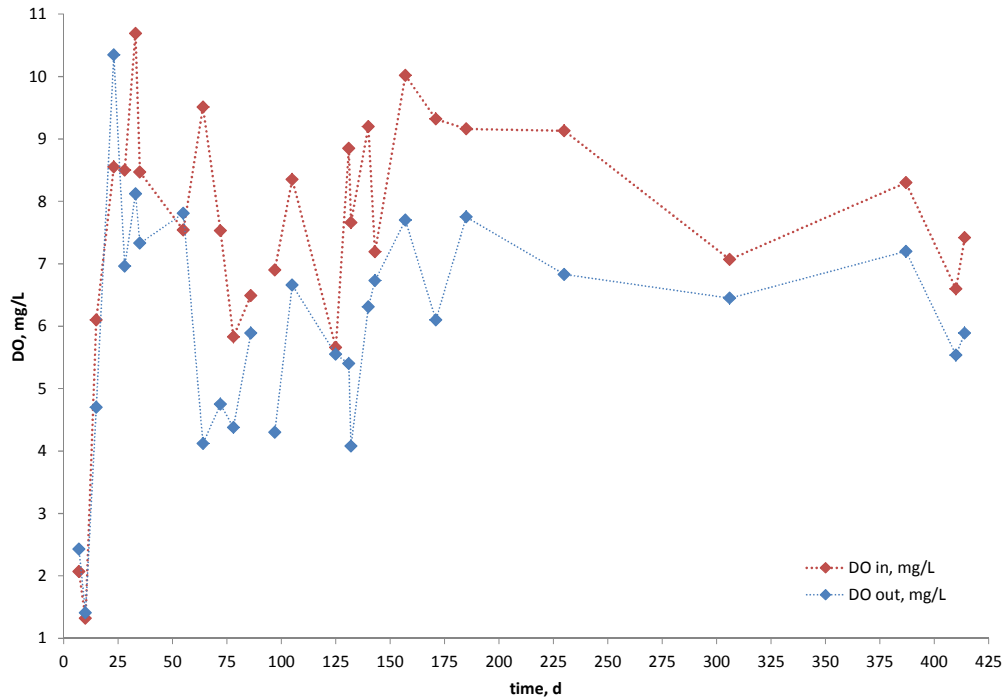


Figure 45: VFR inflow and outflow dissolved oxygen (DO) concentrations over time.

6.4.2.5 Redox-Potential

Redox potentials are measured with secondary electrodes and the results (usually recorded as ORP) have to be converted to the standard hydrogen electrode by adding the temperature dependent factor to the measured cell potential. In addition, the correction factor depends on the electrode used and is usually obtained from tabulated values. Alternatively, the correction factor can be calculated. This was done by applying equation 33 (Wolkersdorfer, 2008) to the actual mV measurements which will be used in this discussion of the field data:

$$E_{0(25^{\circ}\text{C})} = E_T - 0.198 \cdot (T - 25) + \sqrt{a - b \cdot T} \quad [33]$$

with E_0 : converted redox potential, mV; E_t : measured redox potential at temperature T , mV; T measured temperature, °C; a , b : empirical electrode dependent coefficients (for the Hanna Ag/AgCl, KCl, 3.5 mol/L: $a = 49,296$, $b = 298$).

Little variation in the ranges of the inflow and outflow measurements is seen until day 387, after which the inflow and outflow ORP are lower. This was the time when the flow rate through the system was increased by adjustment of the swan neck, to lower the head height in the tank.

Figure 46 shows the corrected ORP values. The range for the inflow water was between 491 and 792 mV, the average was $684 \pm \sigma 79$ mV for the outflow water, the range was between 463 and 785 mV with an average of $714 \pm \sigma 88$ mV (Table 13). Statistically there is a significant difference in the inflow and outflow ORP measurements, the outflow, on average, had a higher ORP than the inflow (Table 11).

The redox data shows that the redox potential of the Cwm Rheidol water is in the field where both Fe(II) and Fe(III) dominates (Figure 3).

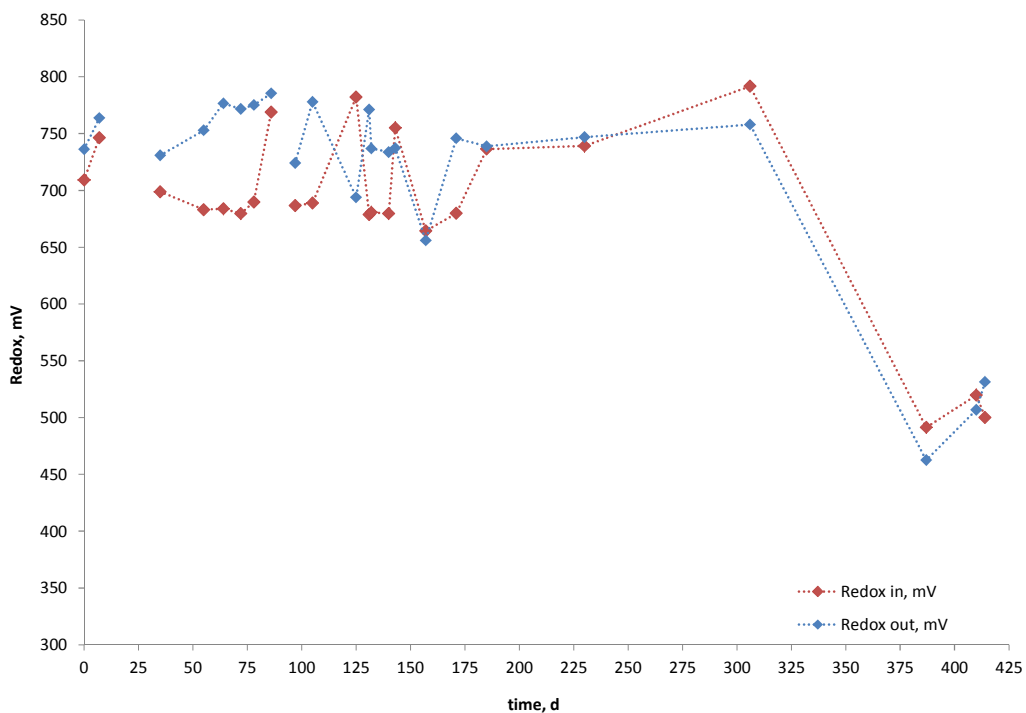


Figure 46: ORP corrected values of the VFR inflow and outflow water over time.

6.4.3 Alkalinity

Alkalinity was not measured as mine waters with a pH below 5.6 (first turning point of alkalimetric titration) don't have relevant amounts of alkalinity and is inexistent at pH values below 4.5.

6.4.4 Metals and Main Ion Concentrations (field data)

6.4.4.1 Zn

Figure 47 shows the total Zn concentrations in the inflow and outflow of the VFR. Zn concentrations in the inflow and outflow vary considerably, with higher concentrations in the early stages of the VFR trial. The inflow concentration ranges between 61 mg/L and 101 mg/L, and the average is $99.7 \pm \sigma 21.6$ mg/L. The outflow concentrations range between 58.2 mg/L to 99.0 mg/L with an average of $97.9 \pm \sigma 21.6$ mg/L (Table 13).

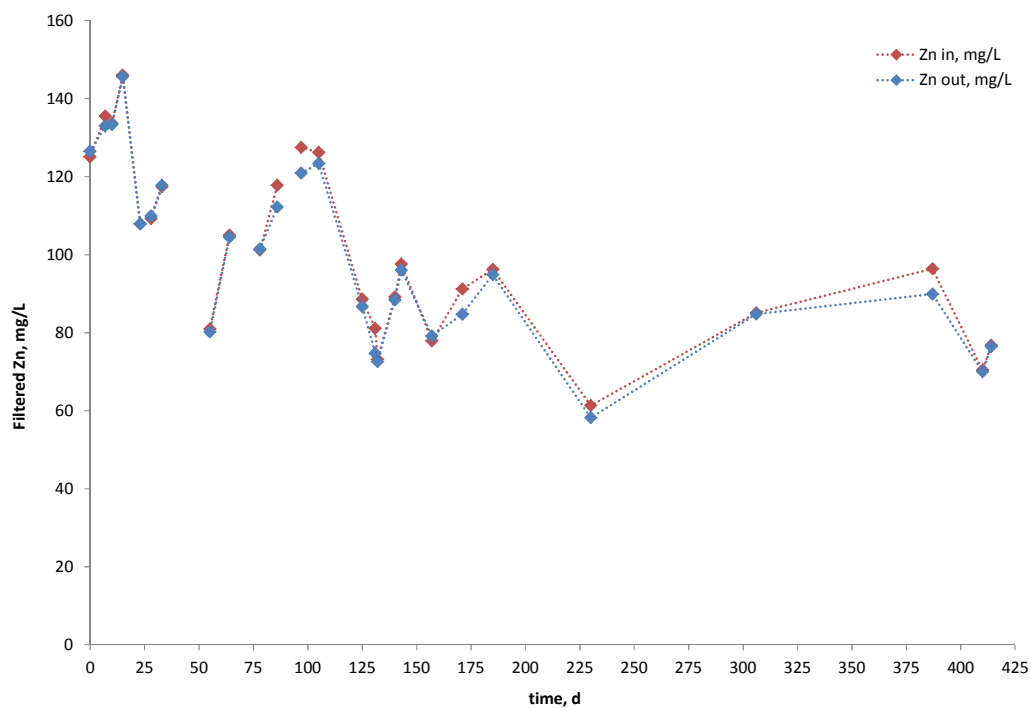


Figure 47: VFR Zn concentrations of the inflow and outflow water over time.

The difference between the inflow and outflow concentrations were consistently close throughout the trial. Whilst there is only a very small Zn amount of 2% being removed on average, the difference is statistically significant in the inflow and outflow concentrations (Table 11).

6.4.4.2 Pb

During the course of the trial period, Pb concentrations in the Cwm Rheidol Adit water ranged between 0.00 and 0.09 mg/L in the inflow, with an average concentration of $0.06 \pm \sigma 0.02$ mg/L (Table 13). The outflow Pb concentrations range between 0.00 and 0.05 mg/L with the average of $0.05 \pm \sigma 0.02$ mg/L. As can be

seen in Figure 48, there are instances where the outflow concentration is less than the inflow, which gives an average removal rate of $7.2 \pm \sigma 11.9\%$. Yet, the Pb concentrations of the inflow and outflow show no statistically significant difference (Table 11).

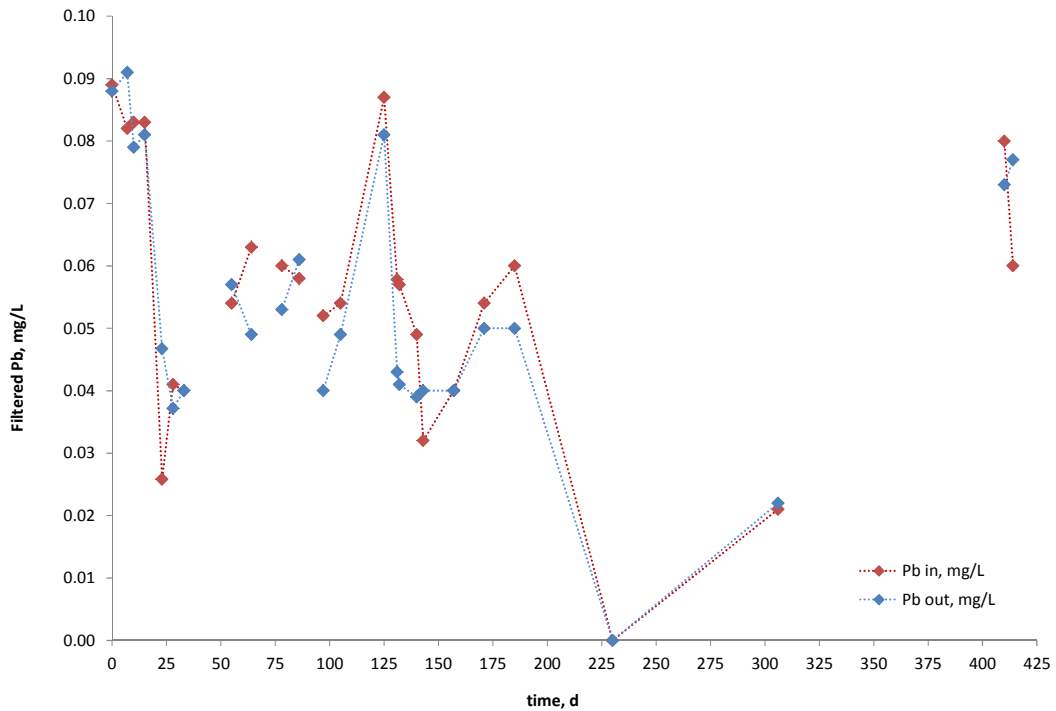


Figure 48: VFR Pb concentrations of the inflow and outflow water over time.

The imperative WQS for dissolved Pb is between 4 and 20 $\mu\text{g/L}$ (depending on water hardness) and consequently, the VFR is not effective at removing Pb in order to meet these standards.

6.4.4.3 Cd

The range of Cd concentrations remained fairly consistent in both the inflow and outflow water throughout the trial period (Figure 49). The inflow Cd concentrations ranged between 0.05 and 0.18 mg/L, the average concentration is $0.1 \pm \sigma 0.03$ mg/L, which is very similar to the outflow concentrations ranging between 0.09 to 0.18 mg/L with an average of $0.1 \pm \sigma 0.03$ mg/L (Table 13). Though there is no statistically significant difference in the inflow and outflow concentrations (Table 11), the average removal rate for Cd in the VFR is 6.55%. However, there is a statistically significant correlation between Zn and Cd in the mine water ($r = 0.75$; $\alpha = 0.01$), which is attributed to the fact that Cd is a dia-

doch replacement for the Zn in the sphalerite, one of the main Zn ores in the lode. The legal limit for Cd total in surface water is 1 µg/L which cannot be met with the VFR.

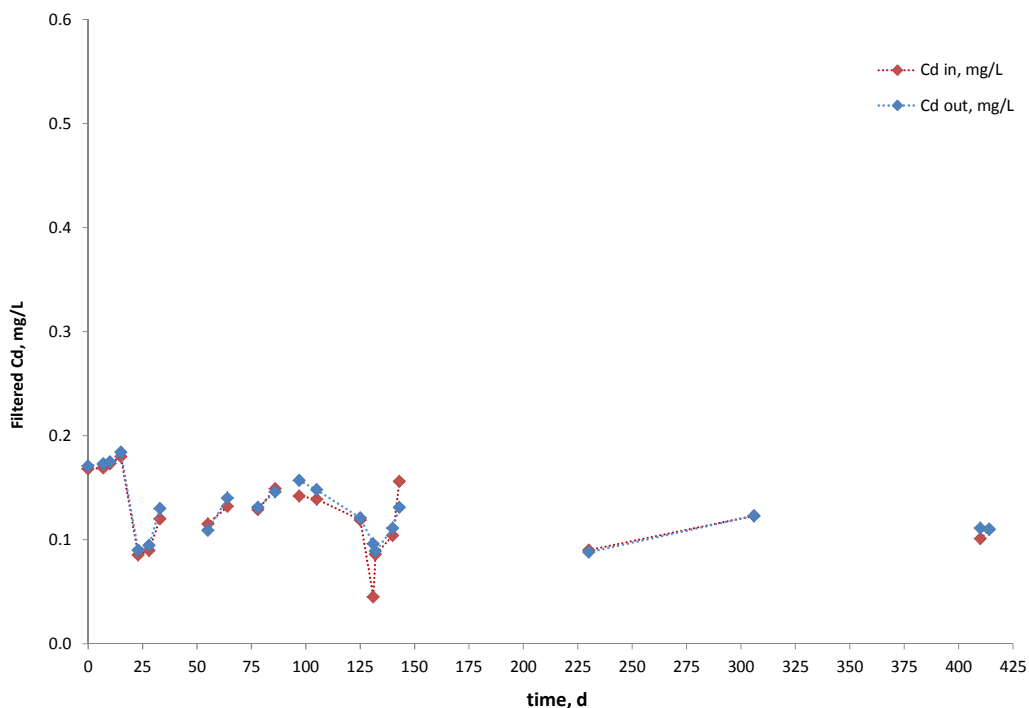


Figure 49: VFR Cd concentrations of the inflow and outflow water over time.

6.4.4.4 Sulphate

Figure 50 shows that the SO_4^{2-} concentrations are high in both the inflow and outflow. The average inflow concentration is $1485.2 \pm \sigma 438.2$ mg/L which is very close to the outflow average concentration of $1477.9 \pm \sigma 415.1$ mg/L (Table 13). Whilst there is a considerable range in both the inflow and outflow waters, the two data sets are very similar. Sulphate concentrations in the inflow range between 715.7 to 2670.7 mg/L and in the outflow the range is between 708.1 and 2083.5 mg/L. On average, the sulphate removal rate is just $2.1 \pm \sigma 2.8\%$. Statistically the difference between the inflow and outflow sulphate concentrations is not significant (Table 11).

Based on the Fe/ SO_4 -mole-ratio of 0.2 for schwertmannite and an average removal of 7.4 mg (0.1 mmol) SO_4^{2-} , 0.5 mmol (28 mg or 47% of the total removed Fe) of Fe can be precipitated as schwertmannite. Consequently, the remaining 32 mg Fe being removed on average from the mine water are other HFO phases.

The same result is obtained from the ESEM analysis where 42% of the Fe is bound to S if all of it is schwertmannite.

On 2012-01-02 (day 230), two samples were given to the laboratory for analysis by ion chromatography. One for the standard parameters used to characterize the VFR efficiency and the other one for a full water analyses. While the first one gave a SO_4^{2-} concentration of 2168 mg/L, the latter result was 1531 mg/L. Using the 1531 mg/L in modelling with PHREEQC showed that this concentration was approximately twice as high as it should be, based on a charge calculation and calculation of the electrical conductivity. Therefore all the SO_4^{2-} analysis reported here must be viewed with caution as the above suggests that there might have been a dilution or any other error in the analytical results.

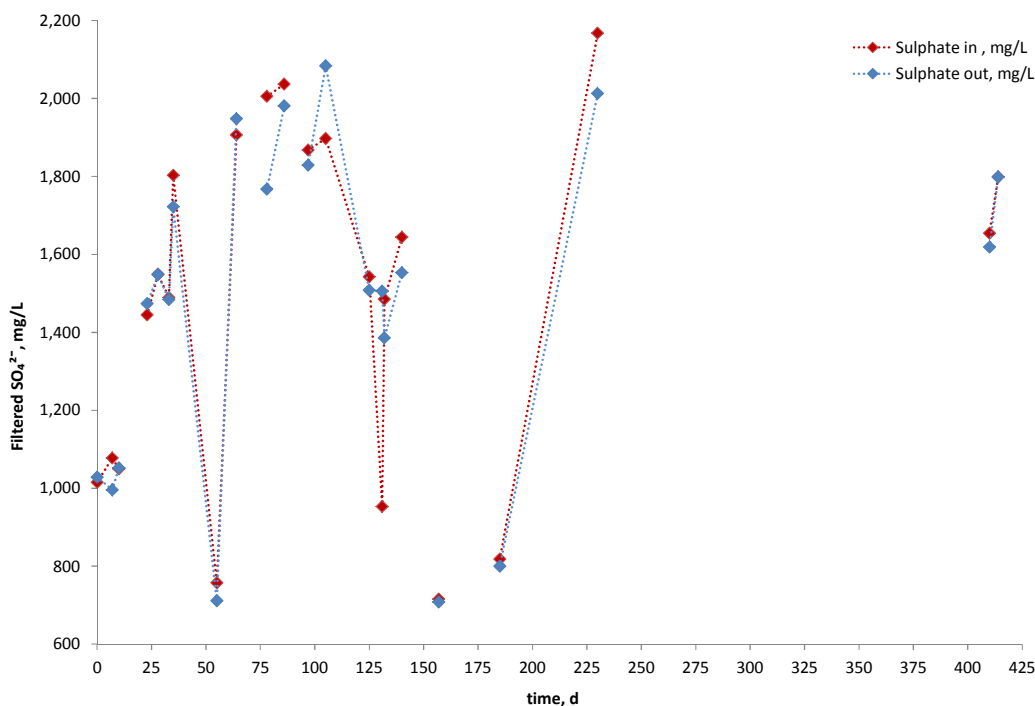


Figure 50: VFR SO_4^{2-} concentrations of the inflow and outflow water over time.

6.4.4.5 Chloride

Cl concentrations in the inflow and outflow are similar (Figure 51). The range is consistent throughout the trial period. The inflow concentration ranges between 9.0 mg/L and 22.0 mg/L with an average of 12.5 ± 3.7 mg/L. In the outflow water, the range is between 9.4 mg/L to 36.9 mg/L. This gives the outflow a

higher average concentration of 13.8 ± 6.5 mg/L (Table 13). However, statistically there is no significant difference between the inflow and outflow Cl^- concentrations (Table 11).

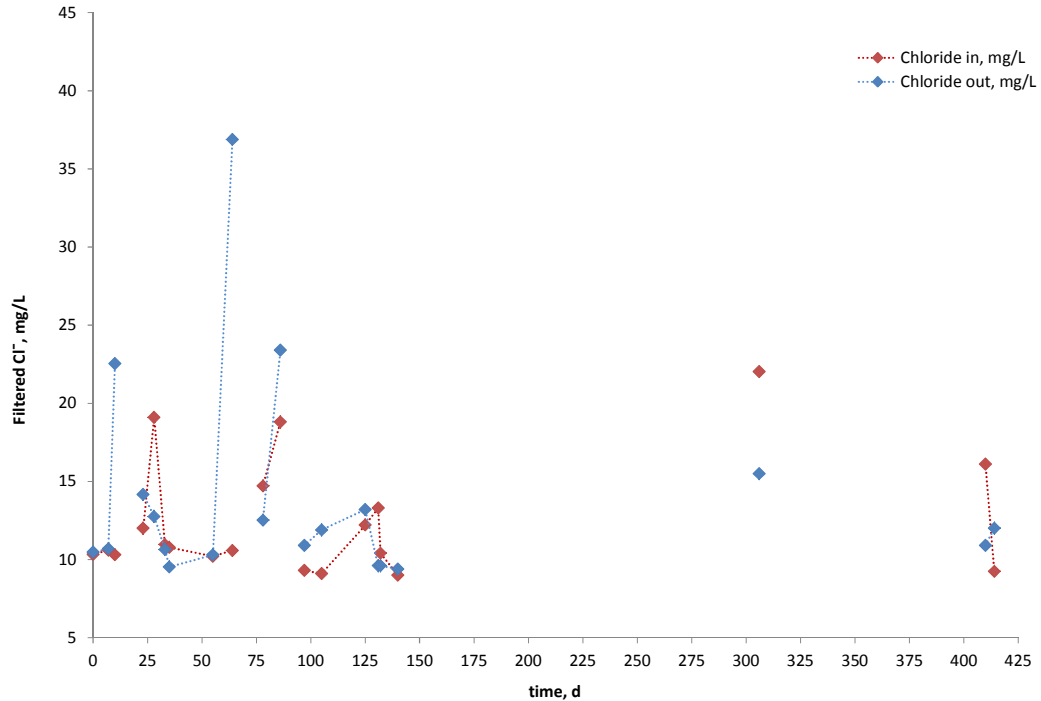


Figure 51: VFR Cl^- concentrations of the inflow and outflow water over time.

6.5 Fe Removal Investigations

6.5.1 Introduction

In order to find the governing mechanisms for the Fe removal in the VFR, a set of Fe-removal experiments were conducted in an iterative process (Table 6). Those experiments aimed to identify the removal mechanisms by varying different parameters and using the VFR sludge with different mine waters to identify the contribution of the sludge itself. Experiments were conducted on site as well as off site in the laboratory.

6.5.2 Cwm Rheidol Aeration and Adsorption Experiments

6.5.2.1 Aeration Experiment

Figure 52 shows the results of the field aeration experiment. Raw mine water was aerated for 120 min and samples collected at 10 min intervals to study the effects of aeration on the Fe total filtered and unfiltered concentrations. Though

the oxygenation rate of Fe is low at a pH around 3 (Singer and Stumm, 1970b), a 120 min experimental time was considered enough to show at least a small decrease of the Fe concentrations in the Cwm Rheidol mine water. The measured mean concentrations were 116.1 ± 6.2 mg/L for the unfiltered and 114.9 ± 2.1 mg/L for the filtered samples and show a statistically significant difference (Table 11). Neither the Fe total filtered nor the unfiltered concentrations decreased over the 2 h of the experiment that was conducted on 2011-06-19. As the regression coefficient of the linear regression for the Fe concentrations over time is very small ($R^2_{\text{filtered}} = 0.106$, $R^2_{\text{unfiltered}} = 0.087$), it is not possible to conclude that there is a systematic change of the Fe concentrations over time. This is supported by the results of a normality test (Kolmogorov-Smirnov) which shows that the Fe concentrations are normally distributed.

During the course of the aeration/oxidation experiment, no precipitation occurred. This is in agreement with the Pourbaix diagram (Figure 3, page 15), which shows that at a redox potential of 773 mV and pH 2.3 the Cwm Rheidol water is in the stability field of Fe(III) (dissolved).

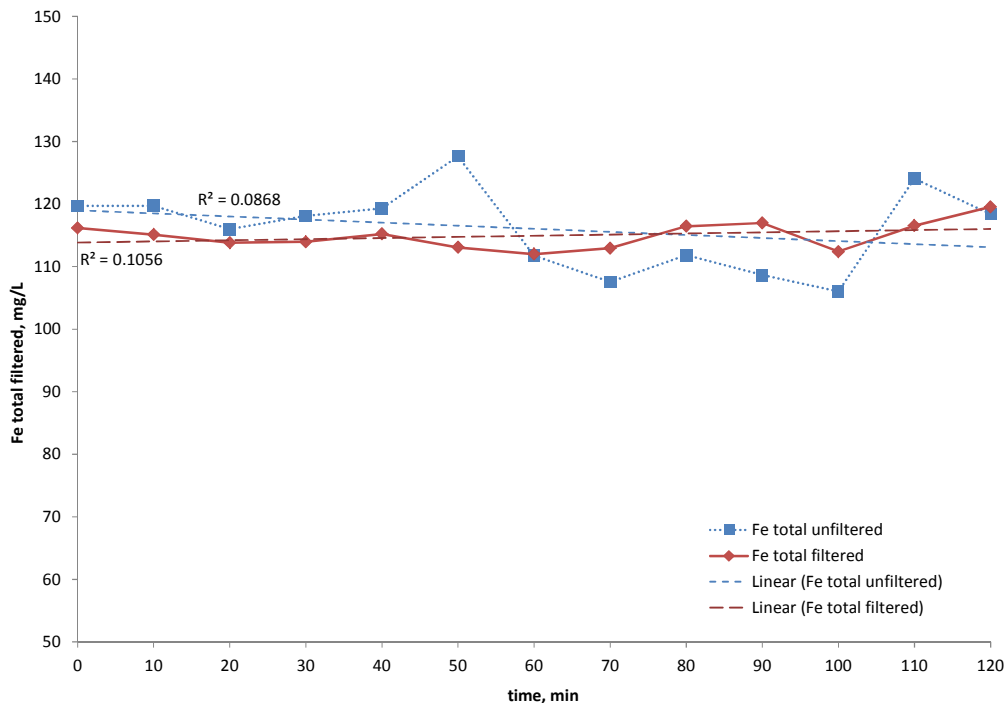


Figure 52: Fe filtered and unfiltered concentration in the raw mine water during aeration over time at Cwm Rheidol (pH 2.3, E_h 772 mV).

6.5.2.2 Adsorption Experiment

Figure 53 shows the results of the adsorption experiment described in methods section 5.10.5.2 (page 97). This experiment was designed to determine the Fe removal mechanism in the VFR. As can be seen, there is an initial steady decline in Fe concentration, which plateaus towards the end of the experiment. Analysis showed that there was < 0.1 mg/L filtered Fe(II) in the untreated mine water and consequently the total filtered Fe concentration is equal to Fe(III). The filtered Fe(III) concentration dropped from 44.8 mg/L to 38.4 mg/L in the first 60 min and to ± 29 mg/L over the next 2 h, stabilizing there for the remaining 48 h. The data follows two first order reactions ($A \xrightarrow{k_1, k_2} B + C$) with rate constants of $k_1 \approx 6.84 \times 10^{-2} \text{ min}^{-1}$ and $k_2 \approx 2.2 \times 10^{-5} \text{ min}^{-1}$ (Figure 53), which implies that both precipitation and sorption occurs.

These data, in conjunction with the aeration experiment without the VFR sludge, where Fe concentrations did not decrease (Figure 52), leads to the conclusion that the Fe is adsorbed to the VFR sludge. As the dry mass of the VFR sludge used for the experiments was 0.38 g, this amount of HFO adsorbed ± 16 mg/L of Fe(III). Consequently, assuming adsorption being responsible for the Fe decrease in this experiment, 1 g of VFR sludge is capable of adsorbing 42 mg/L of Fe(III). The removal rate would be 0.2 mg Fe per mL water and mL sludge.

This experiment also aimed in verifying if the results of the spectrophotometric detection of Fe and the ICP-OES detection are comparable. Throughout the experiment, except the sample after 15 min reaction time, the ICP-OES measured higher Fe-concentrations than the spectrophotometer. The average difference (excluding the 15 min sample) was 1.3 mg/L with a minimum of 0.8 mg/L and a maximum of 1.9 mg/L. It can therefore be concluded that a systematic error in one of the two methods is responsible for this difference. As the spectrophotometric method – other than the ICP-OES – was not compared against a lab standard, the spectrophotometrically detected Fe concentrations are likely to be the ones with the systematic error.

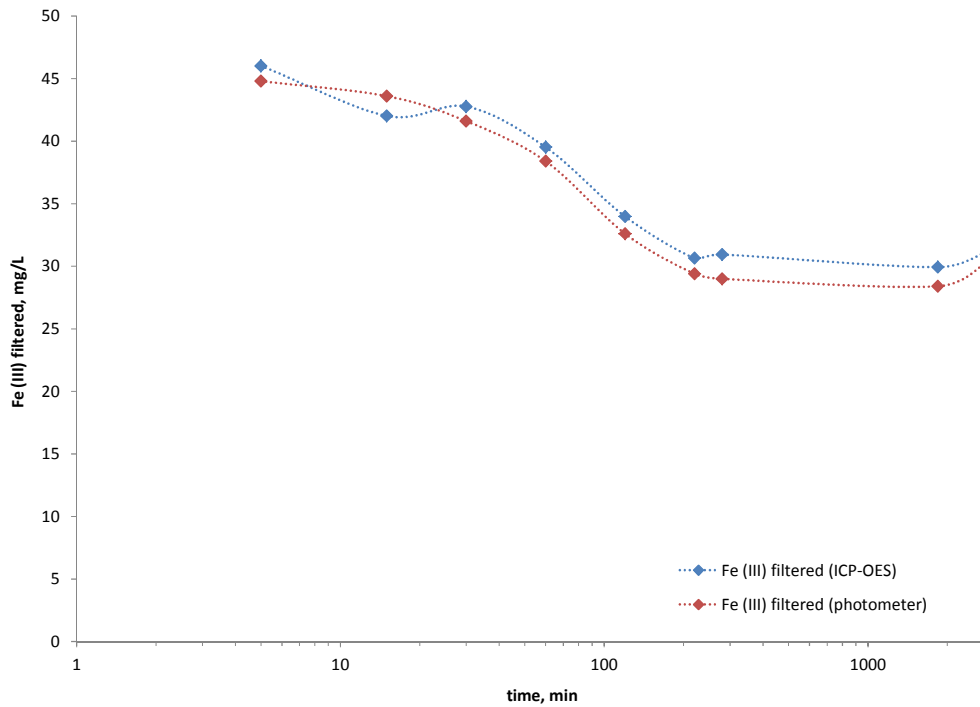


Figure 53: Fe oxidation lab experiment to determine concentration of Fe(III) in raw mine water in contact with VFR ochre over time. Results compare Fe concentrations analysed by the Merck Spectrophotometer and the ICP-OES.

6.5.2.3 *Field Adsorption Experiment*

Fe was constantly removed from the mine water by the VFR, though the difference between filtered (0.2 µm) and unfiltered Fe(III)-concentrations was relatively small. This was an unexpected result and therefore, a field adsorption experiment with fresh sludge and mine water was conducted to evaluate if the Fe removal might be a result of adsorption to the existing VFR sludge.

In this second experimental set up, larger volumes of water and sludge were used: 1 L of sludge was added to 8 L of raw mine water. After an initial drop in Fe total concentration from 102 mg/L to 82 mg/L within the first 10 min, the Fe total concentration decreased only slowly to 64 mg/L until the end of the experiment (1350 min; Figure 54). 3.5 mg/L Fe(II) measured spectrophotometrically were present at the beginning of the test and the concentrations decreased to 2.2 mg/L after 90 min and 1.7 mg/L after 1350 min, showing that there is either Fe(II) oxidation occurring or that the Fe(II) is adsorbed to the sludge as well. During the course of the experiment, the water-sludge suspension was agitated using an aeration pump.

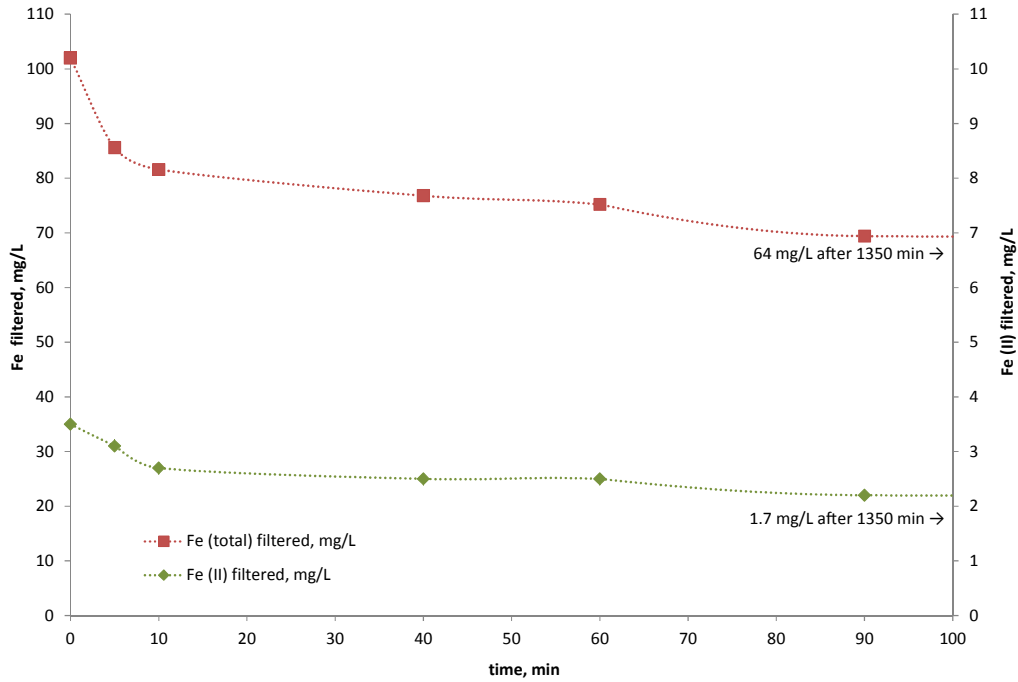


Figure 54: Cwm Rheidol field adsorption experiment, Fe(II) and Fe(total) concentration of aerated raw mine water in contact with VFR sludge over time. Note the different scales for Fe total and Fe(II).

Similar to the lab adsorption experiment, the data follows two first order reactions ($A \xrightarrow{k_1, k_2} B + C$) with rate constants of $k_1 \approx 0.342 \text{ min}^{-1}$ and $k_2 \approx 0.002 \text{ min}^{-1}$, implying again that both precipitation and sorption occurs. Yet, compared to the lab adsorption experiment the Fe removal rate of $4.8 \cdot 10^{-6} \text{ mg/mL per mL}$ sludge was substantially smaller in the field experiment.

6.5.2.4 *Aeration and Adsorption Experiments with Parys Mountain Mine Water*

Containers of the partially dewatered Cwm Rheidol VFR sludge were taken to Parys Mountain for similar experiments as those at Cwm Rheidol (no determination of the solid content was conducted as the experiment primarily aimed in gaining qualitative results only). Parys Mountain is a notorious producer of AMD and another of the priority sites listed in the Metal Mines Strategy for Wales. Experiments carried out using Parys Mountain water were aimed at verifying if the sludge produced in the VFR at Cwm Rheidol was effective at reducing Fe concentrations from another source of mine water or if the reactions occurring at Cwm Rheidol are unique for this site. The experiment lasted approximately 360 minutes in the field immediately after the water was collected.

In general, the water chemistry at Parys Mountain is different from Cwm Rheidol water. Cwm Rheidol has a pH of around 2.9 and the total Fe concentration is around 90 mg/L. At Parys Mountain, the pH is lower (2.2) and the Fe total concentrations of the mine water are around 600 mg/L, of which 412 mg/L are Fe(II). When the unfiltered mine water was stored without exposure to air, no Fe-precipitation in the Parys Mountain mine water occurred, suggesting that no agglomeration of the dissolved and particulate Fe takes place.

Figure 55 shows the decrease in both the Fe total and Fe(II) filtered samples. At each fresh HFO addition to the system (blue arrows) the Fe concentrations again decreased. In principle, the curve follows a similar pattern as at the Cwm Rheidol site and is most probably attributed to adsorption of the dissolved Fe to the HFO particles. It can be shown that the removal of Fe total follows a first-order reaction with $k \approx 7 \times 10^{-4} \text{ min}^{-1}$ and Fe(II) a second order reaction with a rate constant of $k \approx 1.6 \times 10^{-6}$. The pH remained consistent at pH 2.2 throughout the experiment indicating that the concentration decrease is not a result of hydrolysis as this might have further lowered the pH.

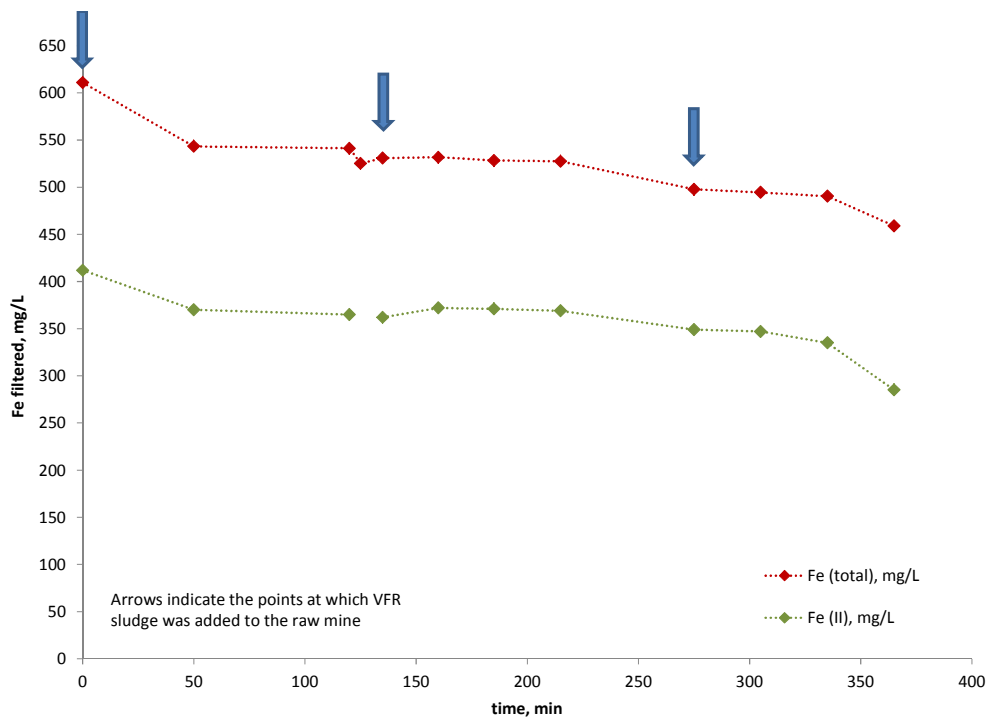


Figure 55: Results of filtered Fe concentrations during the field adsorption experiments at Parys Mountain. Blue arrows indicate the times (0, 150 and 270 min) at which the VFR ochre was added in the following respective quantities: 1 L, 0.5 L, 1 L.

6.5.2.5 *Fe Removal in a Dynamic and Static Field Experiment at Cwm Rheidol*

This dynamic and static Fe removal experiment was set up at the VFR site, Cwm Rheidol, as described in the methods section 5.10.9 and used as a control of the field and lab adsorption experiments. Since those experiments were conducted under aerated/stirred conditions, it was necessary to determine if Fe removal would be different under static conditions in the field. The experiment was timed for 50 h to simulate the expected residence time in the VFR, as the actual residence time was not known at that stage of the project.

The total Fe concentration in the aerated/stirred setup dropped from 90 mg/L to 70 mg/L (Table 15, Figure 32) and from 90 mg/L to 84 mg/L in the static setup. Initially, the raw mine water contained 35 mg/L Fe(II) and decreased to 6 mg/L in the aerated/stirred and 22 mg/L in the static setup. Similarly, Fe(III) decreased to 55 mg/L and 62 mg/L, respectively. The pH stayed nearly stable throughout the experiment, increasing by half a pH unit.

This experiment shows that Fe under aerated/stirred conditions is removed more effectively than under static conditions and that the iron is also more effectively oxidized under those conditions (Figure 56, Table 15). Those results have been reported earlier by others (*e.g.* Stauffer and Lovell, 1969) but needed to be verified under the specific conditions for acid mine water of the Cwm Rheidol Pb/Zn-mine and in the context of identifying potential VFR removal mechanisms.

Table 15: Fe concentrations in aerated and static bucket experiments after 50 h.

Experimental Setup	Time h	pH -	Fe Σ mg/L	Fe(II) mg/L	Fe(III) mg/L
Aerated	0	2.65	90	35	55
	50	2.70	70	6	64
			20	29	-9
			22.2%	82.9%	-16.4%
Static	0	2.65	90	35	55
	50	2.78	84	22	62
			6	13	-7
			6.7%	37.1%	-12.7%

However, as the water at Cwm Rheidol is already typically well oxidised (Figure 45, page 132) this cannot completely explain the conversion of Fe(II) to Fe(III). Rather, it seems as if the aerated/stirred conditions itself are increasing the Fe(III) concentration during treatment. Due to these results it became necessary to determine whether substantial populations of Fe(II) oxidising bacteria were present. Samples of mine water and ochre were collected and transported with the necessary precautions for microbial analysis to Bangor University and analysed there (section 6.7 and Appendix 2).

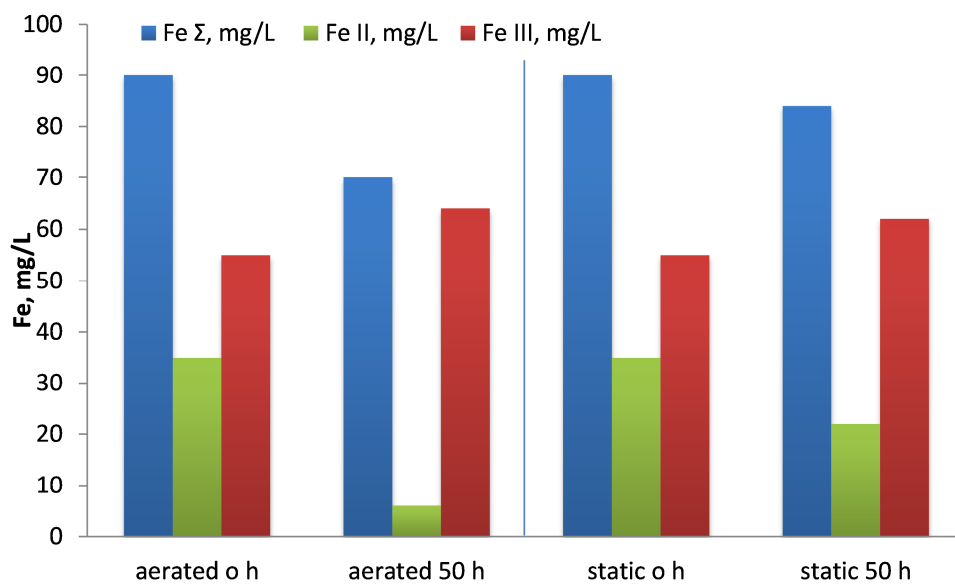


Figure 56: Filtered Fe total, Fe(II) and Fe(III) concentrations in aerated/agitated and static setup of Cwm Rheidol inflow mine water after 50 h reaction time (compare with the results in Figure 59).

6.5.2.6 *Fe Removal in Aerated/Stirred and Static Laboratory Experiments*

This dynamic and static experiment is a repeat of the previous experiment under laboratory conditions. Untreated Cwm Rheidol mine water was collected from the lower Adit drainage pipe and taken back to the CLEER laboratories in Cardiff where it was stored at 4 °C until further use. Before the experiment, the sample was allowed to adapt to room temperature. As known from other laboratory investigations with real mine water, the Fe concentrations in the aged mine water (sample cr21; Appendix 4) had dropped considerably from 111 mg/L to 57 mg/L (Table 16). This was also found to be the case for sample cr30 which was originally meant to be for the stirring experiments described

hereafter, but due to the drop in the Fe-concentrations was replaced by a fresh sample from the site. No Fe(II) was found in sample cr21.

In the aerated/agitated sample (cr21 aged sample) Fe total concentrations decreased from 56.6 mg/L to 18.6 mg/L at the end of the test, whilst stabilising after 24 h (Figure 57, Figure 58). Other than that, in the static sample, Fe total decreased from 57.8 mg/L to 44.6 mg/L during the same experimental time. Whilst the aerated/stirred setup removed 38 mg/L of Fe, the static setup removed only 13 mg/L of Fe, in both cases primarily in the first 2 h (Figure 57). Though the removal rate in the lab experiment (23–67%), is twice as high as in the field experiment (7–22%), the ratio between the Fe removed in the static and aerated/agitated tests (lab: 13.2/38.0; field: 6/20) is similar (0.30–0.34), which gives rise to a specific removal mechanism occurring, which will be further investigated in the next sections. An explanation for the higher removal rate in the lab experiments (aged mine water samples) compared to the field experiments (fresh mine water samples) is that coagulation of the particulate Fe in the lab samples has already occurred, the starting concentration is therefore lower than in the fresh mine water in the field.

Table 16: Starting Fe total concentrations in fresh and aged Cwm Rheidol mine water samples (see also Appendix 4).

Water type	Sample cr21	Sample cr30
Fresh mine water Fe total, mg/L	110.9	102.1
Aged mine water Fe total, mg/L	56.6	45.0
Difference between stored and fresh Fe, mg/L	57.0	54.3

As has been shown earlier, the DO and ORP of the Cwm Rheidol water show that the water is already aerated and oxidised at the Adit and in most cases the Fe(II) concentration is as low as 0 mg/L (Figure 45, Figure 46). This finding is supported by the oxidation experiments (Figure 52) which proved that the mine water after having travelled 600 m in the adit and 200 m downhill in a pipe cannot be further oxidised. Consequently, agitation or some type of sorption or coagulation and not oxidation of the mine water seems to play a key role in reducing the Fe total concentrations. To verify this hypothesis the experiments described in the next section have been designed.

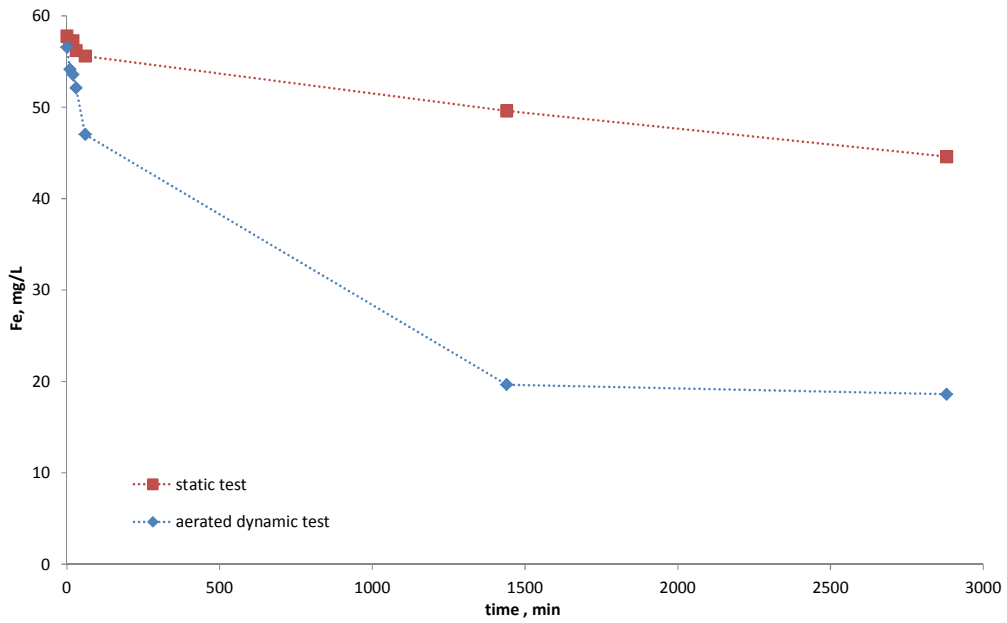


Figure 57: Course of the Fe total concentrations in aerated/stirred and static Cwm Rheidol inflow water over time (lab experiment). Fe(II) was measured at 0 mg/L at beginning of experiment.

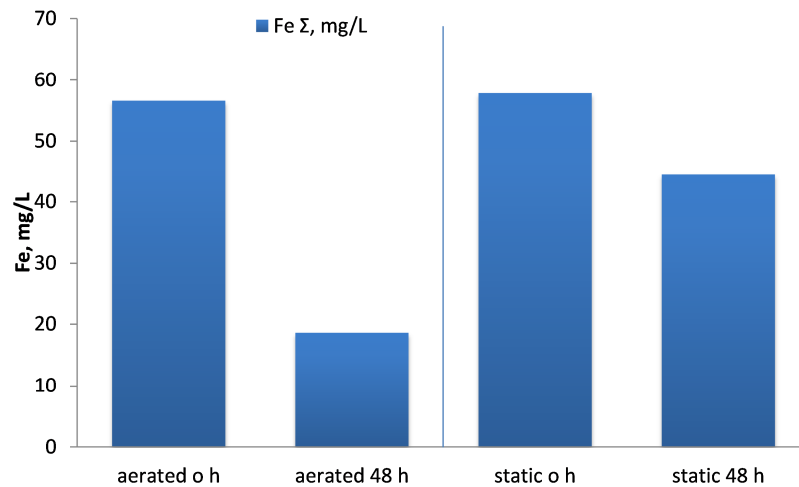


Figure 58: Fe total concentrations in aerated/agitated and laboratory static setup of Cwm Rheidol inflow mine water after 48 h reaction time (compare with the results in Figure 56).

6.5.2.7 Fe Concentrations in Aerated/Agitated, Stirred and Static Samples

As a control to the aeration/agitation experiments in the field and lab, a further experiment to compare all the previous experiments in one single experiment was conducted. The variable experimental conditions were: static, stirring with variable stirring speeds and aeration. The mine water sample was collected af-

ter a storm event and differed from the other samples in that it had a higher turbidity than these samples (Figure 34). It was not expected to obtain substantially different results from the previous experiments but to study the results in more detail.

In each of the four experimental setups, the 0.2 μm filtered Fe total concentrations decreased. The slow stirred sample removed 24.1 mg/L (32.0 %) which was higher than in all others. However, in the static sample 21.0 mg/L (36.7 %) were removed, in the fast stirred sample 19.0 mg/L (29.0 %) and in the aeration setup 18.0 mg/L (27.4 %). In all cases, the concentration was relatively constant for the first 60 min and did change thereafter, plateauing towards the end of the experiment (1500–3000 min). The total Fe concentration in the aerated sample decreased more steadily than in the other experiments. In Figure 59, the light coloured Fe total bar at 35 min in the ‘stirred, fast’ graph is interpolated from the two adjacent readings. For the Fe(II) concentrations in the aerated sample no data was available after 180 min due to a malfunction of the spectrophotometer. The decrease in Fe(II) concentrations was similar in the static, stirred slow and stirred fast samples. This was unexpected, as static experimental conditions in all previous agitation vs static experiments showed that the static sample removed substantially less Fe than the agitated ones.

This experiment showed that Fe(II) is oxidized (70 – 80%) in all experimental conditions after 180 min experimental time and that Fe total decreases after 60 min. Yet, compared to the results with mine water that was taken under non turbid conditions the Fe removal rate was 27 to 37 % substantially smaller than the 23 to 67 % from the non-turbid conditions. This experiment shows that the particulate Fe in the turbid samples contributes to the Fe total concentration in the samples. In addition, turbid samples contain particulate Fe even in the 0.2 μm filtered samples, which are not present in the non-turbid mine water samples (Figure 60). As has been shown by the centrifuging experiments, the particle size of the normally non-turbid Cwm Rheidol mine water consists mainly of particles below 0.05 μm . Yet, the turbid sample used for this test also contains particles in the 0.05 to 0.2 μm range. Those particles were not removed by the

experiment, compared to previous experiments, and therefore the Fe concentration at that experiment is higher than in other experiments.

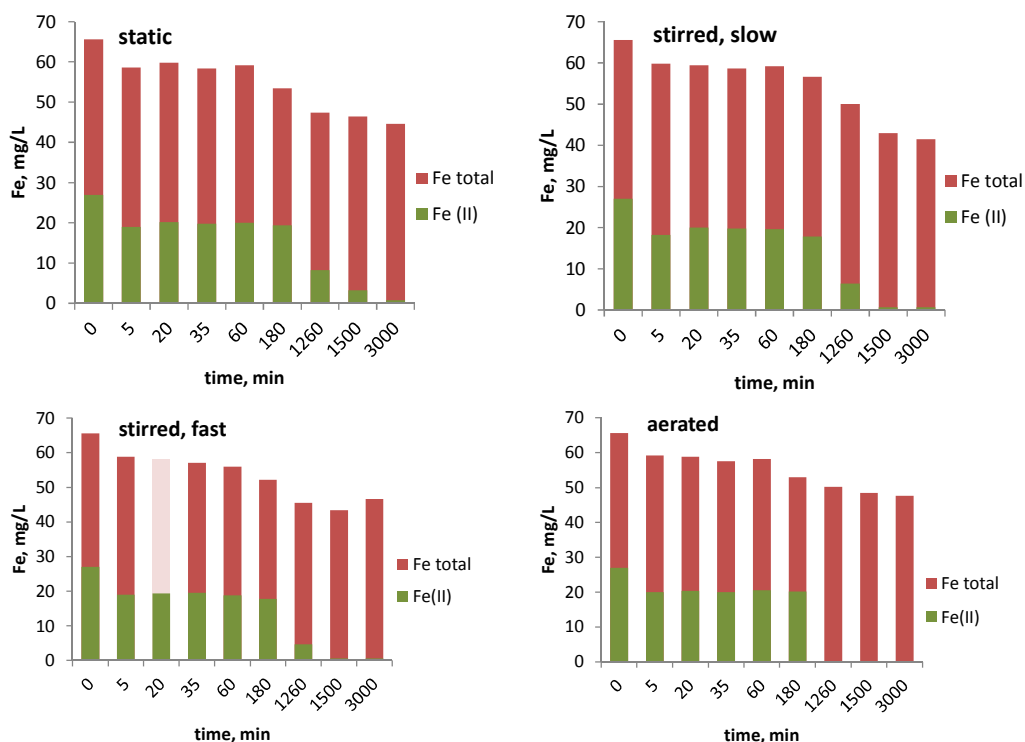


Figure 59: Fe total concentrations in aerated/agitated, stirred and static samples of Cwm Rheidol inflow water over time (lab experiment). 35 min Fe total in fast stirred experiment extrapolated (lighter bar); Fe(II) data for the aerated experiment after 180 min not available due to malfunction of the spectrophotometer.

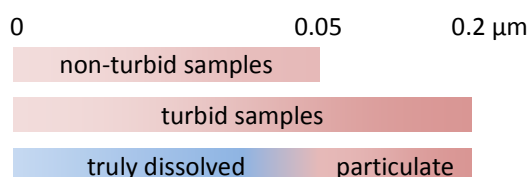


Figure 60: Distribution of Fe in the non-turbid and turbid samples used in the Fe removal experiments. 0.05 μm is considered the threshold of the centrifuging experiments, 0.2 μm is the filter size used in the field and lab experiments.

6.5.2.8 Results of Outflow Aeration/Agitation Experiment

The Cwm Rheidol VFR outflow water was tested to verify if aeration/agitation has an effect on the Fe total concentration and if it can be further decreased. No Fe(II) was present in the outflow water at the start of experiment. Over the 24 h period of the experiment, there was no substantial change in the Fe concentra-

tion (Figure 61). Initially, the Fe concentration was 27 mg/L and at the end of the experiment 26.3 mg/L. The average of the seven samples collected for the experiment was 26.7 ± 0.2 mg/L indicating that no Fe removal occurs. Based on this and the previous experiments it can be concluded that the oxidized residual Fe concentration in the outflow water of the VFR is truly dissolved and at the E_h -pH-conditions cannot be further decreased by the mechanisms occurring in the VFR.

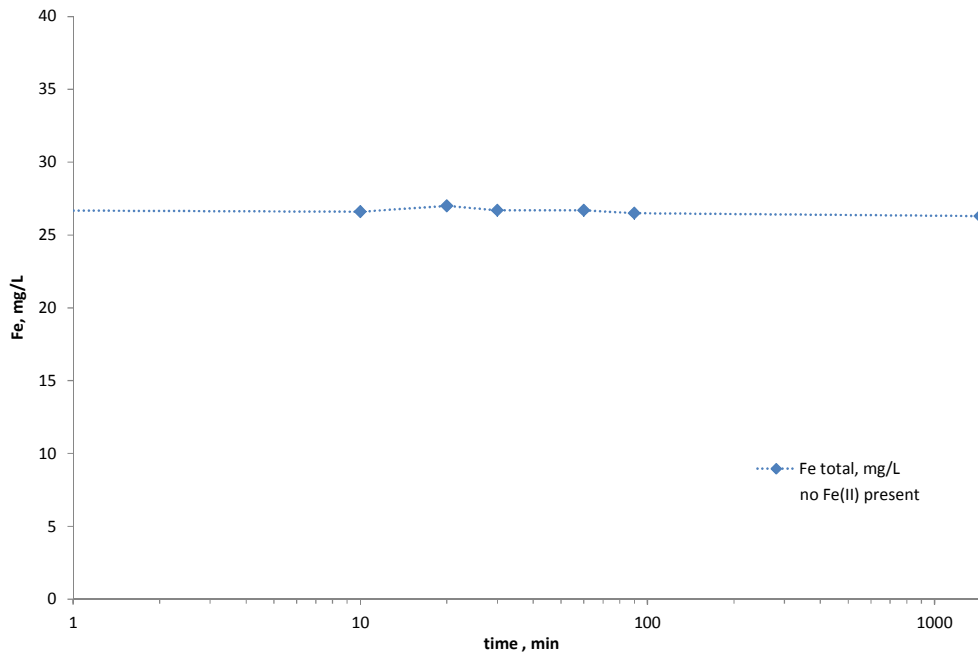


Figure 61: Time dependend Fe total concentrations in aerated/stirred sample of Cwm Rheidol outflow water (lab experiment).

6.6 Limestone Experiments

6.6.1 Cwm Rheidol Open System Limestone Experiment

The Cwm Rheidol open system limestone field experiment was initiated to verify if a limestone channel would be able to remove the acidity and the contaminating metals of concern from the VFR outflow water. Though numerous of these experiments have been done before at other locations, it was designed to investigate if a limestone channel would be an option as a second treatment step following the VFR. The metals of concern in the outflow water are Fe, Zn,

Cd, Pb, Cu and Mn (Table 13, Figure 62), but only Fe and Zn were investigated more detailed in this thesis.

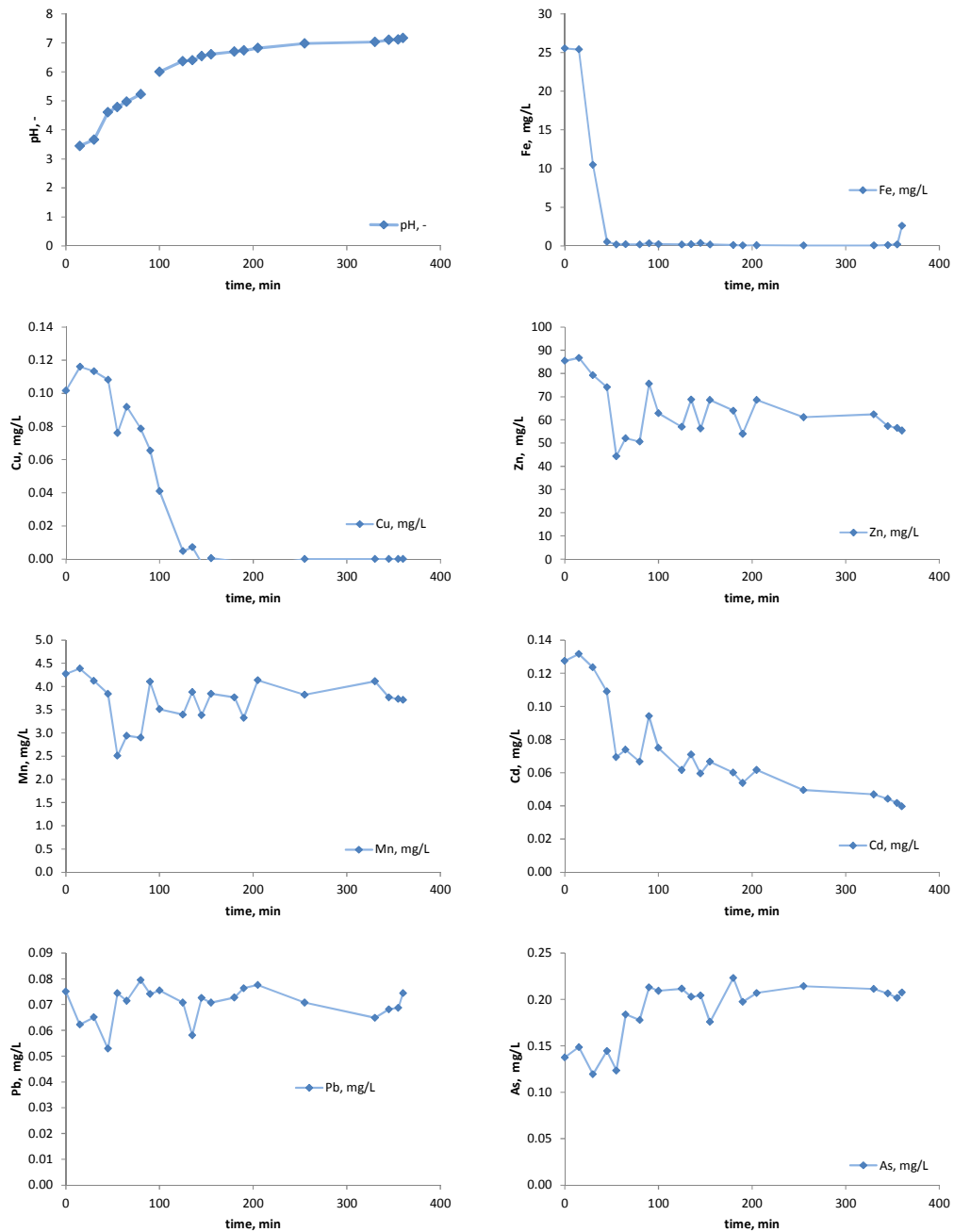


Figure 62: pH and filtered (semi-)metal concentrations in Cwm Rheidol inflow water in contact with limestone.

As expected, adding limestone to the outflow water increased the pH steadily from 3.5 to pH 7.1 over the 6 h of the experiment. Neutral pH 7 was reached in 330 min reaction time. The Zn concentration decreased from 85.47 mg/L to 56.97 mg/L in the first 2 h then stabilised with no further decrease until the end

of the experiment. Further Zn removal was not possible, because minimum Zn solubility is not reached at the final pH of this experiment, as can be seen in Figure 2 (page 8) which shows that the minimum solubility for Zn is between about pH 8.5 and pH 10.5. How much of the Zn removal is attributed to co-precipitation or sorption and how much of the formation of solid Zn-phases (such as Zn(OH)_2) cannot be said with certainty with the results obtained. Ferric Fe, which has a solubility which is particularly pH dependent within the experiment's pH-range, decreased from 25.53 mg/L to 0.52 mg/L within the first 45 min as the pH reached 4.5. Cu was also removed in the first 2 h until the pH reached 6.4, where Cu starts to have its minimum solubility. Mn was not removed, as Mn(II) is very soluble below pH 10. Cd dropped from 0.13 mg/L to 0.06 mg/L in the first 2 h. Given the solubility of Cd being high until pH 10 to pH 13, Cd co-precipitates most likely with the Fe oxyhydroxides. The concentration of the semi-metal As increased from 0.13 mg/L to 0.21 mg/L in the first 2 h and remained stable from then on. There are two possible sources for this increase in As, namely the limestone which can contain between 2.6 to 50 mg/kg of As (Price and Pichler, 2006) or the PVC material of the buckets used in the experiments as antimicrobial chemicals containing As are typically added to PVC (US EPA, 2009). Because potential reasons for the increase in As concentrations were only investigated during write-up of the thesis, no further investigations of the limestone or PVC were conducted.

Consequently, these experiments show that a limestone-based system might remove some of the remaining (semi-)metals of concern given that the chosen mean residence time in the limestone bed is high enough. To avoid additional As input into the Rheidol river, the limestone needs to be chosen carefully to have a low As-content.

6.6.2 Cwm Rheidol Closed System Limestone Experiment to Assess the Potential for a RAPS System as a Second Treatment Stage for Zn Removal Following a VFR

In the lab, limestone was added to untreated Cwm Rheidol water in a closed system. The water had been collected and stored for three days at 4°C before

the experiment started. This is reflected in the Fe total being 66 mg/L at the start of the experiment.

The hypothesis tested in this experiment was that the acidity would dissolve the CaCO_3 thus adding CO_2 plus carbonate species to the water. By doing this in a closed system, the CO_2 would be prevented from escaping. Once the system is degassed during the CO_2 stripping phase, the CO_3^{2-} would increase the pH sufficiently enough to about 8 to precipitate Zn as ZnCO_3 . In the first 48 h, the system remained a closed system and the pH increased to 4.9 in the first 2 h – sufficient to precipitate all of the Fe (Figure 63). After 48 h, the pH has reached approximately 6.6 and the CO_2 stripping phase started. After 65 h, the pH increased to its maximum of 7.3 and remained at this level for the remainder of the experiment. This shows that the closed system followed by air stripping did not increase the pH sufficiently enough to pH 8 where all of the Zn theoretically could have been precipitated.

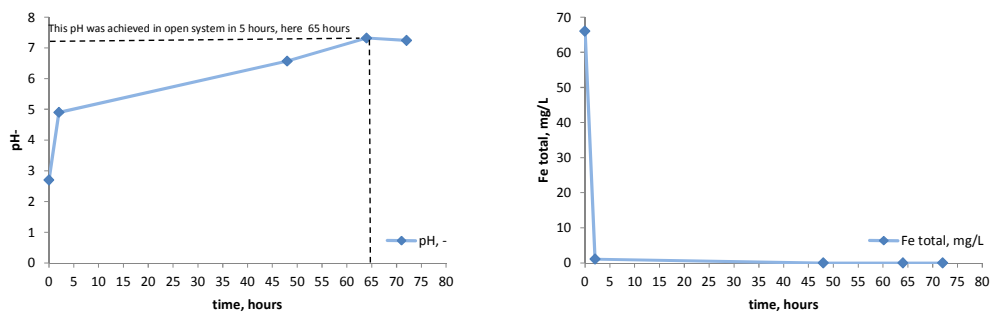


Figure 63: Cwm Rheidol closed system limestone experiment followed by air stripping.

6.6.3 Parys Mountain Limestone Experiment

The following experiment aimed in testing if the above described principles to assess whether a two stage treatment option might be applicable for the Parys Mountain mine site. This experiment was designed to assess if the installation of a VFR to remove the bulk of the Fe could be succeeded by a closed limestone bed. If the acidity of the water from the outflow of a VFR could be harnessed to dissolve the limestone, increase the alkalinity and raise the pH to precipitate metals, this could be considered a feasible treatment option. It is a follow up of the aeration and adsorption experiments described in section 6.5.2.4 on page

142. Because the results of this experiment were not as successful as expected suggesting an unrealistic residence time requirement no additional experiments were designed and conducted.

Limestone was added to the water that previously had been contacted with the Cwm Rheidol VFR sludge (“pre-treated water”) and after 3270 min, aeration was started. Parys Mountain water is different in that the pH is lower at pH 2.2 and the total Fe concentrations in the Adit water are much higher. At the time of this experiment, the raw mine water Fe total concentration was 610 mg/L. The adsorption/aeration experiment in section 6.5.2.4 showed that adding VFR sludge decreases the Fe concentration by 175 mg/L in 4 h and 45 min.

After adding the pre-treated Parys Mountain water to the limestone and maintaining a closed system, the pH increased from 2.2 to 4.77 in the first 4 h (Figure 64). At the time of starting the aeration (3270 min), the pH had increased to 5.9 and the Fe concentration to 140 mg/L. At this pH, all the iron already had precipitated in the Cwm Rheidol experimental setup.

Once aeration began, it took another 18 h before the Fe was completely removed and the pH had reached 7.1. Only after a further 37 h of aeration, the pH reached a maximum of 7.25. The Zn concentration continued to decrease throughout the experiment from initially 79.53 mg/L to a final concentration of 9.17 mg/L. It can be clearly seen that after 3270 min, the concentrations for Fe, Zn, Cu and Cd begin to decrease much more rapidly, which coincides with the pH increasing above 5.4. Almost all the Zn, Cu and Cd was removed by this experiment. Some of the Pb was also removed but the concentrations were rather erratic directly after the aeration started, the reason for this behaviour being unclear. Mn in the pre-treated mine water increases during the experiment from 23 mg/L to 40 mg/L which might be an indication that one of the impurities in the limestone is rhodochrosite: MnCO_3 (Hem, 1985). Again, time frame required to remove Zn and other metals was considered unrealistic and no further investigations were made.

The As concentration increased as well, which might be explained in the same way as in the Cwm Rheidol open limestone experiment (section 6.6.1), where

there was also an As increase. Desorption from the formed HFO can be excluded, because the As-concentration starts to increase right from the beginning of the experiment, indicating a source from the limestone or container used.

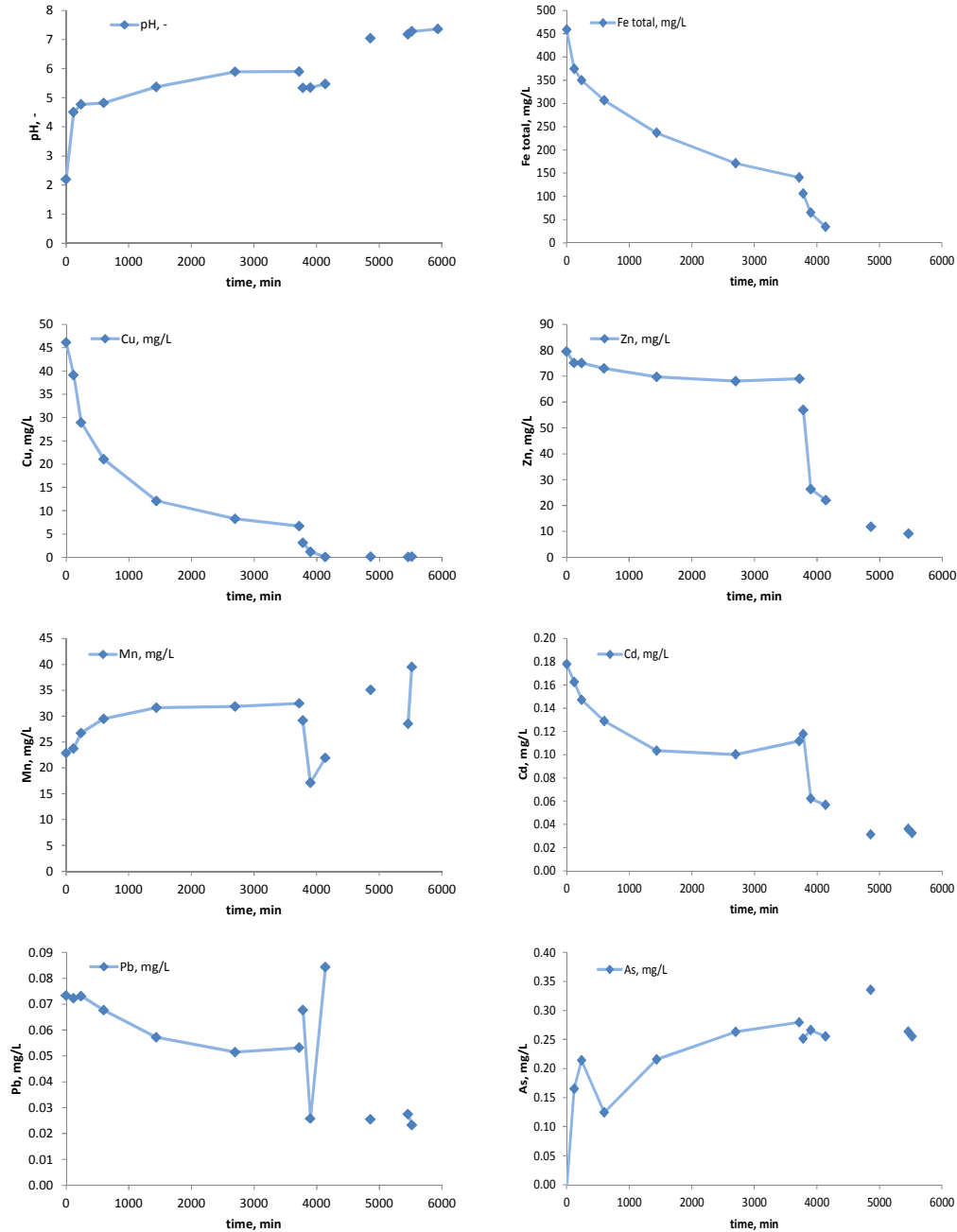


Figure 64: pH and metal concentrations in Parys Mountain water after contact with Cwm Rheidol VFR sludge and then in contact with limestone (closed system followed by air stripping after 54 h 30 min).

6.7 Ultracentrifugation of Cwm Rheidol Water

In order to validate if the residual Fe in the treated water is dissolved or colloidal, two centrifuging experiments were carried out. The first one was done to

determine the dissolved and colloidal Fe fractions in the mine water, whilst the second one aimed in identifying the size distribution of the colloidal fraction in the mine water.

In the first series of experiments, the portion of particulate Fe in the raw mine water and the ultracentrifuged water was determined. As described in chapter 5.10.11, AlSO_4 was added as a coagulant to accelerate the coagulation and settling process and it could be shown that a 60 mg/L AlSO_4 -solution showed the best settling behaviour before centrifuging the samples. After centrifuging the samples for 15 min at 3000 rpm, no substantial difference in the iron concentration could be shown between the samples without and with the AlSO_4 -coagulant (Table 17). For both, centrifuged inflow and outflow water, the filtered Fe-concentrations can be considered the same. The only relevant difference in Fe-concentrations can be seen between the inflow mine water (115 mg/L) and the centrifuged samples (91 and 94 mg/L).

Those results – at first sight – seem to be an indication that most of the iron that passes the 0.2 μm filter is dissolved. Yet, the effective diameter of the particles settling at a centrifugal speed of 3000 rpm and a 15 min centrifugal time, calculated with equation 30, is above 0.113 μm . Therefore, this experiment's results are not sufficient to verify if the Fe in the outflow mine water is dissolved or particulate, as particles with a diameter below 0.113 μm are still colloidal (Figure 60, page 149). Another centrifuging experiment, which is described in section 5.10.12, was conducted to identify the size distribution of the particulate Fe and Zn (Figure 65 and Figure 66).

Table 17: Filtered Fe(III) concentrations in inflow and outflow mine waters after selected centrifuge treatments (3000 rpm, 15 min). Only the results for the 60 mg/L AlSO_4 -solution are shown.

	Mine water	Centrifuge	AlSO_4 + centrifuging
Fe Inflow, mg/L	115	91	94
Fe Outflow, mg/L	24	22	22

Figure 65 shows the results for the centrifuging experiment to determine the Fe particle sizes in the unfiltered Cwm Rheidol inflow water, using the method described in section 5.10.12. This experiment showed that 80–90% of the Fe parti-

cles in the Cwm Rheidol raw water are <35.2 nm in size (<0.035 μm). This explains why, throughout the trial period, on average, 70% of the total Fe concentration in the inflow passed a 0.2 μm filter.

There is no general consensus in the literature, under which threshold size of particles can be considered “truly dissolved”, and the distinction between the two is analytically challenging (Mudashiru, 2008). Commonly, 1–1000 nm are called colloids, 1–100 nm are nanoparticles and several authors call particle sizes under 30–50 nm “truly dissolved” (Daughney et al., 2004). Yet, 1 nm is still larger than the size of a molecule which is in the range of several Ångstroms but in the range of hydrated ions (Ranville and Schmiermund, 1999). Detailed knowledge of the size and distribution in the nano-particle range help to understand the absorbance capacity of those particles, which generally have a large surface area. Based on the results of the ultracentrifuging and this definition of colloid ranges, it can therefore be concluded that the reactions occurring in the VFR are dominated by both nanoparticles as well as truly dissolved molecules.

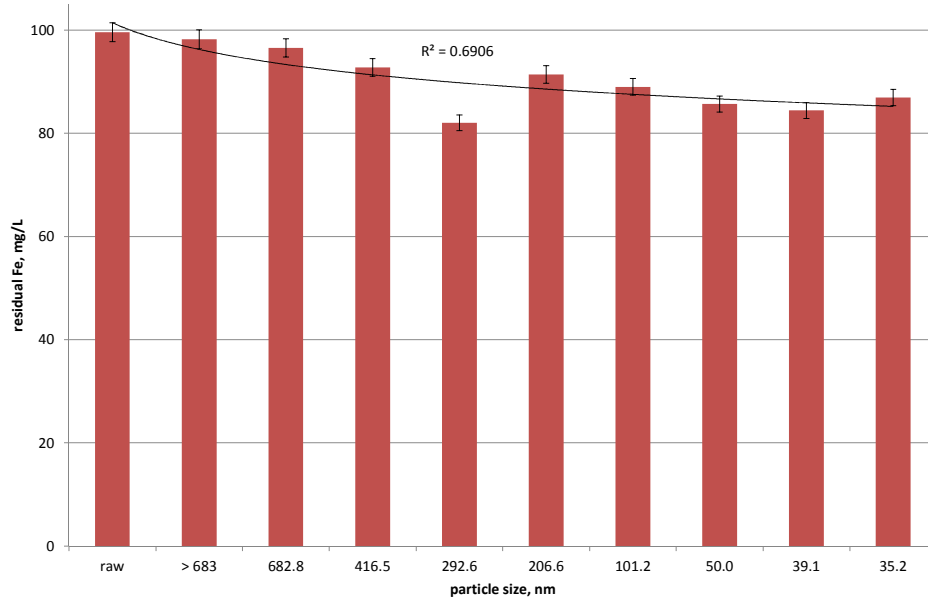


Figure 65: Results of the centrifuge experiment to determine the Fe particle size in the Cwm Rheidol inflow water. Error bars based on duplicate ion determinations.

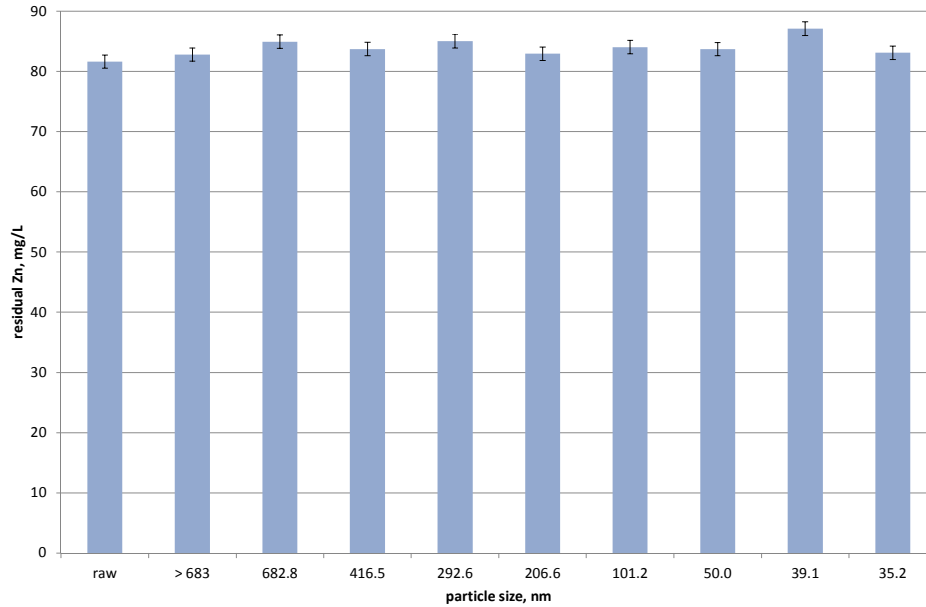


Figure 66: Results of the centrifuging experiment to determine the Zn particle size in the Cwm Rheidol inflow water.

Figure 66 shows the results for Zn from the same experiment. As can be seen, 80–85% of the Zn in the Cwm Rheidol inflow water has particle sizes less than 35.2 nm, which in the context of this experiment is considered dissolved. It is expected that at pH 2.9, the majority of the Zn will be in the dissolved form when referring to the solubility curve in Figure 2. However, taking the Zn-stability-diagram (Figure 5), there is a small portion of 15–30% where co-precipitation or adsorption reactions might be considered responsible for the Zn-removal.

6.8 VRF Microbiology (by Bangor University)

The full report including methods and results for the microbiological analysis of the untreated Lower number 9 adit Cwm Rheidol water analysis and solid ochre samples from the VFR by Bangor University can be found in Appendix 2.

To summarise this report, DNA was successfully extracted from the Cwm Rheidol water samples, which were collected and supplied to the Bangor Acidophile Research Team (BART) as per the method described in section 5.10.14. Amplification of the bacterial 16S rRNA gene DNA was sufficient to carry out T-RFLP analysis. The analysis showed iron oxidising bacteria *Acidithiobacillus ferrivorans* NO-37 (10% relative abundance), *Leptospirillum* species and *Acidi-*

thiobacillus ferrooxidans species at a relative abundance of 9% and 5% respectively. Other minor peaks that were not identifiable in the database were also detected. The most prevalent species present were the iron-oxidizing β -proteobacterium, *Ferrovum myxofaciens*, a simple community with a relative abundance of approximately 50%. These bacteria are increasingly being identified within free flowing waters that are acidic and are associated with long gelatinous formations of extracellular polysaccharide (ESP) matrixes, which stick to both inorganic and organic material allowing attachment of the bacteria in free flowing water, as attachment within the stream provides them access to the soluble Fe(II) energy source.

A good comparison was found from T-RFLP data used with T-RF data in the database with a number of archaeon clones from other very low pH streams such as those that drain the Parys Mountain mine on Anglesey North Wales and the Cantareras mine site in the Huelva Province in Spain (Rowe et al., 2007). Other data was found to correspond to cloned sequences from sediments of acidic pit lakes as well as macroscopic filaments most closely related with the phylum *Euryacrhaeota*, and the order *Thermoplasmatales* from acidic rivers was also identified.

Interesting here is that the 'gelatinous' matrix formed by the bacterial community *Ferrovum myxofaciens* dominating (50% abundance) in the Cwm Rheidol water samples could explain the suspension of the particulate Fe as well as the Fe(II) oxidation rate being faster in moving water as seen in the aeration/agitation experiments. The field data also shows that Fe is mostly oxidised by the time it arrives at the number 9 discharge pipe, where the samples for the bacterial water analysis were collected. It should be noted that the mine water travels 600 m below ground and is then piped over ground through a pipe for a further 200 m to the point at which the water is discharged. Due to the oxidation of the ferrous Fe that forms within the mine workings, the mine adit, as well as the discharge pipe, shows an abundance of soft and harder ochre precipitates that precipitated during the 800 m course of the mine water (Figure 15, Figure 16). This precipitation of particulate iron can be seen as a reason for the water samples containing primarily Fe that passes a 0.2 μm filter.

6.9 VFR Ochre Characterisation

6.9.1 Results of Sequential Extractions

The full table of results for the sequential extractions of the VFR ochre that was collected at the end of the field trial are given in the Appendix 1. The results show that the VFR sludge consisted of 36.11 wt.% Fe and 0.35 wt.% of trace amounts. The remainder of the ochre is likely to be made up of oxygen and organics. Table 18 gives the results as a % of the total mass of the sample and compares them with literature values from Kairies et al. (2001), (Sapsford et al., 2007), (Wolkersdorfer and Baierer, 2013) and (Zinck et al., 1997).

For the phases targeted by the extractions, the results showed that the Fe is mainly bound to the goethite, ankageneite and hematite phase (FeO_{x2}). The Al is bound to the Fe carbonate (Fe_{carb}) phase. Zn is mainly bound to the $\text{Fe}_{\text{ox}2}$ -phases and Cu to the $\text{Fe}_{\text{ox}1}$ and Fe_{PRS} -phases. Other than the results for EC, it seems as no magnetite was formed in the VFR as no investigated elements are bound to the Fe_{mag} -phase.

Table 18: Weight% of constituents of the VFR ochre. ^aVFR sludge, ^bCanadian Active Treatment plants, ^cUS coal mine sludges, ^dactive treatment of fluorspar mine sludge.

Constituent	Cwm Rheidol	Sapsford et al. (2007) ^a	Zinck et al. (1997) ^b	Kairies et al. (2001) ^c	Wolkersdorfer and Baierer (2013) ^d
Fe	36.11	53.6	1.5 – 28.1	25 – 61	2.67
Cu	0.10	0.002	0.001 – 1.48	< 0.0005	0.01
Al	0.08	0.08	0.1 – 11.2	< 2	0.22
Ca	0.06	2.17	3.8 – 26.6		33.53
K	0.06	0.06			0.02
Zn	0.04	0.13	0.03 – 14.4	< 0.076	0.06
As	0.01	0.02	0.002 – 0.098	< 0.3	0.12

6.9.2 TOC and Sulphur Analysis

0.355 g of dried sludge from the VFR at Cwm Rheidol was analysed using the LECO SC-144 DR instrument to determine the sulphur and organic carbon content (CS-analysis). Results following sample preparation and analytical procedure (as described in section 5.7) for the sulphur and carbon content of the VFR ochre (sample by weight %) are given in Table 19. The sample contained 4.4% sulphur which is again an indication that schwertmannite was formed in the

VFR sludge, as already proven earlier. In addition, it is consistent with the microbiology report from Bangor University (Appendix 2) which discusses schwertmannite precipitation by the Fe oxidising bacteria *Ferrovum myxofaciens* in low pH mine water. Differences between the S-content determined by this method and by ESEM Table 20 are due to the heterogeneity of the sample and the different analytical procedures.

Table 19: Sulphur and carbon content by weight % of the Cwm Rheidol VFR ochre.

Sulphur, %	Carbon, %
4.4	0.64

6.9.3 Results of XRD Analysis

VFR ochre was prepared and analysed using XRD as described in the methods section 5.5.1. Initially, the instrument was set for a 6 h scan but this did not produce any detectable results. Consequently, the scan time was increased to 14 h.

The results displayed peaks of an amorphous Fe(III) (hydroxy) oxide (Figure 67) that is characteristic of aged schwertmannite (Peretyazhko et al., 2009) and shows transformation to goethite, the more crystalline modification as shown by others (Regenspurg et al., 2004) and described in chapter 3.1.3.

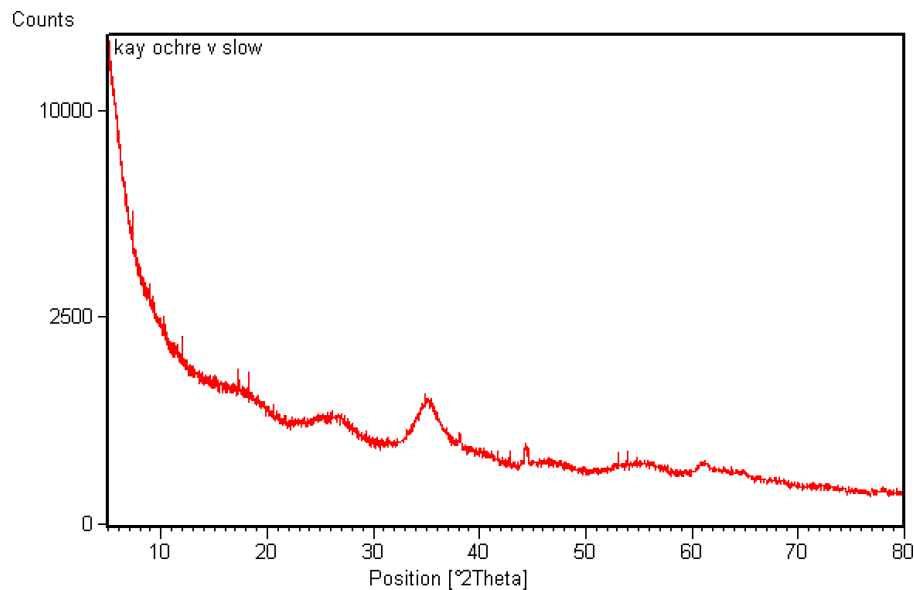


Figure 67: XRD analysis of VFR ochre. The peaks at around 15, 35 and 45°2θ are characteristic for schwertmannite.

6.9.4 Results of ESEM Analysis

ESEM images and elemental composition data were compared for the three different ochre samples relevant to the Cwm Rheidol field trial. The first sample (Figure 68, freshly precipitated ochre) was collected from the VFR during the trial. The second sample (Figure 69) was collected from the ochre bed within the VFR 48 weeks after it had been emptied and completely drained of inflow water. The third sample (Figure 70 the aged pipe scale) was collected from the adit discharge pipe.

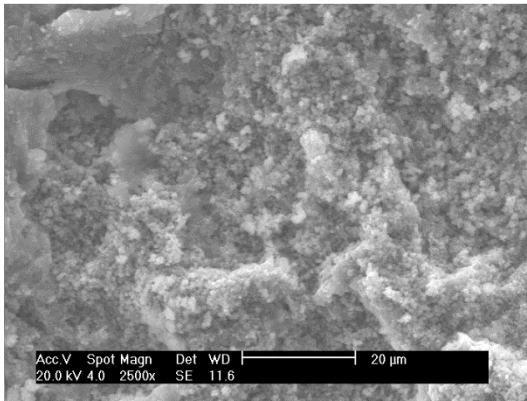


Figure 68: SEM image showing the amorphous structure of the Cwm Rheidol Fe precipitates collected from the VFR when it was in operation

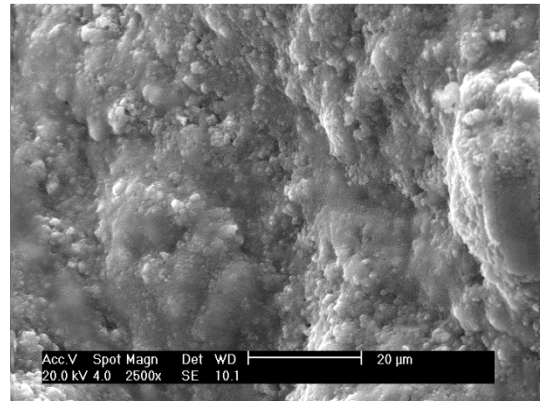


Figure 69: SEM image of amorphous structure of the Cwm Rheidol Fe precipitates (as solid ochre) collected from the VFR after it had been drained down

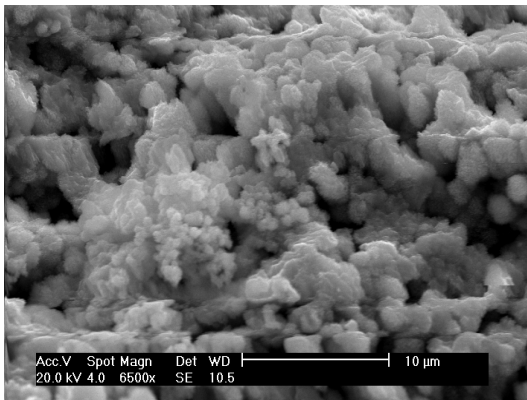


Figure 70: SEM image showing the amorphous structure of the ochre collected from the Cwm Rheidol discharge pipe

Table 20: Emission spectrum data from ESEM analysis of ochre samples from Figure 68, Figure 69 and Figure 70.

Sample description	Figure ref	O, wt %	S, wt %	Fe, wt %	C, wt %	Total, wt %
sample collected in the VFR during operation	Figure 68	41.10	3.74	56.16	0.00	101.00
sample collected from the VFR after the system had been drained	Figure 69	27.94	3.20	68.87	0.00	100.01
ochre collected from the lower number 9 adit discharge pipe	Figure 70	33.26	4.26	41.04	21.44	100.00

Samples were prepared as described in section 5.6.3, (page 87) and analysed/imaged at Cardiff University Earth and Ocean Sciences Department. Table 20 provides the results of the chemical composition for which all elements were analysed. The results are quoted in weight%.

The ESEM image for the sample taken from the VFR during operation (Figure 68) shows that the ochre has an amorphous appearance. There is no obvious crystalline structure to the precipitate, which is typical of un-aged material. The spectrum data for this sample shows the composition as 41.1% O, 56.16% Fe and 3.74% S, which compares well with the LECO furnace data providing an analysis for S at 4.4%. The ESEM image also corresponds with the interpretation of the XRD graph suggesting this is an amorphous Fe(III) (hydroxy) oxide characteristic of ‘Schwertmannite’. Similar results were obtained from the other two samples. The ochre taken from the VRF after it had been drained contained 3.2% S and the pipe scale ochre contained 4.3% S. There was also C present in the pipe scale ochre analysis. This is attributed to the carbon layer that the sample is coated with during the sample preparation stage as a conductive layer necessary for spectrum analysis.

In summary, there was little variation in the composition of the ochres. SEM images of the three samples showed an amorphous structure. The S content ranging between 3.2–4.2% is consistent with the CS analysis and suggests that an iron-oxyhydroxysulphate mineral is accumulating in the VFR. According to Schwertmann and Cornell (2000), Schwertmannite is commonly found in low < pH 3 mine water where bacterial oxidation of pyrite and SO₄²⁻ concentrations in the region of 1 g/L are found. According to Bigham et al. (1996) precipitates

that form in mine drainage that has pH values between 2.4 to 4.5 are typically schwertmannite and he describes laboratory studies where bacterial oxidation of Fe(II) at low pH suggests an optimum pH of 2.8–3.2 for which Schwertmannite precipitates. The ICP-OES data, ESEM images and XRD analysis all correspond well with section 3.1.3, which describes schwertmannite as being a ferric oxyhydroxysulphate, which is poorly crystalline and therefore difficult to characterise. Using the ideal formula for schwertmannite $[\text{Fe}_8\text{O}_8(\text{OH})_{4.8}(\text{SO}_4)_{1.6}]$ (Bigham and Nordstrom, 2000, Bigham et al., 1996, Gagliano et al., 2004), it is possible to make a more calculated approach to characterising the VFR precipitates.

6.10 Total Digest of VFR Ochre

As expected, the ochre from the number 9 adit discharge pipe (Figure 71) and the VFR ochre show a similar elemental composition, which is dominated by iron (Table 21). The combination of the low pH of the water and the S-content of the sludge, again, indicates the formation of Schwertmannite. This also is proven by the results of the XRD analyses (Figure 67) and the CS-analyses (Table 19). Fe binds with oxygen and forms various iron oxyhydrates in the sludge, as can be seen by the SEM images (Figure 68–Figure 70) and the emission spectrum data (Table 20). The Ca and Al are most likely bound to gypsum ($\text{CaSO}_4 \cdot 2\text{H}_2\text{O}$) and jurbanite (AlOHSO_4) as indicated by the PHREEQC modelling (Appendix 3).



Figure 71: Sampling location of the Cwm Rheidol pipe sludge at the end of the No. 9 adit drainage pipe. Width of pipe 300 mm.

Table 21: Results of the total digest for the VFR and lower number 9 adit discharge pipe (Figure 71) sludges (%). B, Be, Bi, Co, Mo, Ni, Sb, Se and Tl below the detection limit. 0.0 means that the element was measured above the detection limit, but below 0.05%.

Element	Cwm Rheidol pipe	VFR
Fe	38.0	36.4
S	4.3	2.5
Cu	0.1	0.0
Al	0.0	0.1
Si	0.0	0.1

6.11 Settling of VFR Precipitates

As described in section 6.3.1, the hydraulic conductivity of the ochre and gravel bed did not decrease throughout the trial period. This is thought to be attributed to the structure of the precipitates that formed within the tank. There, precipitates naturally coagulated to form relatively large flocs in the tank. During site visits, it was noted that the precipitates appeared to have a density that allowed them to settle quickly but they did not compact to form an impermeable dense layer on the bed as expected. It is this property of the forming permeable flocs that resulted in the longevity of the field trial.

Figure 72 and Figure 73 show difference in height of the precipitates in the VFR during and after the field trial. This describes the suspended nature of the flocs which remained consistent throughout the trial period.

Figure 74 shows the properties of the precipitates that formed in the VFR as being similar in nature to high density sludge (HDS), described in section 3.7.5 (page 44). The image was taken immediately after the sample was syringed from the tank. The particles settle rapidly but do not compact into an impermeable layer. The flocs appear to stay separated from each other, thus allowing the permeability to be maintained.



Figure 72: Height of the Fe precipitates in the VFR during the trial is approximately 40 cm from the top of the gravel. Inflow temporarily turned off.

To investigate the settling properties of the VFR ochre, settling experiments in graduated cylinders were performed (Table 22). The images in Figure 75 were taken in the following time sequence: 15, 60, 120, 194, 240 and 284 s (from left to right). The results show a rapid, linear settling behaviour with a settling velocity of 0.9 to 1.1 cm/s within the first 120 s (Figure 76) and a slowing down thereafter with settling velocities stabilizing at around 0.1 cm/s (Figure 77). Compared with the settling rates found by Franco and Balouskus (1974) for sludges from electro treated and aerated mine water, this settling rate is substantially slower. Whilst they were able to settle to approximately 10% after 10 min settling time, the sludge volume of the VFR is still around 30% after the same time interval. Yet, compared to HDS or low density sludge (LDS) mine drainage sludge, the settling rates of the VFR sludge are much faster (Wolkersdorfer and Baierer, 2013).



Figure 73: Height of Fe precipitates in the VFR after it had been drained is approximately 6-7 cm from the top of the gravel bed.

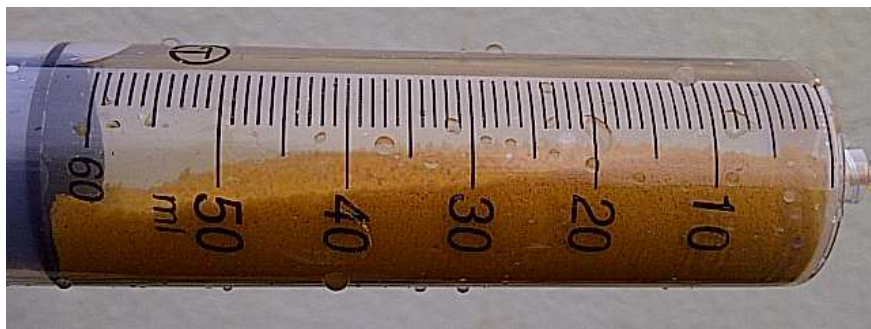


Figure 74: Fe precipitates immediately after the sample was taken from inside the VFR.

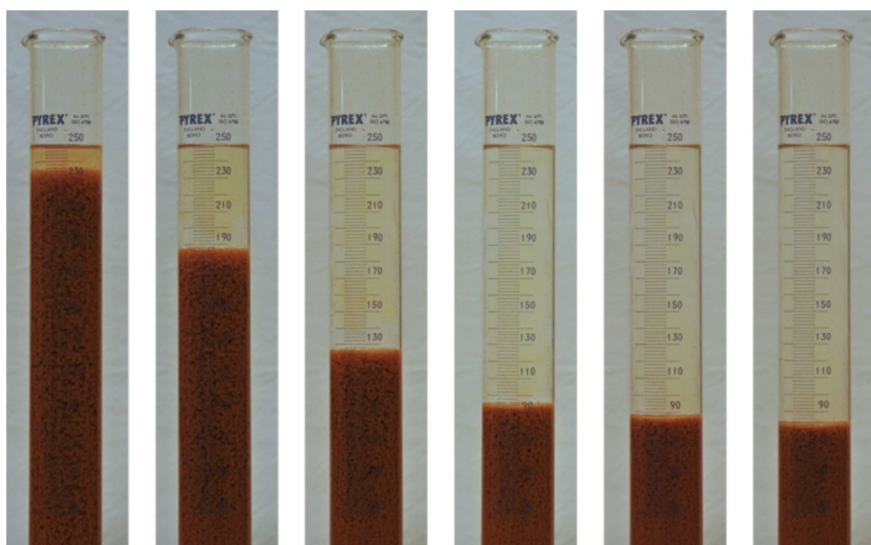


Figure 75: Settling properties of the precipitates that formed in the VFR at 15, 60, 120, 194, 240 and 284 s settling time.

Table 22: Settling rates (v, cm/s) of the VFR sludge.

time, s	reading, mm	percentage	v, cm/s
0	250	100 %	
15	236	94 %	0.93
30	220	88 %	1.07
45	204	82 %	1.07
60	187	75 %	1.13
74	172	69 %	1.07
90	155	62 %	1.06
104	141	56 %	1.00
120	126	50 %	0.94
135	116	46 %	0.67
150	108	43 %	0.53
164	102	41 %	0.43
179	98	39 %	0.27
194	95	38 %	0.20
210	92	37 %	0.19
224	90	36 %	0.14
240	88	35 %	0.13
254	86	34 %	0.14
270	85	34 %	0.06
284	84	34 %	0.07

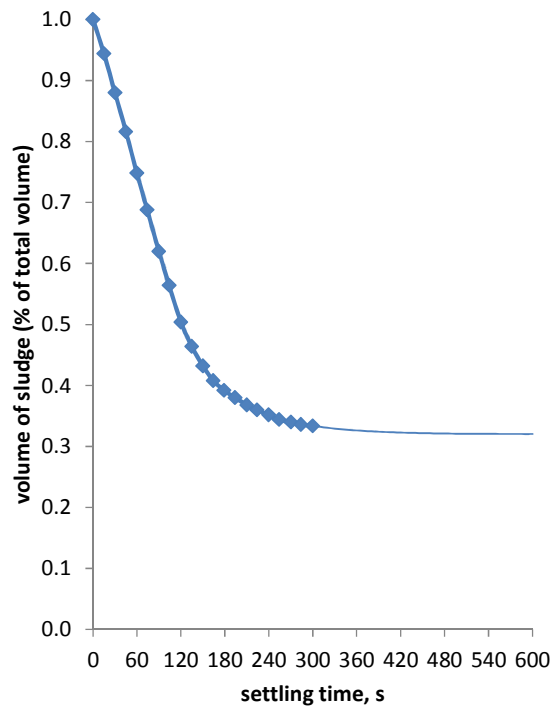


Figure 76: Settling rates of the VFR sludge. 50% settling after the first 120 s. Between 284 and 600 s, extrapolated data.

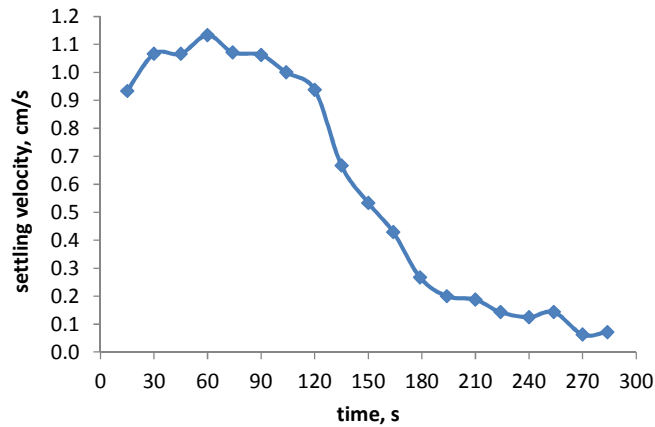


Figure 77: Settling velocities of the VFR sludge. Settling velocity decreases rapidly after 50% of the sludge has settled.

6.12 Geochemical Modelling

Though only one fully chemically characterised water sample (cr25 2012-01-02, Appendix 4) was available for geochemical modelling with PHREEQC (WATEQ4F database) analysis of that sample was carried out at the CLEER laboratories. Those results are imperative for the understanding of the mechanisms before the water enters the VFR and after it leaves the VFR. This sample was taken at the inflow to the VFR, after the water already passed a 800–900 m course through the No. 9 adit and drainage pipe. After a first modelling run with the original data, the ion balance (-42%) showed that the amount of anions is too high compared to the cations. In a second step, the database was changed to PHREEQC and in an iterative process, the original SO_4^{2-} concentration of 1530.64 mg/L was amended until the calculated electrical conductivity matched this of the measured electrical conductivity. At this stage the charge balance (-0.34%) matched the acceptable error ranges of $\pm 5\%$ (AWWA, 1998, Hem, 1985) This calculation showed that the analysed SO_4^{2-} concentration is twice as high as the modelled concentration of 765.32 mg/L.

As expected from the stability diagrams (Figure 5), Zn (61.31 mg/L) in the water sample predominantly consist of the species Zn^{2+} (72%), ZnSO_4^0 (27%) and $\text{Zn}(\text{SO}_4)_2^{2-}$ (1%). In conjunction with the low pH in the VFR, these species explain why Zn could not be removed in the VFR. The controlling phases for Zn are the Zn-sulphates Goslarite and Bianchite. Those phases might be abundant as sphalerite (ZnS) weathering products in the adit and the discharge pipe.

Based on the numerical model, iron, the element of concern in this VFR study, predominantly exists as Fe(III) (91%) and to a lesser degree of Fe(II) (9%). The dominating species are FeSO_4^+ (81%) and Fe(III) (9%) for the ferric and Fe(II) (81%) and FeSO_4^0 (9%) for the ferrous species. Controlling Fe-phases for the mine water are maghemite, jarosite-K, magnetite and jarosite(ss). Especially jarosite can be seen at the surface and walls of the No. 9 discharge adit (Figure 15, Mason (s.a.)).

6.13 Zinc Removal

6.13.1 Characterization of Mine Water

Frongoch mine water has a very low mineralisation, exemplified by the low electrical conductivity of 0.1–0.2 mS/cm and a circumneutral pH (Appendix 3 page 7). The only metal of concern is Zn, which ranges around 12–17 mg/L. Geochemical modelling with PHREEQC (WATEQ4F database) showed that the main Zn-species in the water are Zn(II), ZnSO_4^0 (3%) and ZnHCO_3^+ (1%). The solubility controlling phases for the water are $\text{Al}(\text{OH})_{3(\text{aq})}$, barite, cerussite, schwertmannite, cuprite and $\text{Fe}(\text{OH})_3(\text{aq})$, typical secondary mineral products that can be found in Pb- Zn deposits.

6.13.2 Electrocoagulation of Frongoch Mine Water (steel electrodes)

Figure 78 presents the results for the bench scale EC experiments conducted at Cardiff CLEER laboratories using a fixed voltage of 1.5 A. EC was chosen to investigate for the electrochemical removal of Zn based on previous work at Frongoch (Lauder, 2012).

The first bench test using EC in this thesis aimed to verify if it would be possible to remove Zn from Frongoch mine water using just steel electrodes. The experiment was run for 120 min. Total filtered Zn concentrations decreased from 12.3 mg/L to 9.2 mg/L in the first 20 min. The overall result after 2 h was very promising as Zn was removed to a concentration of 0.1 mg/L. Further work is needed to decrease the time for the EC because a duration of 120 min to remove Zn might not be economically feasible.

It can also be seen that the total filtered Fe concentration increases while the Zn concentration decreases. Frongoch water contains <0.01 mg/L Fe and conse-

quently, the increase in the Fe concentration is from the dissolution of the steel electrodes. During this experiment, the Fe concentration steadily increased from 0 to 5.7 mg/L after 120 min. At the same time, the pH increased from 6.29 to pH 6.63 in the first 10 min (Figure 78). After 60 min, the pH plateaus at around 6.8 for the remainder of the experiment. This experiment shows, that Zn in the presence of Fe can be removed at pH values at around 6–7. This differs from the results of the Zn-titration experiments, where Zn started to precipitate at pH-values of around 8 (Figure 79), being in agreement with the calculated solubility curves (Figure 2).

As can be seen from the course of the Zn- and Fe-concentrations of this experiment, the curve follows first order reactions with a rate constant of $k \approx 1.32 \times 10^{-2} \text{ min}^{-1}$ for Zn and $k \approx 4.6 \times 10^{-3} \text{ min}^{-1}$ for Fe. In accordance with the results of Dzombak and Morel (1990), the Zn in the experimental setup is probably removed by adsorption onto HFO.

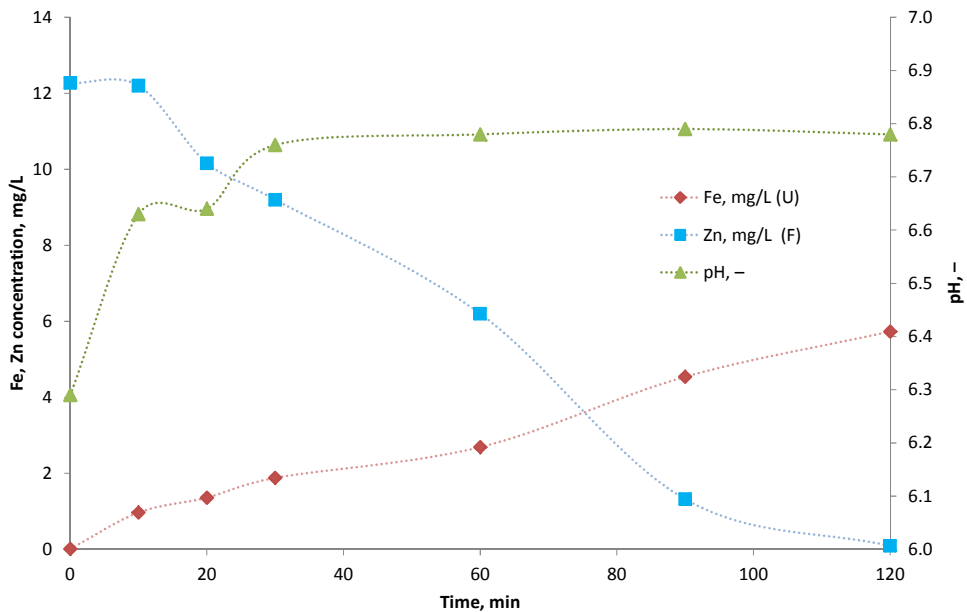


Figure 78: Results for pH, filtered Zn and total Fe removal from Frongoch mine water using steel electrodes at 1.5 A and 30 V.

6.13.3 Zinc Solubility Titration

A Zn solubility titration was performed with a laboratory prepared Zn solution of pH 2 and then titrated against 0.1 M NaOH in order to observe the changes in Zn concentration through the pH of range 2–12.

In Figure 79, the characteristics of Zn can be clearly seen. Between pH 4–7, which is within the pH of many natural waters, the dissolved Zn concentration stays relatively constant over a large pH-range, explaining why the Zn in the Frongoch mine water stays in solution. From pH 2 to 4, the concentration of dissolved Zn decreases by approximately 75% and between pH 9 and 12 the Zn concentration drops to around 1 mg/L.

This experiment showed that Zn is least soluble at pH above 9. This is fairly consistent with Figure 2, page 8 which shows the range for minimum solubility to be between pH 8.5 and 11.

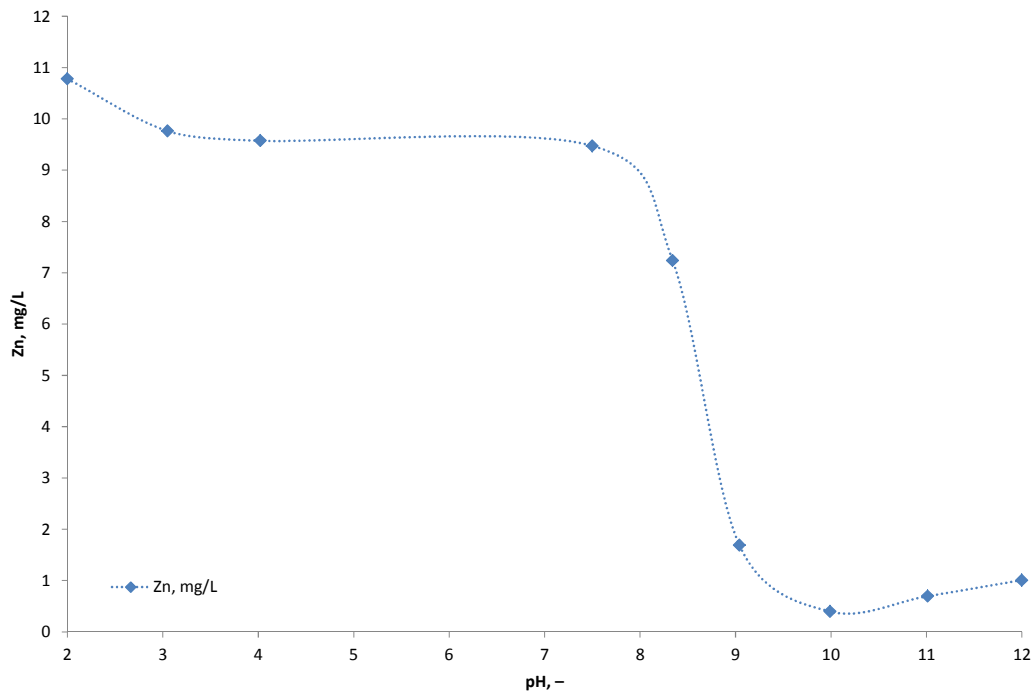


Figure 79: Solubility curve for Zn titrated through the pH range 2–12.

6.13.4 Co-precipitation vs. Adsorption of Zn in Neutral Mine Water

As has been seen in the previous experiments of this thesis, Zn is more effectively removed when Fe is added to the system. Similar findings were reported by

Jenke and Diebold (1984), Casqueira et al. (2006) or (Oncel et al., 2013). Yet, none of the experiments at this stage was able to determine with precision if the removal mechanism is by co-precipitation or by surface adsorption. This set of electrochemical experiments therefore aimed in determining, which of those two processes is more effective in removing Zn from solution. To identify if more Zn is removed by co-precipitation and adsorption rather than adsorption alone, one experiment with Frongoch mine water and four experiments with synthetic mine water and varying setups were conducted (Table 10, page 110).

Frongoch mine water showed a substantial decrease in the Zn concentration during 6 min of treatment with a steep decline after the first 2 min treatment time (Figure 80). The untreated sample initially contained 153 mg/L total unfiltered Zn and less than 6 mg/L total unfiltered Fe. This higher concentration than normally is due to natural fluctuations of Zn concentrations on site, which usually increase during rainfall events (Hartley, 2009). The sample collected at the end of the 6 min EC treatment time contained 0.4 mg/L filtered Zn and 0.7 mg/L total unfiltered Zn. The total unfiltered Zn concentration was shown to increase slightly during the stirring phase to 8.7 mg/L filtered and 22.2 mg/L Zn total unfiltered. After 15 min stirring the last sample was collected, containing 8.3 mg/L filtered Zn and 15.13 mg/L Zn total unfiltered. The total unfiltered Fe concentration at the end of the experiment was 27.63 mg/L. No pH change was observed during the experiment, which started with pH 6.6 and ended with a pH of 6.5 after the stirring phase. Consequently, Zn was removed in the presence of Fe at a pH 6.6, which is normally the pH range in which Zn is most soluble (Figure 79). The increase of the Zn concentrations during the stirring phase can be explained with re-dissolution of the Zn from the sludge formed during EC.

In the next step, synthetic Zn solutions containing 12.4 mg/L Zn (the typical Zn-concentration in Frongoch mine water) were used. The varying setup (Table 10) was designed to identify the governing mechanism for the Zn removal such that experiment 1 tests for co-precipitation and experiments 2–4 for adsorption onto HFO.

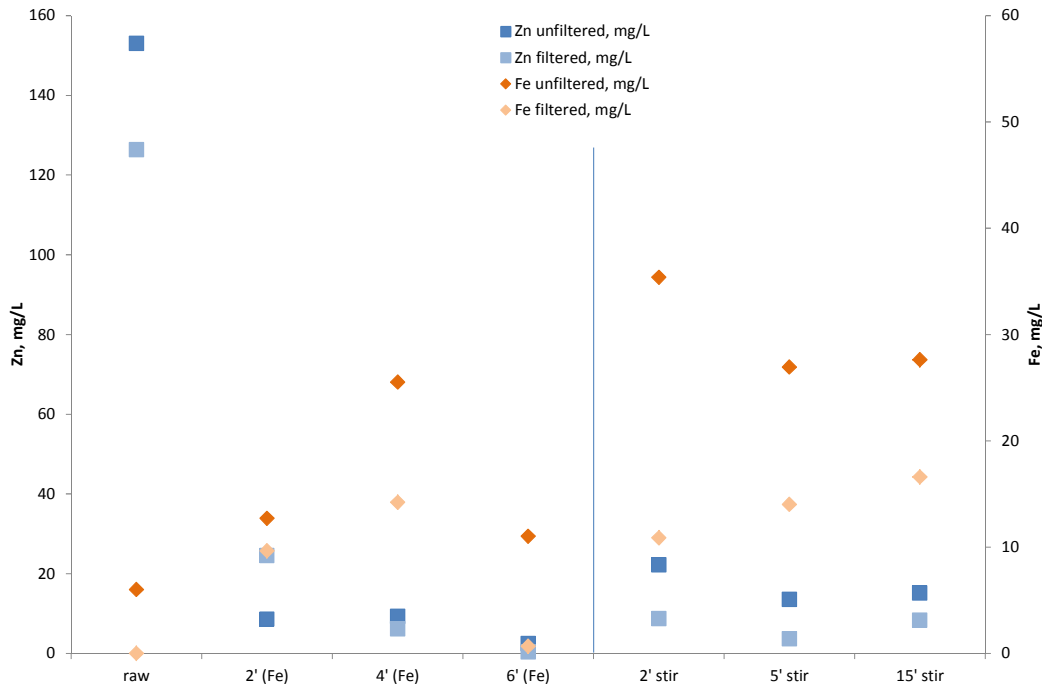


Figure 80: Results for Zn removal from Frongoch mine water by electro co-precipitation with Fe from a sacrificial electrodes spaced 30 mm apart. 1 A, variable voltage. Compare Table 10 for meaning of abscissa.

For experiment 1, Zn was added at the start of the experiment. The results show (Figure 81) that the unfiltered Zn concentration decreased from 12.4 mg/L at the start of the experiment to 1.36 mg/L after 8 min treatment time. The filtered Zn concentration after 8 min was 0.3 mg/L. Fe increased from 0 to a total unfiltered concentration of 10.85 mg/L and a Fe filtered concentration of 1.6 mg/L.

The Zn concentration remained relatively constant during the stirring period, with a maximum of 1.6 mg/L Zn at the start and a slight increase after 15 min stirring. This increase is most likely the result of re-dissolution from the EC sludge.

Figure 82 presents the results for experiment 2, in which the Zn solution was added after the Fe had been electrochemically released into solution and precipitated. During the 8 min EC phase, the Zn concentrations were 0 mg/L and increased to 3.8 mg/L filtered and 4.1 mg/L unfiltered after the addition of the 12 mg/L Zn-solution. After 15 min stirring, the total unfiltered Zn concentration was 2.7 mg/L and the filtered Zn concentration 2.3 mg/L. The total unfiltered Fe concentrations decreased from 28.2 mg/L after 2 min EC to 1.7 mg/L after 15 min stirring. Compared to experiment 1, the terminal Zn concentrations are

higher, indicating that co-precipitation and adsorption is a more efficient Zn-removal mechanism than adsorption. This demonstrates that co-precipitation is important in the EC process.

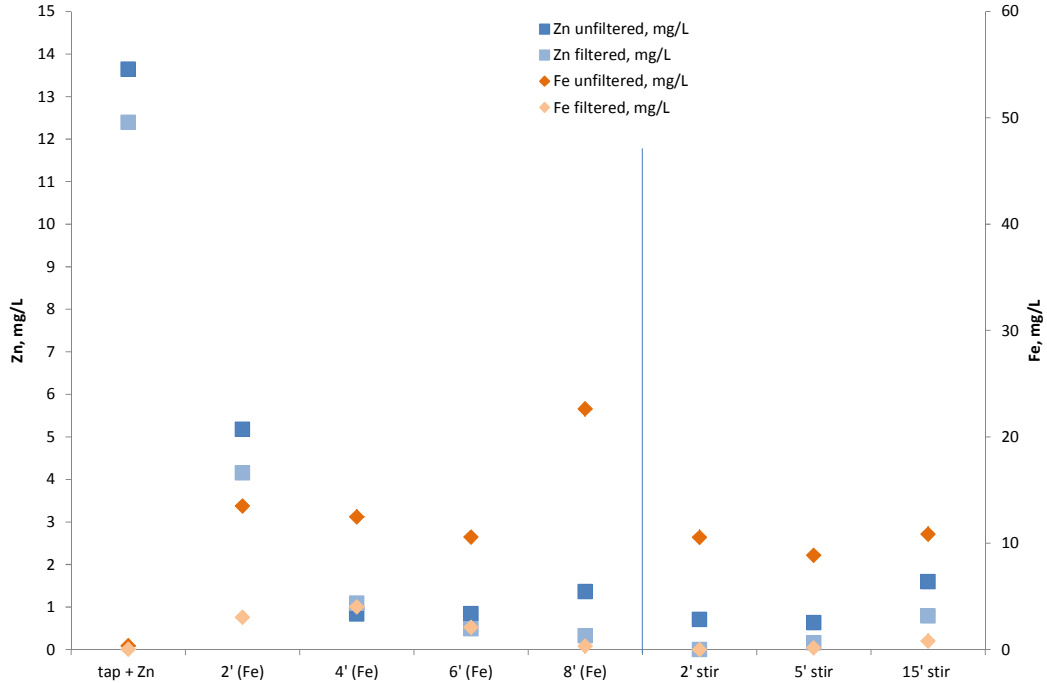


Figure 81: Results for Zn removal by electro co-precipitation with Fe from sacrificial electrodes spaced 30 mm apart. 1 A, variable voltage. Compare Table 10 for meaning of abscissa.

Experiment 2 was repeated as experiment 3 and extended with a 40 min settling time at the end of the experiment to verify if an extended time for adsorption would effect on the amount of Zn being removed. Similar to experiment 2, the Zn filtered and unfiltered concentrations after 15 min stirring range between 1.7 and 2.3 mg/L (Figure 83). During the 40 min settling phase, no substantial changes in the Zn concentrations occurred, remaining between 1.9 and 2.4 mg/L (unfiltered).

Unfiltered Fe concentrations ranged between 9.4 and 26.7 mg/L and filtered between 0 and 2.2 mg/L. At the end of the stirring phase, Fe filtered in the system was ± 10 mg/L and did not change during the settling phase. These results show that there is no substantial difference between experiment 2 and 3.

Kay Florence | Removal Mechanisms of Metals from Mine Water

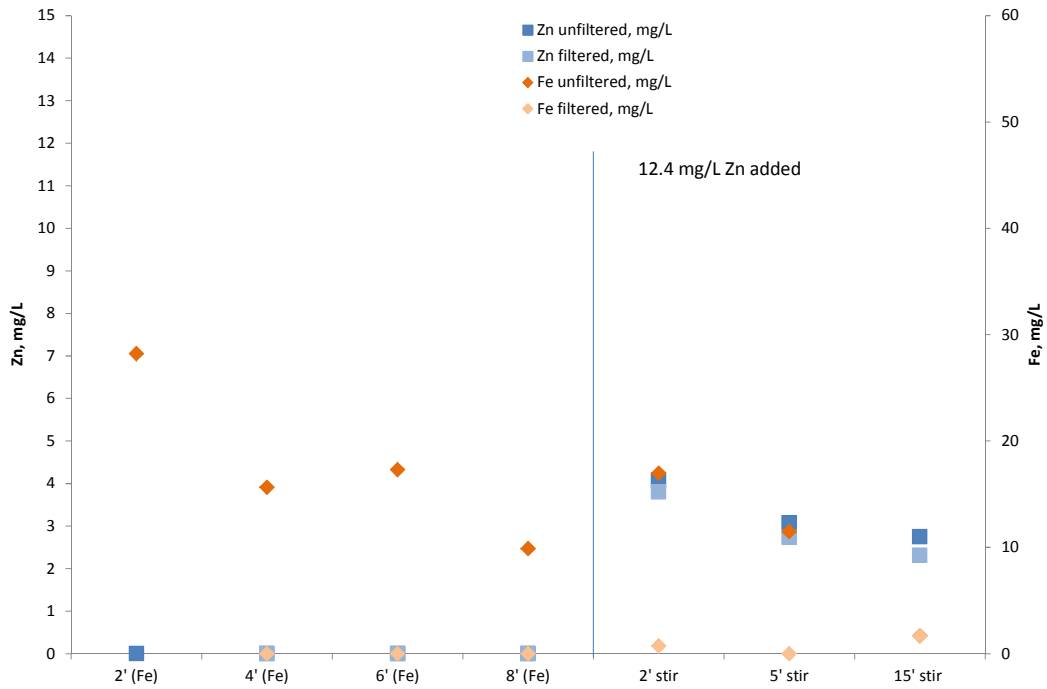


Figure 82: Results for Zn removal by adsorption to HFO particles that were added and precipitated electrically using Fe electrodes spaced at 30 mm 1 A, variable voltage. using Zn added at the end of the EC stage, before stirring. Fe unfiltered and filtered concentrations after 15 min stirring were identical, therefore the data plots on the same data point. Compare Table 10 for meaning of abscissa.

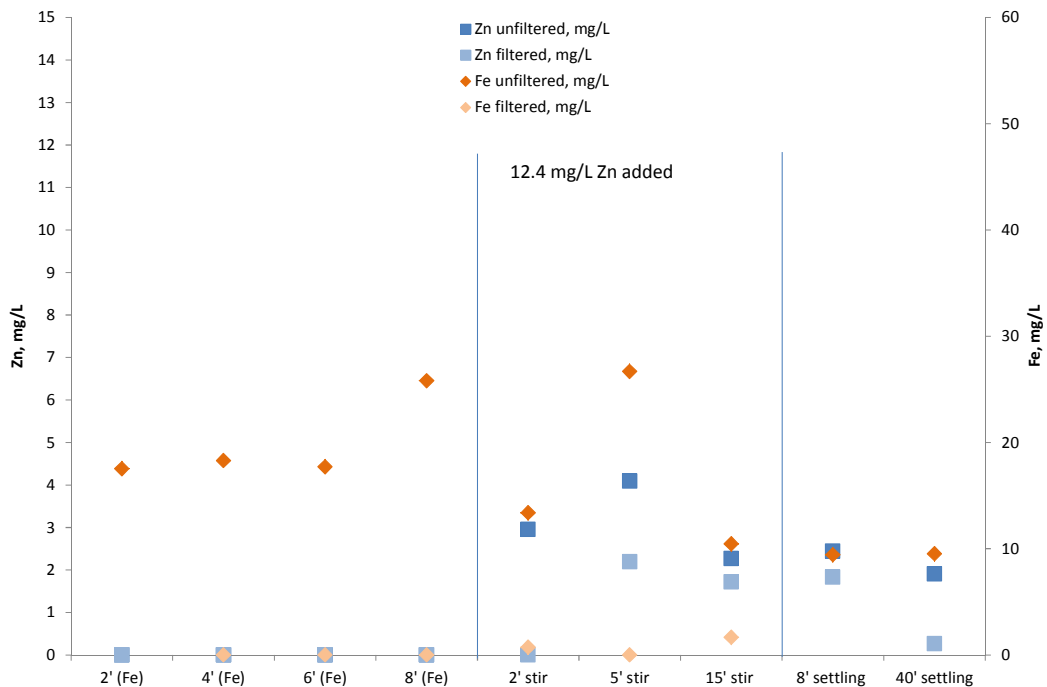


Figure 83: Results for Zn removal by adsorption to HFO particles that were added and precipitated electrically using Fe electrodes spaced 30 mm apart, 1A, variable voltage. Zn added at the end of the EC stage, before stirring and the experiment extended to include a 40 min settling time. Compare Table 10 for meaning of abscissa.

A final experiment 4 was conducted, where the Zn solution was added after the stirring period (Table 10). As in the experiments before, the Fe concentrations fluctuate during the course of the experiment, but the Fe unfiltered concentrations of 12.7–33.7 mg/L (Figure 84) were higher than in experiments 1 to 3.

Zn unfiltered during the final settling phase ranges between 6.9 and 7.9 mg/L and Zn filtered between 5.8 and 6.2 mg/L, which is higher than in experiment 3. These results suggest that for Zn removal by adsorption, the agitation of the solution influences the adsorption kinetics.

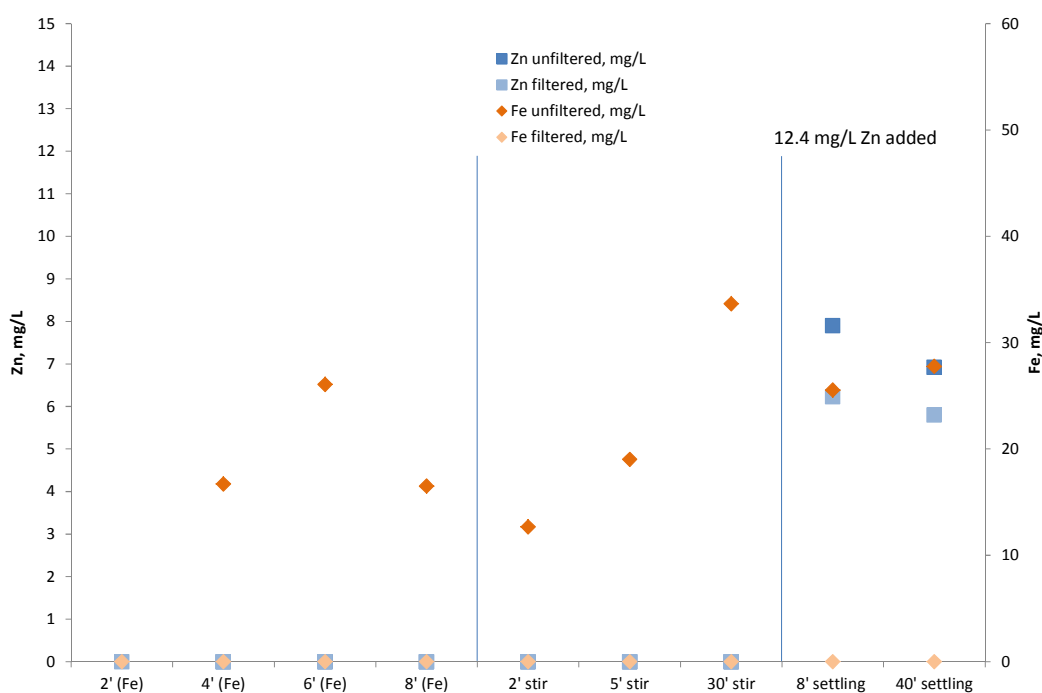


Figure 84: Results for Zn removal by adsorption to HFO particles that were added and precipitated electrically using Fe electrodes spaced 30 mm apart, 1A, variable voltage. Zn added after the stirring phase and before the settling phase. Compare Table 10 for meaning of abscissa.

For all experiments, the pH after the initial EC phase was in the range of 7–9 and the electrical conductivity between 83 and 231 $\mu\text{S}/\text{cm}$ (average 160 $\mu\text{S}/\text{cm}$). The redox potential after the EC phase ranged around 150 mV and increased to ± 250 mV in the final experimental phases.

In conclusion, the Zn removal experiments with electrocoagulation showed that the Zn is primarily removed by co-precipitation, which can be improved by an

adequate settling time. In addition, the experiments showed that the agitation of the solution is essential to improve the Zn removal kinetics.

6.14 Advanced Oxidation of Ynysarwed Coal Mine Drainage

Electrochemical oxidation using Pt (inert) electrodes was applied to Ynysarwed coal mine drainage that had an initial total filtered Fe concentration of 73.7 mg/L. The procedure for the method is described in section 5.11.2. The physicochemical lab parameters of the untreated mine water and the results after treating 800 mL samples with inert Pt electrodes (4 min; 1–8 A in 1 A steps) are presented in Table 23. Figure 85 shows the concentration of filtered Fe(II) for each experiment carried out at increasing applied current. As can be seen, there is a correlation between the increase in applied current and the reduction of filtered Fe(II) concentrations. At currents above 5 A the filtered total Fe(II) concentration stayed stable between 0 and 2 mg/L.

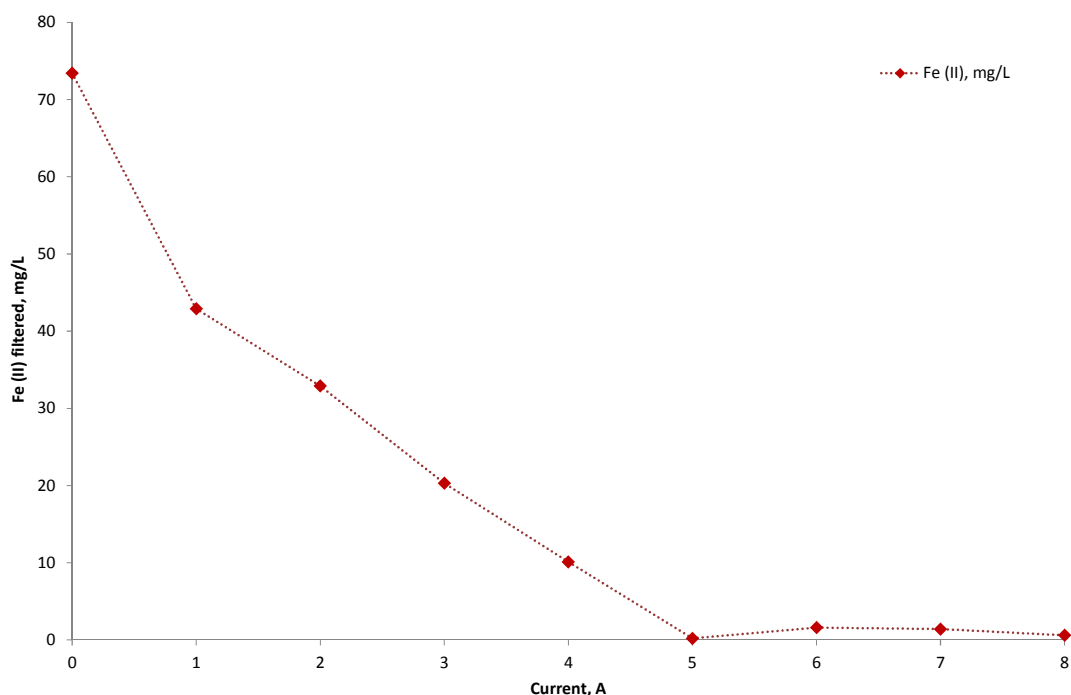


Figure 85: Fe(II) concentration of Ynysarwed coal mine water at increasing current using Pt electrodes. 4 min reaction time.

Table 23 shows the changes in the measured parameters for each amperage increase. While the amperage increased from 0–5 A, the pH decreased by 2.1 pH values from 6.7 in the untreated sample to 4.6 at 5 A. The pH changed only ± 0.3

pH values for the 6, 7 and 8 A experiments. Given the minimal Fe(II) concentration and pH change in treatments with an amperage greater than 5 A, suggests that 5 A is the most efficient amperage setting to remove the Fe(II) from Ynysarwed mine water. As expected, the ORP and the dissolved oxygen concentrations increased at higher amperages. The table also shows that the uncorrected ORP value for the 5 A treatment was 151 mV. When plotted on a Pourbaix diagram the conditions at 5 A are in the stability field for Fe(II) in natural waters (Figure 3); however, in the diffusion layer of the electrode the Fe(II) is oxidized to Fe(III) (Figure 87) which subsequently precipitates and therefore is removed from the water.

Table 23: Change in parameters at the end of each amperage step (el. cond.: electrical conductivity; ORP uncorrected). Pt electrodes, 4 min reaction time.

Parameter	Untreated	1 A	2 A	3 A	4 A	5 A	6 A	7 A	8 A
pH	6.7	6.8	6.2	5.9	5.6	4.6	4.9	4.6	4.8
DO, %	31.2	50.3	54.4	54.4	56.5	57.8	56.4	59.4	55.0
el. cond., $\mu\text{S}/\text{cm}$	1813	1736	1651	1726	1280	1341	1734	1845	1765
ORP, mV	-15.7	-10.5	26.1	42.7	70.7	151.6	154.9	169.4	174.8
Fe(II), mg/L	73.4	42.9	32.9	20.3	10.1	0.2	1.6	1.4	0.6
Fe(III), mg/L	0.3	0.1	0.2	0.1	0.2	0.2	0.1	0.2	0.1
Temp, $^{\circ}\text{C}$	14.3	21.3	21.27	22.06	26.58	39.14	37.6	41.8	45.07

During the AOP process, substantial increases in temperature were recorded. Table 23 gives the results after the samples had been cooled. As already has been observed by (Stauffer and Lovell, 1969), a 10 K temperature increase can result in an increase in Fe(II) oxidation rate by a factor of 3 to 15. Therefore, a control experiment for temperature was performed with the untreated water to verify if the temperature increase might be responsible for the reduction of Fe(II) concentrations in the Ynysarwed mine water. Figure 86 shows the Fe(II) filtered concentration at temperatures between 10 and 50.5 $^{\circ}\text{C}$. It should be noted that the Fe(II) was measured as soon as the desired temperature was reached. The starting Fe(II) concentration in the untreated water was less than in the EC experiment because the sample had begun to oxidise in the laboratory. However, no substantial decrease in Fe(II) concentrations could be observed between 15 and 41 $^{\circ}\text{C}$. Yet, between 40 and 45 $^{\circ}\text{C}$ the Fe(II) concentrations decreased by 12.6 ± 5.5 mg/L indicating that the oxidation rate seems to increase

above ± 40 °C. It can therefore be concluded that the reduction in Fe(II) concentrations during the EC experiment are not a result of the temperature change during the experiment, but a result of the electrochemical reactions occurring in the sample.

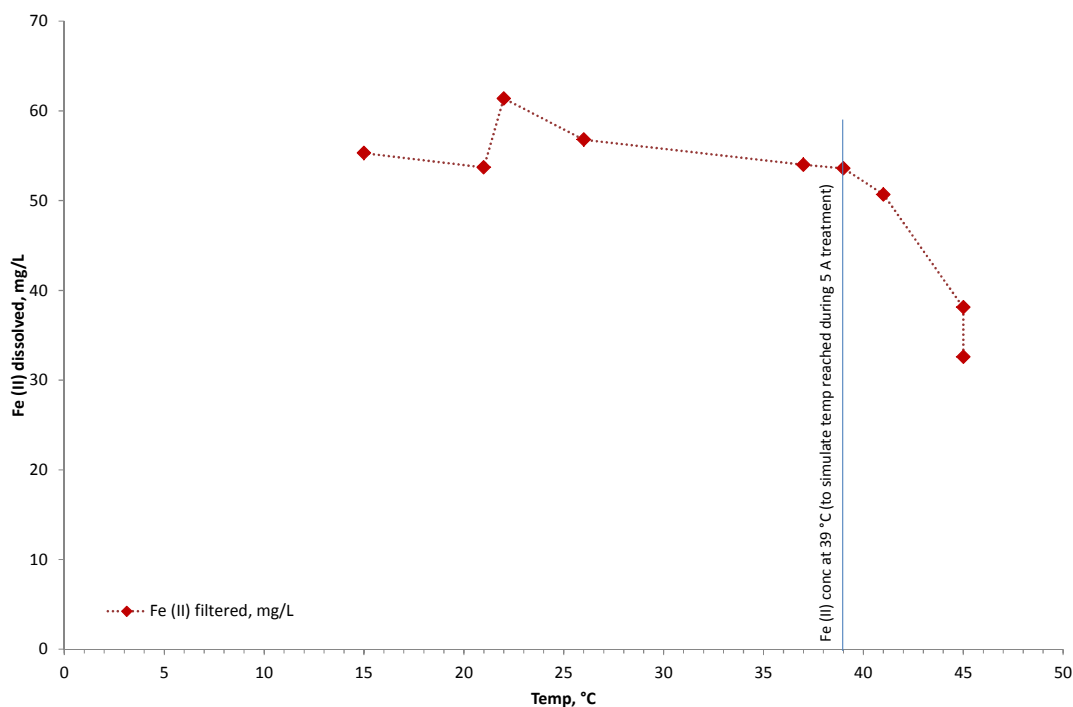


Figure 86: Filtered Fe(II) concentration of Ynysarwed coal mine water through the temperature range 15–45 °C.

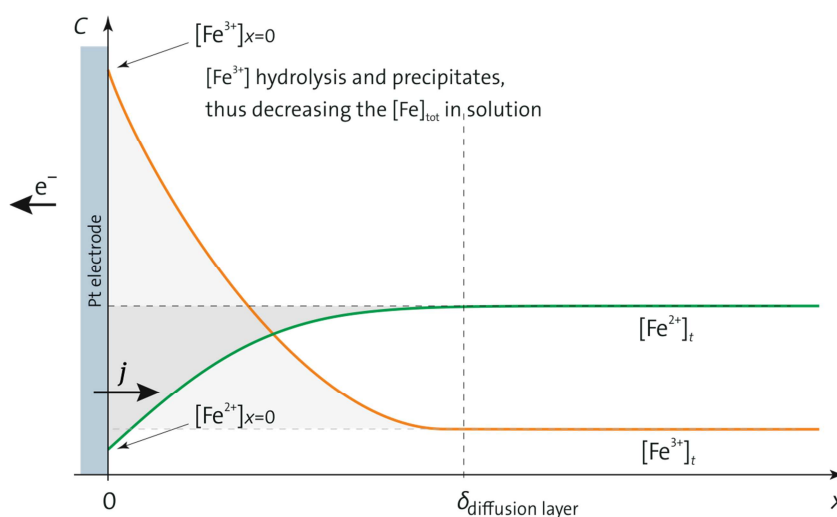


Figure 87: Diagram showing the conversion of Fe(II) to Fe(III) in the diffusion layer between the Pt electrode and the sample (modified after Lefrou et al., 2012).

Figure 87 describes the situation that is seen in the Ynysarwed water treated with Pt electrodes. The oxidation reaction that converts Fe(II) to Fe(III) in the sample occurs in the diffusion layer between the electrode and the sample (Lefrou et al., 2012).

The results have shown that the oxidation of Fe(II) to Fe(III) takes 4 min within an electrochemical cell using Pt electrodes and that the Pt electrodes are covered with a thin layer of Fe precipitates. The AOP process in this system can be explained by the following reactions, where the application of an electric current to the sample is represented by equations 34 and 35



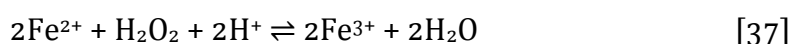
and 2, the electrolysis of water:



Equations 34 and 35 occur simultaneously and the production of hydrogen peroxide ensues by equation:



The hydrogen peroxide is utilised in the rapid oxidation of ferrous Fe by the following equation:



Once the Fe from the Ynysarwed was sufficiently oxidised as to precipitate out of solution, it was found that a second stage of treatment, using sacrificial Fe electrodes for 20 min altered the redox conditions sufficiently to reduce the sample back to a magnetic form of Fe within the EC reactor. Figure 88 shows the Ynysarwed sample after AOP and the addition of Fe using 2 × Fe electrodes for a 20 min treatment time at 5 A. The sample turned very dark to black and when a magnetic stirrer was added, a globule of the sample stuck to it as can be seen in Figure 88 left. Figure 88 middle shows some of this material stuck to the Fe cathode. This material was collected and dried at 60 °C until the mass was constant. It has a granular texture and as can be seen in the bottom centre image of Figure 88, the dried granules stuck readily to the side of a clean dry sample con-

tainer with a magnet against the outside. This indicates that in the case of the Ynysarwed mine water, EC can be used to create a recoverable form of Fe. This is possible, because using EC causes reactions within the cell that rapidly alter the redox-conditions and create the conditions necessary for stable minerals to form. Total digest of that sludge (Table 26) showed that it consists primarily of Fe (43.7%), Zn (1.2%) and S (0.9%). Mass balance calculations based on those results, the E_h -pH-conditions during that treatment step and the stability fields for the stable phases of Fe and Zn (Figure 5, Figure 89) show that the sludge consists of 96 wt % magnetite (Fe_2O_3), 3 wt % sphalerite (ZnS) and 2 wt % FeS.

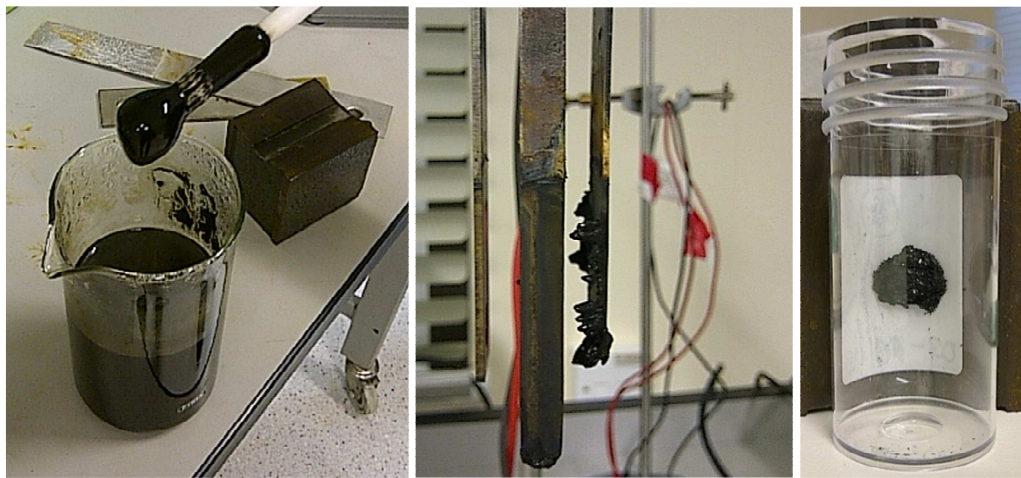


Figure 88: left: Magnetic Fe phase in Ynysarwed sample after oxidation followed by addition of Fe using sacrificial electrodes. Middle: Magnetic material adhered to the cathode. Left: Dried magnetic material from Ynysarwed sample.

The reactions and observations in the EC process in which magnetite is produced from Ynysarwed mine water can be compared to previous work on magnetic nanoparticle formation from mine water by chemical methods. According to Wei and Viadero Jr (2007), the recovery of usable Fe and the subsequent production of magnetite nanoparticles from AMD can be achieved through a number of stages of chemical oxidation and precipitation reactions. They found that magnetite particles could be formed when the ratio of Fe(II) to Fe(III) was 2:1 (as required for magnetite) and state this being a critical parameter in the production of magnetite. They added ferrous Fe to ferric Fe extracted from AMD by oxidising the sample with hydrogen peroxide and adjusting the pH to 3.5. This precipitated ferric Fe(III) as Fe-oxyhydroxides thus separating clean Fe sludge

from the other dissolved contaminants in the mine water. To ensure purity of the ferric Fe, a pH increase to 6.7 was required. Fe was then re-solubilised by addition of sulphuric acid and used as a ferric Fe source for the Fe(II):Fe(III) ratio. On mixing, the pH raised to 9.5 and the solution was bubbled with nitrogen for 30 min to encourage crystal growth.

In the EC system using Ynysarwed coal mine drainage, the ferric Fe source comes from the oxidation of Fe(II) to Fe(III) by equations 34 to 37. Subsequently, this is followed by the addition of Fe(II) formed by the back reduction of Fe from the Fe electrodes, which creates reducing conditions with an increase in the pH. The purpose of this experiment was to attempt using AOP followed by EC to manipulate the conditions required to form magnetic phases of Fe.

To construct a stability diagram for understanding the system behaviour, the following data was used (collected at the end of the experiment when the black magnetic material was formed): pH 8.9, RedOx -355 mV, temperature 40 °C, the sum of the concentrations of untreated total unfiltered Fe and the Fe from the electrode and the SO_4^{2-} concentration. Given that the conversion of Fe(II) + Fe(III) to form solid magnetic Fe occurs at the surface of the electrode, it is likely that only a nominal amount of sulphate entered into the reactions. This is supported by the solids analysis of the magnetic sludge shown in Table 26 (page 188). Therefore, the stability diagram shows the system with SO_4^{2-} (Figure 89, left) and without SO_4^{2-} (Figure 89, right). In the diagram where SO_4^{2-} is included, magnetite resides on the boundary between pyrite and hematite, outside the experiment's E_h -pH-conditions, whereas in the diagram where no SO_4^{2-} is included (Figure 89, right), magnetite is closer to the hematite/magnetite boundary and the experiment's conditions.

In addition to this, the ESEM images of the Ynysarwed magnetic Fe (Figure 89) have similar characteristics to SEM images of the magnetite nanoparticles formed by chemical oxidation and precipitation (Wei and Viadero Jr, 2007).

Though it cannot be said conclusively that magnetite is being extracted from the Ynysarwed mine water, results show that a stable magnetic material was produced (Figure 88). This could have implications for mine water treatment. Mag-

netite (Fe_3O_4) could be extracted as a saleable by product from AMD. Alternatively, magnetite nanoparticles and other forms of magnetic Fe such maghemite (Fe_3O_3) could be used as effective adsorbent materials for the removal of contaminant metals such as Cu(II) , Ni(II) and Cr(VI) (Akhbarizadeh et al., 2013, Hao et al., 2010).

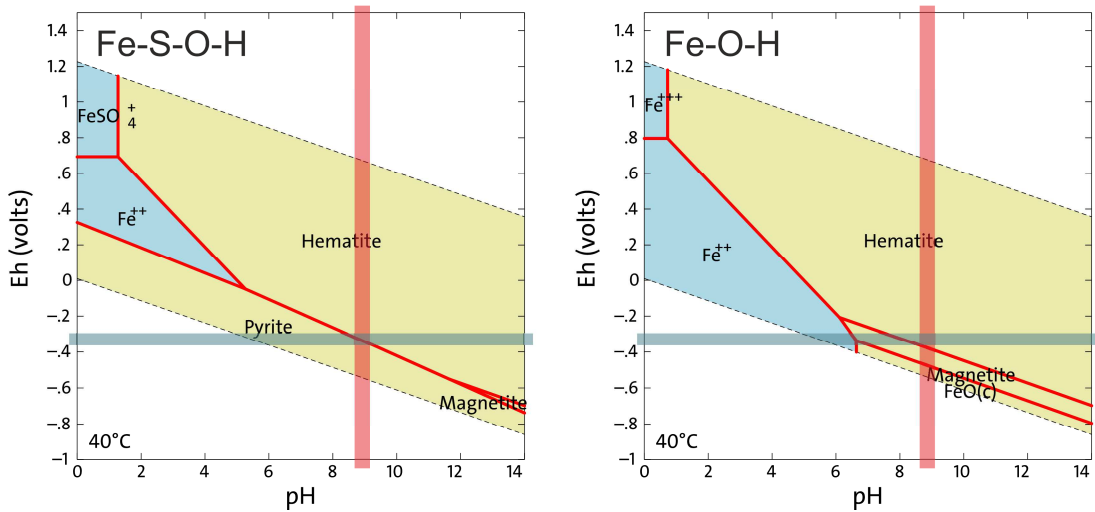


Figure 89: Pourbaix-diagram for Fe-S-O-H and Fe-O-H phases with superimposed Eh-pH-conditions at the end of the experiment. Temp: 40 °C, p = 1 bar, $\text{Fe(aq)} = 10^{-2.7}$, $\text{H}_2\text{O(aq)} = 1$, $\text{SO}_4^{2-}(\text{aq}) = 10^{-2.7}$. Diagrams constructed using Geochemist's Workbench 9.

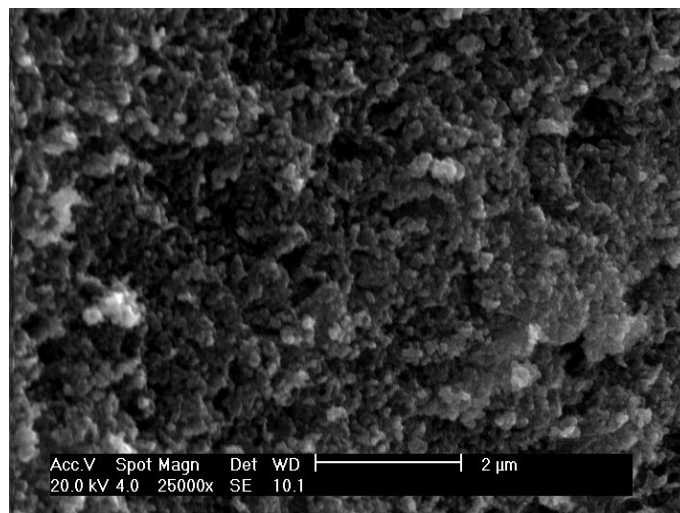


Figure 90: ESEM images of the electrochemically produced magnetic sludge formed in Ynysarwed water after a two stage process of AOP followed by EC with Fe electrodes.

6.15 Electrochemical Treatment of Cwm Rheidol Water

Different electrode materials were investigated in order to assess EC as a method for targeting the common problems associated with metal mine water treatment. In the UK, the main problems are the low pH and high dissolved (semi-)metal concentrations whereas in other countries, such as South Africa, high sulphate concentrations are also a major challenge. Sulphate for these experiments was measured using the NOVA60 Spectrophotometer and Merck sulphate test cells in order to get an on the spot reading for sulphate concentrations. A number of experiments using different combinations of electrodes, treatment times, aeration, no aeration were carried out. The Cu cathode experiments were the only ones to show promising results and therefore chosen for further investigation. Full data sets were not collected for all these variations as sulphate and pH were used to monitor the best parameters/materials and treatment times. Optimum treatment time to achieve the best sulphate removal and pH increase was 40 min using 5 A, although all experiments were continued for 60 min but no further improvement was seen between 40 and 60 min. Consequently, 40 min treatment time at 5 A were the chosen treatment parameters for the data presented in Table 24.

Mine water from the Cwm Rheidol lower number 9 adit discharge pipe was considered to be representative of very acid AMD in the UK and other countries and therefore chosen for the EC scoping studies in which Al, Pt, Cu and Fe electrodes were tested. The method as described in section 5.11.3 was developed to add aeration during the EC process, which produced a more vivid green colour sludge. This procedure was followed for each of the electrode combinations presented (Table 24) and the experiments were continued for a total of 60 min. Every 10 min, the treatment was stopped so that filtered and unfiltered samples for ICP-OES analysis could be collected. pH increased substantially in each electrode combination. In the experiments using Pt or Al as the cathode, the pH increased from 3 to 6.2. When Fe was used as the cathode, the pH increased to 5.2.

For targeting Zn and Fe as the main elements of concern, the best combinations were Cu + Cu and Cu + Al, both reducing the Zn concentration to < 1 mg/L. Sulphate was also considerably reduced in the case of Cu + Al and Cu + Cu from

1324 mg/L in the untreated sample to 112 and 350 mg/L respectively. Considering Faraday's law, a substantial amount of Cu will have been lost from the anode during 40 min of treatment time. Yet in all cases with the exception of the Fe + Cu + Fe combination, the amount of Cu in solution was < 1 mg/L.

Cu electrodes generated a green sludge (Figure 92) which was sampled and oven dried at 60 °C until the mass was constant. Once dried, samples were analysed by ESEM in order to examine the structure of the sludges as almost all of the metals are precipitated and the sulphate is also incorporated in the solid phases (Figure 91 and Figure 92).

Table 24: Parameters for untreated and EC treated Cwm Rheidol water in mg/L; Cu anode with Al, Pt, Cu and Fe cathode materials and a treatment time of 40 min at 5 A. ORP is uncorrected.

Parameter (filtered)	untreated mine water	Cu anode with various cathode materials			
		Cu + Cu	Cu + Pt	Cu + Al	Fe + Cu + Fe
Fe	107.7	0	3.8	0	262.3
Zn	117.6	0.5	5.5	0.5	109.3
Mg	54.6	27.4	37.2	6.7	57.2
Cu	0.2	0.9	0.5	0.9	28
Mn	5.4	0.9	1.4	1.3	6.9
Ca	74.7	43.9	68.2	29.3	81.4
Al	41	0	1.5	0	0
Pb	0	0	0	0	0
Cd	0.1	0	0	0	0.1
SO ₄	1323.8	349.8	398.6	111.5	1230.4
Cl	-	6.4	6.1	6.5	-
pH	3	6.2	6.2	6.2	5.2
ORP	366	31	33	31	-0.5
TDS	1070	120	310	120	750

Figure 92 shows cubic crystalline structures that formed during the EC treatment of Cwm Rheidol water using Cu and Al electrodes. The ESEM spectrum data (Table 25) shows that 63.5 wt% is Cu. Relatively small amounts of Fe (0.43%), S (0.42%), Al (0.36%), Cl (2.41%) were shown and the remaining 9.8% is O. 23.03 wt% C comes from the carbon that is used to coat the sample before it is placed in the instrument. It should be noted that the spectrum data is from one precise point on the sample surface and can not be considered representative of the sample as a whole. In future studies, XRD analysis of the sludges formed are imperative for further conclusions. However, the crystal structure of the

mineral, the ESEM and total digest composition of the sample (Table 25, left column), indicate that this mineral is cuprite (Cu_2O), a cubic copper oxide mineral, which was also found in ochres within the Cornish Levant mine (Bowell and Bruce, 1995)



Figure 91: Unfiltered Cwm Rheidol sludge and dried sludge produced in the EC reactor after 60 min treatment time with Cu + Al electrodes.

Various stability diagrams of the elements analysed in the sludge were used to identify the stable phases in the sludge (Figure 93 shows only the Cu-S-O phases in addition to the E_h -pH conditions during the experiment). It was possible to determine that the sludge consists of cuprite (Cu_2O), chalcocite (Cu_2S), elemental copper (as can also be seen in the sample vial in Figure 91), sphalerite (ZnS), gibbsite ($\text{Al}(\text{OH})_3$), FeS and Mg-spinell (MgAl_2O_4). Though all the elements analysed in the sludge were used as input to construct the stability diagram, only the Cu-O-S phases appear therein. The other minerals were identified by setting the Cu-activity to 0 (those diagrams not shown here).

The formation of cuprite and Cu metal in this system could have implications for the future of mine water treatment where the requirements are pH adjustment, a substantial decrease in sulphate concentrations and the removal of other contaminant metals. Whilst Cu is added from the sacrificial anode, there is the potential for the Cu to be recovered, recycled and reused.

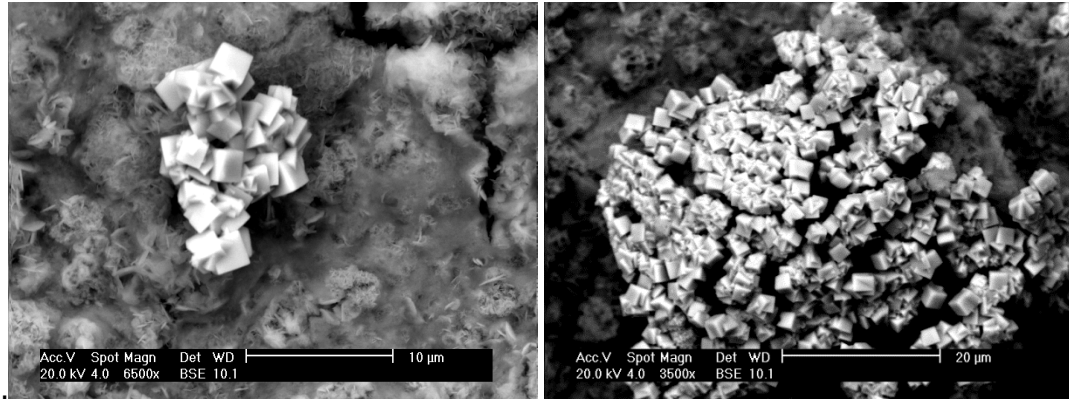


Figure 92: ESEM images of the sludge from the Cu + Al electrode treated water. The cubic mineral in the centre is probably cuprite (Cu₂O).

Table 25: Emission spectrum data from ESEM analysis of the cubic mineral in Figure 92.

Sample (Cwm Rheidol)	C	O	Al	S	Cl	Fe	Cu	Total weight %
Cu + Al	23.03	9.80	0.36	0.42	2.41	0.48	63.5	100

Table 26: Results for the total digest of sludges from the EC treatment of Cwm Rheidol and Ynysarwed water (%). 0.0 means that the element was measured above the detection limit, but below 0.05%.

Element	Cwm Rheidol EC treatment (Cu+Al)	Ynysarwed EC treatment (Pt+Fe)
Al	3.4	0.5
Be	0.0	<DL
Ca	0.0	0.3
Cr	0.0	0.4
Cu	10.6	0.1
Fe	1.2	43.7
Mg	0.5	0.3
Mn	0.0	0.2
Ni	0.0	0.2
S	3.9	0.9
Se	0.0	<DL
Si	0.1	0.2
Zn	1.1	1.2

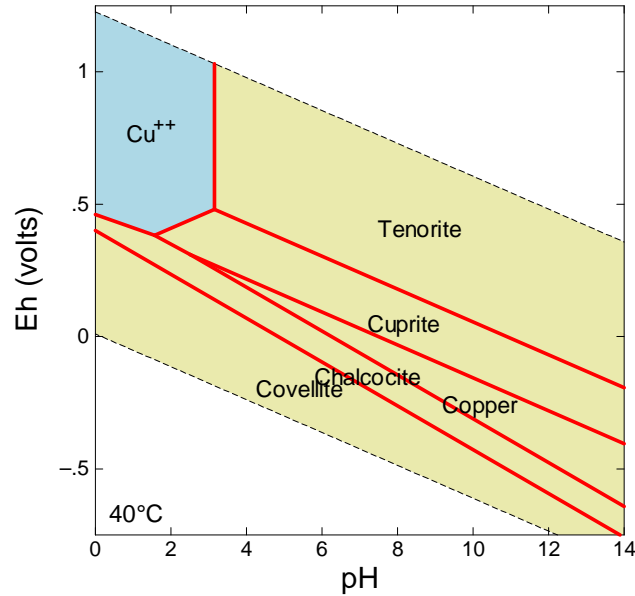


Figure 93: Stability diagram for Cu phases using the analysis in Table 26 at 40 °C. Diagram constructed using Geochemist’s Workbench 9. Conclusions.

6.16 Vertical Flow Reactor (VFR)

A vertical flow reactor (VFR) has shown to be effective at removing dissolved and particulate iron from low pH multi element contaminated mine water from the lower number 9 adit discharge pipe at Cwm Rheidol. Figure 94 is a cross section of the abandoned Cwm Rheidol mine used to explain the mechanisms leading to the mine water chemistry at the end of the discharge pipe and occurring in the VFR. This cross section will be used to draw the conclusions for the thesis and the occurring mechanisms ① to ⑤. It is based on an extensive literature study of the mine layout (Edwards and Potter, 2007, Jones, 1922, Levins, 2007, Lord, 2013, Mason, Rees et al., 2004) and the results in the previous section of the thesis. The cross section illustrates the chemical reactions responsible for this site being a producer of AMD and how the VFR is removing Fe from the mine water.

① Surface infiltration of rain and surface water through the abandoned mine workings starts the process.

② Weathering of pyrite/marcasite in the ore veins causes the oxidation of di-sulphides and is responsible for causing the water at Cwm Rheidol to become acidic (equation 38):

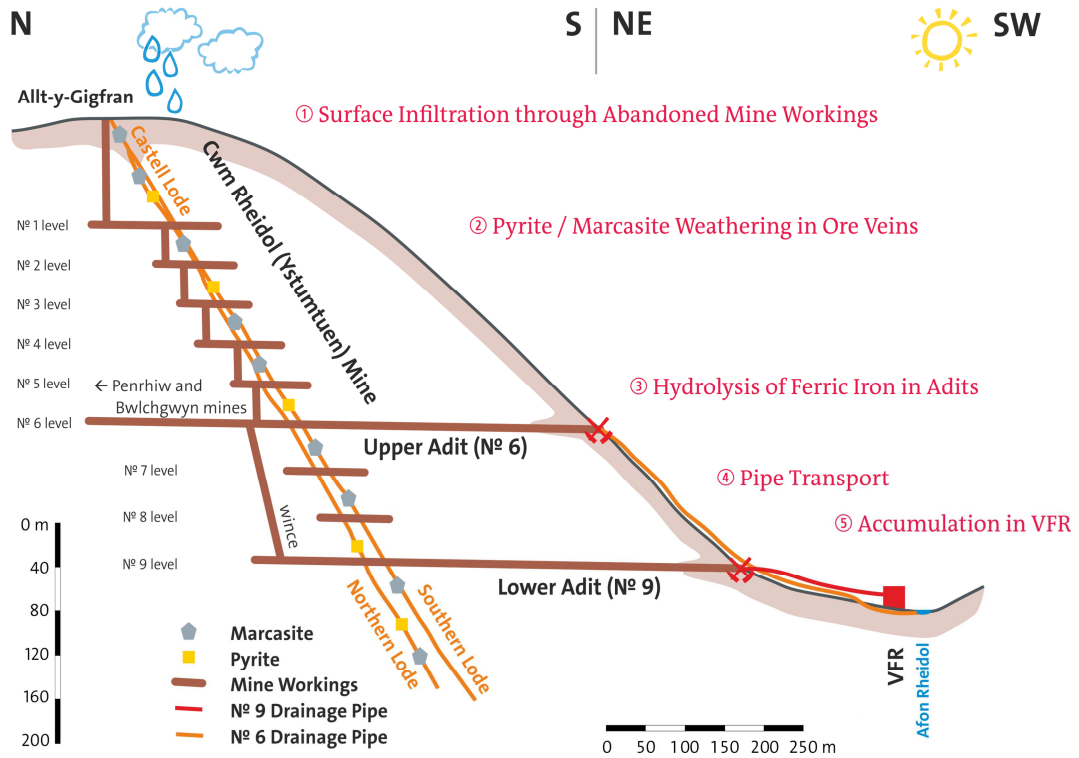
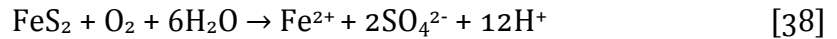
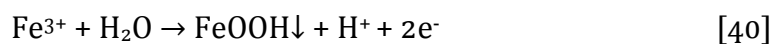


Figure 94: Cross section of the Cwm Rheidol mine and the mechanisms leading to the mine water chemistry and the Fe oxidation/precipitation reactions occurring in the VFR. Mine layout based on literature mentioned in the text and dozens of underground images found in the internet.

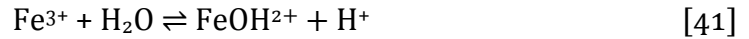
③ Next, hydrolysis of Fe(II) occurs in the extended adits and mine workings by the following set of reactions. In the first step, Fe(II) is oxidised to Fe(III) by reaction 39:



This is followed by two reactions as shown by the PHREEQC modelling. Considering an adit length of 600 m, a flow rate of 3 L/min in a 0.5–1 m wide and 0.05–0.1 m deep, convex channel (Figure 15) results in a flow of 0.10 ± 0.06 m/min. Consequently, based on Stoke's law, the flow rate and the settling velocity, it can be calculated, that particles above $0.2 \mu\text{m}$ already settle in the adit after a flow path of 300–500 m. Therefore, the first reaction occurring is the partial ochre precipitation in the adits and mine workings by the following reaction 40:



Yet, as the PHREEQC calculation and the chemical analysis at the discharge pipe shows, part of the iron does not precipitate and keeps dissolved as (nano-)particles < 0.2 µm in the acid mine water according to equation 41:



④ After leaving the mine portal, the mine water is further aerated and agitated during the pipe transport and more ochre forms in the pipe. The mine water that is now collected from the adit discharge pipe and drained to the VFR contains the following aqueous components (based on PHREEQC results)



⑤ In the VFR, due to the slow flow and prolonged residence time compared to the adit and pipe flow, the (nano-)particles and the dissolved Fe react further:

Table 27: Fe removal processes occurring in the VFR at Cwm Rheidol.

Fe-removal by sorption, coagulation and precipitation	Fe(III) leaves VFR
70 %	30 %
$\text{FeOH}^{2+} + \text{H}_2\text{O} \rightarrow \text{FeOOH}\downarrow + 2\text{H}^+$ (nano-)particles coagulate to form larger particles that settle in the VFR	Fe^{3+} leaves VFR predominantly unreacted

- The mechanisms responsible for the removal of iron were initially thought to be a combination of microbial Fe(II) oxidation and self-filtration of nano-particulate Fe(III).
- When Fe(II) was found to be present, oxidation of Fe(II) was shown to be occurring between the inflow and outflow of the VFR.
- Analysis of the Cwm Rheidol influent water by Bangor University has shown the dominance of *Ferrovum myxofaciens* Fe(II) oxidising bacteria in water samples from the number 9 adit at Cwm Rheidol which support the settling of the (nano-)particles in the VFR, adit and discharge pipe.
- Fe(III) is shown to be present as particles less than 35 nm in size as determined by centrifuging studies.
- Chemical analysis as well as XRD, SC and SEM analysis of the VFR sludge suggest that the mineralogy of the VFR ochre is schwertmannite.

- The permeability of the VFR remained consistent after the initial filling phase. Bacterial presence is thought to be responsible for the consistency of the flocs in the VFR.
- Build-up of ochre in VFR does not substantially affect the hydraulic conductivity of the system over time.

6.17 Electrochemistry for Fe and Zn Removal

6.17.1 Zn removal Before and After EC Using Iron Electrodes

- Zn removal during EC with a Fe electrode has shown to be due to co-precipitation and adsorption rather than just adsorption alone.
- Results showed consistently that if zinc was added after the formation of $\text{Fe}(\text{OH})_3$ from the electrode (*i.e.* adsorption only) that the overall removal of Zn was generally lower than if Zn had been present during the electrical production of $\text{Fe}(\text{OH})_3$

6.17.2 AOP for Fe Removal at Ynysarwed

- Fe removal from Ynysarwed was shown to be rapid using inert Pt electrodes.
- The conversion of Fe(II) to Fe(III) followed by precipitation of Fe(III) was shown to be most effective at 5 A for a 4 min duration experiment.
- The removal mechanism is thought to be the electrochemical oxidation of Fe(II) to Fe(III) taking place in the diffusion layer between the Pt electrode and the sample
- When a two stage treatment was performed whereby Fe was added electrically after the AO process, the sample was shown to produce a magnetic form of Fe after 20 min treatment time with an Fe electrode.
- Characterisation of the sludge combined with modelling of the Fe phases with Geochemist's workbench indicate that the precipitate formed is magnetite.

6.17.3 Electroprecipitation at Cwm Rheidol Using Cu Electrodes

- Using copper electrodes at 5 A for 40 min was shown to be effective at removing dissolved cations and anions from low pH mine water

- The pH was shown to increase from pH 2.9 to pH 6.2 in the first 10 min of treatment.
- The removal mechanism is thought to be electro precipitation (induced initially by the electrically manipulated change in redox and pH conditions) and adsorption co-precipitation reactions.
- Use of a Cu cathode and Al anode in EC bench scale trials was shown to be effective at removing Fe, Al and Cd and reduction of Cu from 0.2 to 0.9 mg/L, Zn from 117.6 to 0.5 mg/L and SO_4^{2-} from 1323.8 to 111.5 mg/L from Cwm Rheidol low pH mine water.
- SEM images of the sludge formed using the copper electrodes showed that when the sample is also aerated during the EC process, that distinct cubic mineral structures are formed.
- Stability diagrams show that Cu added from the electrode during the EC treatment process forms cuprite and Cu metal.
- Whilst Cu is added to the system from a sacrificial electrode, all other metals are removed and sulphate concentrations substantially reduced which has implications for future mine water treatment

6.18 Relevance for Mine Water Treatment and Further Work

6.18.1 VFR Relevance

The main focus of this study was to examine the potential use of a VFR at removing Fe from low pH mine water. This study showed that at pH 3, an average of 65% of the total Fe concentration was removed in a 5 h residence time. The system operated for over a year without compromising the permeability of the bed. This has implications for the future of mine water treatment where a modular approach can be adopted. An initial stage of treatment where a substantial amount of the Fe can be removed ahead of other treatment stages (where possibly as hybrid passive/active treatment system) could substantially increase the longevity of conventional treatment plants by reducing the problems of passivation and clogging of pipes and systems. Another interesting factor in this trial was that the Fe was removed as a clean HFO sludge despite this being a multi metal contaminated mine water. Benefits of this might include the disposal costs being much lower for clean HFO than for a multi contaminated waste.

However, the detailed removal mechanisms were not completely understood and it remains uncertain if the VFR is suitable for other low pH mine water or if it is dependent purely on the geochemical and microbiological conditions at Cwm Rheidol. Either way, further work needs to be carried out to determine if the VFR is capable of treating higher flows at Cwm Rheidol, a site in need of remediation, and if it will work at other metal mine sites. Further investigations into the contribution of the microbiological factor on the success of the VFR in terms of long term operation, *i.e.* to the stability of the flocs in the system and the mineral precipitates formed is also recommended. The findings in this study could well be applied to many abandoned low flow sites where a passive, low operational cost system is required.

6.18.2 Zn Removal

The ability to remove Zn from neutral mine pH water using EC proved relevant in that Zn can be removed without the addition of pH adjusting chemicals. It was proven that co-precipitation and adsorption reactions with Fe using EC are sufficient to remove Zn from neutral mine water at pH values lower than for the least solubility for Zn. While this is an effective method, further work needs to be carried out to assess the operating costs of supplying Fe electrodes to remote sites and also the power usage required. Power electronics is also a developing area of research and should be combined with EC research. Geochemically and electrochemically, there is great potential for EC if the reactions become better understood so that a more specific, targeted approach can be adopted in order to minimise power and material usage.

Further to this, in more complex systems, EC was capable of removing Zn and other metals from AMD using Cu electrodes. In fact several benefits of EC using copper were highlighted. This metal at the cathode achieved good results for three main mine water treatment requirements, namely an increase in pH without the use of chemicals, removal of unwanted residual contaminant metals and a substantial drop in sulphate concentrations. Further to this ESEM images, sludge analysis and the use of stability diagrams indicated that the Cu being added to the system from the electrodes was likely precipitating as the Cu mineral cuprite Cu_2O and native Cu. This is also a valuable starting point for mine

water treatment because of the potential for material recycling recovery and reuse. Further work needs to be directed at determining the mineralogy of the precipitates and the factors that control those formations. Again, the methods need to be investigated to mine water from different sites.

6.18.3 Advanced Oxidation and Electrocoagulation

The AOP process proved successful as a single stage oxidation/precipitation method for the removal of Fe(II) from coal mine water at Ynysarwed. This was achieved using inert electrodes (non-sacrificial) and is potentially comparable to aeration and chemical dosing which produces a higher volume of sludge and thus higher disposal costs. Furthermore, it was found that adding Fe back into the system to generate an Fe(II):Fe(III) ratio under the appropriate RedOx and pH conditions (formed by electrochemical manipulation) meant that a stable magnetic form of Fe could be produced. Potentially this could be a method of turning a waste product (HFO) into a saleable resource. Further work into understanding the conditions created in the electrochemical cell, the precise mineralogy of the magnetic precipitates and whether this conversion can be reliably maintained needs to be carried out.

7 Literature

- Abdulgader, H. A., Kochkodan, V. & Hilal, N. 2013. Hybrid ion exchange – Pressure driven membrane processes in water treatment – A review. *Separation and Purification Technology*, 116, 253-264.
- Aceró, P., Ayora, C., Torrentó, C. & Nieto, J.-M. 2006. The behavior of trace elements during schwertmannite precipitation and subsequent transformation into goethite and jarosite. *Geochimica et Cosmochimica Acta*, 70, 4130-4139.
- Adler, R., Funke, N., Kieran, F., & Turton, A. 2007. An Assessment of the Relationship Between the Government, the Mining Industry and the Role of Science in the Far West Rand of South Africa. *Emerging Issues Paper: Mine Water Pollution*. South Africa, Pretoria Department of Environmental Affairs and Rural Affairs.
- Akhbarizadeh, R., Shayestehfar, M. R. & Darezereshki, E. 2013. Ability of Maghemite Nanoparticles (λ -Fe₂O₃) to Competitive Removal and Recovery of Cr (IV) and Ni (II) from Mine Wastewater. *Journal of Environmental Studies*, 38, 1-8.
- Amos, P. W. & Younger, P. L. 2003. Substrate characterisation for a subsurface reactive barrier to treat colliery spoil leachate. *Water Research*, 37, 108-120.
- Andrews, E. J., Dejournett, T. D., Friel, J. M. & Richard, D. E. 2009. Membrane processes for the reuse and reclamation of non-ferrous mine process water.
- Atkins, P. W. & Beran, J. A. 1992. *General Chemistry*, New York, Scientific American Books
- Authority, T. C. 2009. *Ynysarwed Minewater Treatment Scheme* [Online]. Available: <http://webarchive.nationalarchives.gov.uk/20090506125027/http://www.coal.gov.uk/environmental/minewatertreat/wales/ynysarwed/ynsarwedminewatertreatmentscheme.cfm> [Accessed 2015-04-27].
- AWWA 1998. *Standard Methods for the Examination of Water and Wastewater*, Washington, DC, American Public Health Association.
- Baas Becking, L. G. M., Kaplan, I. R. & Moore, D. 1960. Limits of the Natural Environment in Terms of pH and Oxidation-Reduction Potentials. *J. of Geol.*, 68, 243-284.
- Baird, C. 1995. *Environmental Chemistry USA*, W. H. Freeman and Company.
- Barkley, N. P., Farrell, C. W. & Gardnerclayson, T. W. 1993. Alternating-Current Electrocoagulation for Superfund Site Remediation. *Journal of the Air & Waste Management Association*, 43, 784-789.
- Barnes, A. 2008. *The Rates and Mechanisms of Fe (II) Oxidation in a Passive Vertical Flow Reactor for the Treatment of Ferruginous Mine Water* Ph.D., Cardiff.
- Barrera-Díaz, C., Bilyeu, B., Roa, G. & Bernal-Martinez, L. 2011. Physicochemical aspects of electrocoagulation. *Separation and Purification Reviews*, 40, 1-24.
- Barrett, T. J., MacLean, W. H. & Tennant, S. C. 2001. Volcanic Sequence and Alteration at the Parys Mountain Volcanic-Hosted Massive Sulfide

- Deposit, Wales, United Kingdom: Applications of Immobile Element Lithogeochemistry. *Economic Geology*, 96, 1279-1305.
- Bayless, E. R. & Olyphant, G. A. 1993. Acid-generating salts and their relationship to the chemistry of groundwater and storm runoff at an abandoned mine site in southwestern Indiana, U.S.A. *J. Contam. Hydrol.*, 12, 313-328.
- Bearcock, J., A Palumbo-Roe, B., A Banks, V. & A Klinck, B. 2010. The hydrochemistry of Frongoch Mine, mid Wales. Nottingham, UK: British Geological Society
- Bearcock, J. M. 2007. *Laboratory studies using naturally occurring "green rust" to aid metal mine water remediation*. Ph.D., Aberystwyth University
- Bearcock, J. M., Perkins, W. T. & Pearce, N. J. G. 2011. Laboratory studies using naturally occurring "green rust" to aid metal mine water remediation. *Journal of Hazardous Materials*, 190, 466-473.
- Benjamin, M. M. & Leckie, J. O. 1981. Multiple-site adsorption of Cd, Cu, Zn, and Pb on amorphous iron oxyhydroxide. *Journal of Colloid and Interface Science*, 79, 209-221.
- Benner, S. G., Blowes, D. W., Gould, W. D., Herbert Jr, R. B. & Ptacek, C. J. 1999. Geochemistry of a permeable reactive barrier for metals and acid mine drainage. *Environmental Science and Technology*, 33, 2793-2799.
- Best, G. A. & Aikman, D. I. 1983. The treatment of ferruginous ground water from an abandoned colliery. *Water Pollution Control*, 82, 557-566.
- Bick, D. 1978. *The Old Metal Mines of Mid-Wales*. [Online]. Newent, Gloucestershire: The Pound House
- Bick, D. 1996. British Mining No 30 - Frongoch Lead and Zinc mine
- Bigham, J. M., Carlson, L. & Murad, E. 1994. Schwertmannite, A New Iron Oxyhydroxysulphate From Pyhasalmi, Finland, And Other Localities. *Mineralogical Magazine*, 58, 641-648.
- Bigham, J. M. & Nordstrom, D. K. 2000. Iron and aluminum hydroxysulfates from acid sulfate waters. *Sulfate Minerals - Crystallography, Geochemistry and Environmental Significance*, 40, 351-403.
- Bigham, J. M., Schwertmann, U., Traina, S. J., Winland, R. L. & Wolf, M. 1996. Schwertmannite and the chemical modeling of iron in acid sulfate waters. *Geochimica et Cosmochimica Acta*, 60, 2111-2121.
- Blowes, D. W., Ptacek, C. J., Benner, S. G., McRae, C. W. T., Bennett, T. A. & Puls, R. W. 2000. Treatment of inorganic contaminants using permeable reactive barriers. *Journal of Contaminant Hydrology*, 45, 123-137.
- Blowes, D. W., Ptacek, C. J., Cherry, J. A., Gillham, R. W. & Robertson, W. D. 1995. Passive remediation of groundwater using in situ treatment curtains. *Geotechnical Special Publication*, 46, 1588-1607.
- Blowes, D. W., Ptacek, C. J., Jambor, J. L. & Weisener, C. G. 2003. The Geochemistry of Acid Mine Drainage. In: Heinrich, D. H. & Karl, K. T. (eds.) *Treatise on Geochemistry*. Oxford: Pergamon, 149-204.
- Bothwell, D. N., Mair, E. A. & Cable, B. B. 2003. Chronic ingestion of a zinc-based penny. *Pediatrics*, 111, 689-691.
- Bowell, R. J. & Bruce, I. 1995. Geochemistry of iron ochres and mine waters from the Levant mine, Cornwall. *Applied Geochemistry*, 10, 237-250.
- British Geological Survey. 2014. *Plans history* [Online]. Available: <http://www.bgs.ac.uk/nocomico/history.htm> [Accessed 31/05/2014].

- Brodie, A., G., Britt, C. R., Tomaszewski, T. M. & Taylor, H. N. 1991. Anoxic Limestone Drains to Enhance Performance of Aerobic Acid Drainage Treatment Wetlands – Experiences of the Tennessee Valley Authority. *In: Wildeman T., B. G., Gusek J (ed.) Wetland Design for Mining Operations, chapt. III. Proceedings, International Conference on Constructed Wetlands for Water Quality Improvement.* Pensacola.
- Brodie, G. A. 1991. Staged, Aerobic Constructed Wetlands to Treat Acid Drainage – Case History of Fabius Impoundment 1 and Overview of the Tennessee Valley Authority's Program. *In: Wildeman T., B. G., Gusek J. (ed.) Wetland Design for Mining Operations, chapt III. Proceedings, International Conference on Constructed Wetlands for Water Quality Improvement.* Pensacola.
- Brookins, D. G. 1988. *Eh-pH diagrams for geochemistry*, Berlin, Springer.
- Brown, B. E. 1977. Effects of mine drainage on the river hayle, cornwall a) factors affecting concentrations of copper, zinc and iron in water, sediments and dominant invertebrate fauna. *Hydrobiologia*, 52, 221-233.
- Brown, M., Barley, B. & Wood, H. 2002. *Minewater Treatment – Technology, Application and Policy*, London, IWA Publishing.
- Cartwright, P. S. 2012. *Application of Membrane Separation Technologies to Wastewater Reclamation and Reuse*, Littleton, SME.
- Casqueira, R. G., Torem, M. L. & Kohler, H. M. 2006. The removal of zinc from liquid streams by electroflotation. *Miner. Eng.*, 19, 1388-1392.
- Chen, G. 2004. Electrochemical technologies in wastewater treatment. *Separation and Purification Technology*, 38, 11-41.
- Cherns, L., Cocks, L. R. M., Davies, J. R., Hillier, R. D., Waters, R. A. & Williams, M. 2006. Silurian: the influence of extensional tectonics and sea-level changes on sedimentation in the Welsh Basin and on the Midland Platform. *In: Rawson, P. F. & Brenchley, P. J. (eds.) The Geology of England and Wales.* London: Geological Society, 75-102.
- Clayton, C. R., Matthews, M. C. & Simms, N. E. 1995. *Site Investigation*, Oxford Wiley-Blackwell.
- Comninellis, C. & Chen, G. 2010. *Electrochemistry for the Environment*, Heidelberg, Springer.
- Coulton, R., Bullen, C. & Hallett, C. 2003. The design and optimisation of active mine water treatment plants. *Land Contamination and Reclamation*, 11, 273-280.
- Cox, P. A. 1995. *The Elements on Earth. Inorganic Chemistry in the Environment.*, Oxford, Oxford University Press.
- Cravotta, C. A., III 2010. Abandoned Mine Drainage in the Swatara Creek Basin, Southern Anthracite Coalfield, Pennsylvania, USA: 2. Performance of Treatment Systems. *Mine Water and the Environment*, 29, 200-216.
- Cravotta, C. A. I. 1998. Oxidic Limestone Drains for the Treatment of Dilute, Acid Mine Drainage. *Annual Symposium of the West Virginia Surface Mine Drainage Task Force West Virginia*
- Cravotta, C. A. I. 2007. Passive aerobic treatment of net-alkaline, iron-laden drainage from a flooded underground anthracite mine, Pennsylvania, USA. *Mine Water and the Environment*, 26, 128-149.
- Cravotta, C. A. I. 2008. Dissolved metals and associated constituents in abandoned coal-mine discharges, Pennsylvania, USA. Part 2:

- Geochemical controls on constituent concentrations. *Applied Geochemistry*, 23, 203-226.
- Cravotta, C. A. I. & Trahan, M. K. 1999. Limestone drains to increase pH and remove dissolved metals from acidic mine drainage. *Applied Geochemistry*, 14, 581-606.
- Crosby, S. A., Glasson, D. R., Cuttler, A. H., Butler, I., Turner, D. R., Whitfield, M. & Millward, G. E. 1983. Surface areas and porosities of iron(III)- and iron(II)-derived oxyhydroxides. *Environmental Science & Technology*, 17, 709-713.
- Daughney, C. J., Châtellier, X., Chan, A., Kenward, P., Fortin, D., Suttle, C. A. & Fowle, D. A. 2004. Adsorption and precipitation of iron from seawater on a marine bacteriophage (PWH3A-P1). *Marine Chemistry*, 91, 101-115.
- Davies, J. R., A Fletcher, C. J. N., A Waters, R. A. & A Wilson, D. 1994. *Geology of the country around Llanilar and Rhayader : memoir for 1:50 000 geological sheets 178 and 179 (England and Wales)*, London, UK, Stationery Office.
- Demchak, J., Morrow, T. & Skousen, J. 2001. Treatment of acid mine drainage by four vertical flow wetlands in Pennsylvania. *Geochemistry: Exploration, Environment, Analysis*, 1, 71-80.
- Deul, M. & Mihok, E. A. 1967. Mine Water Research – Neutralization. *Bureau of Mines Report of Investigations*, 6987, 1-24.
- Dey, M., Sadler, P. J. K. & Williams, K. P. 2003. A novel approach to mine water treatment. *Land Contamination and Reclamation*, 11, 253-258.
- Dold, B. & Fontboté, L. 2001. Element cycling and secondary mineralogy in porphyry copper tailings as a function of climate, primary mineralogy, and mineral processing. *Journal of Geochemical Exploration*, 74, 3-55.
- Doležal, F., Kulhavý, Z., Švihla, V., Cmelík, M. & Fucík, P. 2007. Uncertainty in Estimating Runoff and Water Quality Characteristics in Agricultural Catchments and Tile Drainage Systems. In: Pfister, L. & Hoffmann, L. (eds.) *Uncertainties in the 'monitoring-conceptualisation-modelling' sequence of catchment research*. Luxembourg: International Hydrological Programme (IHP) of the United Nations Educational Scientific and Cultural Organization (UNESCO).
- Drever, J. I. 1997. *The Geochemistry of Natural Waters: Surface and Groundwater Environments*. 3rd ed. University of California Prentice Hall 436.
- Dyck, W. 1968. Adsorption and coprecipitation of silver on hydrous ferric oxide. *Canadian Journal of Chemistry*, 46, 1441-1444.
- Dzombak, D. A. & Morel, F. M. M. 1987. Development Of A Data Base For Modelling Adsorption Of Inorganics On Iron And Aluminum Oxides. *Environmental Progress*, 6, p 133-137.
- Dzombak, D. A. & Morel, F. M. M. 1990. *Surface Complexation Modelling* Canada, John Wiley & Sons.
- Edwards, P. & Potter, H. 2007. The Cwm Rheidol Metal Mines Remediation Project – Phase 1. *International Mine Water Association* Italy.
- Environment Agency 2002. *Metal Mines Strategy for Wales*.
- European Parliament 2006. Directive 2006/11/EC Of The European Parliament And Of The Council On Pollution Caused By Certain Dangerous

- Substances Discharged Into The Aquatic Environment Of The Community. *Official Journal of the European Union*, 56-52.
- Evangelou, V. P. 1998. *Environmental Soil and Water Chemistry: Principles and Applications*, Canada, John Wiley & Sons.
- Evans, K. A., Watkins, D. C. & Banwart, S. A. 2006. Rate controls on the chemical weathering of natural polymineralic material II. Rate controlling mechanisms and mineral sources and sinks for element release from four UK mine-sites, and implications for comparison of laboratory and field scale weathering studies. *Applied Geochemistry*, 21, 377-403.
- Farley, K. J., Dzombak, D. A. & Morel, F. M. M. 1985. A surface precipitation model for the sorption of cations on metal oxides. *Journal of Colloid and Interface Science*, 106, 226-242.
- Faure, G. 1998. *Principles and Applications of Geochemistry* New Jersey, Prentice Hall.
- Fernandez-Martinez, A., Timon, V., Romaman-Ross, G., Cuello, G. J., Daniels, J. E. & Ayora, C. 2010. The structure of schwertmannite, a nanocrystalline iron oxyhydroxysulfate. *American Mineralogist* 95, 1312-1322.
- Fernández-Rubio, R., Fernández-Lorca, S. & Esteban Arlegui, J. 1987. Preventive Techniques for Controlling Acid Water in Underground Mines by Flooding. *Int. J. Mine Water*, 6, 39-52.
- Figuerola, L. A. & Wolkersdorfer, C. 2014. Electrochemical Recovery of Metals in Mining Influenced Water: State of the Art. In: Sui, W. et al. (eds.) *An Interdisciplinary Response to Mine Water Challenges - IMWA 2014*. Xuzhou.
- Fitzpatrick, R. W. & Self, P. G. 1997. Iron Oxyhydroxides, Sulfides and Oxyhydroxysulfates as Indicators of Acid Sulfate Weathering Environments. *Advances in GeoEcology* 30, 227-240.
- Florence, T. M. 1980. *Speciation of Zinc in the Natural Environment*, New York, Wiley-Interscience.
- Fosmire, G. J. 1990. Zinc toxicity. *American Journal of Clinical Nutrition*, 51, 225-227.
- Franco, N. B. & Balouskus, R. A. 1974. Electrochemical removal of heavy metals from acid mine drainage. *Environmental Protection Technology Series*, EPA-670/2-74-023, 86.
- Fuge, R., Laidlaw, I. M. S., Perkins, W. T. & Rogers, K. P. 1991. The influence of acidic mine and spoil drainage on water quality in the mid-Wales area. *Environmental Geochemistry and Health*, 13, 70-75.
- Fuge, R., Pearce, F. M., Pearce, N. J. G. & Perkins, W. T. 1994. Acid mine drainage in Wales and influence of ochre precipitation on water chemistry. *ACS Symposium Series*, 550, 261-274.
- Gagliano, W. B., Brill, M. R., Bigham, J. M., Jones, F. S. & Traina, S. J. 2004. Chemistry and mineralogy of ochreous sediments in a constructed mine drainage wetland. *Geochimica et Cosmochimica Acta*, 68, 2119-2128.
- Gaikwad, R. W. 2010. Review and research needs of active treatment of acid mine drainage by ion exchange. *Electronic Journal of Environmental, Agricultural and Food Chemistry*, 9, 1343-1350.
- Gandy, C. J. & Younger, P. L. 2002. A Review of Saline Mine Waters in the Silesian Region and Methods for Managing them. University of Newcastle

- Geldenhuis, A. J., Maree, J. P., Fourie, W. J., Smit, J. J., Bladergroen, B. J. & Tjati, M. 2003. *Acid mine drainage treated electrolytically for recovery of hydrogen, iron (II) oxidation and sulphur production*, Johannesburg, Proceedings, 8th International Mine Water Association Congress.
- Geroni, J. 2011. *Rates and mechanisms of chemical processes affecting the treatment of ferruginous mine water* Ph.D., Cardiff University.
- Gill, R. 1996. *Chemical Fundamentals of Geology* London.: Chapman & Hall, 290.
- Glaze, W. H., Kang, J.-W. & Chapin, D. H. 1987. *Chemistry Of Water Treatment Processes Involving Ozone, Hydrogen Peroxide And Ultraviolet Radiation*. 335-352.
- Griffith, J. J. 1919. Influence of mines upon land and livestock in Cardiganshire. *Journal of Agricultural Science*, 9, 366-395.
- Hao, Y. M., Man, C. & Hu, Z. B. 2010. Effective removal of Cu (II) ions from aqueous solution by amino-functionalized magnetic nanoparticles. *Journal of Hazardous Materials*, 184, 392-399.
- Hartley, S. 2009. *Remediation of Abandoned Metal Mine Drainage Using Dealginated Seaweed*. Ph.D Unpublished thesis Aberystwyth University.
- Heaney, S. I. & Davison, W. 1977. The determination of ferrous iron in natural waters with 2,2' - bipyridyl. *Limnology and Oceanography*, 22, 753-760.
- Hedin, R., Narin, W. R. & Kleinmann, L. P. 1994. Passive Treatment of Coal Mine Drainage *Bureau of Mines Information Circular* 1-35.
- Hedin, R. S. 2003. Recovery of marketable iron oxide from mine drainage in the USA. *Land Contam. Reclam.*, 11, 93-97.
- Hedin, R. S., Nairn, R. W. & Watzlaf, G. R. 1991. A Preliminary Review of the Use of Anoxic Limestone Drains in the Passive Treatment of Acid Mine Drainage. *Proceedings, West Virginia Surface Mine Drainage Task Force Symposium* 12.
- Hedrich, S. & Johnson, D. B. 2012. A modular continuous flow reactor system for the selective bio-oxidation of iron and precipitation of schwertmannite from mine-impacted waters. *Bioresource Technology*, 106, 44-49.
- Heidmann, I. & Calmano, W. 2008. Removal of Zn(II), Cu(II), Ni(II), Ag(I) and Cr(VI) present in aqueous solutions by aluminium electrocoagulation. *Journal of Hazardous Materials*, 152, 934-941.
- Hem, J. D. 1985. Study and Interpretation of the Chemical Characteristics of Natural Water. *U.S. Geological Survey, Water Supply Paper*, 2254, 263.
- Herbert Jr, R. B. 1999. *MiMi – Sulfide oxidation in mine waste deposits – A review with emphasis on dysoxic weathering*, Luleå, MiMi Print.
- Holt, P. K., Barton, G. W. & Mitchell, C. A. 2005. The future for electrocoagulation as a localised water treatment technology. *Chemosphere*, 59, 355-367.
- Holt, P. K., Barton, G. W., Wark, M. & Mitchell, C. A. 2002. A quantitative comparison between chemical dosing and electrocoagulation. *Colloids and Surfaces A: Physicochemical and Engineering Aspects*, 211, 233-248.
- Huisman, L. & Wood, W. E. 1974. *Slow sand filtration*, World Health Organization.
- Hunt, A. 2003. *Complete A-Z Chemistry Handbook*, London., Hodder & Stoughton.
- Hüttig, G. & Zänker, H. 2004. Kolloidgetragene Schwermetalle im Entwässerungsstollen einer stillgelegten Zn-Pb-Ag-Grube. *Wissenschaftlich-Technische Berichte*, FZR-403, 1-33.

- International Union of Pure and Applied Chemistry 2012. *Compendium of Chemical Terminology – Gold Book*, International Union of Pure and Applied Chemistry.
- Ixer, R. & Budd, P. 1998. The Mineralogy of Bronze Age Copper Ores from the British Isles: Implications for the Composition of Early Metalwork. *Oxford Journal of Archaeology*, 17, 15-41.
- Jarvis, A., Fox, A., Gozzard, E., Hill, S. & Mayes, W. M. 2007. Prospects for Effective National Management of Abandoned Metal Mine Water Pollution in the UK. *International Mine Water Association Italy*.
- Jarvis, A. P. & Younger, P. L. 2001. Passive treatment of ferruginous mine waters using high surface area media. *Water Research*, 35, 3643-3648.
- Jasinski, R. & Gaines, L. 1972. Electrochemical treatment of acid mine wastes. *Wat. Poll. Contr. Res. Ser.*, 14010 FNQ 02-72, 81.
- Jenke, D. R. & Diebold, F. E. 1984. Electroprecipitation treatment of acid mine wastewater. *Water Research*, 18, 855-859.
- Jennings, S. R., Neuman, D. R. & Blicher, P. S. 2008. Acid Mine Drainage and Effects on Fish Health and Ecology: A review. *Reclamation Research Group Publication*
- Johnson, D. B. 2014. Recent Developments in Microbiological Approaches for Securing Mine Wastes and for Recovering Metals from Mine Waters. *Minerals*, 4, 279-292.
- Johnson, D. B. & Hallberg, K. B. 2005. Acid mine drainage remediation options: a review. *Science of the Total Environment*, 338, 3-14.
- Johnston, D. 2004. A Metal Mines Strategy for Wales In: Jarvis A. P., D. B. A., Younger P. L. (ed.) *mine water 2004 – International Mine Water Association Symposium*. Newcastle Upon Tyne: University of Newcastle.
- Johnston, D., Parker, K. & Pritchard, J. 2007. Management of Abandoned Minewater Pollution in the United Kingdom. *International Mine Water Association Italy*.
- Jones, A. N. & Howells, W. R. 1975. *The partial recovery of the metal polluted River Rheidol*, Oxford, Blackwell.
- Jones, O. T. 1922. *Lead and Zinc – The Mining District of North Cardiganshire and West Montgomeryshire*, London, Geological Survey.
- Jones, O. T. & Pugh, W. J. 1935. The geology of the districts around Machynlleth and Aberystwyth. *Proceedings of the Geologists' Association*, 46, 247-IN2.
- Kairies, C. L., Watzlaf, G. R., Hedin, R. S. & Capo, R. C. 2001. Characterization and resource recovery potential of precipitates associated with abandoned coal mine drainage. *Proceedings of the Annual Meeting of the American Association for Surface Mining and Reclamation*. Scottsdale.
- Karthikeyan, K. G., Elliott, H. A. & Cannon, F. S. 1997. Adsorption and Coprecipitation of Copper with the Hydrous Oxides of Iron and Aluminum. *Environmental Science & Technology*, 31, 2721-2725.
- Kelly, D. P. & Wood, A. P. 2000. Reclassification of some species of *Thiobacillus* to the newly designated genera *Acidithiobacillus* gen. nov., *Halothiobacillus* gen. nov. and *Thermithiobacillus* gen. nov. *International Journal of Systematic and Evolutionary Microbiology*, 50, 511-516.
- Kelly, M. 1988. *Mining and the Freshwater Environment* England, UK, Elsevier.

- Kepler, D. A. & McCleary, E. C. 1994. *Successive Alkalinity-Producing Systems (SAPS) for the Treatment of Acid Mine Drainage*, Pittsburgh, Proceedings, International Land Reclamation and Mine Drainage Conference.
- Kickuth, R. 1977. Degradation and Incorporation of nutrients from rural wastewaters by plant hydrosphere under limnic conditions.
- Kirby, C. S., Dennis, A. & Kahler, A. 2009. Aeration to degas CO₂, increase pH, and increase iron oxidation rates for efficient treatment of net alkaline mine drainage. *Applied Geochemistry*, 24, 1175-1184.
- Konhauser, K. O. 2006. *Introduction to Geomicrobiology*, Malden, Wiley-Blackwell.
- Kostenbader, P. D. & Haines, G. F. 1970. High-density sludge treats acid mine water. *Coal Age*, 75, 90-97.
- Langmuir, D. 1997. *Aqueous Environmental Geochemistry*, New Jersey, Prentice-Hall.
- Lauder, M. 2012. *Electrocoagulation to Treat Metal Mine Drainage – A Feasibility Study*. MSc Cardiff University
- Leblanc, M., Morales, J. A., Borrego, J. & Elbaz-Poulichet, F. 2000. 4,500-Year-Old Mining Pollution in Southwest Spain: Long-Term Implications from Modern Mining Pollution. *Econ. Geol.*, 95, 655-662.
- Lefrou, C., Fabry, P. & Poignet, J.-C. 2012. *Electrochemistry: The Basics, With Examples* Berlin Springer
- Levins, G. 2007. Temple Mine Survey. Edgbaston: Welsh Mines Preservation Trust.
- Levinson, A. A. 1974. *Introduction to Exploration Geochemistry*, Calgary, Applied Publishing Ltd.
- Lord, I. R. 2013. The mines of Cwm Rheidol. *Welsh Mines Preservation Trust Newsletter - Special Edition*, 36-47.
- Lottermoser, B. 2007. *Mine Wastes – Characterization, Treatment and Environmental Impacts*, Heidelberg, Springer.
- Macías, F., Caraballo, M. A., Nieto, J. M., Rötting, T. S. & Ayora, C. 2012. Natural pretreatment and passive remediation of highly polluted acid mine drainage. *Journal of Environmental Management*, 104, 93-100.
- Majzlan, J. & Myneni, S. C. B. 2004. Speciation of Iron and Sulfate in Acid Waters: Aqueous Clusters to Mineral Precipitates. *Environmental Science & Technology*, 39, 188-194.
- Maree, J. P., Hlabela, P., Nengovhela, R., Geldenhuys, A. J., Mbhele, N., Nevhulaudzi, T. & Waanders, F. B. 2004. Treatment of mine water for sulphate and metal removal using barium sulphide. *Mine Water and the Environment*, 23, 195-203.
- Maree, J. P., Mujuru, M., Bologo, V., Daniels, N. & Mpholoane, D. 2013. Neutralisation treatment of AMD at affordable cost. *Water SA*, 39, 245-250.
- Mason, J. S. *Prevention of Environmental Disaster at Cwmrheidol Mine, Central Wales, Early 1990s* [Online]. Available: <http://www.geologywales.co.uk/cwmrheidol.htm> [Accessed 2014-06-17].
- Mason, J. S. 1997. Regional polyphase and polymetallic vein mineralization in the Caledonides of the Central Wales Orefield. *Transactions of the Institution of Mining and Metallurgy Section B-Applied Earth Science*, 106, B135-B143.

- Mason, J. S. s.a. *Prevention of Environmental Disaster at Cwmrheidol Mine, Central Wales, Early 1990s* [Online]. Available: <http://www.geologywales.co.uk/cwmrheidol.htm> [Accessed 2014-06-17].
- Matteson, M. J., Dobson, R. L., Glenn Jr, R. W., Kukunoor, N. S., Waits Iii, W. H. & Clayfield, E. J. 1995. Electrocoagulation and separation of aqueous suspensions of ultrafine particles. *Colloids and Surfaces A: Physicochemical and Engineering Aspects*, 104, 101-109.
- Matthies, R., Aplin, A. C., Boyce, A. J. & Jarvis, A. P. 2012. Geochemical and stable isotopic constraints on the generation and passive treatment of acidic, Fe-SO₄ rich waters. *Science of the Total Environment*, 420, 238-249.
- McKnight, D. & Feder, G. 1984. The ecological effect of acid conditions and precipitation of hydrous metal oxides in a Rocky Mountain stream. *Hydrobiologia*, 119, 129-138.
- Merkel, B., Planer-Friedrich, B. & Nordstrom, D. K. 2005. *Groundwater geochemistry : a practical guide to modeling of natural and contaminated aquatic systems*, Berlin ; New York, Springer.
- Mermet, J. M., Otto, M., Kellner, R. & Cases, M. V. 2004. *Analytical chemistry: a modern approach to analytical science*, Wiley-VCH.
- Metcalf & Eddy, I. 2002. *Wastewater Engineering: Treatment and Reuse*, New York, McGraw-Hill.
- Mollah, M. Y. A., Schennach, R., Parga, J. R. & Cocke, D. L. 2001. Electrocoagulation (EC) – science and applications. *Journal of Hazardous Materials*, 84, 29-41.
- Morin, K. A. & Hutt, N. M. 2006. *Case Studies of Costs and Longevities of Alkali-Based Water-Treatment Plants for ARD*, St. Louis, Proceedings 7th International Conference on Acid Rock Drainage (ICARD).
- Mudashiru, L. K. 2008. *Electrochemical Determination of Dissolved and Particulate Iron in Mine-waters*, Newcastle, unpubl. PhD Thesis Univ. Newcastle upon Tyne.
- Mullinger, N. 2007. Assessing the Impacts of Metal Mines in Wales. *International Mine Water Association* Newcastle, UK
- Muyssen, B. T. A., De Schampelaere, K. A. C. & Janssen, C. R. 2006. Mechanisms of chronic waterborne Zn toxicity in *Daphnia magna*. *Aquatic Toxicology*, 77, 393-401.
- Nkwonta, O. & Ochieng, G. M. 2009. Passive Treatment of Mine Water Using Roughing Filters as a Pre-Treatment Option. International Mine Water Conference, Pretoria.
- Nordstrom, D. K. 2011. Mine waters: Acidic to circumneutral. *Elements*, 7, 393-398.
- Nordstrom, D. K. & Alpers, C. N. 1999. Negative pH, efflorescent mineralogy, and consequences for environmental restoration at the Iron Mountain Superfund site, California. *Proc Natl Acad Sci USA*, 96, 3455-62.
- Nordstrom, D. K., Alpers, C. N., Ptacek, C. J. & Blowes, D. W. 2000. Negative pH and extremely acidic mine waters from Iron Mountain, California. *Environmental Science and Technology*, 34, 254-258.
- Noubactep, C. 2012. Investigating the processes of contaminant removal in Fe⁰/H₂O systems. *Korean Journal of Chemical Engineering*, 29, 1050-1056.

- Oncel, M. S., Muhcu, A., Demirbas, E. & Kobya, M. 2013. A comparative study of chemical precipitation and electrocoagulation for treatment of coal acid drainage wastewater. *J. Environm. Chem. Eng.*, 1, 989-995.
- Palumbo-Roe, B. & Colman, T. 2010. The nature of waste associated with closed mines in England and Wales., 82.
- Palumbo-Roe, B., Klinck, B., Banks, V. & Quigley, S. 2009. Prediction of the long-term performance of abandoned lead zinc mine tailings in a Welsh catchment. *Journal of Geochemical Exploration*, 100, 169-181.
- Parkhurst, D. L. & Appelo, C. A. J. 2013. Description of Input and Examples for PHREEQC Version 3 – A Computer Program for Speciation, Batch-Reaction, One-Dimensional Transport, and Inverse Geochemical Calculations. *U.S. Geological Survey Techniques and Methods*, 6, 1-497.
- Pearce, F. M. 1993. Great Opencast, Parys Mountain, Anglesey
- Pearce, N. J. G. 1994. *Development and conservation at Parys Mountain, Anglesey, Wales. In: Geological and Landscape Conservation*, Geological Society London.
- Pearson, F. H. & McDonnell, A. J. 1974. Neutralization of acidic wastes by crushed limestone. *NTIS*.
- Peretyazhko, T., Zachara, J. M., Boily, J. F., Xia, Y., Gassman, P. L., Arey, B. W. & Burgos, W. D. 2009. Mineralogical transformations controlling acid mine drainage chemistry. *Chemical Geology*, 262, 169-178.
- Philips Electron Optics & Johnson, R. 1996. *Environmental scanning electron microscopy – an introduction to ESEM*, Eindhoven, Netherlands, Philips Electron Optics.
- PIRAMID Consortium 2003. Engineering guidelines for the passive remediation of acidic and/or metalliferous mine drainage and similar wastewaters
- Pointon, C. R. & Ixer, R. A. 1980. Parys Mountain mineral deposit, Anglesey, Wales – Geology and ore mineralogy. *Transactions of the Institution of Mining and Metallurgy*, 89, 43-155.
- Pollio, F. & Kunin, R. 1967. Ion exchange processes for the reclamation of acid mine drainage waters. *Environmental Science and Technology*, 1, 235-241.
- Pretorius, W. A., Johannes, W. G. & Lambert, G. G. 1991. Electrolytic Iron Flocculant Production With a Bipolar Electrode in Series Arrangement *Water (South Africa)* 17.
- Price, R. E. & Pichler, T. 2006. Abundance and mineralogical association of arsenic in the Suwannee Limestone (Florida): Implications for arsenic release during water–rock interaction. *Chemical Geology*, 228, 44-56.
- Rajeshwar, K. & Ibanez, J. 1997. *Environmental Electrochemistry Fundamentals and Applications in Pollution Sensors and Abatement* Academic Press
- Ranville, J. F. & Schmiermund, R. L. 1999. *General Aspects of Aquatic Colloids in Environmental Geochemistry*, Littleton, Society of Economic Geologists.
- Raybould, J. G. 1973. *Studies of variations in the paragenic sequence and zoning in the mineral veins of Cardiganshire and Montgomeryshire*. Unpublished Ph.D thesis University of Wales, Aberystwyth
- Razowska-Jaworek, L., Pluta, I. & Chmura, A. 2008. Mine Waters and Their Usage in the Upper Silesia in Poland – Examples from Selected Regions. *Proceedings, 10th International Mine Water Association Congress*, 537-539.

- Rees, B. 2005. *An Update on Parys Mountain Remediation and Welsh Metal Mine Management*, Oviedo, University of Oviedo.
- Rees, S. B., Bright, P., Connelly, R., Howell, R. J. & Szabo, E. 2004. Application of the Welsh Mine Water Strategy - Cwmrheidol Case Study. In: Jarvis, A. P. et al. (eds.) *mine water 2004 – International Mine Water Association Symposium*. Newcastle Upon Tyne: University of Newcastle.
- Regenspurg, S., Brand, A. & Peiffer, S. 2004. Formation and stability of schwertmannite in acidic mining lakes. *Geochimica et Cosmochimica Acta*, 68, 1185-1197.
- Rhee, I. H. & Dzombak, D. A. 1998. Surface Complexation/Gouy–Chapman Modeling of Binary and Ternary Cation Exchange. *Langmuir*, 14, 935-943.
- Richardson, J. B. 1974. *Metal Mining* London Allen Lane
- Ríos, C. A., Williams, C. D. & Roberts, C. L. 2008. Removal of heavy metals from acid mine drainage (AMD) using coal fly ash, natural clinker and synthetic zeolites. *Journal of Hazardous Materials*, 156, 23-35.
- Rose, A. W. & Dietz, J. M. 2002. *Case Studies of Passive Treatment Systems – Vertical Flow Systems*, Lexington, Proceedings 19th Annual National Meeting – American Society for Surface Mining and Reclamation.
- Rowe, O. F. & Johnson, D. B. 2009. Enhanced rates of iron oxidation in mine waters by the novel acidophilic bacterium “*Ferroplasma myxofaciens*” immobilized in packed-bed bioreactors. *Proceedings, Securing the Future 2009 & 8th ICARD*. Skellefteå.
- Rowe, O. F., Sánchez-España, J., Hallberg, K. B. & Johnson, D. B. 2007. Microbial communities and geochemical dynamics in an extremely acidic, metal-rich stream at an abandoned sulfide mine (Huelva, Spain) underpinned by two functional primary production systems. *Environmental Microbiology*, 9, 1761-1771.
- Sahoo, P. K., Tripathy, S., Panigrahi, M. K. & Equeenuddin, S. M. 2012. Mineralogy of Fe-Precipitates and Their Role in Metal Retention from an Acid Mine Drainage Site in India. *Mine Water and the Environment*, 31, 344-352.
- Sanders, M. J., Du Preez, H. H. & Van Vuren, J. H. J. 1999. Monitoring cadmium and zinc contamination in freshwater systems with the use of the freshwater river crab, *Potamonautes warreni*. *Water SA*, 25, 91-98.
- Sapsford, D. 2013. New perspectives on the passive treatment of ferruginous circumneutral mine waters in the UK. *Environmental Science and Pollution Research* 20, 7827-7836.
- Sapsford, D., Barnes, A., Dey, M., Williams, K., Jarvis, A. & Younger, P. 2007. Low Footprint Passive Mine Water Treatment: Field Demonstration and Application. *Mine Water Environ.*, 26, 243-250.
- Sapsford, D. J., Barnes, A., Dey, M., Liang, L. & Williams, K. P. 2005. *A novel method for passive treatment of mine water using a vertical flow accretion system*, Oviedo, University of Oviedo.
- Sapsford, D. J., Barnes, A., Dey, M., Williams, K. P., Jarvis, A., Younger, P. & Liang, L. 2006. Iron and manganese removal in a vertical flow reactor for passive treatment of mine water. 7th ICARD, St. Louis, 1831 - 1843. 1831-1843.
- Sasson, M. B., Calmano, W. & Adin, A. 2009. Iron-oxidation processes in an electroflocculation (electrocoagulation) cell. *Journal of Hazardous Materials*, 171, 704-709.

- Schoeman, J. J. & Steyn, A. 2001. Investigation into alternative water treatment technologies for the treatment of underground mine water discharged by Grootvlei Proprietary Mines Ltd into the Blesbokspruit in South Africa. *Desalination*, 133, 13-30.
- Schwertmann, U. & Carlson, L. 2005. The pH-dependent transformation of schwertmannite to goethite at 25 degrees C. *Clay Minerals*, 40, 63-66.
- Schwertmann, U. & Cornell, R. M. 2000. *Iron Oxides in the Laboratory* WILEY-VCH
- Seidel, K. 1996. Reinigung von Gewässern durch höhere Pflanzen. *Naturwissenschaften*, 53, 289-297.
- Senes Consultants Limited 1994. *Acid Mine Drainage – Status of Chemical Treatment and Sludge Management Practices*, Richmond Hill, The Mine Environment Neutral Drainage [MEND] Program.
- Sheoran, A. S. & Sheoran, V. 2006. Heavy metal removal mechanism of acid mine drainage in wetlands: A critical review. *Minerals Engineering*, 19, 105-116.
- Shiller, A. M. 2003. Syringe Filtration Methods for Examining Dissolved and Colloidal Trace Element Distributions in Remote Field Locations. *Environ. Sci. Technol.*, 37, 3953-3957.
- Sierra, C., Álvarez Saiz, J. R. & Gallego, J. L. R. 2013. Nanofiltration of Acid Mine Drainage in an Abandoned Mercury Mining Area. *Water, Air and Soil Pollution*, 224, 1-12.
- Singer, P. C. & Stumm, W. 1969. The Rate-Determining Step in the Production of Acidic Mine Wastes. *Am. Chem. Soc., Div. Fuel Chem., Prepr.*, 13, 80-87.
- Singer, P. C. & Stumm, W. 1970a. Acidic mine drainage: The rate-determining step. *Science*, 167, 1121-1123.
- Singer, P. C. & Stumm, W. 1970b. Direct oxidation by adsorbed oxygen during acidic mine drainage. *Science*, 169, 98.
- Skelly & Loy 1974. Processes, Procedures and Methods to Control Pollution From Mining Activities.
- Skousen, J. G. 1991a. Anoxic limestone drains for acid mine drainage treatment. *Green Lands* 21, 30-35.
- Skousen, J. G. 1991b. An evaluation of acid mine drainage treatment systems and costs. In: Lootens, D. J., ed. *Environmental Management for the 1990's*, Littleton. Soc. Mining, Metall. and Exploration, 173-178.
- Skousen, J. G., Sexstone, A. & Ziemkiewicz, P. F. 2000. *Acid Mine Drainage Control and Treatment*, Madison, Wis., American Society of Agronomy.
- Smith, K. S., Figueroa, L. A. & Plumlee, G. S. 2013. *Can treatment and disposal costs be reduced through metal recovery?*, Golden, International Mine Water Association.
- Smith, K. S. & Huyck, H. L. O. 1999. *An Overview of the Abundance, Relative Mobility, Bioavailability, and Human Toxicity of Metals*, Littleton, Society of Economic Geologists.
- Sørensen, S. P. L. 1909. Über die Messung und die Bedeutung der Wasserstoffionenkonzentration bei enzymatischen Prozessen. *Biochemische Zeitschrift*, 21, 131-200.
- Stauffer, T. E. & Lovell, H. L. 1969. The Oxygenation of Iron II Solutions – Relationships to Coal Mine Drainage Treatment. *Am. Chem. Soc., Div. Fuel Chem., Prepr.*, 13, 88-94.

- Strathmann, H. 2012. *Membranes and Membrane Separation Processes, 1. Principles*, Weinheim, Wiley-VCH.
- Stumm, W. & Morgan, J. J. 1996. *Aquatic Chemistry - Chemical Equilibria and Rates in Natural Waters*, New York, John Wiley & Sons.
- Suvio, P., Sapsford, D., Griffiths, A. J., Williams, K., Davies, J. D. & Maynard, S. 2010. High Density Sludge process applied to metal-containing effluent. 289-299.
- Tischendorf, G. & Ungethüm, H. 1965. Zur Anwendung von Eh-pH-Beziehungen in der geologischen Praxis. *Z. Angew. Geol.*, 11, 57-67.
- Trapido, M. 2008. Ozone-Based Advanced Oxidation Processes In: Munter, R. (ed.) *Encyclopedia of Life Support Systems (EOLSS), Developed under the Auspices of the UNESCO*. Oxford, UK: Eolss Publishers, 1-17.
- US EPA 2009. 10,10'-Oxybisphenoxarsine (OBPA) Summary Document: Registration Review.
- Valente, T. M., Antunes, M., Braga, A. S., Prudencio, M. I., Marques, R. & Pamplona, J. 2012. Mineralogical attenuation for metallic remediation in a passive system for mine water treatment. *Environmental Earth Sciences*, 66, 39-54.
- Vepsäläinen, M. 2012. *Electrocoagulation in the treatment of industrial waters and wastewaters*, Espoo, VTT.
- Walton-Day, K. 2003. *Passive and Active treatment of Mine Drainage*.
- Walton, K. C. & Johnson, D. B. 1992. Microbiological and chemical characteristics of an acidic stream draining a disused copper mine. *Environmental Pollution*, 76, 169-175.
- Warrender, R., Pearce, N. J. G., Perkins, W. T., Florence, K. M., Brown, A. R., Sapsford, D. J., Howell, R. J. & Dey, M. 2011. Field Trials of Low-cost Reactive Media for the Passive Treatment of Circum-neutral Metal Mine Drainage in Mid-Wales, UK. *Mine Water and the Environment*, 30, 82-89.
- Waybrant, K. R., Blowes, D. W. & Ptacek, C. J. 1998. Selection of reactive mixtures for use in permeable reactive walls for treatment of mine drainage. *Environmental Science and Technology*, 32, 1972-1979.
- Wei, X. & Viadero Jr, R. C. 2007. Synthesis of magnetite nanoparticles with ferric iron recovered from acid mine drainage: Implications for environmental engineering. *Colloids and Surfaces A: Physicochemical and Engineering Aspects*, 294, 280-286.
- Weiner, E. R. 2010. *Applications of Environmental Aquatic Chemistry – A Practical Guide*, Boca Raton, CRC Press.
- Wendt, H., Vogt, H., Kreysa, G., Goldacker, H., Jüttner, K., Galla, U. & Schmieder, H. 2012. *Electrochemistry, 2. Inorganic Electrochemical Processes*, Weinheim, Wiley-VCH.
- Whitlow, R. 2000. *Basic Soil Mechanics*, Prentice Hall.
- WHO 2004. *Water Treatment and Pathogen Control: Process Efficiency in Achieving Safe Drinking Water*. Alliance House, London SW1H 0QS
- Wildeman, T., Brodie, G. & Gusek, J. 1993. *Wetland Design for Mining Operations*, Richmond, BC, BiTech.
- Wolkersdorfer, C. 2008. *Water Management at Abandoned Flooded Underground Mines – Fundamentals, Tracer Tests, Modelling, Water Treatment*, Heidelberg, Springer

- Wolkersdorfer, C. 2013. *Grubenwasserreinigung – Verfahren und Vorgehensweisen*, Pretoria, Sächsisches Landesamt für Umwelt Landwirtschaft und Geologie.
- Wolkersdorfer, C. & Baierer, C. 2013. Improving Mine Water Quality by Low Density Sludge Storage in Flooded Underground Workings. *Mine Water and the Environment*, 32, 3-15.
- Younger, P. 2000. The adoption and adaptation of passive treatment technologies for mine waters in the United Kingdom. *Mine Water and the Environment*, 19, 84-97.
- Younger, P., Banwart, S. A. & Hedin, R. S. 2002. *Mine Water Hydrology, Pollution, Remediation*, Dordrecht, , Kluwer.
- Ziemkiewicz, P. F., Skousen, J. & Lovett, R. J. 1994. Open Limestone Channels for Treating Acid Mine Drainage: A new Look at an Old Idea *Green Lands* 24, 36-41.
- Ziemkiewicz, P. F., Skousen, J. G., Brant, D. L., Sterner, P. L. & Lovett, R. J. 1997. Acid mine drainage treatment with armored limestone in open limestone channels. *Journal of Environmental Quality*, 26, 1017-1024.
- Zinck, J. M. 2005. *Review of Disposal, Reprocessing and Reuse Options for Acidic Drainage Treatment Sludge*, Ottawa, Mine Environment Neutral Drainage (MEND) Program.
- Zinck, J. M. 2006. *Disposal, reprocessing and reuse options for acidic drainage treatment sludge*, St. Louis, Proceedings 7th International Conference on Acid Rock Drainage (ICARD).
- Zinck, J. M., Wilson, J. L., Chen, T. T., Griffith, W., Mikhail, S. & Turcotte, A. M. 1997. *Characterization and Stability of Acid Mine Drainage Sludge*, Ottawa, Mine Environment Neutral Drainage (MEND) Program.